

Possible high-temperature superconductors predicted from electronic structure and data-filtering algorithms

M. Klintenberg^{1,*} and O. Eriksson^{1,†}

¹ *Department of Physics and Astronomy, Uppsala University, Box 516, SE-75120, Uppsala, Sweden*
(Dated: September 30, 2011)

We report here the completion of the electronic structure of the majority of the known stoichiometric inorganic compounds, as listed in the International Crystal Structure Data-base (ICSD). We make a detailed comparison of the electronic structure, crystal geometry and chemical bonding of cuprate high temperature superconductors, with the calculated over sixty thousand electronic structures. Based on compelling similarities of the electronic structures in the normal state and a data-filtering technique, we propose that high temperature superconductivity is possible for electron- or hole-doping in a much larger group of materials than previously considered. The identified materials are composed of over one hundred layered compounds, most which hitherto are untested with respect to their superconducting properties. Of particular interest are the following materials; $\text{Ca}_2(\text{CuBr}_2\text{O}_2)$, K_2CoF_4 , $\text{Sr}_2(\text{MoO}_4)$ and $\text{Sr}_4\text{V}_3\text{O}_{10}$, which are discussed in detail.

Electronic structure, and the chemical binding which is the direct consequence of it, is responsible for all materials properties. This applies to the equation of state, hardness, elasticity, catalytic activity, surface tension, work function, magnetism, conductivity, lattice dynamics and superconductivity. Theory based on density functional theory[1], so called *ab-initio* theory, has recently matured to reliably reproduce the electronic structure of materials, and almost all properties associated with it. Hence, *ab-initio* theory has become an indispensable tool for analyzing experimental results, and even for predicting novel properties[2]. We report here on the completion of the calculation of the electronic structures of the majority of the synthesized stoichiometric compounds reported in ICSD[3], which amounts to over sixty thousand compounds. Our study may be viewed as the materials scientists counterpart to the Human Genome mapping[4, 5] in bio-medical science, with a similar potential for impact, albeit with the ambition to identify new functional materials. In this comparison between materials science and life-science, the electronic structure of a material corresponds to the genome of a biological system. It is the electronic structure which ultimately governs the materials property. Having established an electronic structure data-base we argue that it is possible to use what is best described as a data-filtering approach,[6] so that several

new materials with selected properties can be identified. For example, the methodology was recently used to successfully predict several new topological insulators[7]. In this report it is high temperature superconductors we focus on.

The electronic structure data-base was first generated by extracting structural information from the Inorganic Crystal Structure Database (ICSD)[3], and using this structural information we performed first principles calculations of the electronic structure. The electronic structure was calculated within the local density approximation (LDA) in combination with a full potential linear muffin-tin orbital (FP-LMTO) method[8]. Although large data-bases of any kind may be used in a variety of ways, we aim to illustrate one particular application. The method may best be described as data-filtering. The basic philosophy is to identify a known class of materials which has been well characterized with respect to a certain property (e.g. superconductivity). If these materials have conspicuous and unique similarities in the underlying electronic structure (the 'code'), one may make a comparison of the electronic structure of other materials, which may not have been subjected to a detailed experimental investigation of the relevant materials property. If a large similarity is found in the electronic structure and possibly also other materials properties like the crystal structure, one may expect a similarity in the materials properties in general.

One hundred years ago superconductivity was discovered[9]. Seventy five years later the field of high temperature superconductivity started, with the discovery of doped La_2CuO_4 , that had an ordering temperature of 30 K[10]. This discovery of a so called cuprate (copper oxide) superconductor, was quickly followed by several other cuprates with high superconducting temperature. Among the most studied cuprate superconductors is $\text{YBa}_2\text{Cu}_3\text{O}_{6+x}$ (YBCO)[11], which has a critical temperature of 93 K. The critical temperature of $\text{Bi}_2\text{Sr}_2\text{CaCu}_2\text{O}_8$ (BISCO)[12] is similar. Currently, the highest critical temperature is found in $\text{HgBa}_2\text{Ca}_2\text{Cu}_3\text{O}_{8+x}$ at $\sim 135\text{-}160$ K[13, 14]. Unfortunately a well established theory is lacking for the origin of the d-wave superconductivity in these materials, and several reviews outlining different mechanisms may be found, e.g. in Refs.15–19. The lack of a firm theoretical understanding of the microscopic mechanism behind the pairing in these materials has made it impossible to pre-

dict new compounds with higher critical superconducting temperatures, critical fields or critical currents. This unfortunately makes this sub-branch of materials science unique, since most other properties of the materials, e.g. magnetism, optical conductivity, elasticity, phase- and structural stability, in general can now be predicted from *ab-initio* theory[20] with good accuracy.

The resonant valence bond model[21] was suggested early on as a possible mechanisms for superconductivity in the cuprates. In addition, spin-bag theories, antiferromagnetic Fermi liquid theory, nested Fermi liquid theory, and a van Hove scenario have been reviewed in Ref.19 and references therein. Here mechanisms based on spinon, holon and anyons are also described. Furthermore, one has considered microscopic mechanisms based on the Hubbard model,[22] antiferromagnetic paramagnons[23] as well as the so called t-J model[24]. In addition a skyrmion like electronic state has been suggested, where a hole is suggested to be moving clock-wise or counter clock-wise on the oxygen plaquette, and this movement couples to transversal magnetic excitations[25].

The basic hypothesis of the present study is that whatever the mechanism or combination of mechanisms that cause the pairing of charge carriers, there is a crucial aspect in that this takes place in a unique electronic structure and crystal geometry. Namely, that of a quasi two-dimensional/layered crystal structure, in which the d-shell of a transition metal atom hybridizes strongly with p-orbitals of ligand atoms. In the cuprates this is manifested in a band of primary $d_{x^2-y^2}$ character that hybridizes with oxygen p-orbitals. We also suggest that it is important that in the normal state, only one single hybridized band cuts through the Fermi level (E_F), for each CuO_2 -plane. This is exactly the situation for the cuprate superconductors, and angular resolved photoemission of the over-doped compounds result in a Fermi surface which is in agreement with that of electronic structure calculations (e.g. as noted in Ref.26 and references therein). One should of course bare in mind that undoped cuprates are Mott insulators (see e.g.Ref.19), where the direct incorporation of electron-electron interaction must be taken into account in order to get the correct electronic structure. Once this is done, the hole doping that drives superconductivity appears in a single band of Cu $d_{x^2-y^2}$ and O p-character. It is this feature we focus on.

A natural question is if there are other compounds that may be promising candidates for superconductivity, due to a similar electronic structure and crystal geometry as those of the cuprates. We suggest that this is the case and as we shall see below we propose over one hundred compounds which have a crystal geometry and electronic structure which is similar to that of the normal state of the cuprates. Amongst previous studies of superconductivity and the electronic structure we note in particular the work of Pavarini et al.[27] who correlated parameters

which determine the electronic structure of cuprates to the critical temperature of these materials, and the works of Refs.28 and 29, where the electronic structure of a nice-late material was tuned by confinement and correlation effects to give an electronic structure that is similar to that of the cuprates.

We have identified potential superconducting compounds by the following data-filtering approach. We have let almost all known stoichiometric compounds as listed by ICSD pass through this filter which has resulted in a list of 139 materials. There are three criteria used in this filtering process: i) A layered crystal structure, with characteristics of the electronic structure reflecting this layered geometry. This can be achieved by inspection of the crystal structure itself, but it is sufficient to investigate the size of the Brillouin-zone, which for two-dimensional materials is compressed in one direction and in addition has a very weak dispersion of the energy bands along this direction. ii) The electronic structure of the cuprates have in the normal state a characteristic feature in that only one band (per CuO_2 -layer) cuts through E_F , and that this band has a dispersion that roughly follows a cosine like dispersion (which is easily understood from tight-binding analysis). iii) The bands the cut through E_F are the result of strongly hybridization between ligand state p and transition metal d orbitals. This last criteria can be fulfilled by analyzing the character of the eigenstates close to E_F , i.e the orbital character for each atom (and site) in the unit cell.

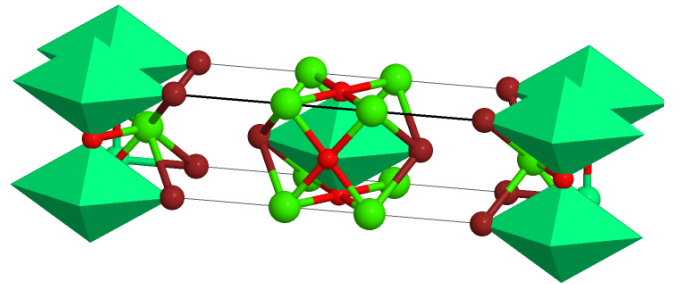


FIG. 1: (Color) Crystal structure of $\text{Ca}_2(\text{CuBr}_2\text{O}_2)$. The Br, Ca, Cu and O atoms are shown in brown, light green, dark green, and red, respectively [3]. The Cu atom sits in an octahedron (marked in green) built up of four oxygen atoms and two Br atoms in apical position.

In the appendix (presented in the Supplementary Information) a list of the suggested 139 superconducting compounds is given, together with figures of these materials electronic- and crystal structures. The 139 compounds are materials that result from the data-filtering criteria outlined above. Slightly different criteria would

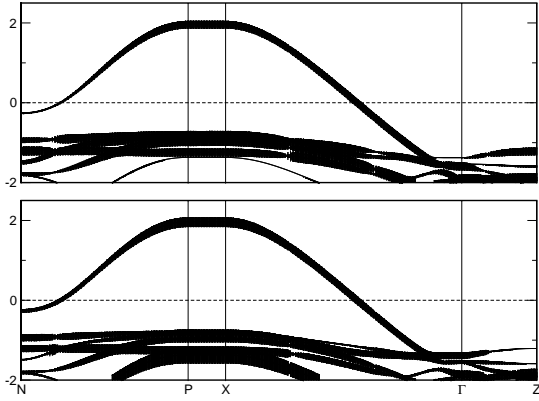


FIG. 2: Electronic structure of the normal state of $\text{Ca}_2(\text{CuBr}_2\text{O}_2)$. The upper panel shows the d-projected bands and the lower panel the p-projected bands, in a so called fat-band representation where the amount of d- or p wave character is represented by the thickness of the bands. The Fermi level is at zero and is marked by a horizontal dashed line.

result in a slightly modified list of possible superconductors. We suggest that electron/hole doping of this list of materials should also be tried in order to find possible new high-temperature superconductors. It is also possible that compounds where a substitution of iso-valent elements to the materials given in the appendix are strong candidates for superconductivity.

Note that for each compound the electronic structure is given in the so called fat-band representation, to highlight the angular momentum character of the bands. This means that the fatter a band is, the higher degree of a certain angular momentum does it have. In particular we show the amount of transition metal d-character and the ligand p-character of the energy bands.

Before entering a discussion about possible new superconductors we note that in the list of suggested materials one finds all established high-temperature superconducting cuprates. This is not surprising since the data-filtering algorithms were set to capture materials with a cuprate like electronic and crystalline structure. Nevertheless it is rewarding that these materials are found, and this may be viewed as an internal test of the filtering algorithms. Also, other materials with strong electron-phonon coupling are found, e.g. NbSe_2 which is known to have a charge density wave state.

The compounds listed in the Appendix form in tetragonal, hexagonal, orthorhombic, monoclinic and cubic crystal structures. Oxides form a large group of compounds in this list, but many non-oxygen based compounds are also found. A detailed analysis of all the materials suggested to be superconducting that are listed in the appendix, is too lengthy for this communication, but we

point out that all identified materials have a layered crystal structure as well as few bands (per chemical building block) that cut E_F . In addition, these bands are for the majority of compounds, composed of strongly hybridized transition metal d-orbitals and ligand p-orbitals. To give an example of the information that is available in our list of suggested materials, the nature of the chemical bonding, geometry and the electronic structure of four of these materials have been selected, and are analyzed in full detail below.

$\text{Ca}_2(\text{CuBr}_2\text{O}_2)$

The compound $\text{Ca}_2(\text{CuBr}_2\text{O}_2)$ crystallizes in the space group I 4/mmm (139), in a tetragonal body centered structure (see Fig.1). The Cu atoms are in a 2+ state and are located in a layered crystal structure, with O atoms in the same plane as the Cu atoms forming CuO_2 -plaquettes. Unlike the cuprates there is in this compound no apical oxygen atom. Instead there is in the out-of-plane position a Br atom that has a Ca atom as a nearest neighbor (see Fig.1). The crystal structure is clearly a layered one with a Cu-O network in a planar geometry that is similar to that of the cuprates.

The electronic structure of the normal state is shown in Fig.2 and is seen to be very similar to that of the cuprates, with a single hybridized Cu d - O p band that cuts E_F and with an energy dispersion that roughly follows what is expected from a tight-binding analysis, where $\epsilon(\mathbf{k}) = \epsilon_0 - 2t(\cos(k_x a) + \cos(k_y a))$ (here t is the hopping parameter and a the in-plane lattice constant). A symmetry analysis of the orbitals that build up this band is that it is composed of Cu $d_{x^2-y^2}$ character that hybridizes with oxygen p_x and p_y orbitals. In the fat-band representation shown in Fig.2, it is seen that this band is essentially an equal mixture of O p and Cu d orbitals. This feature of the electronic structure is similar as that of the known cuprate superconductors.

Electron or hole-doping of this material may be an possible route towards finding new high-temperature superconductors. In this search it is of-course necessary to consider other halides than Br and other alkali earths than Ca. Oxygen doping on the Br site should also be tried.

K_2CoF_4

The compound K_2CoF_4 crystallizes in the space group I 4/mmm (139), also in a tetragonal body centered structure (see Fig.3). The Co atoms are positioned in layers together with a square network of F atoms. There is in addition F atoms in apical positions, in a way that is very similar to that of the oxygen positions in the cuprate

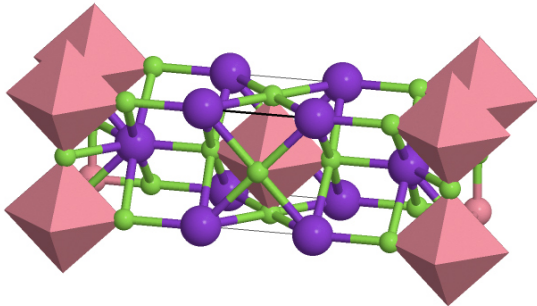


FIG. 3: (Color) Crystal structure of K_2CoF_4 . The K, Co and F atoms are shown in purple, pink and green, respectively [3]. The F atoms form octahedral cages (marked in pink) which surround the Co atoms.

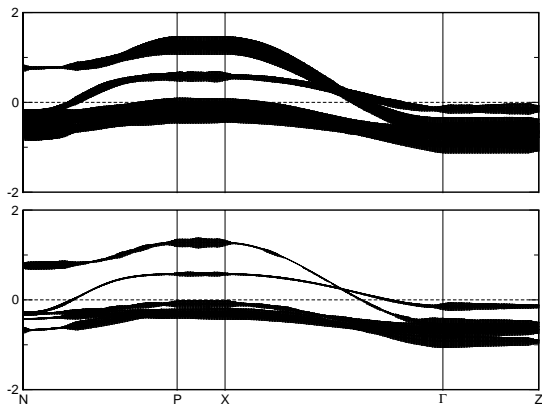


FIG. 4: Electronic structure of the normal state of K_2CoF_4 . The upper panel shows the d-projected bands and the lower panel the p-projected bands, in a fat-band representation where the amount of d- or p wave character is represented by the thickness of the bands. The Fermi level is at zero and is marked by a horizontal dashed line.

superconductors. The Co atom is in a +2 state in this compound.

The electronic structure is shown in Fig.4 and is found to be very similar to that of the cuprates. The wave-function characters of the two bands that cut E_F and have cosine like dispersion, are mainly composed of Co d (e_g) and F p_x and p_y orbitals. The lowest band also has some admixture of d_{xz} and d_{yz} orbitals. Electron or hole-doping of this material may be a possible route towards finding new high-temperature superconductors. In this search it is of-course necessary to consider other halides than F and other Group IX elements than Co. Oxygen doping for F should also be tried.

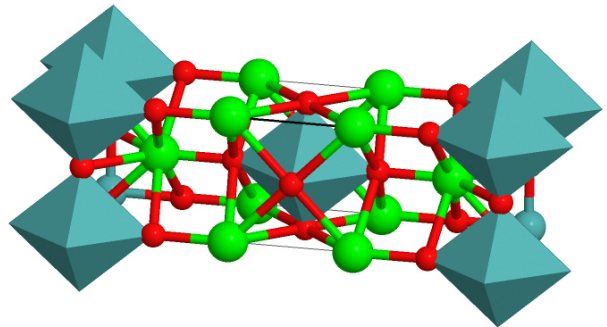


FIG. 5: (Color) Crystal structure of $\text{Sr}_2(\text{MoO}_4)$. The Sr, Mo and O atoms are shown in green, grayish blue and red, respectively [3]. The O atoms form octahedral cages (marked in grayish blue) which surround the Cu atoms.

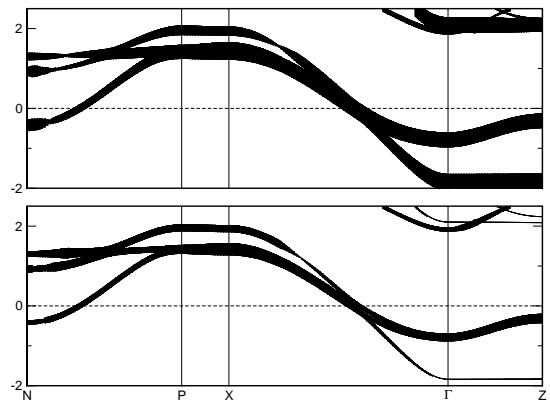


FIG. 6: Electronic structure of the normal state of $\text{Sr}_2(\text{MoO}_4)$. The upper panel shows the d-projected bands and the lower panel the p-projected bands, in a fat-band representation where the amount of d- or p wave character is represented by the thickness of the bands. The Fermi level is at zero and is marked by a horizontal dashed line.

$\text{Sr}_2(\text{MoO}_4)$

The compound $\text{Sr}_2(\text{MoO}_4)$ crystallizes in the space group $I4/mmm$ (139), also in a tetragonal body centered structure (see Fig.5). The Mo atoms are positioned in layers together with a square network of O atoms. There is in addition O atoms in apical positions, and the crystal structure is indeed the same as that of La_2CuO_4 , with Mo taking the place of the Cu atoms. The Mo atom is in a +4 state in this compound.

The electronic structure is shown in Fig.6 and we note that the three bands that cross E_F have a cosine like

dispersion, where the upper band has mainly Mo $d_{x^2-y^2}$ character hybridized with O p_x and p_y orbitals. The two lower bands have mainly Mo d_{xz} and Mo d_{yz} character that hybridize with O p_z states. The hybridization between the Mo d-states and ligand p-states is stronger than for K_2CoF_4 , as is clear when comparing Fig.4 and Fig.6. Electron or hole-doping of this material may be a possible route towards finding new high-temperature superconductors. In this search it is of-course necessary to consider other alkali-earths than Sr and other Group VI elements than Mo.

$Sr_4V_3O_{10}$

The compound $Sr_4V_3O_{10}$ crystallizes in the space group I 4/mmm (139), also in a tetragonal body centered structure (see Fig.7). The V atoms are located in layers with each V atom in the center of a octahedron which is built up of O atoms. The V atom is in a 4+ state in this compound which means that it is the electron-hole symmetric counterpart of a Cu atom in a 2+ configuration.

The electronic structure is similar to that of the cuprates with a single hybridized band along the P-N direction of the Brillouin-zone, that crosses E_F . Along the Γ -X direction, three bands cross E_F . The bands around E_F are composed of V d orbitals that hybridize with O p orbitals. Electron or hole-doping of this material may be a possible route towards finding new high-temperature superconductors. In this search it is of-course necessary to consider other alkali-earths than Sr and other Group V elements than vanadium.

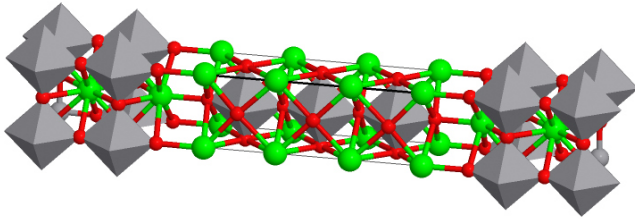


FIG. 7: (Color) Crystal structure of $Sr_4V_3O_{10}$. The Sr, V and O atoms are shown in green, gray and red, respectively [3]. Octahedra (marked in gray) built up of O atoms surround each V atom.

We report the completion of the calculation of almost all known inorganic compounds, which we combine with a data-filtering approach to identify new candidate materials for high-temperature superconductivity. Criteria

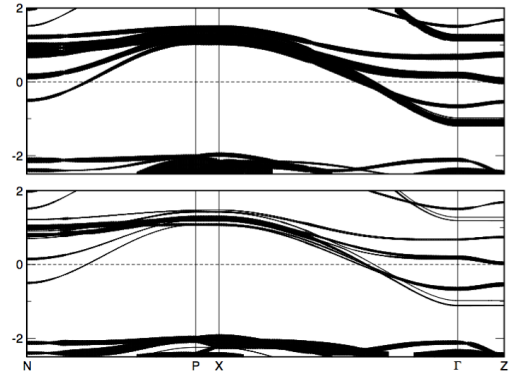


FIG. 8: Electronic structure of the normal state of $Sr_4V_3O_{10}$. The upper panel shows the d-projected bands and the lower panel the p-projected bands, in a fat-band representation where the amount of d- or p wave character is represented by the thickness of the bands. The Fermi level is at zero and is marked by a horizontal dashed line.

involving known properties of the normal state of the cuprate superconductors was used in the filtering process. There is one more conspicuous property of the known cuprate superconductors, namely the strong anti-ferromagnetic inter-atomic exchange interaction between Cu atoms, which is caused by a superexchange mechanism. Since it is unknown if or how this influences the superconductivity we did not use this property as a filtering criterion. Several of the discussed materials are, however, likely to be spin-polarized, but to allow for a larger group of possible new superconductors we did not use spin-polarization as a criterion in the data-filtering process. Instead we used electronic structures from spin-degenerate calculations. If spin-polarization would occur for some of the discussed materials, it is likely to not change the characteristic electronic structure, with the cosine like band that cuts E_F . Experience with the cuprates show this.

It is not unlikely that the materials presented here as candidates for high temperature superconductivity have an electronic structure that is best described from a theory that includes electron-correlation effects somewhat more accurately than that given by the LDA. A natural extension of our work is hence to use dynamical mean field theory to address this issue, and such studies are indeed underway. It is however important to point out that the characteristics of the electronic structure we have used in our filtering approach is a feature which for the cuprate superconductors is in some sense independent of the level of electron correlation. Namely, the high T_C cuprates are all doped in such a way that they in the normal state have an electronic structure which coincides with the filtering criterion used here.

Combining an accurate data-base of the electronic structure with efficient data-filtering protocols to identify new materials, can of course be adapted also for the new class of FeAs based superconductors, albeit, with different filtering criteria than used above. In addition, other properties like thermo electricity, solid state lubrication, new permanent magnets and materials relevant for renewable energy technology are other examples where the described methodology for finding new materials may be applied.

We acknowledge support from the Swedish Research Council (VR), Göran Gustafssons Stiftelse, Swedish Foundation for Strategic Research (SSF), eSSSENCE, and the Swedish National Allocations Committee (SNIC/SNAC). O.E. also acknowledges support from ERC (project 247062 - ASD) and the KAW foundation. We thank Oscar Granäs for helpful discussion regarding the implementation of fat-bands. The authors have contributed equally to this work. Critical reading of Dr.L.Kurland is highly appreciated.

* Electronic address: mattias@physics.uu.se

† Electronic address: olle.eriksson@physics.uu.se

- [1] P. Hohenberg and W. Kohn, "Inhomogeneous electron gas", Phys. Rev. **136**, B864-B871(1964); W. Kohn and L.J.Sham, "Self-consistent equations including exchange and correlation effects", Phys. Rev. **140**, A1133A1138 (1965).
- [2] J. O. Sofo, A. S. Chaudhari, and G. D. Barber, "Graphane: A two-dimensional hydrocarbon", Phys. Rev. B **75**, 153401-4 (2007).
- [3] G. Bergerhoff and I. D.Brown, in Crystallographic Databases, F. H. Allen et al. (Hrsg.) Chester, International Union of Crystallography, (1987). The figures were generated using ICSD Web (<http://icsd.fz-karlsruhe.de/icsd>) using version 2.1.0.
- [4] Venter, J. Craig; Adams, Mark D.; Myers, Eugene W.; et al., "The sequence of the human genome" Science **291** 13041351 (2001).
- [5] Lander, E.S.; Linton, L.M.; Birren, B.; Nusbaum, C.; Zody, M.C.; Baldwin, J.; Devon, K.; Dewar, K. et al., "Initial sequencing and analysis of the human genome", Nature **409** 860921, (2001).
- [6] C.Ortiz, O.Eriksson, and M.Klintenberg, "Data mining and accelerated electronic structure theory as a tool in the search for new functional materials", Computational Materials Science **44**, 1042-1049 (2009).
- [7] M. Klintenberg, arXiv:1007.4838.
- [8] For the most recent description see: J.M.Wills, M.Alouani, P.Andersson, A.Delin, O.Eriksson, A.Grechnev, "Full-potential electronic structure method, energy and force calculations with density functional and dynamical mean field theory" (Springer Series in Solid-State Sciences, Volume 167, 2010).
- [9] H.K. Onnes, "Further experiments with liquid helium D - On the change of the electrical resistance of pure metals at very low temperatures, etc V The disappearance of the resistance of mercury", Proceedings of the Koninklijke Akademie van Wetenschappen te Amsterdam **14**, 113-115 (1911).
- [10] Bednorz, G. and K. Muller, "Possible high- T_C superconductivity in the Ba-La-O system", Z. Phys. B: Condens. Matter **64**, 189-193 (1986).
- [11] Wu, M., J. Ashburn, C. Torng, G. Peng, F. Szofran, P. Hor, and C. Chu, "Superconductivity at 93 K in a new mixed-phase Y-Ba-Cu-O compound system at ambient pressure", Phys. Rev. Lett. **58**, 908-910 (1987).
- [12] Ito, T., H. Takagi, T. Ido, S. Ishibashi, and S. Uchida, "Normal-state conductivity between CuO₂ planes in copper-oxide superconductors", Nature **350**, 596-598 (1991).
- [13] C. W. Chu, L. Gao, F. Chen, et al., "Superconductivity above 150 K in HgBa₂Ca₂Cu₃O_{8+δ} at high pressures", Nature **365** 323-325 (1993).
- [14] L. Gao, Y. Y. Xue, F. Chen, Q. Xiong, R. L. Meng, D. Ramirez, C. W. Chu, J. H. Eggert, and H. K. Mao, "Superconductivity up to 164 K in HgBa₂Ca_{m-1}Cu_mO_{2m+2+δ} (m=1, 2, and 3) under quasi-hydrostatic pressures", Phys. Rev. B **50** 42604263 (1994).
- [15] M.R.Norman, "The challenge of unconventional superconductivity", Science **332**, 196-200 (2011).
- [16] J.P.Attfield, "Chemistry and high temperature superconductivity", J. of Materials Chemistry **21**, 4756-4764 (2011).
- [17] V.P.Mineev, "Recent developments in unconventional superconductivity theory", J. Low. Temp. Phys. **158**, 615-630 (2010).
- [18] M.A.Katner, "Magnetic, transport, and optical properties of monolayer copper oxides", Rev. Mod. Phys. **70**, 897-928 (1998).
- [19] E.Dagotto, "Correlated electrons in high-temperature superconductors", Rev. Mod. Phys. **66**, 763-840 (1994).
- [20] O. Eriksson, "Electronic structure calculations of phase stability: cohesive and elastic properties" in *Encyclopedia of Materials: Science and technology*, Elsevier, (2006) p1-11.
- [21] P.W.Andersen, "The resonating valence bond state in La₂CuO₄ and superconductivity", Science **235** 1196 - 1198 (1987).
- [22] S.R.White, D.J.Scalapino, R.L.Sugar, N.Bickers, and R.Scalettar, "Attractive and repulsive pairing interaction vertices for the two-dimensional Hubbard model", Phys. Rev. B **39**, 839-842 (1989).
- [23] P. Monthoux, A. V. Balatsky and D. Pines, "Toward a theory of high-temperature superconductivity in the antiferromagnetically correlated cuprate oxides", Phys. Rev. Lett. **67** 3448-3451 (1991).
- [24] F.C.Zhang and T.M.Rice, "Effective Hamiltonian for the superconducting Cu oxides", Phys. Rev. B **37**, 3759-3761 (1988).
- [25] R.J.Gooding, "Skyrmion ground states in the presence of localizing potentials in weakly doped CuO₂ planes", Phys. Rev. Lett. **66**, 2266-2269 (1991).
- [26] W.E.Pickett, H.Krakauer, R.E.Cohen, and D.J.Singh, "Fermi surfaces, fermi liquids and high-temperature superconductors", Science **255**, 46-54 (1992).
- [27] E.Pavarini, I.Dasgupta, T.Saha-Dasgupta, O.Jepsen, and O.K.Andersen, "Band-structure trend in hole-doped cuprates and correlation with T_{cmax} ", Phys. Rev. Lett. **87**, 47003-4 (2001).
- [28] J. Chaloupka and G. Khaliullin, "Orbital order and possi-

- ble superconductivity in $\text{LaNiO}_3/\text{LaMO}_3$ superlattices", *Phys. Rev. Lett.* **100**, 016404-4 (2008).
- [29] P. Hansmann, Xiaoping Yang, A. Toschi, G. Khaliullin, O.K. Andersen, K Held, "Turning a nickelate Fermi surface into a cuprate-like one through heterostructuring", *Phys. Rev. Lett.* **103**, 016401-4 (2009).

Supplementary information

The table below shows compound name, space group, space group number, bravais lattice and ICSD reference number. Using the ICSD web-site [1], and the ICSD reference number, allows the reader to generate pictures of the crystal structure.

In the fat-band representation the thickness of the band corresponds to the amount of s -, p - or d -character of the band. This is calculated as follows. Let $n(\mathbf{k})$ be the occupation at \mathbf{k} given by

$$n(\mathbf{k}) = \text{Tr}(O(\mathbf{k})\rho(\mathbf{k}))$$

where $O(\mathbf{k})$ and $\rho(\mathbf{k})$ is the overlap and density, respectively. The fatness f_l for eigenvalue ν can then be calculated using

$$f_l = \frac{\text{Tr}(O(\mathbf{k})\rho^{\nu_l}(\mathbf{k}))}{\text{Tr}(O(\mathbf{k})\rho(\mathbf{k}))}$$

where element ij of the density matrix is given in terms of weights (w) and eigenvectors (Z) by:

$$\rho_{ij}(\mathbf{k}) = \sum_{\nu} w_{\nu,\mathbf{k}} Z_i(\mathbf{k}, \nu) Z_j^{\dagger}(\mathbf{k}, \nu)$$

$$\rho_{ij}^{\nu_l}(\mathbf{k}) = w_{\nu_l,\mathbf{k}} Z_i(\mathbf{k}, \nu_l) Z_j^{\dagger}(\mathbf{k}, \nu_l)$$

$\sum_l f_l$ sums up to one electron and l runs over the complete basis. Note that in the figures below the Fermi level is at zero. Also, in the band plots we make a projection on atomic and l-resolved fat bands.

-
- [1] G. Bergerhoff and I. D. Brown, in Crystallographic Databases, F. H. Allen et al. (Hrsg.) Chester, International Union of Crystallography, (1987). The figures were generated using ICSD Web (<http://icsd.fiz-karlsruhe.de/icsd>) using version 2.1.0.

Material	Space group	(#)	Bravais lattice	ICSD #
AuCuZn ₂	F m -3 m	(225)	cubic face-centred	150571
AgAuZn ₂	F m -3 m	(225)	cubic face-centred	604792
CuNi ₂ Sb	F m -3 m	(225)	cubic face-centred	53320
CuNi ₂ Sn	F m -3 m	(225)	cubic face-centred	103068
ErPt ₂	F d -3 m S	(227)	cubic face-centred	103287
EuPt ₂	F d -3 m S	(227)	cubic face-centred	103430
HoPt ₂	F d -3 m S	(227)	cubic face-centred	104441
NaPt ₂	F d -3 m S	(227)	cubic face-centred	644945
BaPt ₂	F d -3 m S	(227)	cubic face-centred	616039
CuSe	P 63/m m c	(194)	hexagonal primitive	240
KAuTe	P 63/m m c	(194)	hexagonal primitive	40165
RbAuTe	P 63/m m c	(194)	hexagonal primitive	75026
CdInGaS ₄	P -3 m 1	(164)	hexagonal primitive	20785
ZrNCl	P -3 m 1	(164)	hexagonal primitive	25506
KCuSe	P 63/m m c	(194)	hexagonal primitive	12157
KCuTe	P 63/m m c	(194)	hexagonal primitive	12158
Li ₂ ZnGe	P -3 m 1	(164)	hexagonal primitive	53678
Li ₂ ZnSi	P -3 m 1	(164)	hexagonal primitive	16221
AuYO ₂	P 63/m m c	(194)	hexagonal primitive	95675
AgAlO ₂	P 63/m m c	(194)	hexagonal primitive	300020
CuBr	P 63 m c	(186)	hexagonal primitive	30092
Ca ₂ CuZn ₂ P ₃	P 63/m m c	(194)	hexagonal primitive	89517
Al ₅ C ₃ N	P 63 m c	(186)	hexagonal primitive	26859
Ca ₃ Cu ₂ Zn ₂ P ₄	P -3 m 1	(164)	hexagonal primitive	89515
Eu ₃ Cu ₂ Zn ₂ P ₄	P -3 m 1	(164)	hexagonal primitive	89516
Cu ₄ (S ₂) ₂ (CuS) ₂	P 63/m m c	(194)	hexagonal primitive	26968

Material	Space group	(#)	Bravais lattice	ICSD #
LaKPdO ₃	C 1 2/m 1	(12)	monoclinic base-centred	417108
BaY ₂ F ₈	C 1 2/m 1	(12)	monoclinic base-centred	74359
AgCuS	C m c m	(63)	orthorhombic base-centred	30233
LaSeTe ₂	C m c m	(63)	orthorhombic base-centred	413171
NbS ₂	C m 2 m	(38)	orthorhombic base-centred	67443
BaNiY ₂ O ₅	I m m m	(71)	orthorhombic body-centred	68795
RuOCl ₂	I m m m	(71)	orthorhombic body-centred	83883
Bi ₂ (CO ₃)O ₂	I m m 2	(44)	orthorhombic body-centred	94740
Al ₂ Ba ₃ Ge ₂	I m m m	(71)	orthorhombic body-centred	52612
Ba ₃ Al ₂ Si ₂	I m m m	(71)	orthorhombic body-centred	100128
Ba ₃ Al ₂ Sn ₂	I m m m	(71)	orthorhombic body-centred	9565
NbSe ₂	F m 2 m	(42)	orthorhombic face-centred	71339
TaS ₂	F m 2 m	(42)	orthorhombic face-centred	280988
TaSe ₂	F 2 m m	(42)	orthorhombic face-centred	67651
TaSe ₂	F m 2 m	(42)	orthorhombic face-centred	72198
Tl ₂ Ba ₂ CuO ₆	F m m m	(69)	orthorhombic face-centred	41569
TiNCl	P m m n S	(59)	orthorhombic primitive	27396
Pb ₂ Ba ₂ YCuCu ₂ O ₈	P 2 21 2	(17)	orthorhombic primitive	66088
Pb ₂ Sr ₂ YCu ₃ O ₈	P 2 21 2	(17)	orthorhombic primitive	66587
YBa ₂ Cu ₃ O _{6.5}	P m m m	(47)	orthorhombic primitive	75697
YBa ₂ Cu ₃ O _{6.5}	P m m m	(47)	orthorhombic primitive	96016
EuBa ₂ Cu ₃ O ₇	P m m m	(47)	orthorhombic primitive	81171
Ba ₂ GdCu ₃ O ₇	P m m m	(47)	orthorhombic primitive	56514
HoBa ₂ Cu ₃ O ₇	P m m m	(47)	orthorhombic primitive	68044
LaBa ₂ Cu ₃ O ₇	P m m m	(47)	orthorhombic primitive	81167
NdBa ₂ Cu ₃ O ₇	P m m m	(47)	orthorhombic primitive	81169
PrBa ₂ Cu ₃ O ₇	P m m m	(47)	orthorhombic primitive	81168
SmBa ₂ Cu ₃ O ₇	P m m m	(47)	orthorhombic primitive	71705
Ba ₂ YCu ₃ O ₇	P m m m	(47)	orthorhombic primitive	202770
Ba ₂ YCu ₃ O ₇	P m m m	(47)	orthorhombic primitive	77737
LaBa ₂ Cu ₃ O ₈	P m m m	(47)	orthorhombic primitive	85291
Na ₃ Cu ₄ S ₄	P b a m	(55)	orthorhombic primitive	10004
Sr ₄ V ₃ O ₁₀	I 4/m m m	(139)	tetragonal body-centred	73698
MoB	I 41/a m d S	(141)	tetragonal body-centred	24280
WB	I 41/a m d S	(141)	tetragonal body-centred	24281
Yb(AgS ₂)	I 41 m d	(109)	tetragonal body-centred	27091
LaI ₂	I 4/m m m	(139)	tetragonal body-centred	202452
SmCu ₂ Si ₂	I 4/m m m	(139)	tetragonal body-centred	106843
TbCu ₂ Si ₂	I 4/m m m	(139)	tetragonal body-centred	106844
Cu ₂ TmSi ₂	I 4/m m m	(139)	tetragonal body-centred	53349
Cu ₂ YSi ₂	I 4/m m m	(139)	tetragonal body-centred	23551
Li ₂ PdH ₂	I 4/m m m	(139)	tetragonal body-centred	108534
Na ₂ PdH ₂	I 4/m m m	(139)	tetragonal body-centred	68071
(Cu ₂ S ₂)(Sr ₂ NiO ₂)	I 4/m m m	(139)	tetragonal body-centred	88424
Ca ₂ (CuBr ₂ O ₂)	I 4/m m m	(139)	tetragonal body-centred	1028
Sr ₂ CoO ₂ Br ₂	I 4/m m m	(139)	tetragonal body-centred	151789
CuSr ₂ Br ₂ O ₂	I 4/m m m	(139)	tetragonal body-centred	1178
Ca ₂ (CuCl ₂ O ₂)	I 4/m m m	(139)	tetragonal body-centred	1027
Ca ₂ CuO ₂ Cl ₂	I 4/m m m	(139)	tetragonal body-centred	83117
Sr ₂ CuO ₂ Cl ₂	I 4/m m m	(139)	tetragonal body-centred	4087
Tl ₂ Ba ₂ CaCu ₂ O ₈	I 4/m m m	(139)	tetragonal body-centred	78592
Bi ₂ Sr ₂ CaCu ₂ O ₈	I 4/m m m	(139)	tetragonal body-centred	68188
Ce ₂ BiO ₂	I 4/m m m	(139)	tetragonal body-centred	9099
Ce ₂ SbO ₂	I 4/m m m	(139)	tetragonal body-centred	9100
CePd ₂ Si ₂	I 4/m m m	(139)	tetragonal body-centred	621852
CePt ₂ Si ₂	I 4/m m m	(139)	tetragonal body-centred	52895
Cu ₂ ErGe ₂	I 4/m m m	(139)	tetragonal body-centred	53251
ErCu ₂ Si ₂	I 4/m m m	(139)	tetragonal body-centred	106845
Cu ₂ GdSi ₂	I 4/m m m	(139)	tetragonal body-centred	64825

Material	Space group	(#)	Bravais lattice	ICSD #
Cu ₂ HoGe ₂	I 4/m m m	(139)	tetragonal body-centred	53270
YCu ₂ Ge ₂	I 4/m m m	(139)	tetragonal body-centred	52764
Cu ₂ HoSi ₂	I 4/m m m	(139)	tetragonal body-centred	53289
NdCu ₂ Si ₂	I 4/m m m	(139)	tetragonal body-centred	106842
Eu ₂ (VO ₄)	I 4/m m m	(139)	tetragonal body-centred	89000
K ₂ (NiF ₄)	I 4/m m m	(139)	tetragonal body-centred	15576
K ₂ (NiF ₄)	I 4/m m m	(139)	tetragonal body-centred	631720
Rb ₂ (NiF ₄)	I 4/m m m	(139)	tetragonal body-centred	69682
La ₂ (NiO ₄)	I 4/m m m	(139)	tetragonal body-centred	1179
La ₂ (NiO ₄)	I 4/m m m	(139)	tetragonal body-centred	33536
La ₂ PdO ₄	I 4/m m m	(139)	tetragonal body-centred	40262
Sr ₂ (MoO ₄)	I 4/m m m	(139)	tetragonal body-centred	152123
Sr ₂ (RuO ₄)	I 4/m m m	(139)	tetragonal body-centred	157401
Sr ₂ VO ₄	I 4/m m m	(139)	tetragonal body-centred	72219
Cs ₂ AgF ₄	I 4/m m m	(139)	tetragonal body-centred	16254
K ₂ CoF ₄	I 4/m m m	(139)	tetragonal body-centred	33522
Rb ₂ CoF ₄	I 4/m m m	(139)	tetragonal body-centred	69683
Gd ₂ (CuO ₄)	I 4/m m m	(139)	tetragonal body-centred	41844
In ₂ CuO ₄	I 4/m m m	(139)	tetragonal body-centred	39475
La ₂ (CuO ₄)	I 4/m m m	(139)	tetragonal body-centred	41643
Ba ₂ CoF ₆	I 4/m m m	(139)	tetragonal body-centred	21057
Ba ₂ NiF ₆	I 4/m m m	(139)	tetragonal body-centred	21056
Ba ₂ (ZnF ₆)	I 4/m m m	(139)	tetragonal body-centred	21054
(Cu ₂ S ₂)(Sr ₂ CuO ₂)	I 4/m m m	(139)	tetragonal body-centred	88423
Ba ₂ Cu ₃ O ₄ Br ₂	I 4/m m m	(139)	tetragonal body-centred	36128
Ba ₂ Cu ₃ O ₄ Cl ₂	I 4/m m m	(139)	tetragonal body-centred	355
Ca ₃ Cu ₂ O ₄ Br ₂	I 4/m m m	(139)	tetragonal body-centred	69182
Ca ₃ Cu ₂ O ₄ Cl ₂	I 4/m m m	(139)	tetragonal body-centred	69181
La ₃ Ni ₂ O ₆	I 4/m m m	(139)	tetragonal body-centred	249209
K ₃ Ni ₂ F ₇	I 4/m m m	(139)	tetragonal body-centred	33523
Sr ₃ V ₂ O ₇	I 4/m m m	(139)	tetragonal body-centred	71320
Sr ₃ (V ₂ O ₇)	I 4/m m m	(139)	tetragonal body-centred	71451
K ₃ Co ₂ F ₇	I 4/m m m	(139)	tetragonal body-centred	33524
K ₃ Cu ₂ F ₇	I 4/m m m	(139)	tetragonal body-centred	15373
La ₄ Ni ₃ O ₈	I 4/m m m	(139)	tetragonal body-centred	173372
K ₅ Te ₃	I 4/m	(87)	tetragonal body-centred	96743
CaSmCuO ₃ Cl	P 4/n m m Z	(129)	tetragonal primitive	86428
HgBa ₂ CaCu ₂ O ₆	P 4/m m m	(123)	tetragonal primitive	75725
HgBa ₂ CaCu ₂ O ₆	P 4/m m m	(123)	tetragonal primitive	83087
TlYBa ₂ Cu ₂ O ₇	P 4/m m m	(123)	tetragonal primitive	74163
TlCaSr ₂ Cu ₂ O ₇	P 4/m m m	(123)	tetragonal primitive	74165
NdBa ₂ Cu ₂ NbO ₈	P 4/m m m	(123)	tetragonal primitive	44255
Sr ₂ CoO ₃ Cl	P 4/n m m Z	(129)	tetragonal primitive	91750
HgBa ₂ CuO ₄	P 4/m m m	(123)	tetragonal primitive	75720
Sr ₂ CuO ₂ (CO ₃)	P 4 21 2	(90)	tetragonal primitive	83096
KCeSe ₄	P 4/n b m Z	(125)	tetragonal primitive	67656
NdLi ₂ Sb ₂	P 4/n m m Z	(129)	tetragonal primitive	36020
HgBa ₂ Ca ₂ Cu ₃ O ₈	P 4/m m m	(123)	tetragonal primitive	75730
HoBa ₂ Cu ₃ O ₆	P 4/m m m	(123)	tetragonal primitive	68047
LuBa ₂ Cu ₃ O ₆	P 4/m m m	(123)	tetragonal primitive	98113
NdBa ₂ Cu ₃ O ₆	P 4/m m m	(123)	tetragonal primitive	83074
Cs(Cu ₄ Se ₃)	P 4/m m m	(123)	tetragonal primitive	75196
KCu ₄ S ₃	P 4/m m m	(123)	tetragonal primitive	23336
KCu ₄ Se ₃	P 4/m m m	(123)	tetragonal primitive	280072

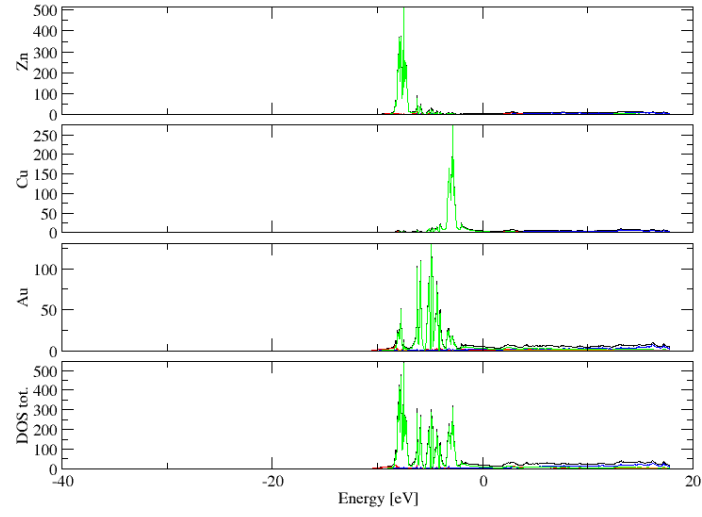


FIG. 1: (Color online) PDOS of AuCuZn₂ (ICSD #150571). The *s*-, *p*- and *d*-projected states are in red, blue and green, respectively. AuCuZn₂ crystallizes in space group $Fm\bar{3}m$ (#225), in a cubic face-centred structure.

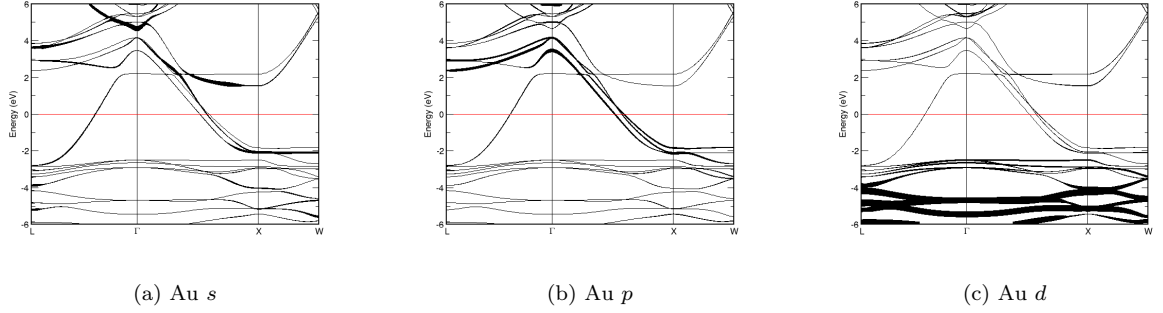


FIG. 2: Fat band representation of Au in AuCuZn₂

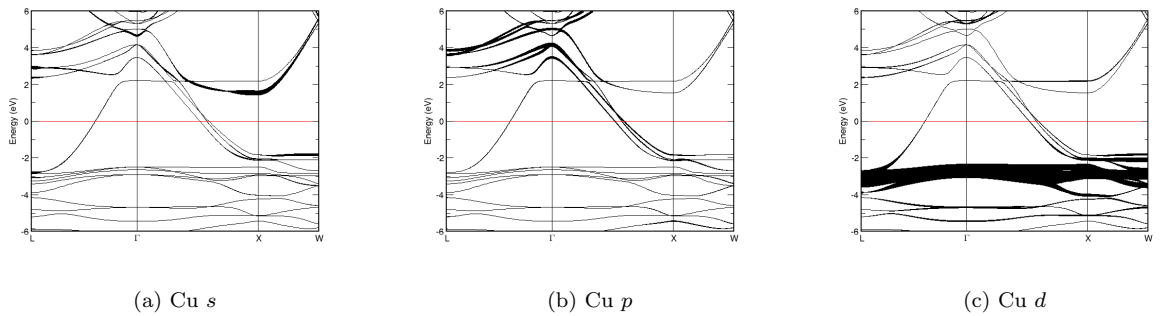


FIG. 3: Fat band representation of Cu in AuCuZn₂

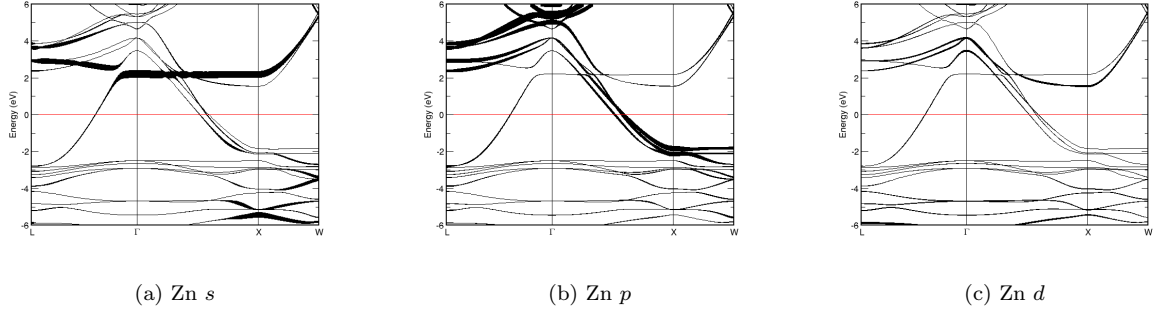


FIG. 4: Fat band representation of Zn in AuCuZn₂

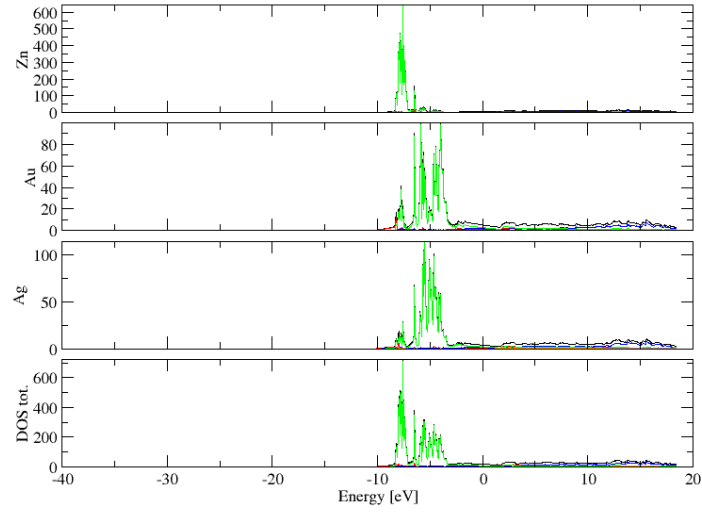


FIG. 5: (Color online) PDOS of AgAuZn₂ (ICSD #604792). The *s*-, *p*- and *d*-projected states are in red, blue and green, respectively. AgAuZn₂ crystallizes in space group Fm-3m (#225), in a cubic face-centred structure.

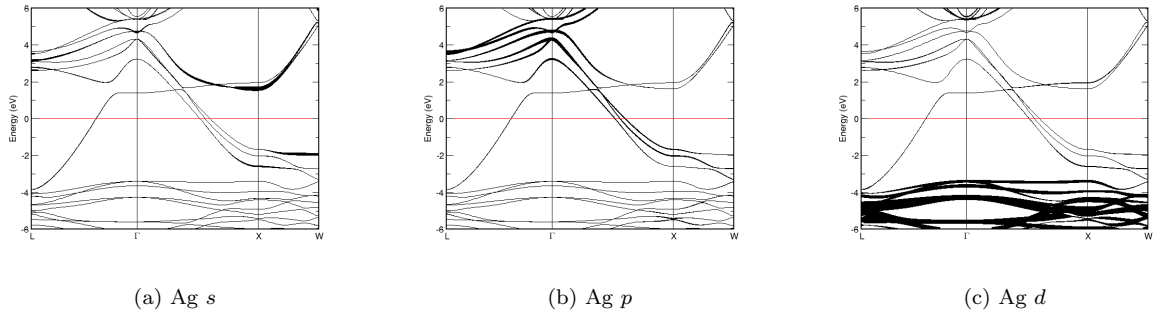


FIG. 6: Fat band representation of Ag in AgAuZn₂

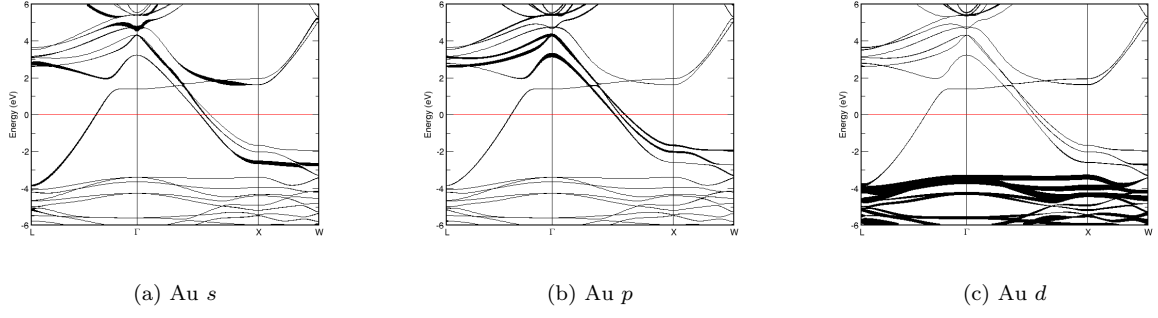


FIG. 7: Fat band representation of Au in AgAuZn₂

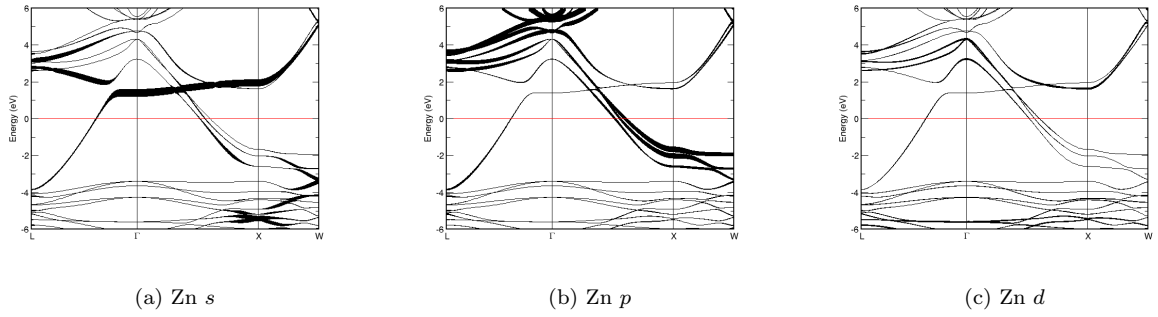


FIG. 8: Fat band representation of Zn in AgAuZn₂

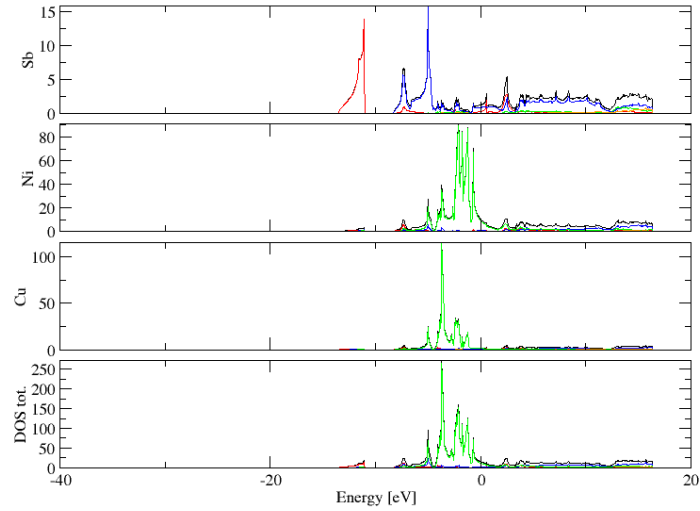


FIG. 9: (Color online) PDOS of CuNi₂Sb (ICSD #53320). The *s*-, *p*- and *d*-projected states are in red, blue and green, respectively. CuNi₂Sb crystallizes in space group *Fm* $\bar{3}$ *m* (#225), in a cubic face-centred structure.

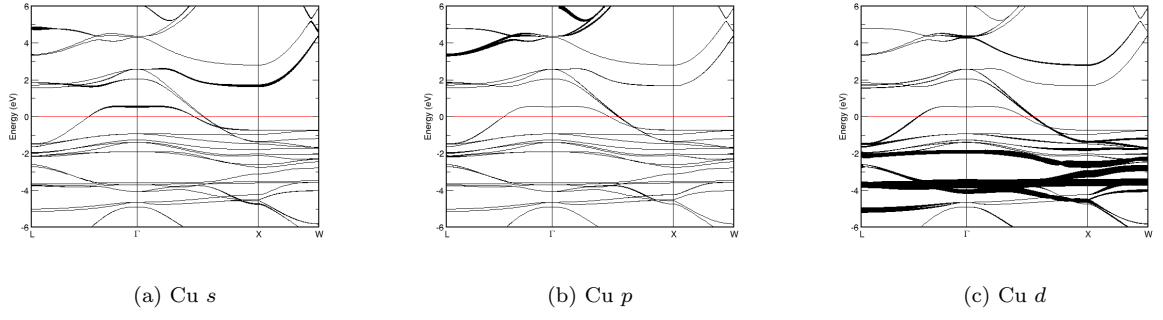


FIG. 10: Fat band representation of Cu in CuNi₂Sb

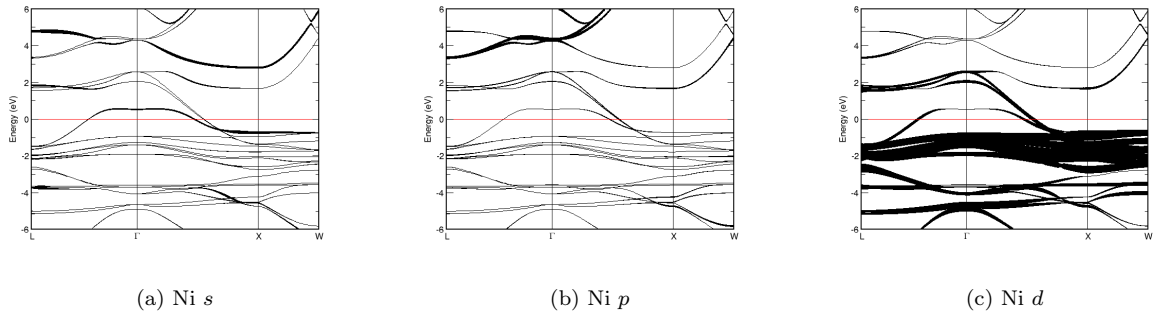


FIG. 11: Fat band representation of Ni in CuNi₂Sb

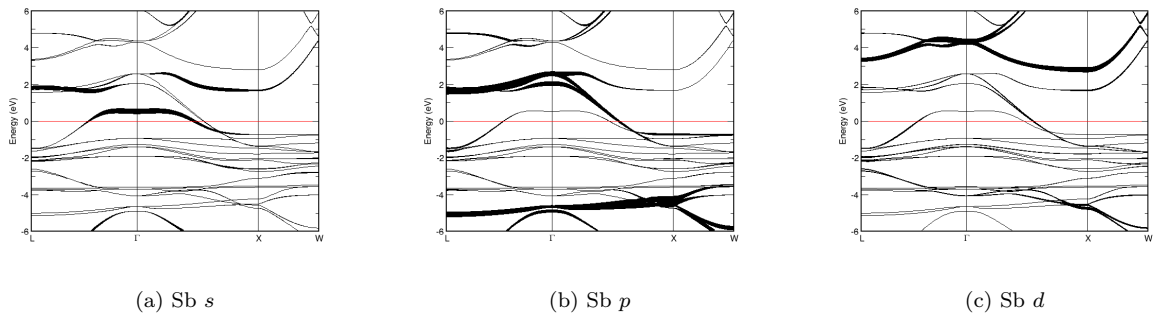


FIG. 12: Fat band representation of Sb in CuNi₂Sb

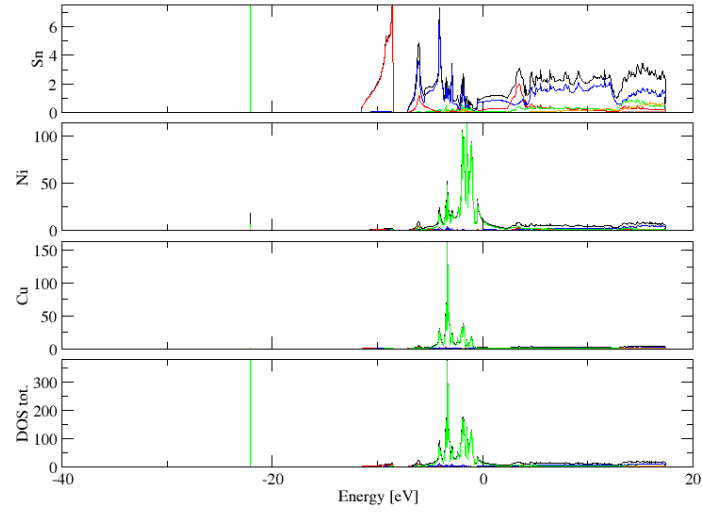


FIG. 13: (Color online) PDOS of CuNi_2Sn (ICSD #103068). The s -, p - and d -projected states are in red, blue and green, respectively. CuNi_2Sn crystallizes in space group $Fm\bar{3}m$ (#225), in a cubic face-centred structure.

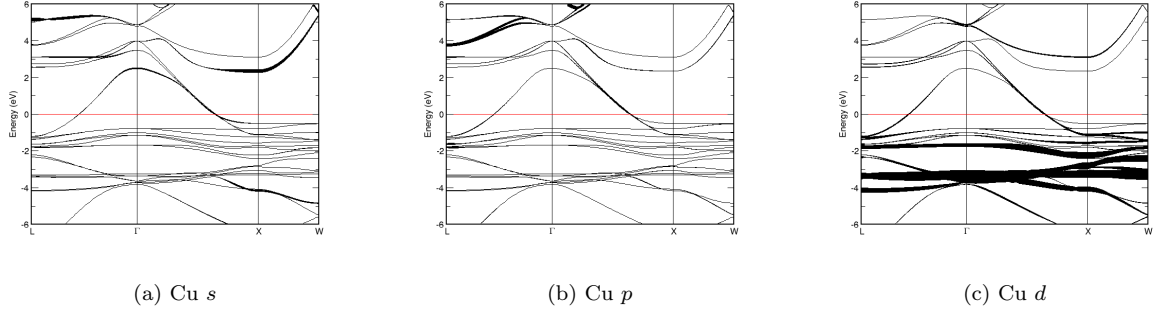


FIG. 14: Fat band representation of Cu in CuNi_2Sn

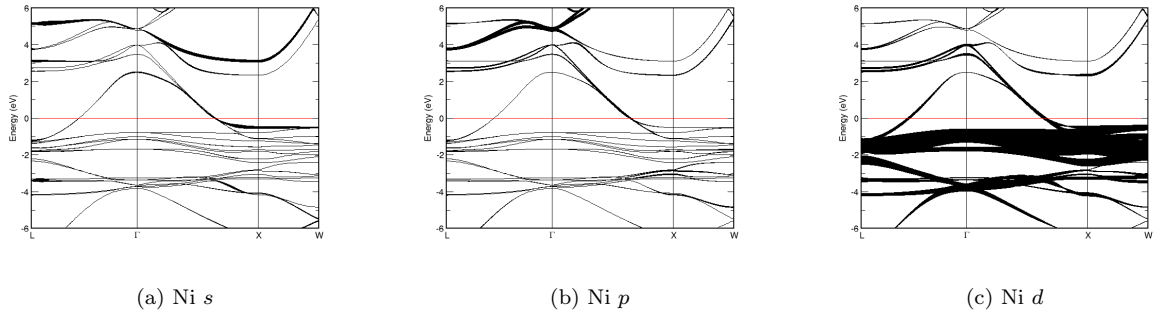


FIG. 15: Fat band representation of Ni in CuNi_2Sn

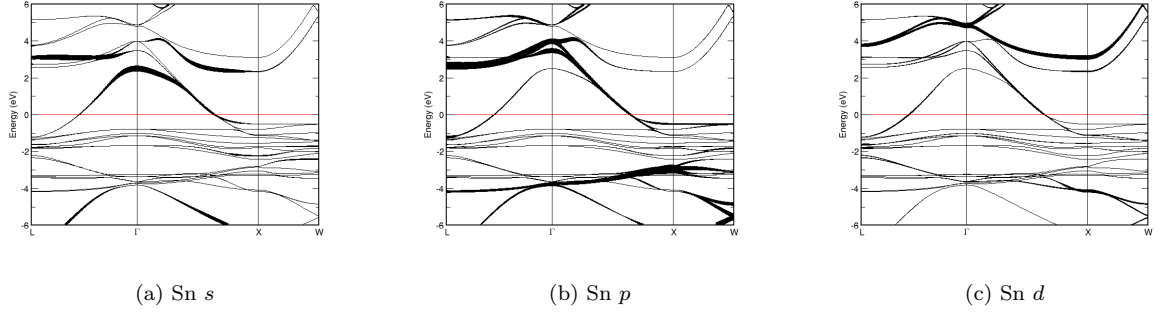


FIG. 16: Fat band representation of Sn in CuNi_2Sn

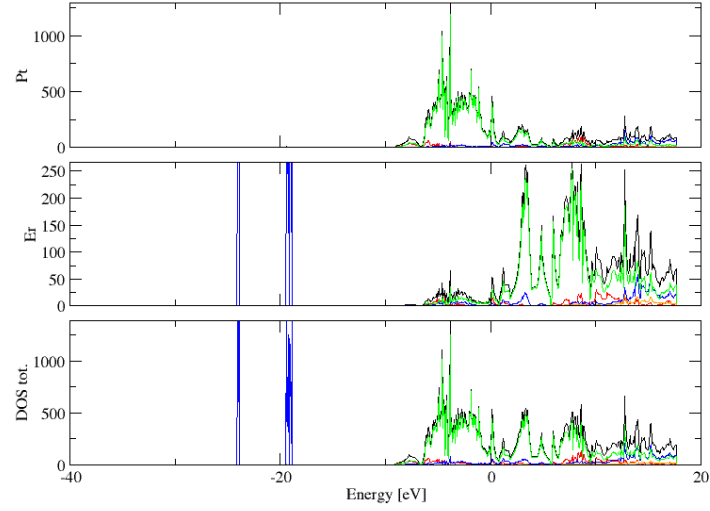
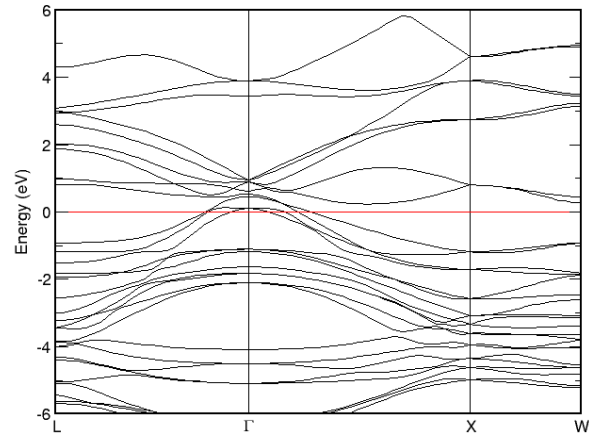


FIG. 17: (Color online) PDOS of ErPt_2 (ICSD #103287). The s -, p - and d -projected states are in red, blue and green, respectively. ErPt_2 crystallizes in space group $Fm\bar{3}m$ (#227), in a cubic face-centred structure.



(a) E vs. k

FIG. 18: Band structure of ErPt_2

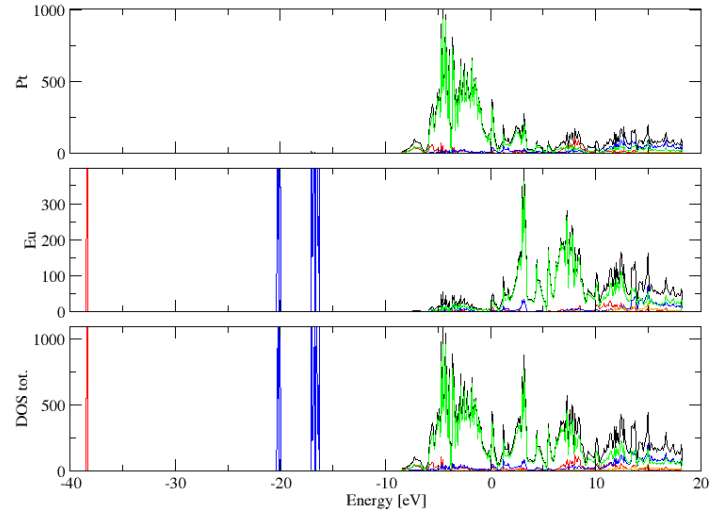
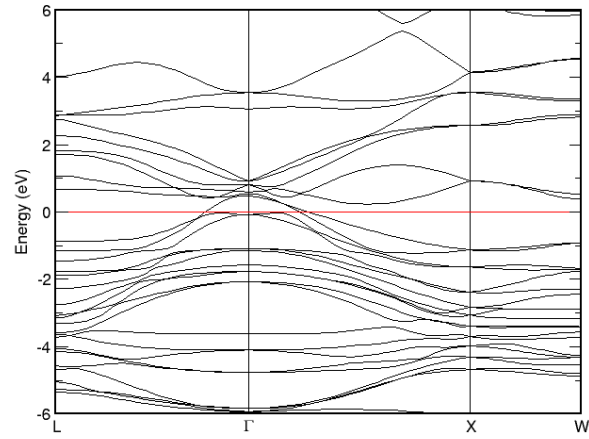


FIG. 19: (Color online) PDOS of EuPt_2 (ICSD #103430). The s -, p - and d -projected states are in red, blue and green, respectively. EuPt_2 crystallizes in space group $F d \bar{3} m S$ (#227), in a cubic face-centred structure.



(a) E vs. k

FIG. 20: Band structure of EuPt_2

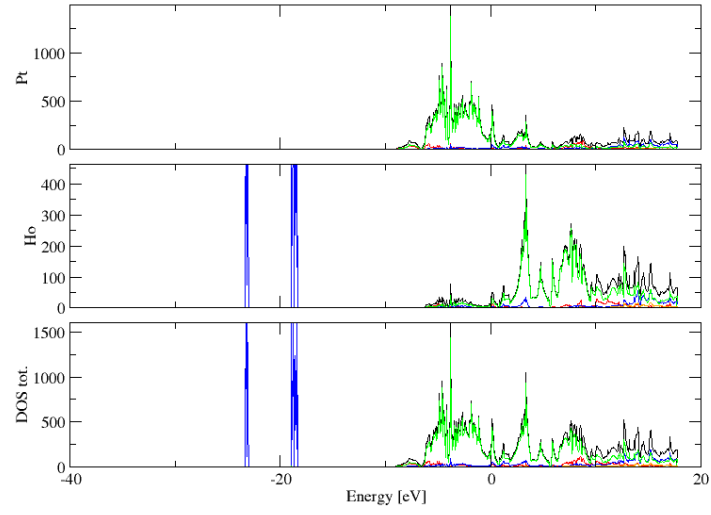
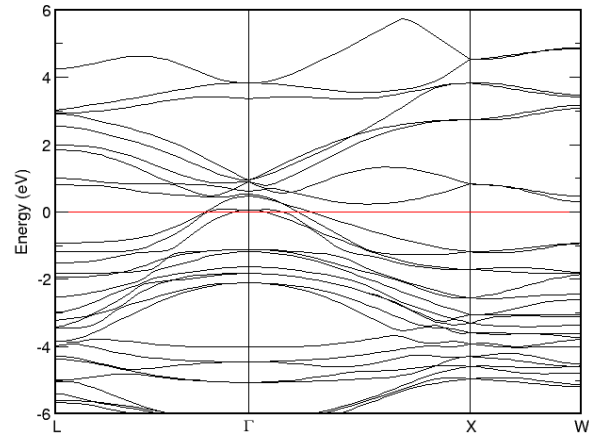


FIG. 21: (Color online) PDOS of HoPt_2 (ICSD #104441). The s -, p - and d -projected states are in red, blue and green, respectively. HoPt_2 crystallizes in space group $F d -3 m S$ (#227), in a cubic face-centred structure.



(a) E vs. k

FIG. 22: Band structure of HoPt_2

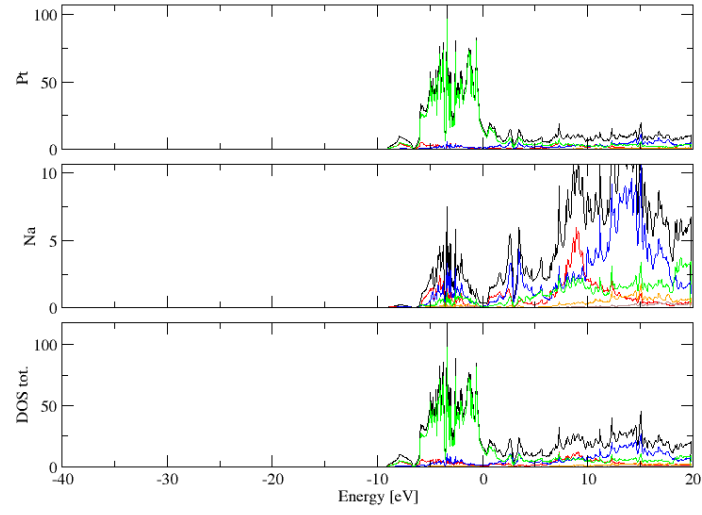


FIG. 23: (Color online) PDOS of NaPt₂ (ICSD #644945). The *s*-, *p*- and *d*-projected states are in red, blue and green, respectively. NaPt₂ crystallizes in space group F d -3 m S (#227), in a cubic face-centred structure.

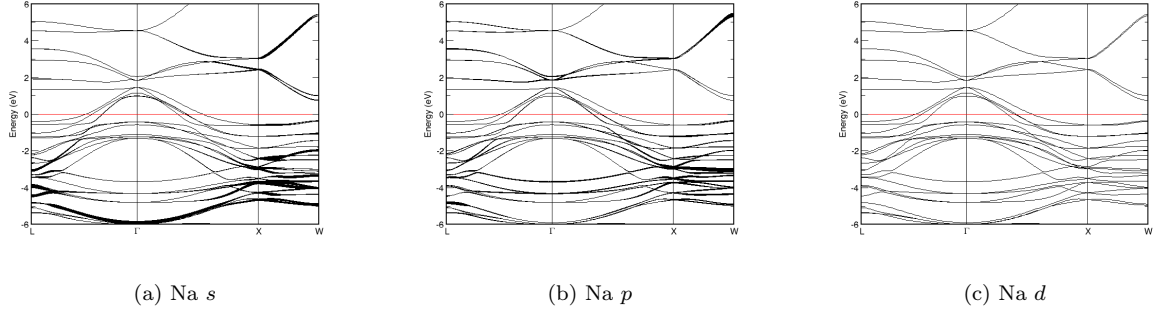


FIG. 24: Fat band representation of Na in NaPt₂

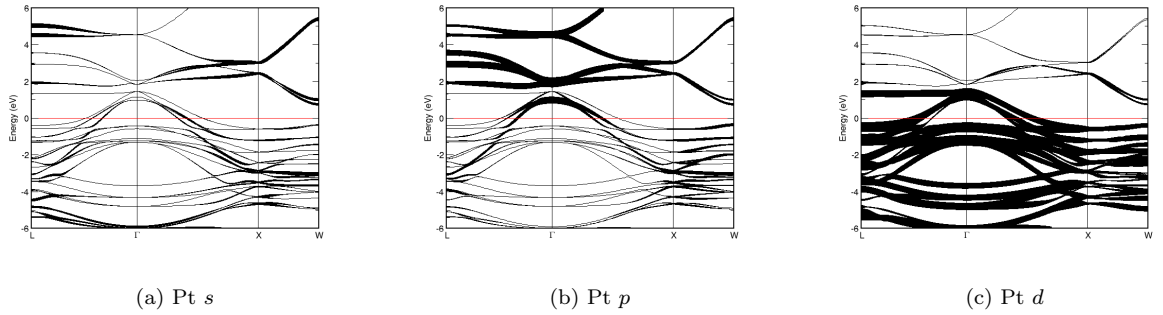


FIG. 25: Fat band representation of Pt in NaPt₂

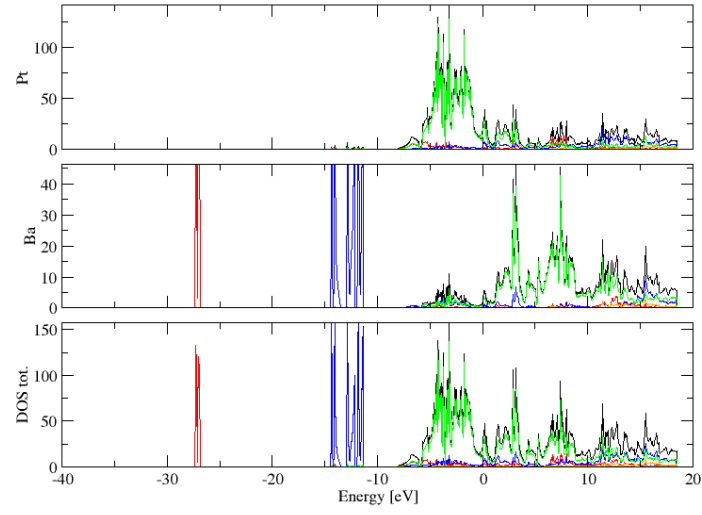


FIG. 26: (Color online) PDOS of BaPt₂ (ICSD #616039). The *s*-, *p*- and *d*-projected states are in red, blue and green, respectively. BaPt₂ crystallizes in space group *F* *d* -3 *m* *S* (#227), in a cubic face-centred structure.

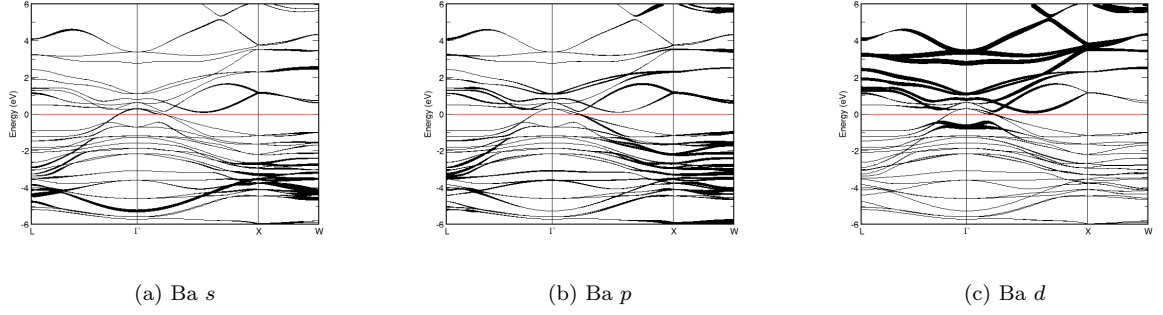


FIG. 27: Fat band representation of Ba in BaPt₂

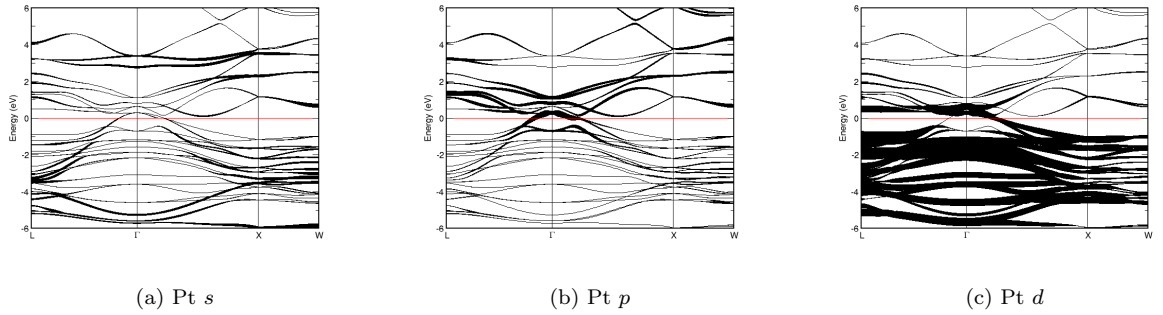


FIG. 28: Fat band representation of Pt in BaPt₂

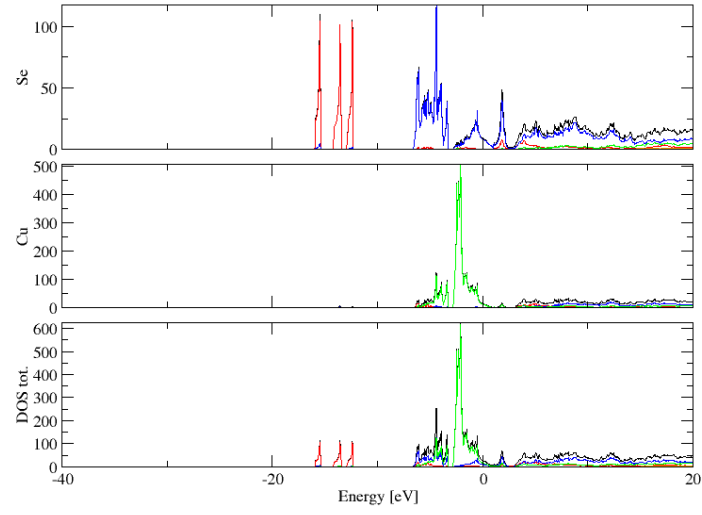


FIG. 29: (Color online) PDOS of CuSe (ICSD #240). The s -, p - and d -projected states are in red, blue and green, respectively. CuSe crystallizes in space group $P 63/m m c$ (#194), in a hexagonal primitive structure.

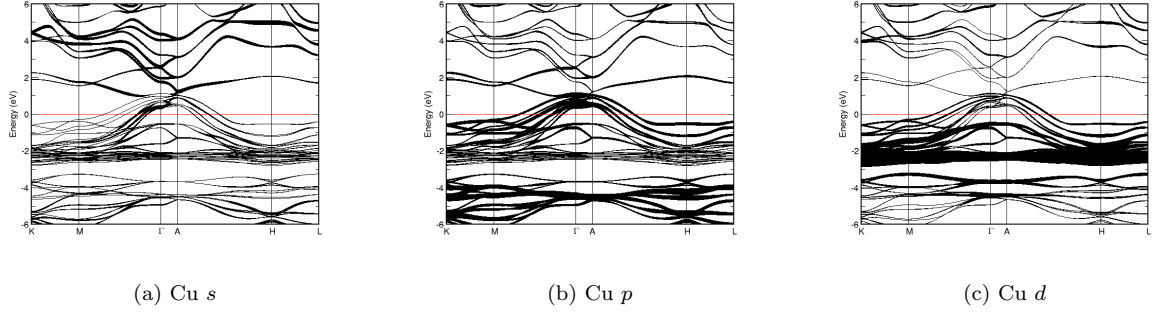


FIG. 30: Fat band representation of Cu in CuSe

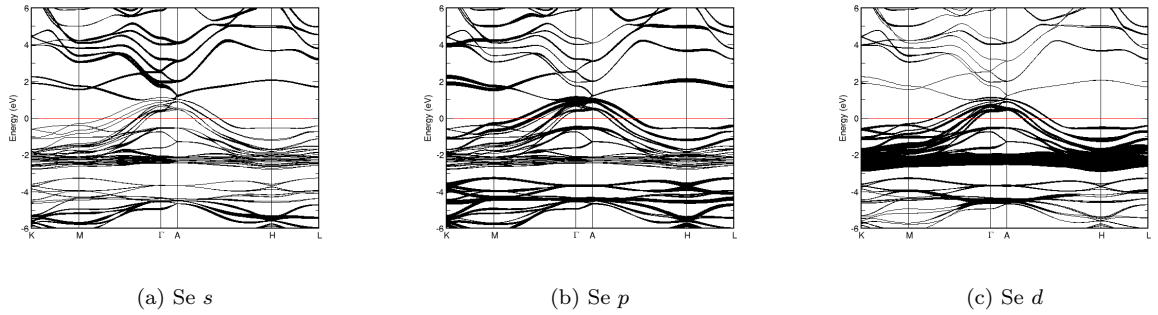


FIG. 31: Fat band representation of Se in CuSe

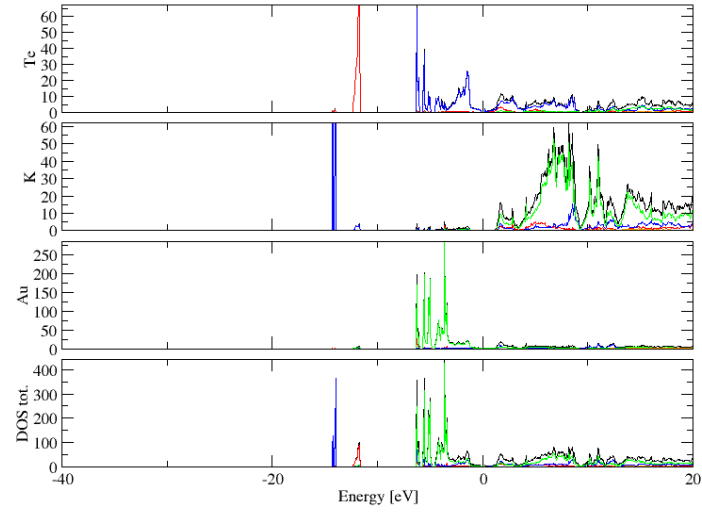


FIG. 32: (Color online) PDOS of KAuTe (ICSD #40165). The s -, p - and d -projected states are in red, blue and green, respectively. KAuTe crystallizes in space group P 63/m m c (#194), in a hexagonal primitive structure.

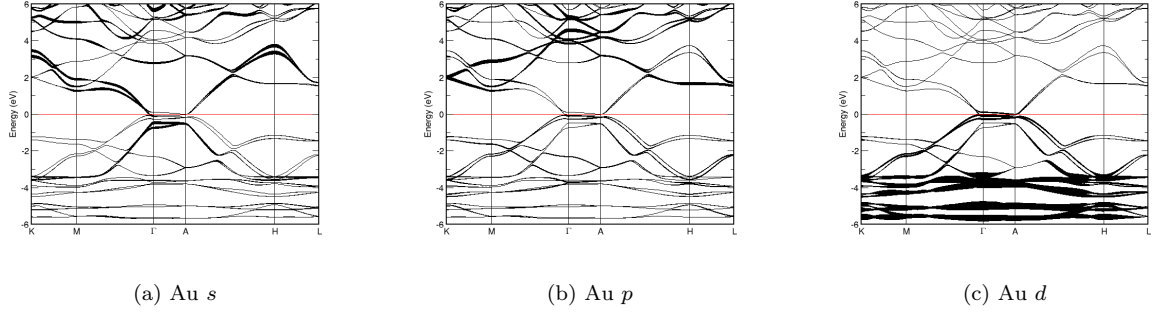


FIG. 33: Fat band representation of Au in KAuTe

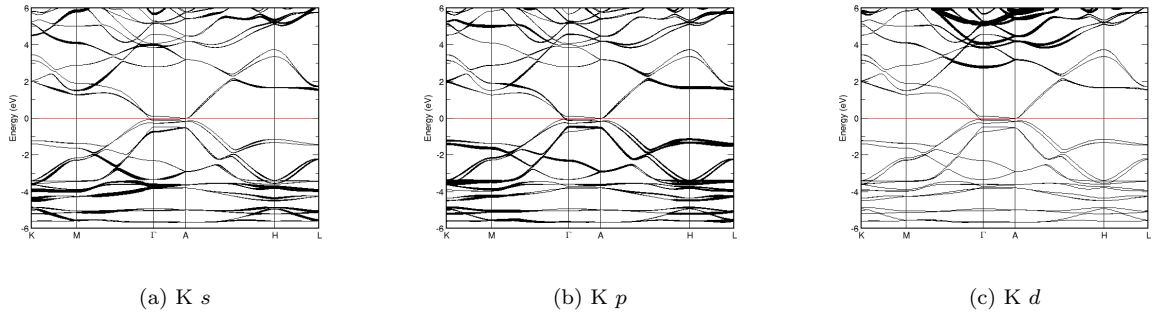


FIG. 34: Fat band representation of K in KAuTe

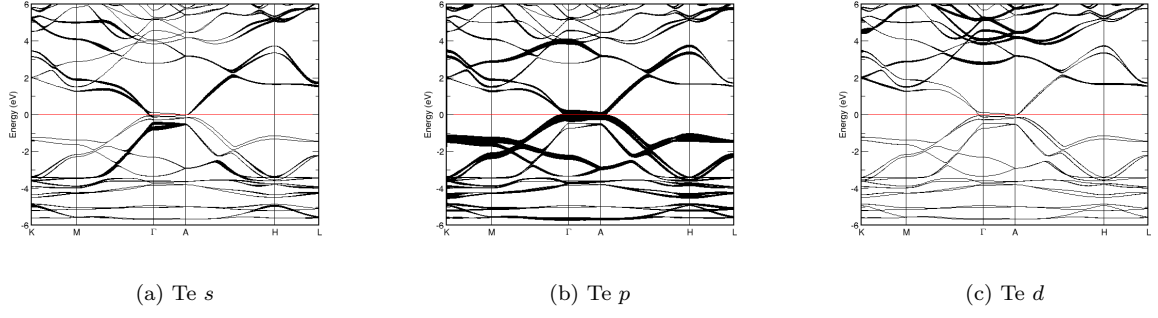


FIG. 35: Fat band representation of Te in KAuTe

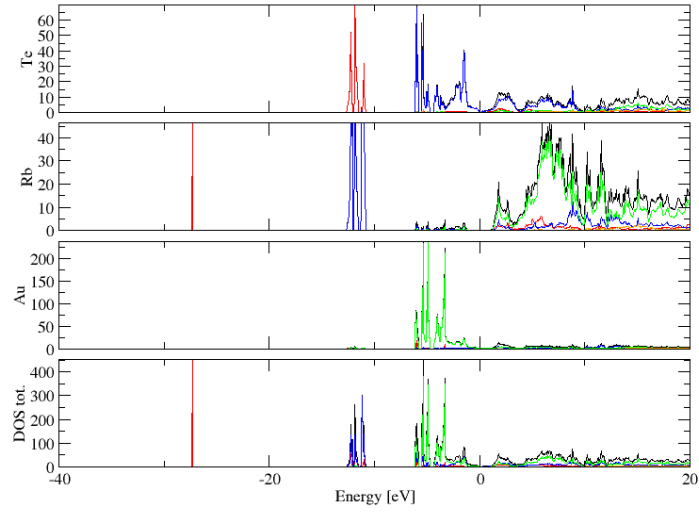
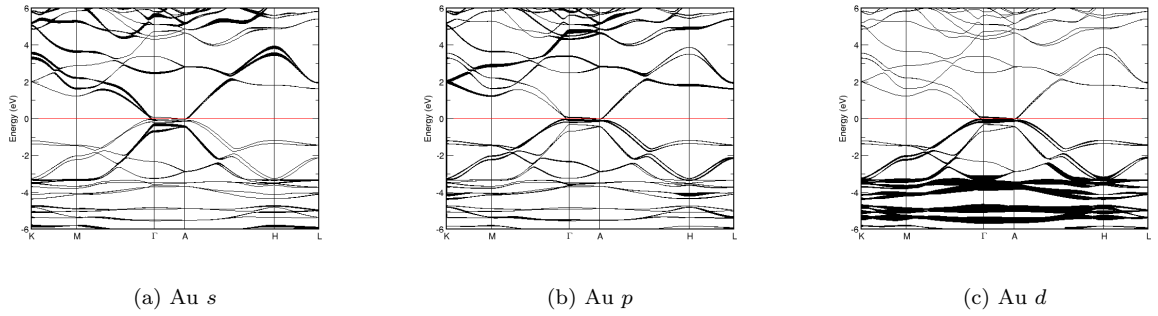
FIG. 36: (Color online) PDOS of RbAuTe (ICSD #75026). The s -, p - and d -projected states are in red, blue and green, respectively. RbAuTe crystallizes in space group $P 63/m m c$ (#194), in a hexagonal primitive structure.

FIG. 37: Fat band representation of Au in RbAuTe

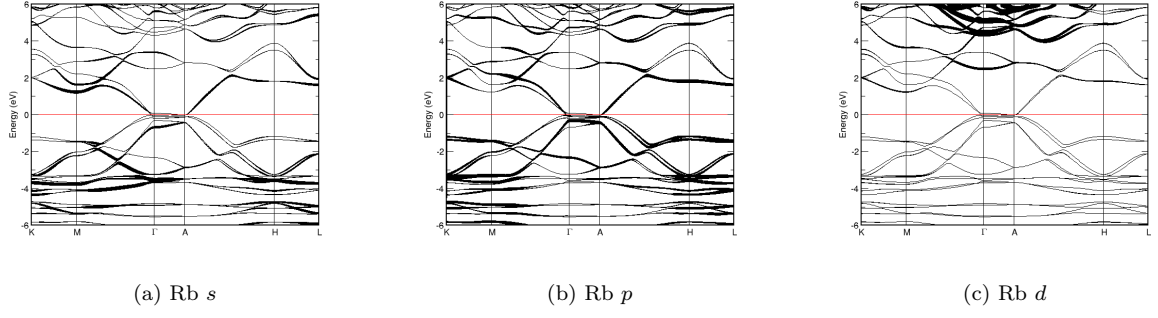


FIG. 38: Fat band representation of Rb in RbAuTe

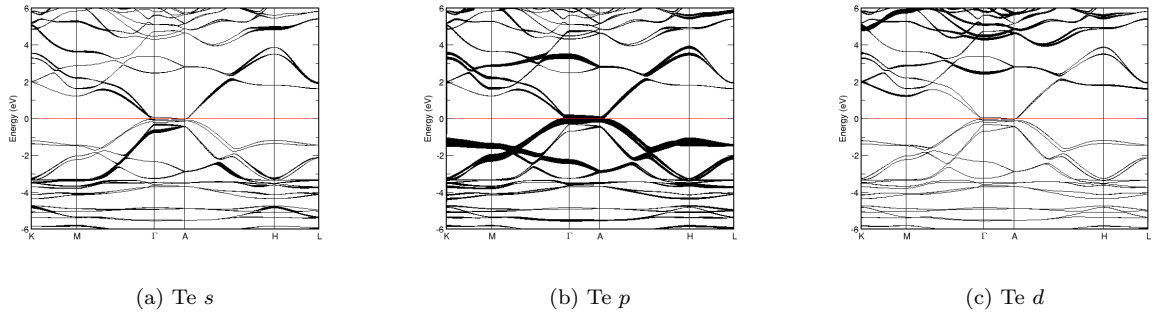


FIG. 39: Fat band representation of Te in RbAuTe

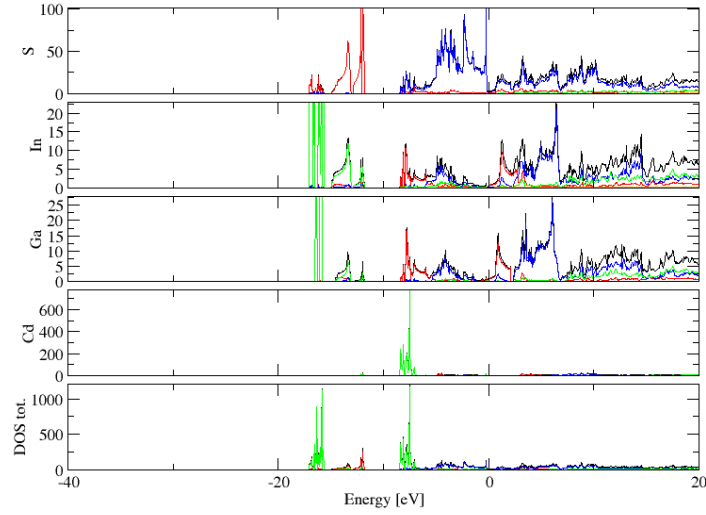
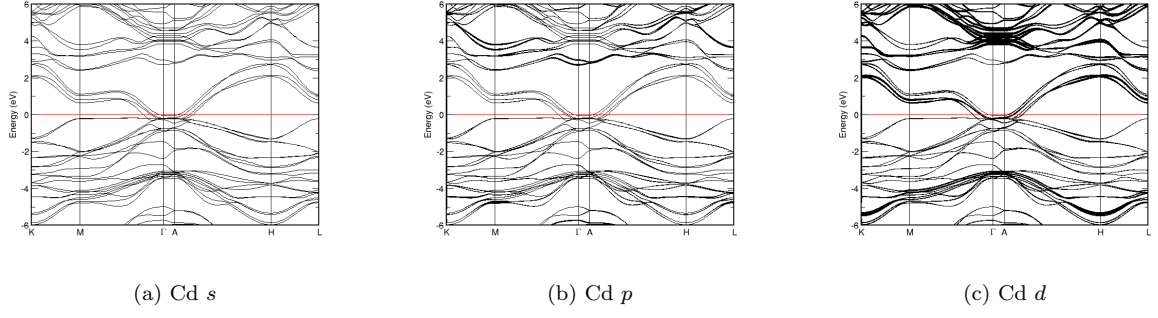
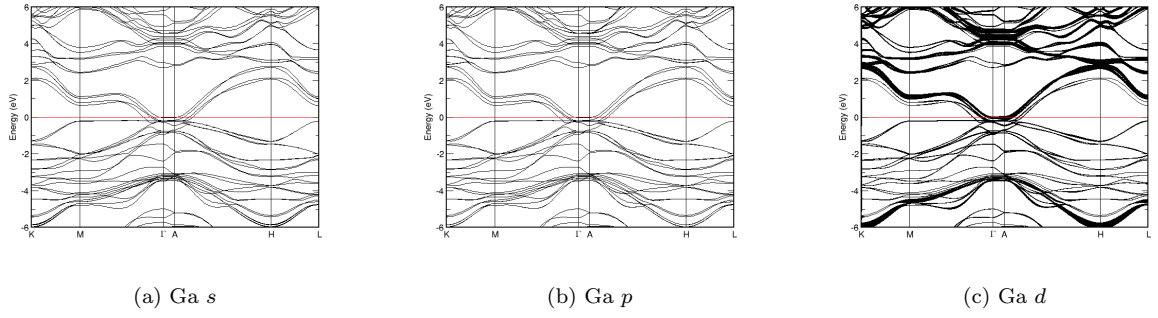
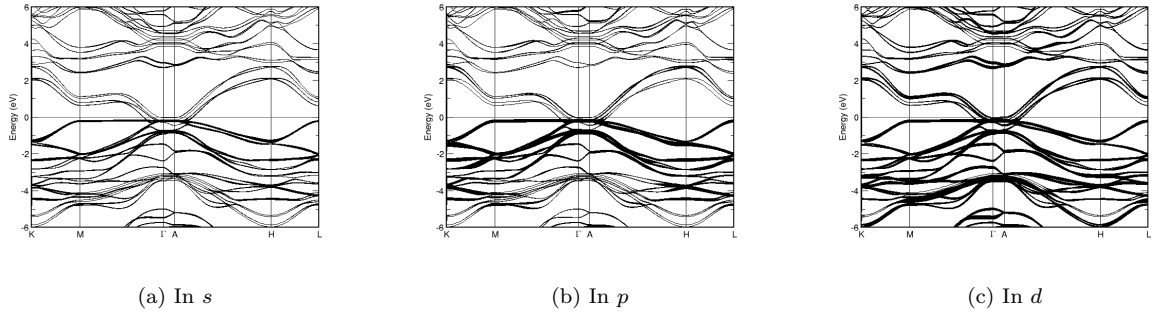
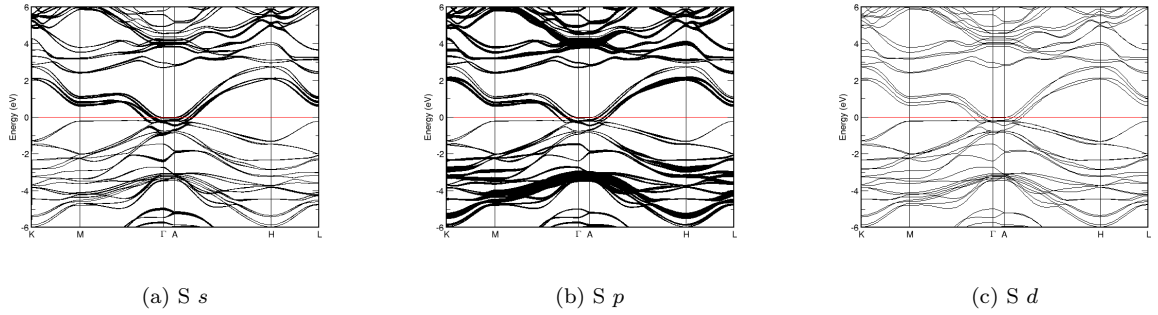


FIG. 40: (Color online) PDOS of CdInGaS₄ (ICSD #20785). The s -, p - and d -projected states are in red, blue and green, respectively. CdInGaS₄ crystallizes in space group $P\bar{3}m1$ (#164), in a hexagonal primitive structure.

FIG. 41: Fat band representation of Cd in CdInGaS₄FIG. 42: Fat band representation of Ga in CdInGaS₄FIG. 43: Fat band representation of In in CdInGaS₄FIG. 44: Fat band representation of S in CdInGaS₄

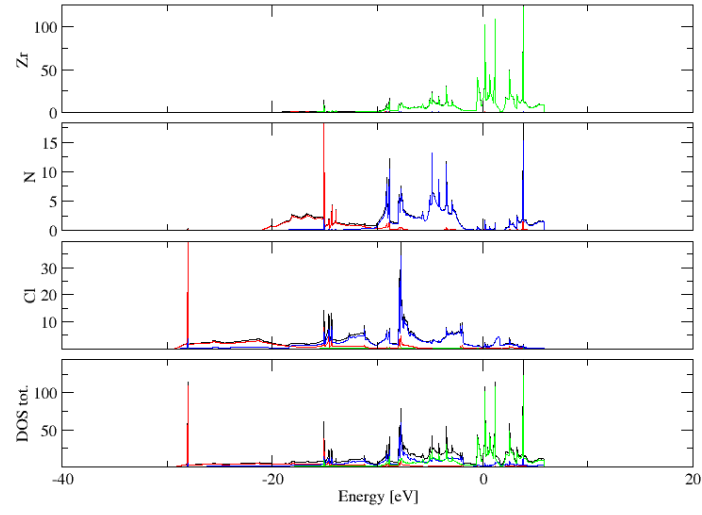


FIG. 45: (Color online) PDOS of ZrNCl (ICSD #25506). The s -, p - and d -projected states are in red, blue and green, respectively. ZrNCl crystallizes in space group $P-3m1$ (#164), in a hexagonal primitive structure.

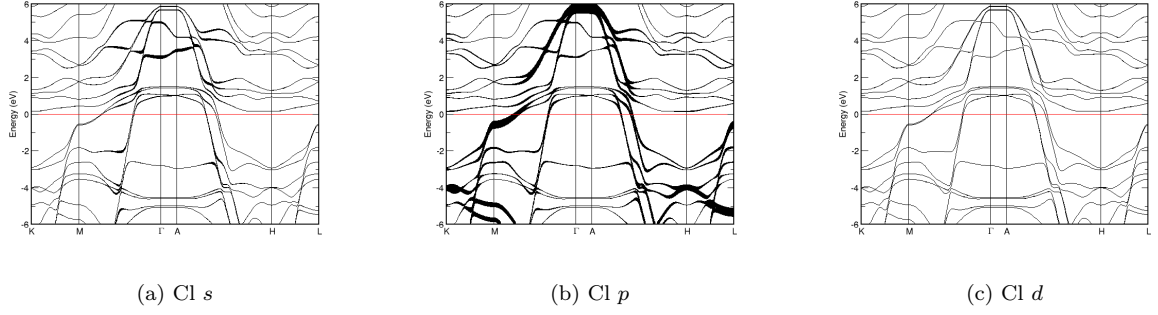


FIG. 46: Fat band representation of Cl in ZrNCl

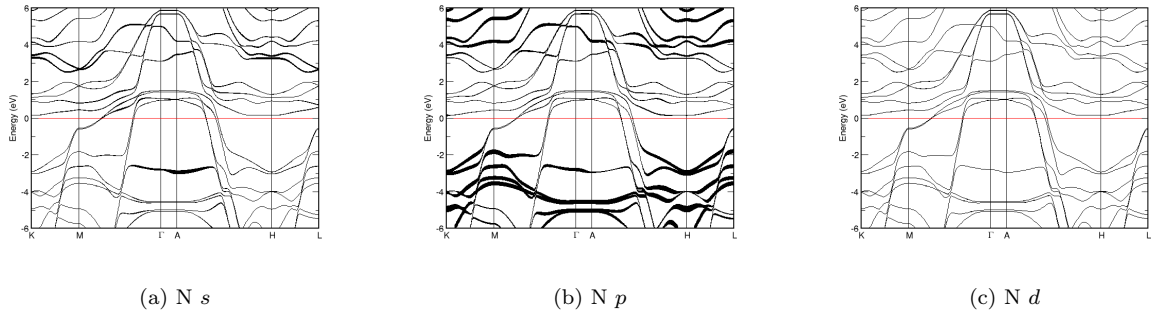


FIG. 47: Fat band representation of N in ZrNCl

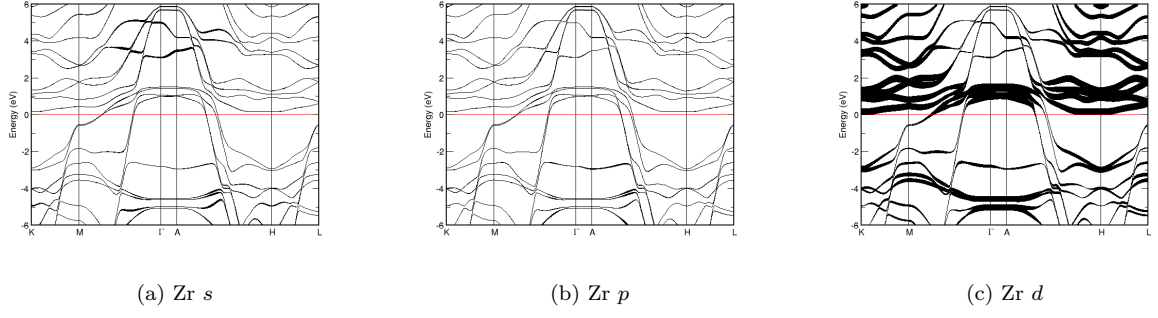


FIG. 48: Fat band representation of Zr in ZrNCl

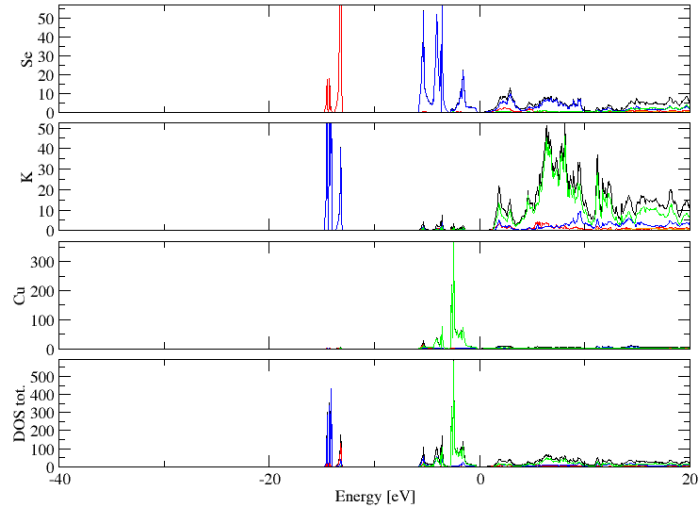
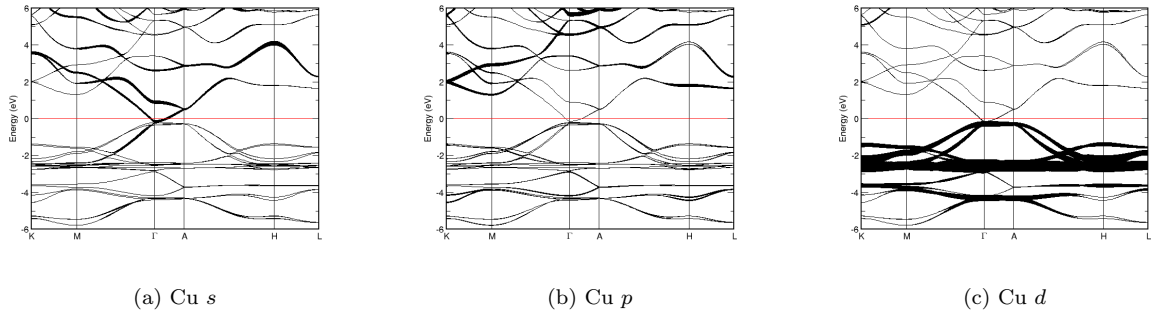
FIG. 49: (Color online) PDOS of KCuSe (ICSD #12157). The *s*-, *p*- and *d*-projected states are in red, blue and green, respectively. KCuSe crystallizes in space group $P 6_3/m m c$ (#194), in a hexagonal primitive structure.

FIG. 50: Fat band representation of Cu in KCuSe

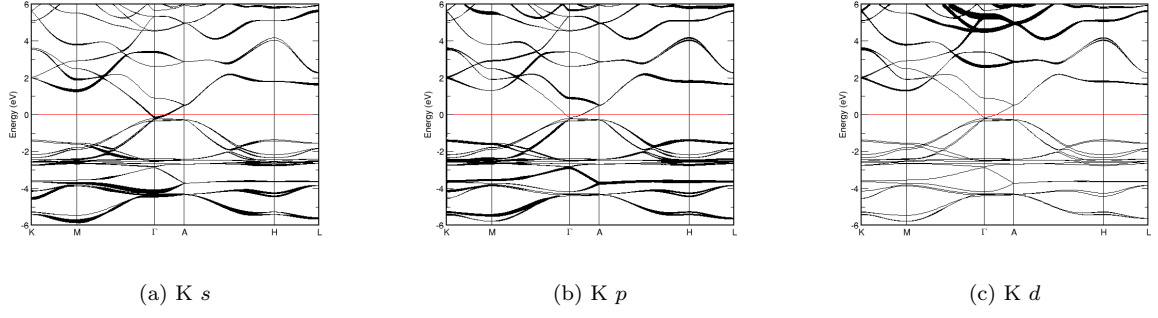


FIG. 51: Fat band representation of K in KCuSe

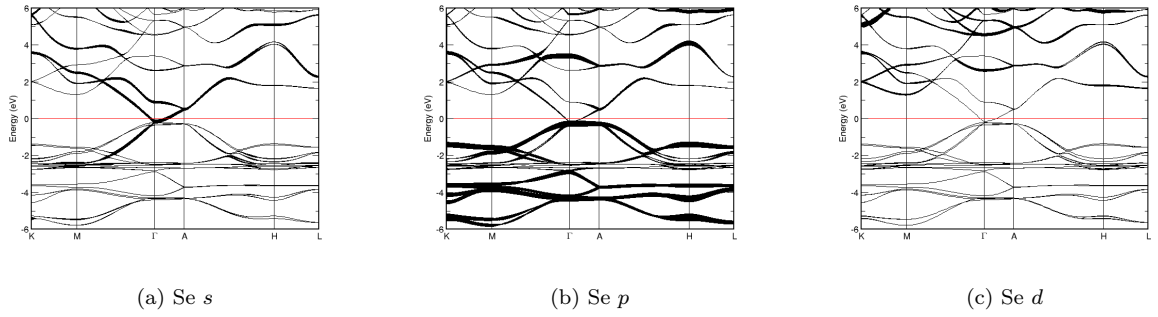
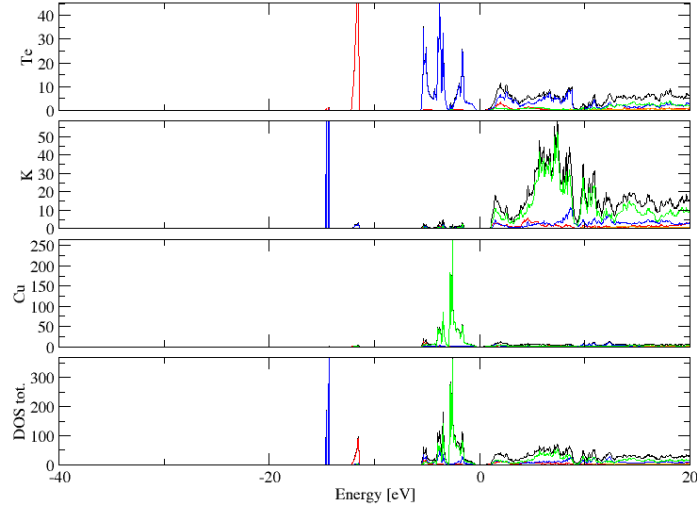


FIG. 52: Fat band representation of Se in KCuSe

FIG. 53: (Color online) PDOS of KCuTe (ICSD #12158). The s -, p - and d -projected states are in red, blue and green, respectively. KCuTe crystallizes in space group P 63/m m c (#194), in a hexagonal primitive structure.

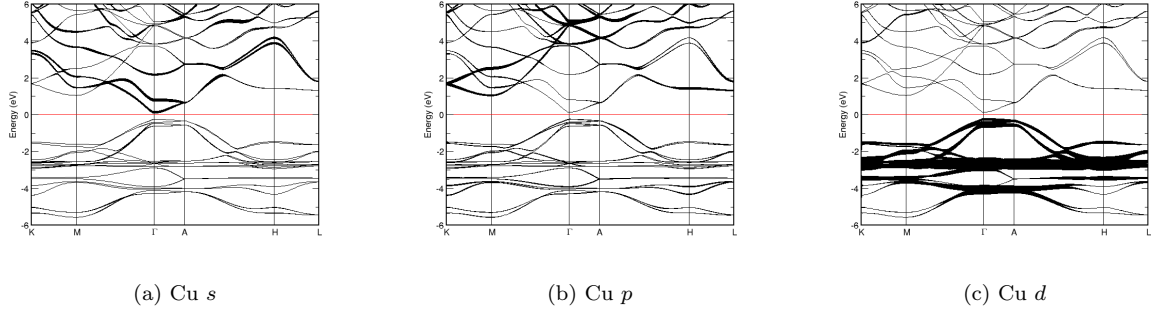


FIG. 54: Fat band representation of Cu in KCuTe

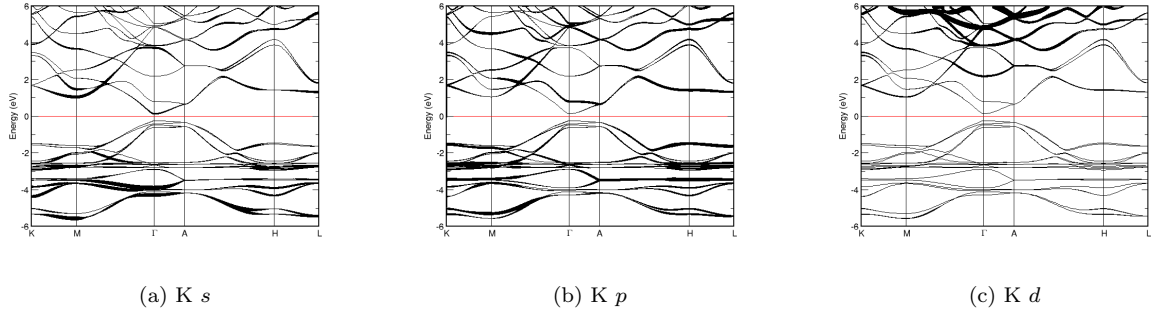


FIG. 55: Fat band representation of K in KCuTe

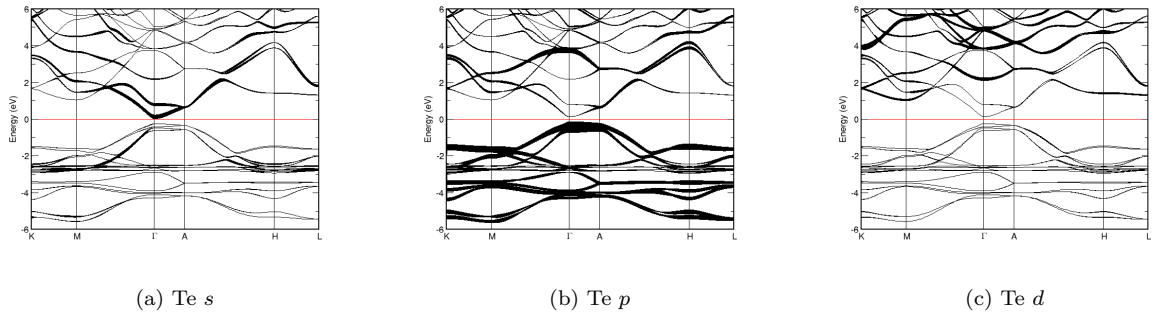


FIG. 56: Fat band representation of Te in KCuTe

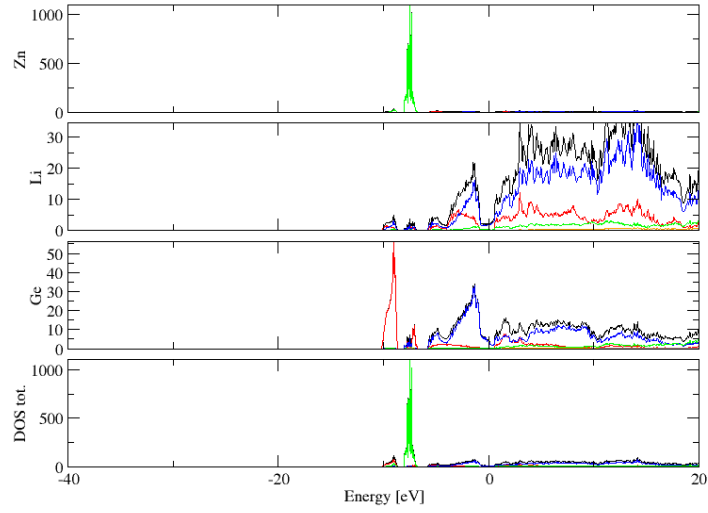


FIG. 57: (Color online) PDOS of Li_2ZnGe (ICSD #53678). The s -, p - and d -projected states are in red, blue and green, respectively. Li_2ZnGe crystallizes in space group $P-3m1$ (#164), in a hexagonal primitive structure.

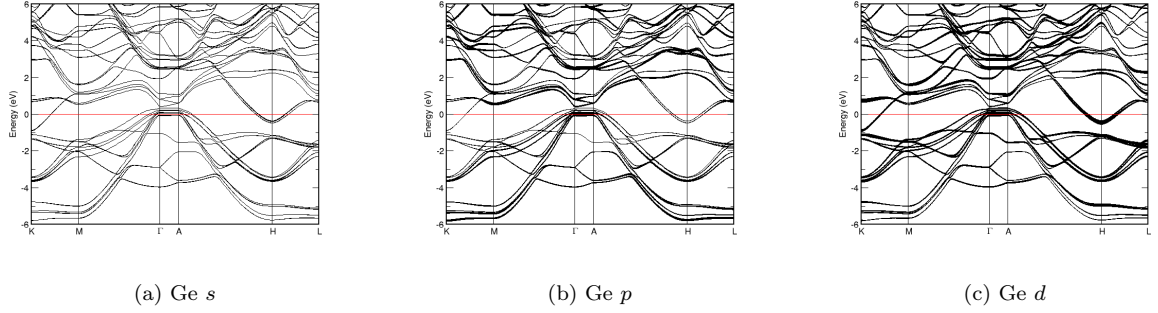


FIG. 58: Fat band representation of Ge in Li_2ZnGe

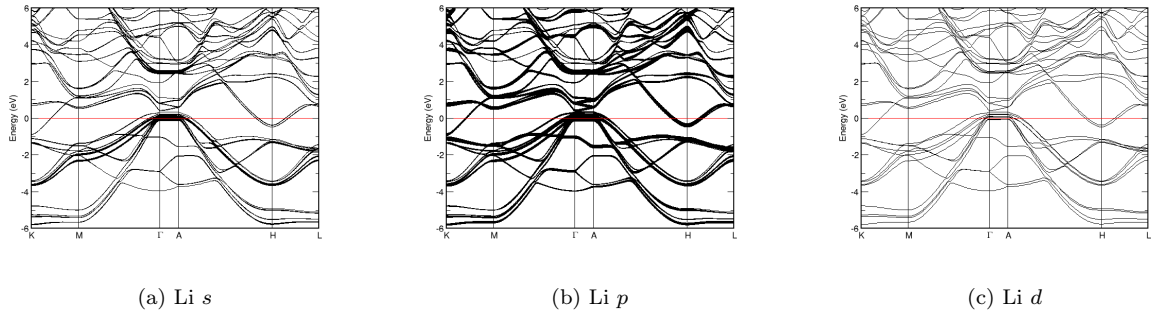
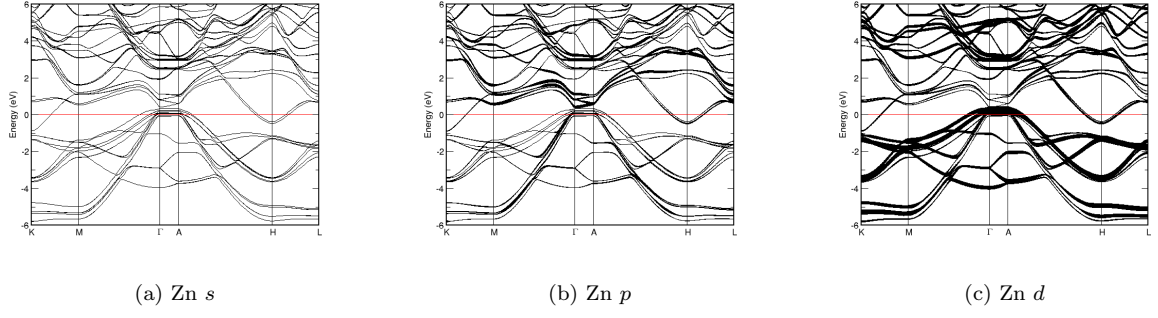
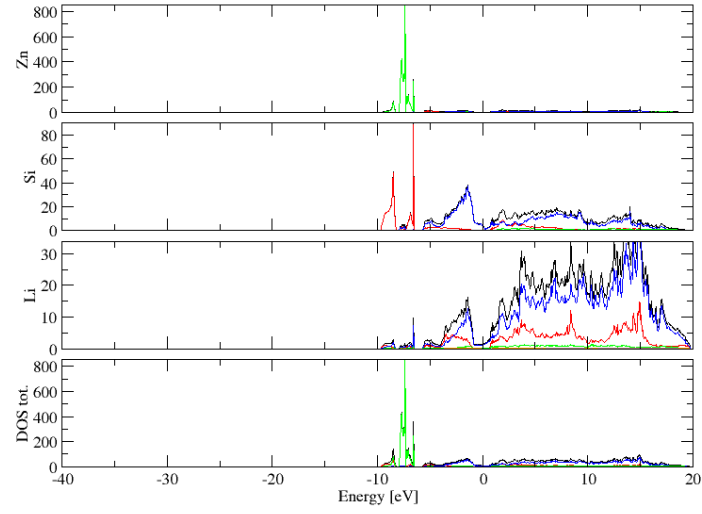
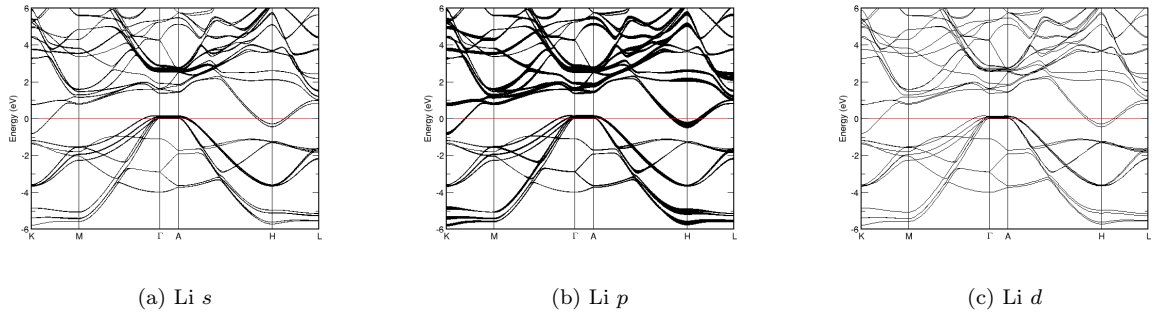
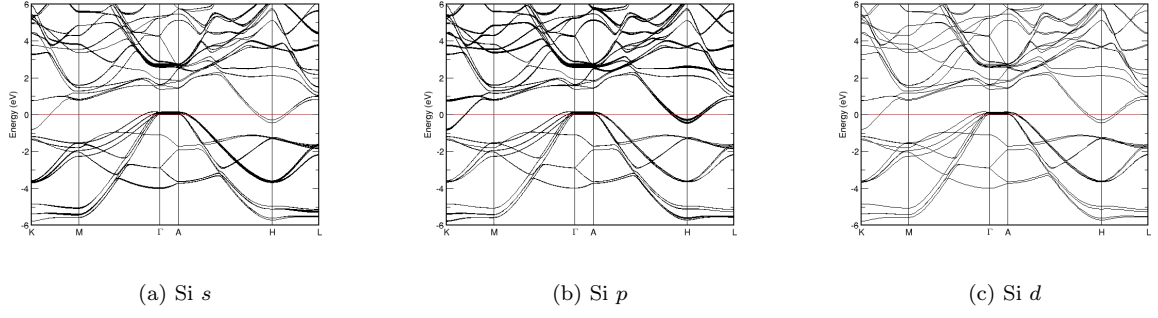
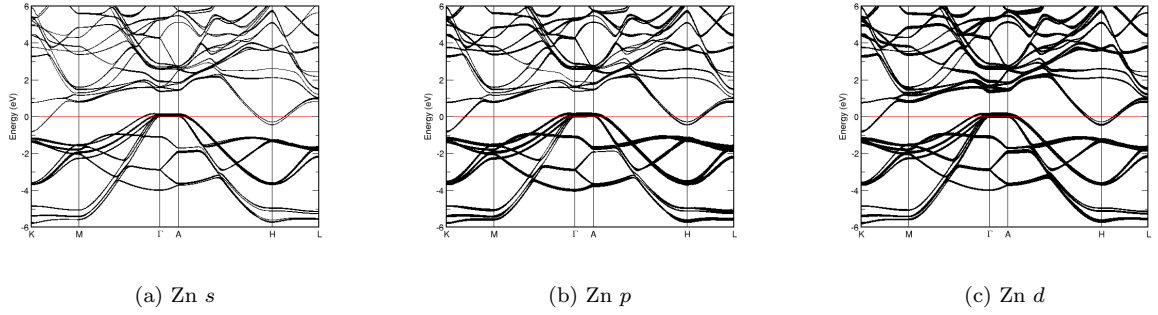
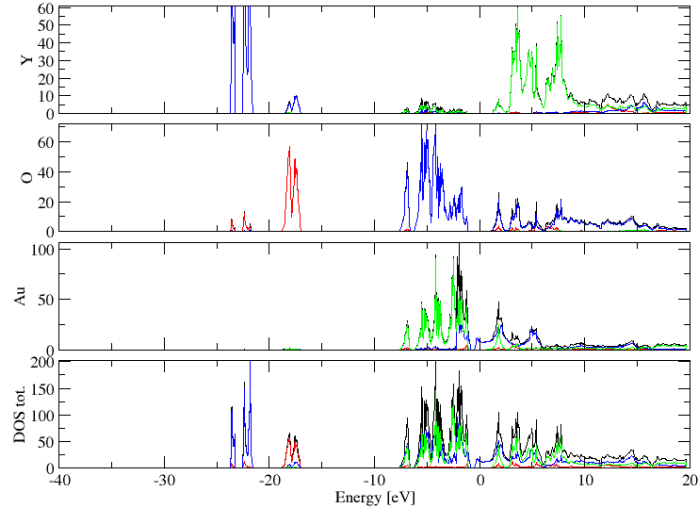
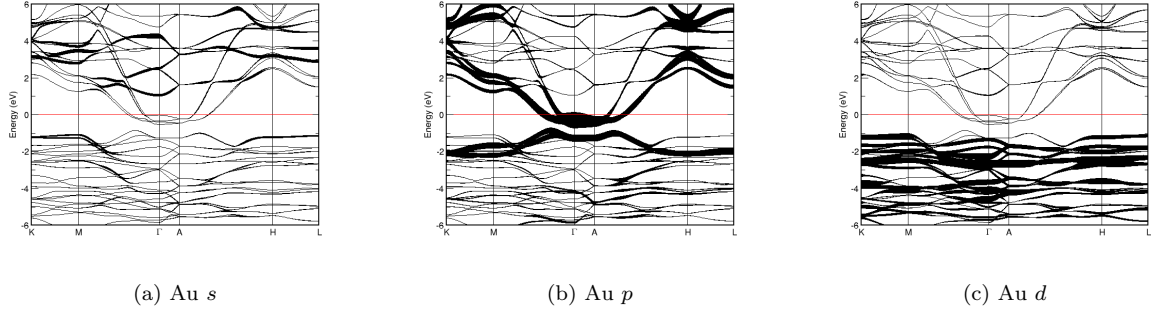
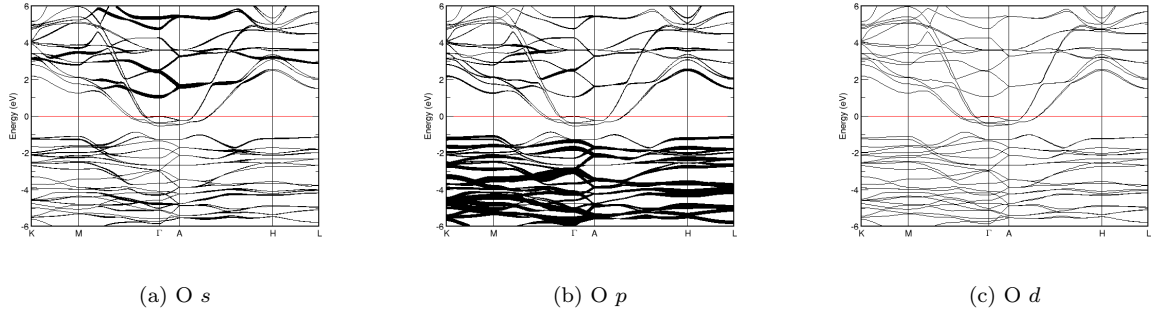
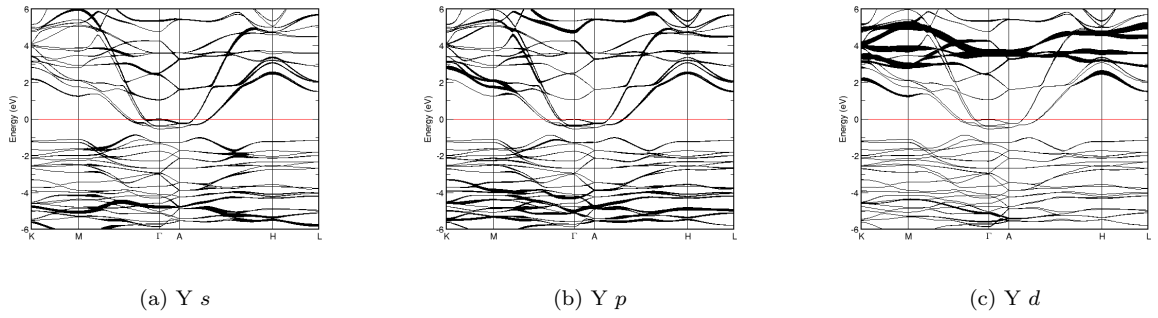


FIG. 59: Fat band representation of Li in Li_2ZnGe

FIG. 60: Fat band representation of Zn in Li_2ZnGe FIG. 61: (Color online) PDOS of Li_2ZnSi (ICSD #16221). The *s*-, *p*- and *d*-projected states are in red, blue and green, respectively. Li_2ZnSi crystallizes in space group $P\bar{3}m1$ (#164), in a hexagonal primitive structure.FIG. 62: Fat band representation of Li in Li_2ZnSi

FIG. 63: Fat band representation of Si in Li_2ZnSi FIG. 64: Fat band representation of Zn in Li_2ZnSi FIG. 65: (Color online) PDOS of AuYO_2 (ICSD #95675). The s -, p - and d -projected states are in red, blue and green, respectively. AuYO_2 crystallizes in space group $P 63/m m c$ (#194), in a hexagonal primitive structure.

FIG. 66: Fat band representation of Au in AuYO₂FIG. 67: Fat band representation of O in AuYO₂FIG. 68: Fat band representation of Y in AuYO₂

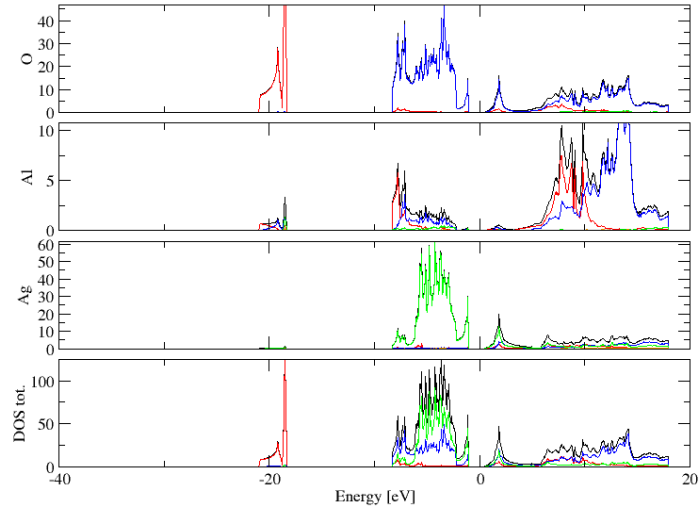


FIG. 69: (Color online) PDOS of AgAlO_2 (ICSD #300020). The s -, p - and d -projected states are in red, blue and green, respectively. AgAlO_2 crystallizes in space group $P 63/m m c$ (#194), in a hexagonal primitive structure. We also note that several other members of the delafossite structure family qualify as possible high-temperature superconductors, after appropriate electron/hole doping, because of layered structure, $p - d$ -hybridization and cosine-like dispersion around E_F .

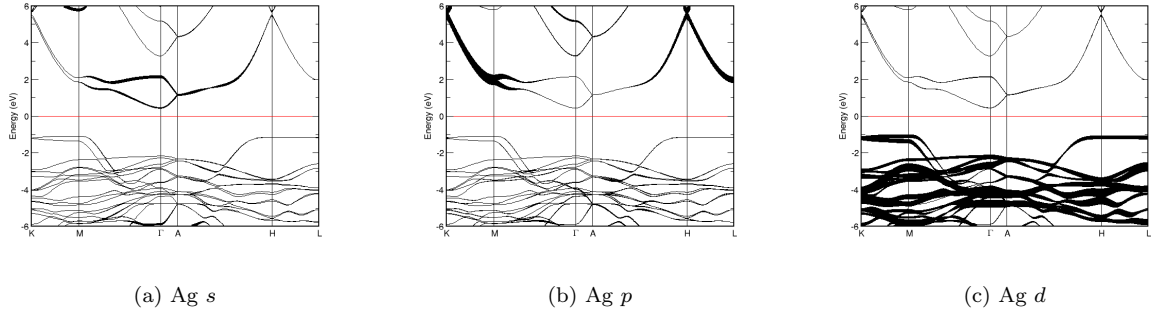


FIG. 70: Fat band representation of Ag in AgAlO_2

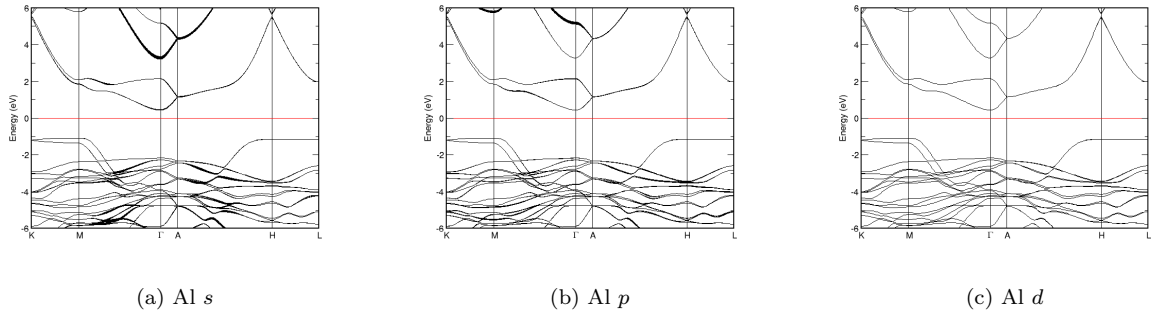


FIG. 71: Fat band representation of Al in AgAlO_2

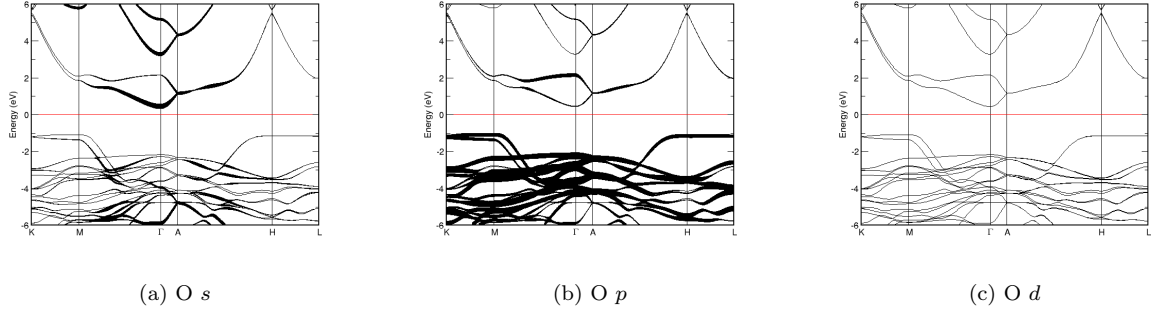
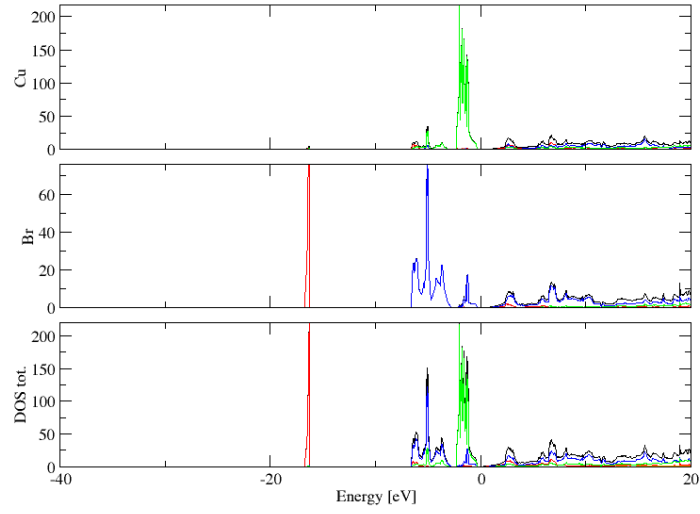
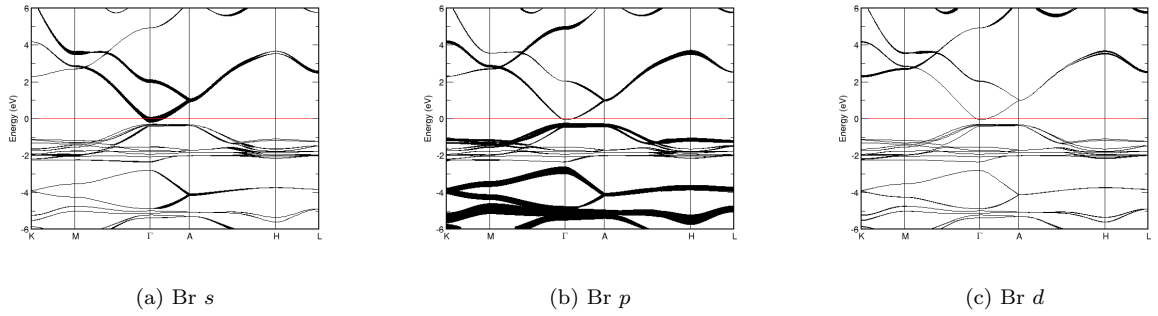
FIG. 72: Fat band representation of O in AgAlO₂FIG. 73: (Color online) PDOS of CuBr (ICSD #30092). The *s*-, *p*- and *d*-projected states are in red, blue and green, respectively. CuBr crystallizes in space group P 63 m c (#186), in a hexagonal primitive structure.

FIG. 74: Fat band representation of Br in CuBr

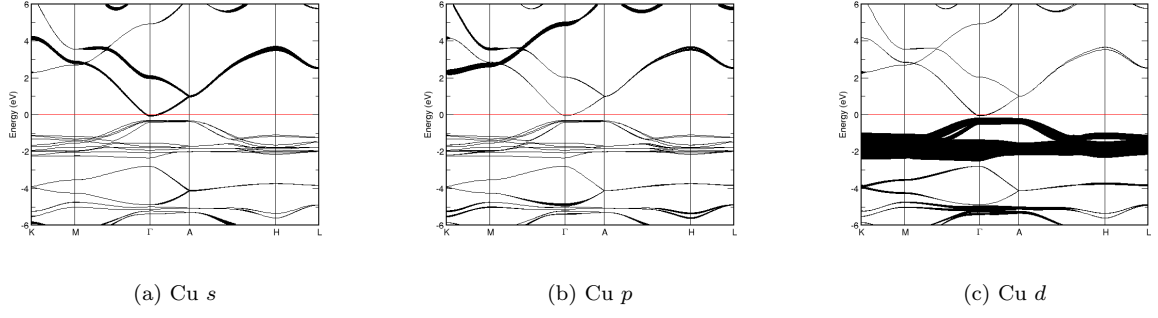
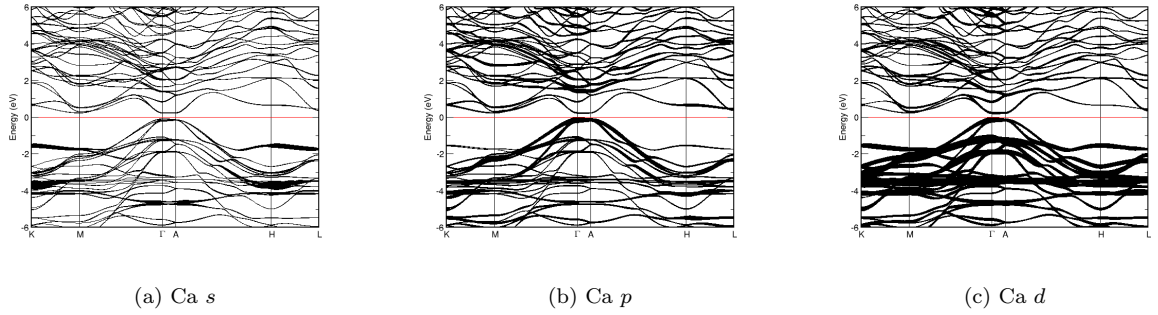
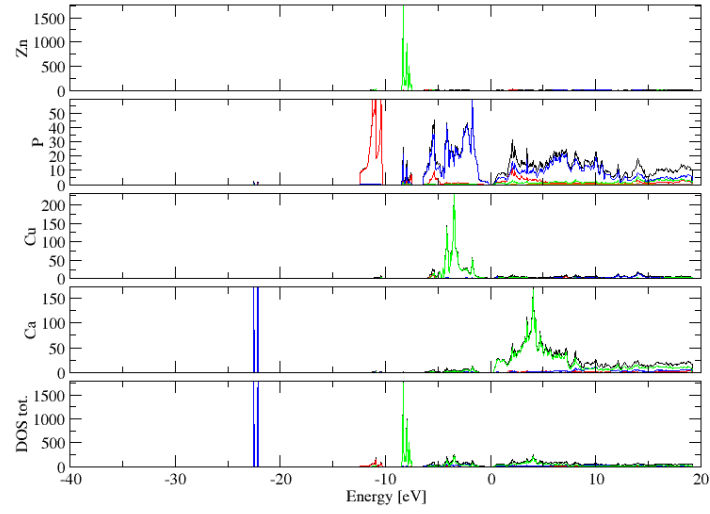
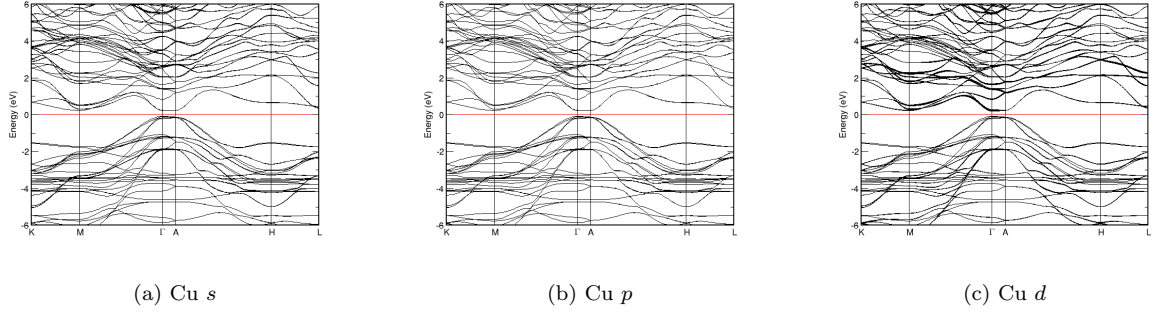
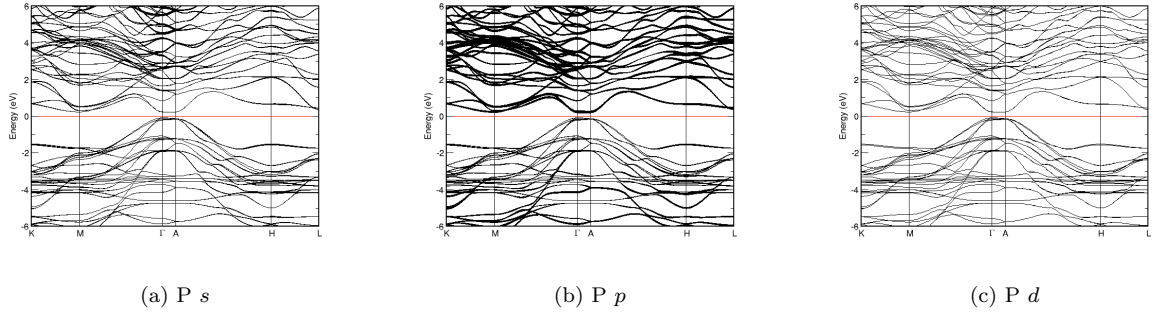
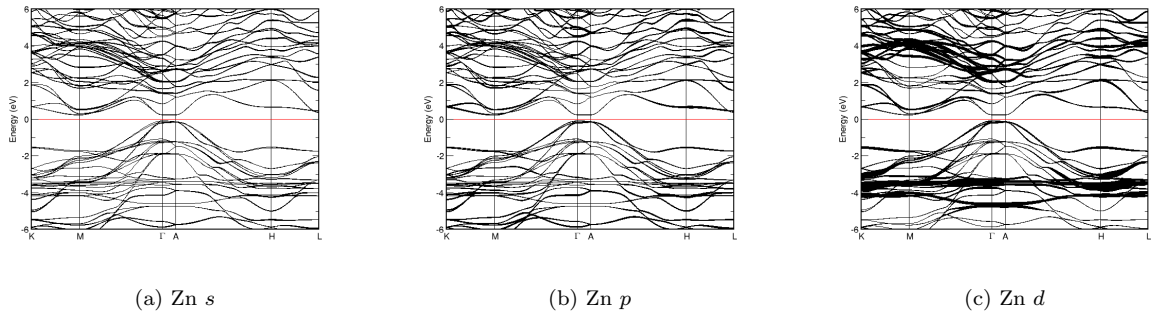


FIG. 75: Fat band representation of Cu in CuBr

FIG. 77: Fat band representation of Ca in $\text{Ca}_2\text{CuZn}_2\text{P}_3$

FIG. 78: Fat band representation of Cu in $\text{Ca}_2\text{CuZn}_2\text{P}_3$ FIG. 79: Fat band representation of P in $\text{Ca}_2\text{CuZn}_2\text{P}_3$ FIG. 80: Fat band representation of Zn in $\text{Ca}_2\text{CuZn}_2\text{P}_3$

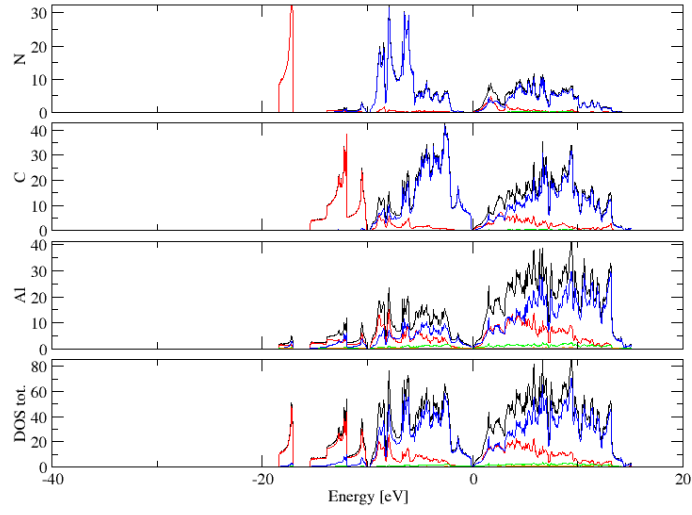


FIG. 81: (Color online) PDOS of $\text{Al}_5\text{C}_3\text{N}$ (ICSD #26859). The s -, p - and d -projected states are in red, blue and green, respectively. $\text{Al}_5\text{C}_3\text{N}$ crystallizes in space group P 63 m c (#186), in a hexagonal primitive structure.

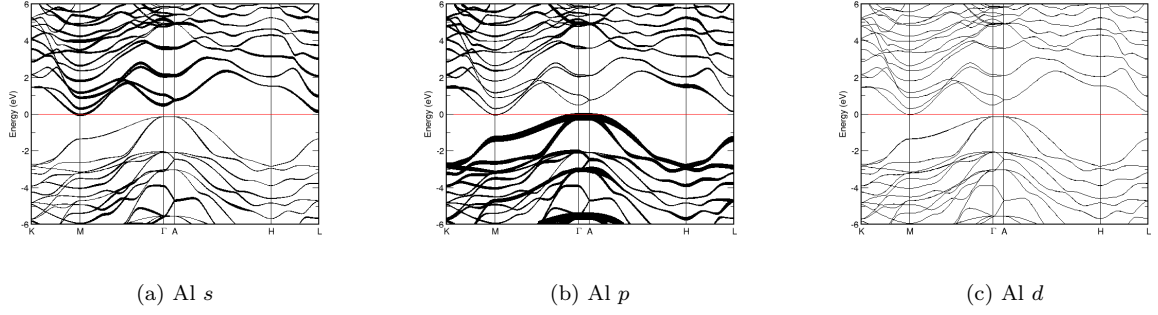


FIG. 82: Fat band representation of Al in $\text{Al}_5\text{C}_3\text{N}$

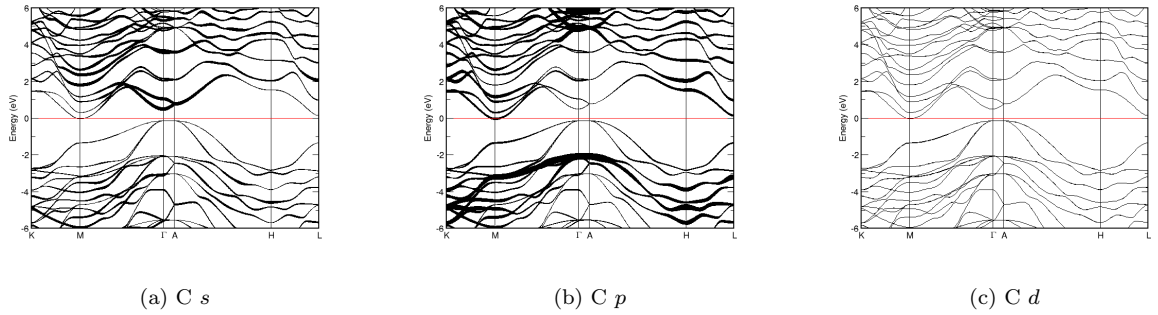
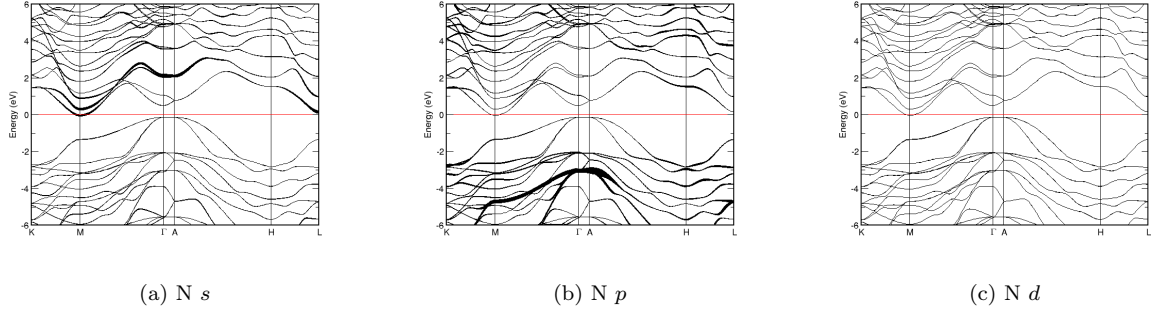
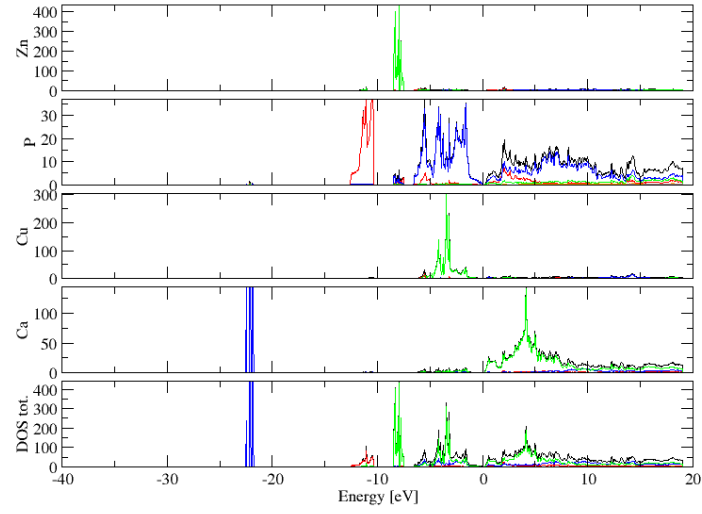
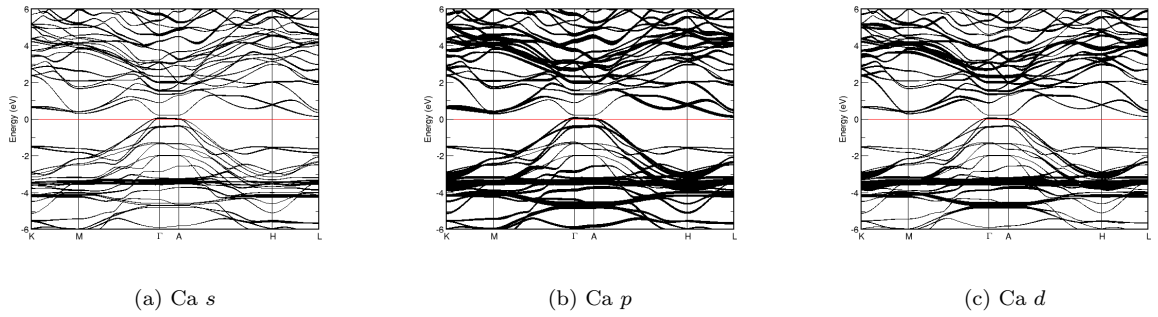
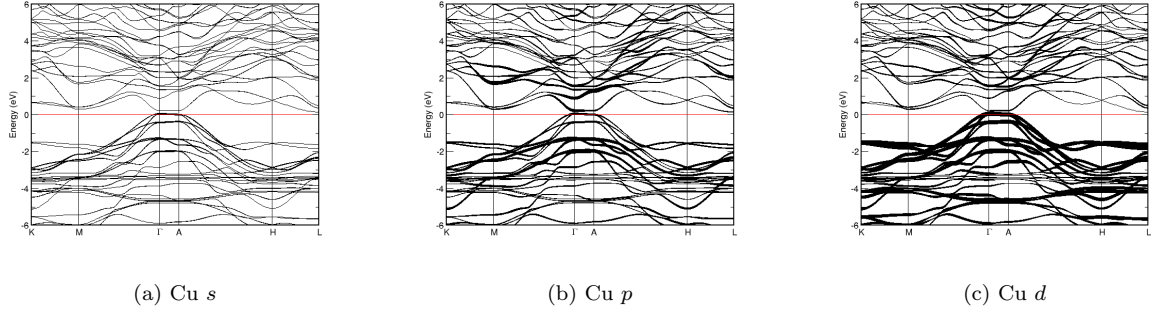
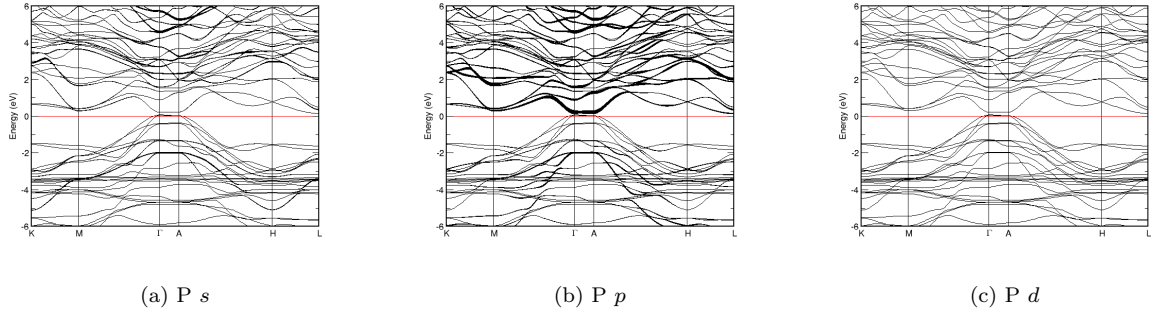
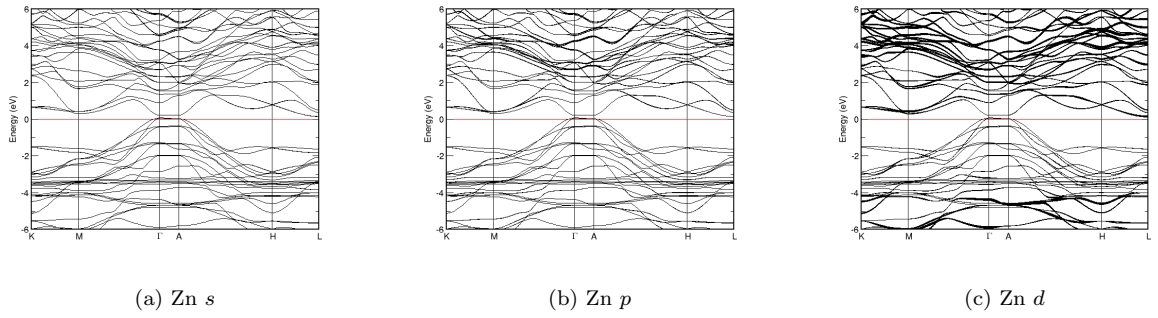


FIG. 83: Fat band representation of C in $\text{Al}_5\text{C}_3\text{N}$

FIG. 84: Fat band representation of N in $\text{Al}_5\text{C}_3\text{N}$ FIG. 85: (Color online) PDOS of $\text{Ca}_3\text{Cu}_2\text{Zn}_2\text{P}_4$ (ICSD #89515). The *s*-, *p*- and *d*-projected states are in red, blue and green, respectively. $\text{Ca}_3\text{Cu}_2\text{Zn}_2\text{P}_4$ crystallizes in space group $P\bar{3}m1$ (#164), in a hexagonal primitive structure.FIG. 86: Fat band representation of Ca in $\text{Ca}_3\text{Cu}_2\text{Zn}_2\text{P}_4$

FIG. 87: Fat band representation of Cu in $\text{Ca}_3\text{Cu}_2\text{Zn}_2\text{P}_4$ FIG. 88: Fat band representation of P in $\text{Ca}_3\text{Cu}_2\text{Zn}_2\text{P}_4$ FIG. 89: Fat band representation of Zn in $\text{Ca}_3\text{Cu}_2\text{Zn}_2\text{P}_4$

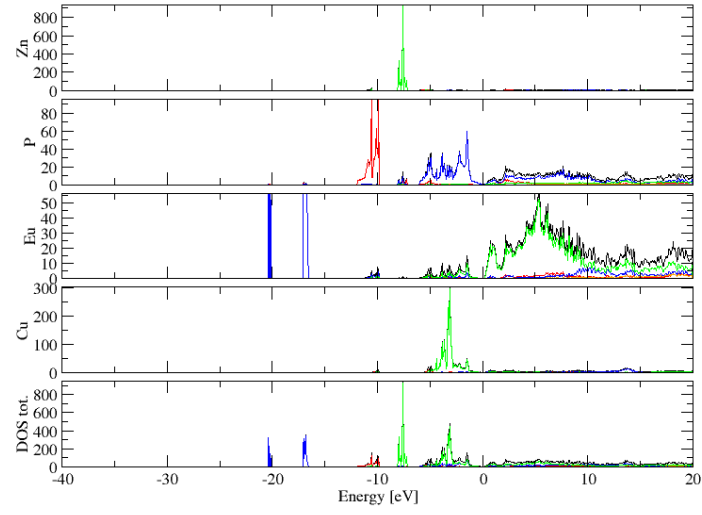


FIG. 90: (Color online) PDOS of $\text{Eu}_3\text{Cu}_2\text{Zn}_2\text{P}_4$ (ICSD #89516). The s -, p - and d -projected states are in red, blue and green, respectively. $\text{Eu}_3\text{Cu}_2\text{Zn}_2\text{P}_4$ crystallizes in space group $P\bar{3}m1$ (#164), in a hexagonal primitive structure.

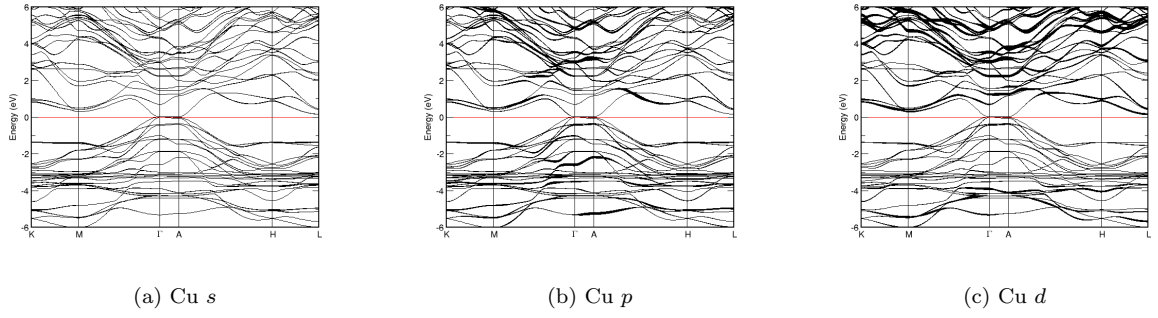


FIG. 91: Fat band representation of Cu in $\text{Eu}_3\text{Cu}_2\text{Zn}_2\text{P}_4$

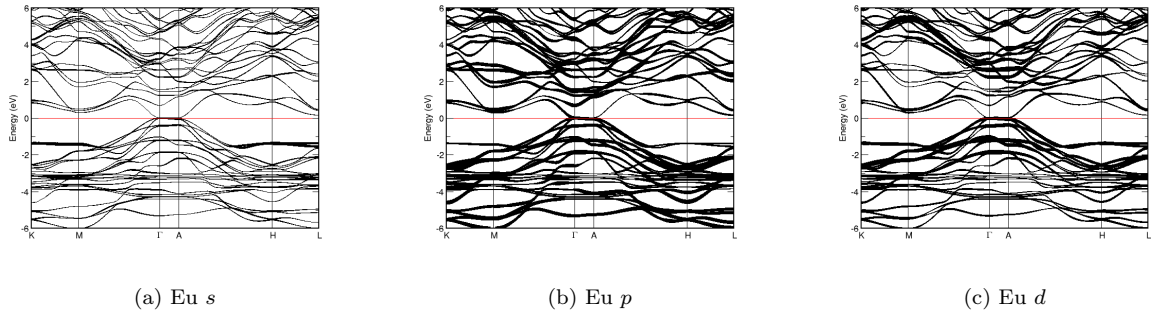
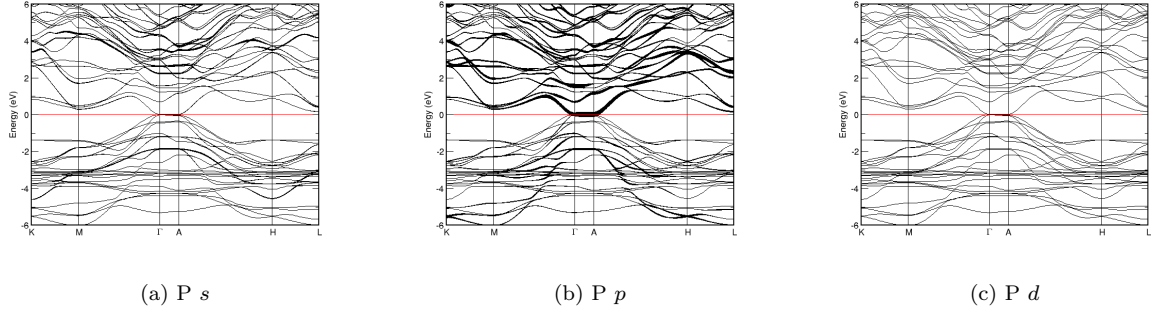
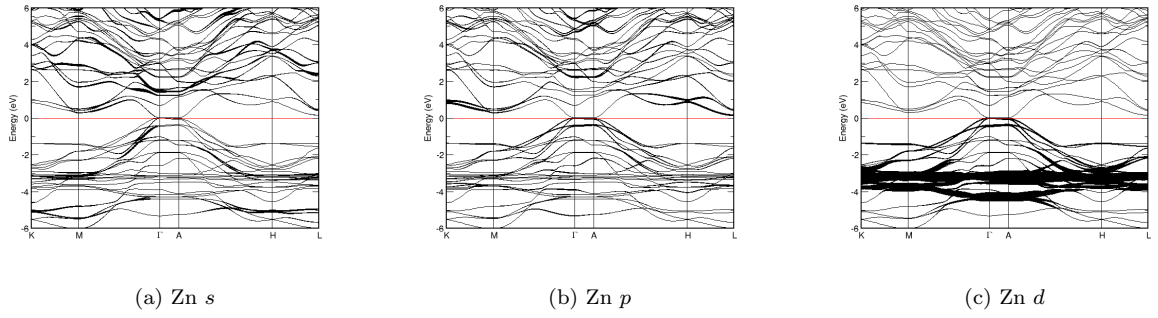
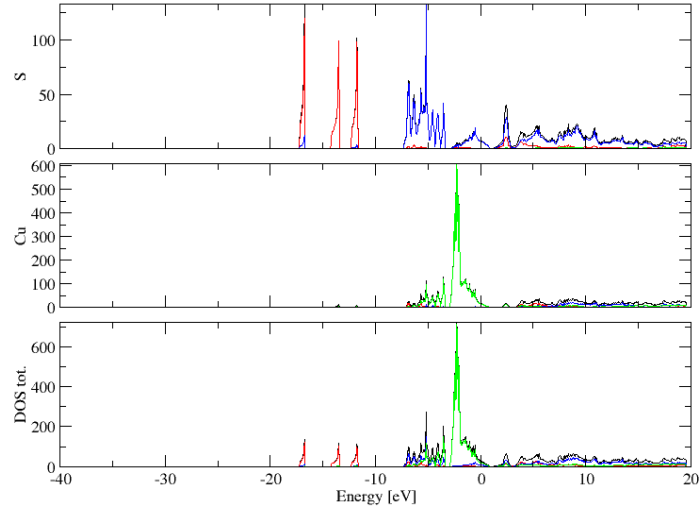
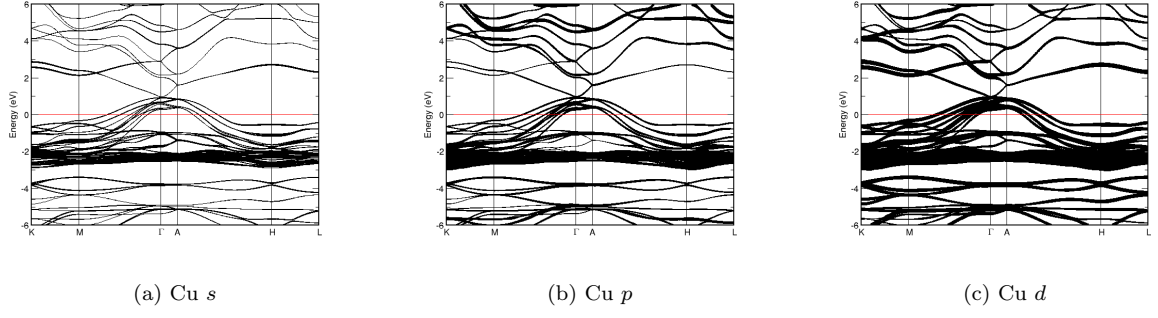
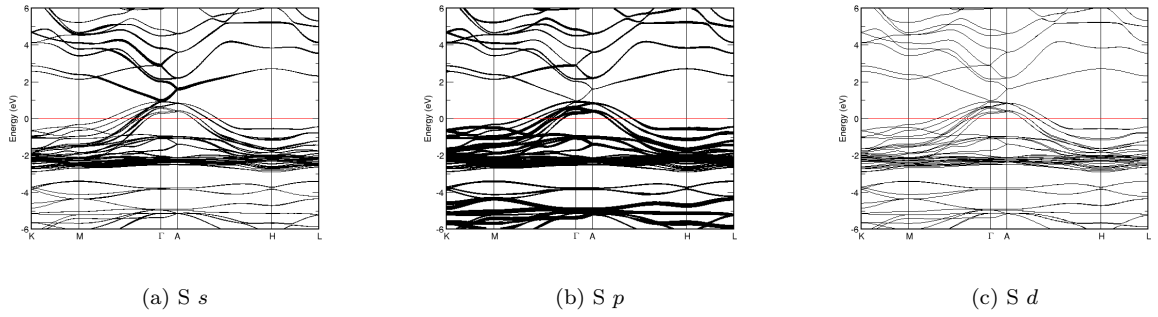
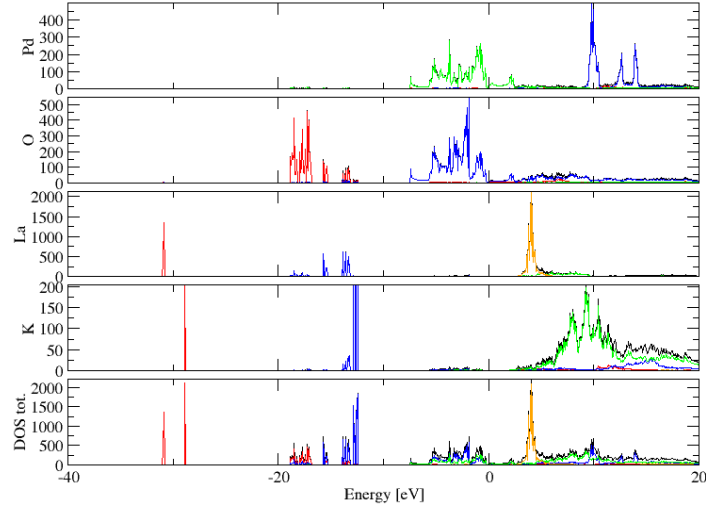
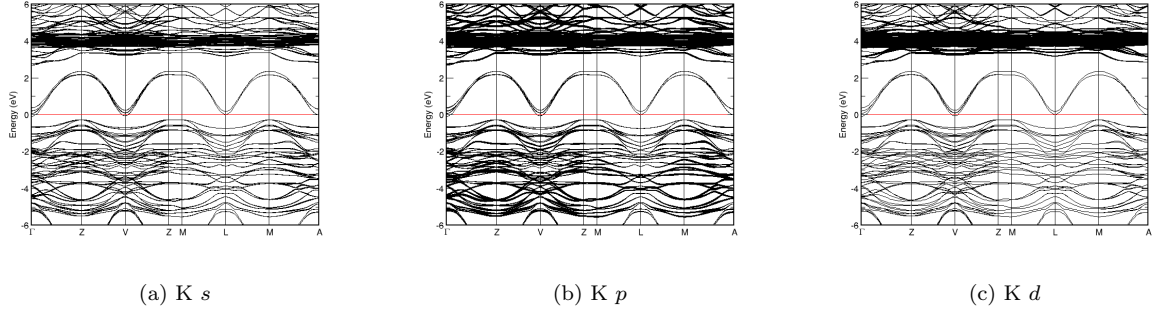
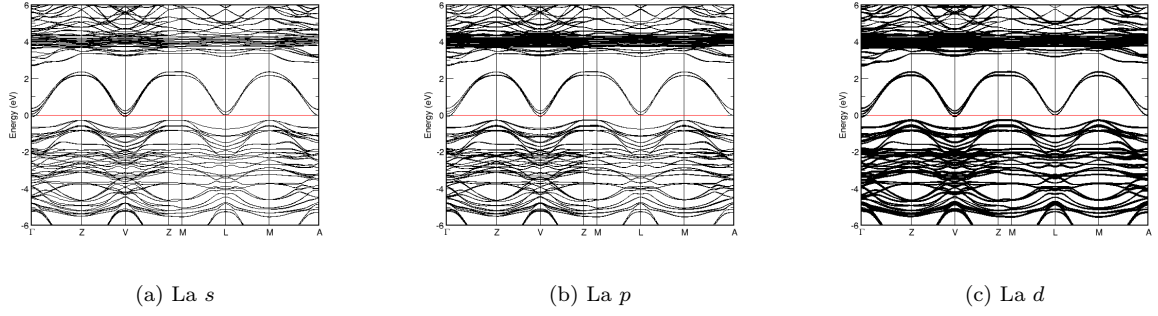
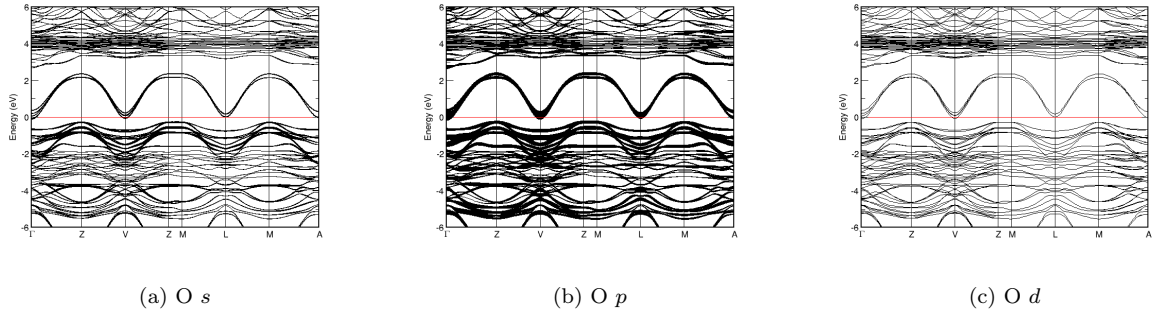
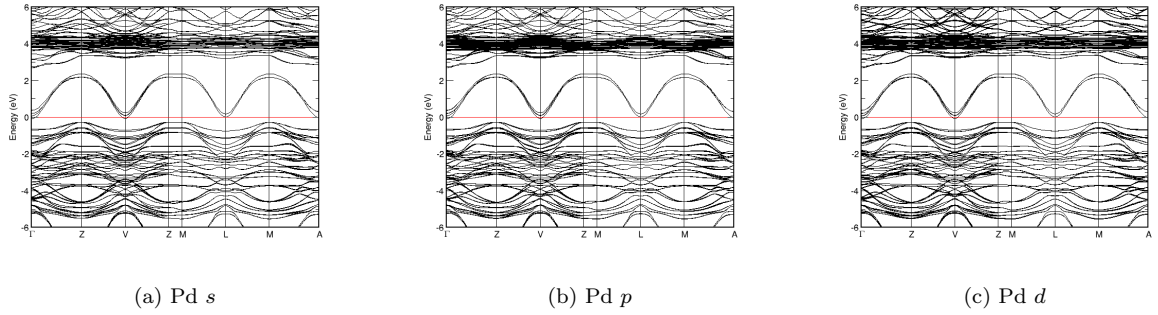


FIG. 92: Fat band representation of Eu in $\text{Eu}_3\text{Cu}_2\text{Zn}_2\text{P}_4$

FIG. 93: Fat band representation of P in $\text{Eu}_3\text{Cu}_2\text{Zn}_2\text{P}_4$ FIG. 94: Fat band representation of Zn in $\text{Eu}_3\text{Cu}_2\text{Zn}_2\text{P}_4$ FIG. 95: (Color online) PDOS of $\text{Cu}_4(\text{S}_2)_2(\text{CuS})_2$ (ICSD #26968). The *s*-, *p*- and *d*-projected states are in red, blue and green, respectively. $\text{Cu}_4(\text{S}_2)_2(\text{CuS})_2$ crystallizes in space group P 63/m m c (#194), in a hexagonal primitive structure.

FIG. 96: Fat band representation of Cu in $\text{Cu}_4(\text{S}_2)_2(\text{CuS})_2$ FIG. 97: Fat band representation of S in $\text{Cu}_4(\text{S}_2)_2(\text{CuS})_2$ FIG. 98: (Color online) PDOS of LaKPdO_3 (ICSD #417108). The *s*-, *p*- and *d*-projected states are in red, blue and green, respectively. LaKPdO_3 crystallizes in space group $C 1 2/m 1$ (#12), in a monoclinic base-centred structure.

FIG. 99: Fat band representation of K in LaKPdO₃FIG. 100: Fat band representation of La in LaKPdO₃FIG. 101: Fat band representation of O in LaKPdO₃FIG. 102: Fat band representation of Pd in LaKPdO₃

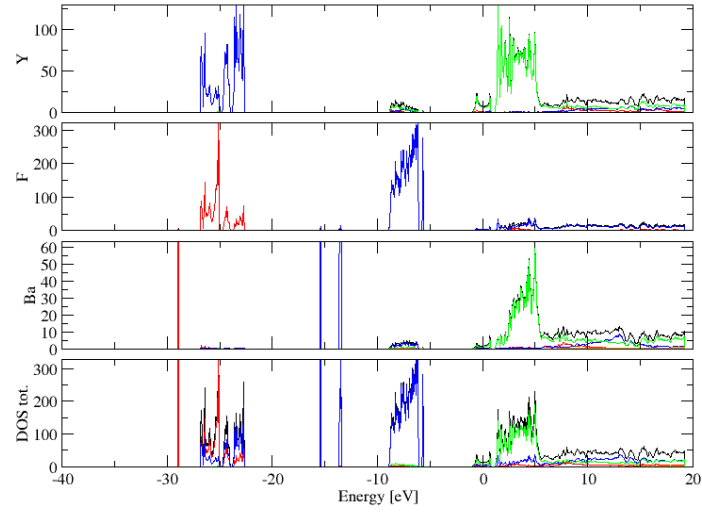


FIG. 103: (Color online) PDOS of BaY_2F_8 (ICSD #74359). The s -, p - and d -projected states are in red, blue and green, respectively. BaY_2F_8 crystallizes in space group $C 1 2/m 1$ (#12), in a monoclinic base-centred structure.

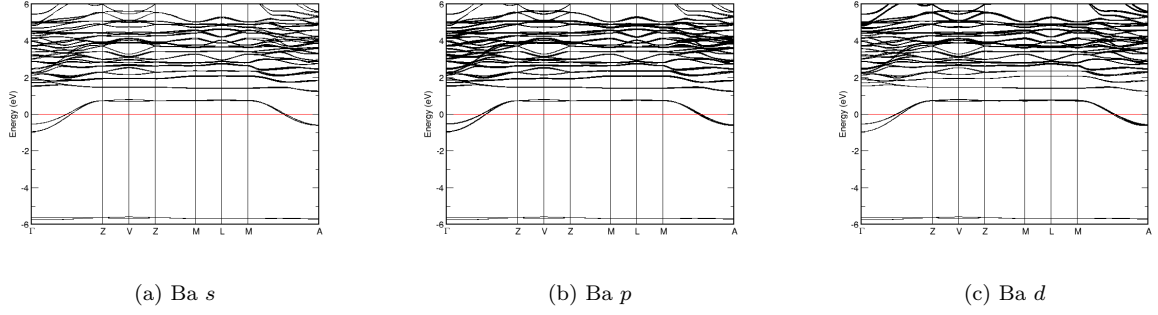


FIG. 104: Fat band representation of Ba in BaY_2F_8

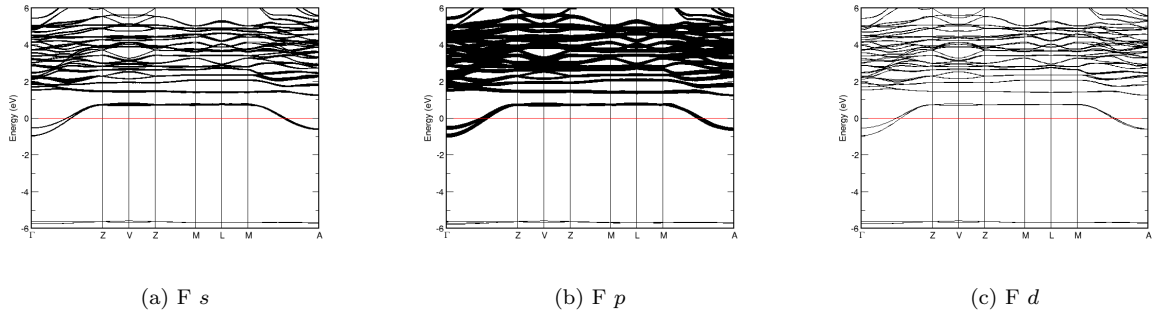


FIG. 105: Fat band representation of F in BaY_2F_8

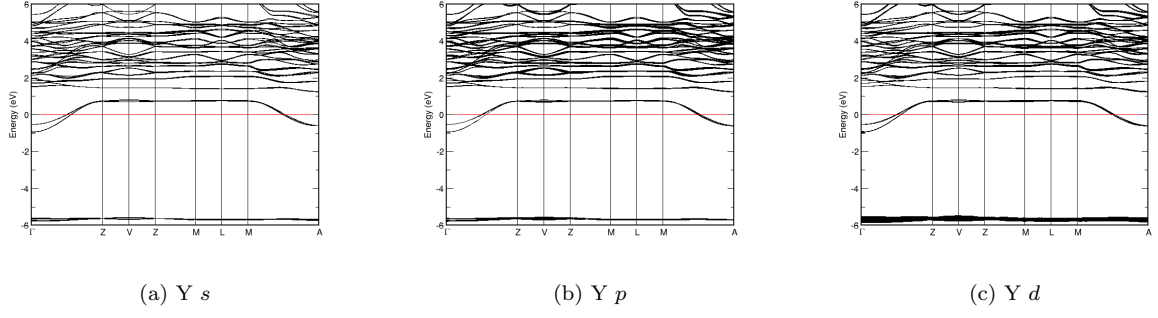
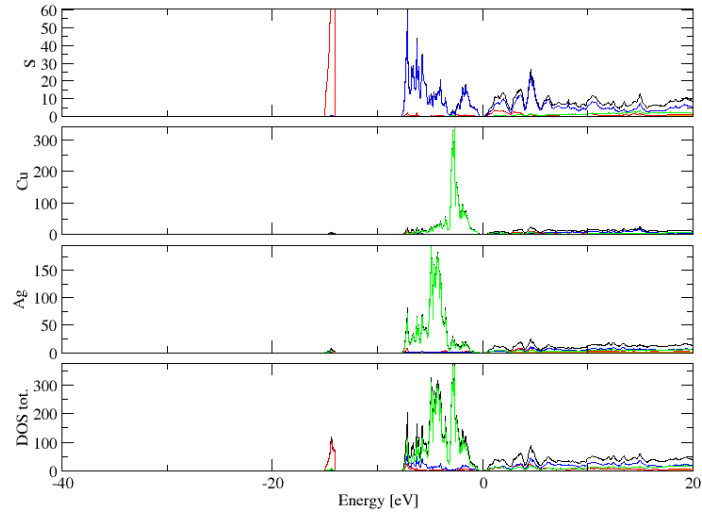
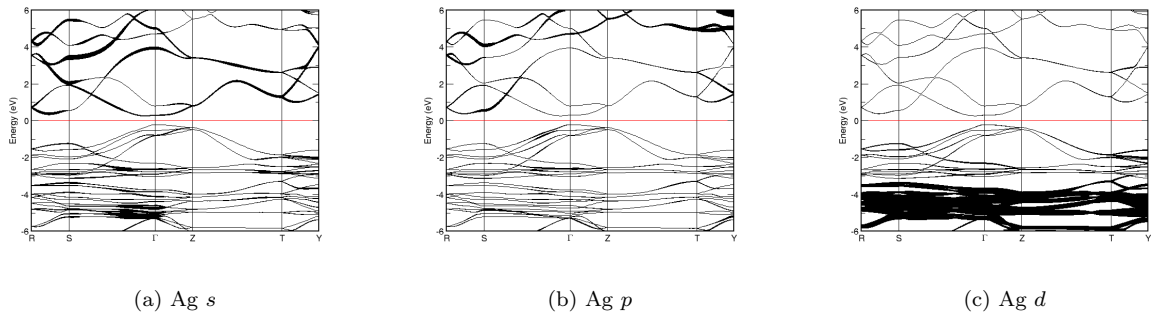
FIG. 106: Fat band representation of Y in BaY_2F_8 FIG. 107: (Color online) PDOS of AgCuS (ICSD #30233). The *s*-, *p*- and *d*-projected states are in red, blue and green, respectively. AgCuS crystallizes in space group $C m c m$ (#63), in a orthorhombic base-centred structure.

FIG. 108: Fat band representation of Ag in AgCuS

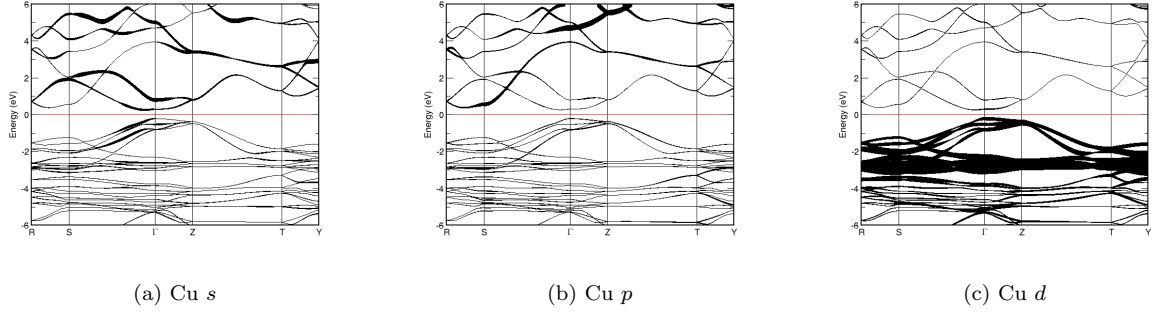


FIG. 109: Fat band representation of Cu in AgCuS

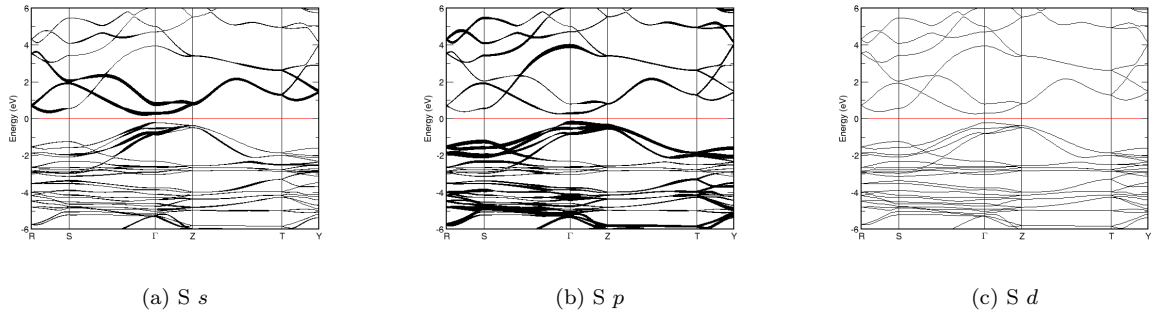
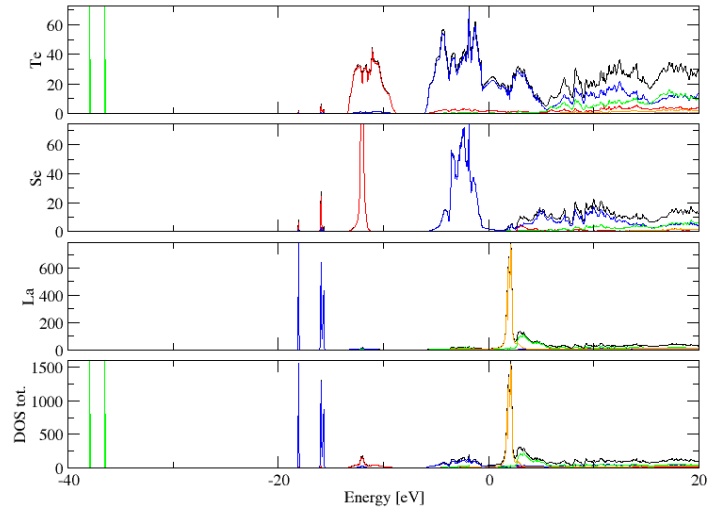
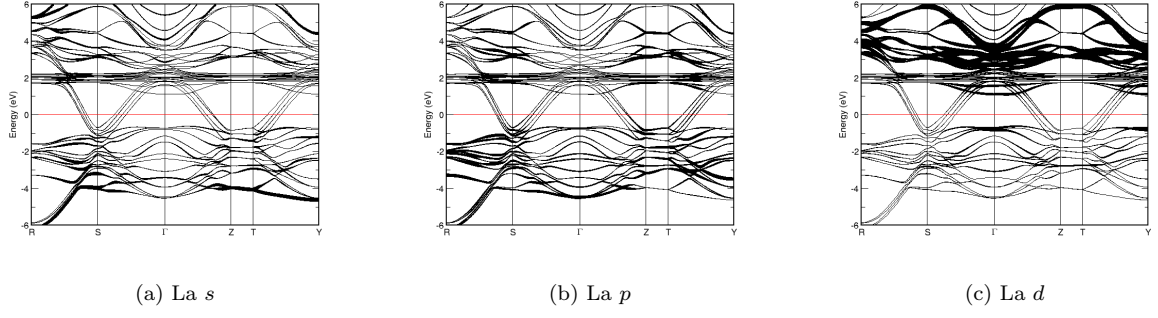
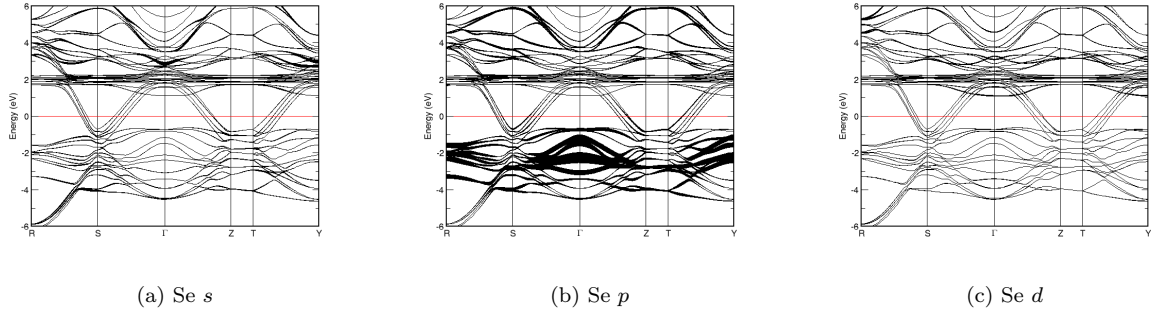
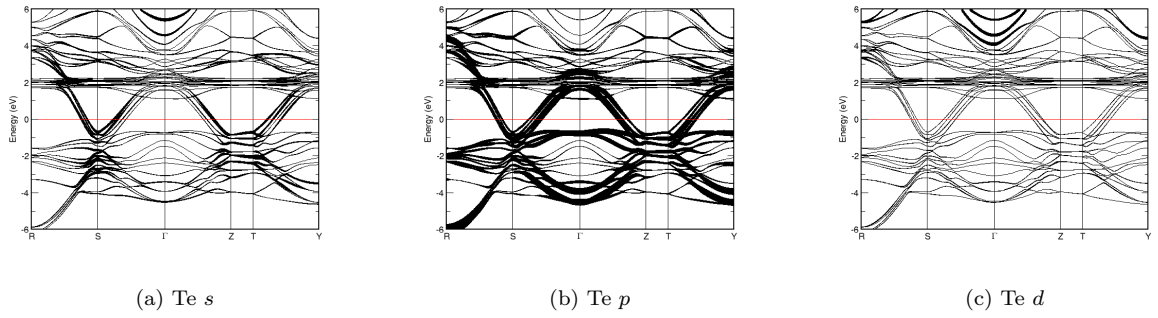


FIG. 110: Fat band representation of S in AgCuS

FIG. 111: (Color online) PDOS of LaSeTe₂ (ICSD #413171). The s -, p - and d -projected states are in red, blue and green, respectively. LaSeTe₂ crystallizes in space group $C m c m$ (#63), in a orthorhombic base-centred structure.

FIG. 112: Fat band representation of La in LaSeTe_2 FIG. 113: Fat band representation of Se in LaSeTe_2 FIG. 114: Fat band representation of Te in LaSeTe_2

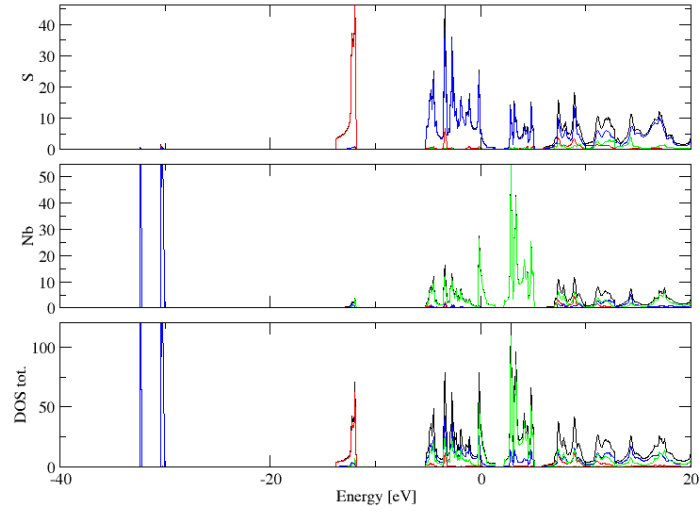


FIG. 115: (Color online) PDOS of NbS₂ (ICSD #67443). The *s*-, *p*- and *d*-projected states are in red, blue and green, respectively. NbS₂ crystallizes in space group C m 2 m (#38), in a orthorhombic base-centred structure.

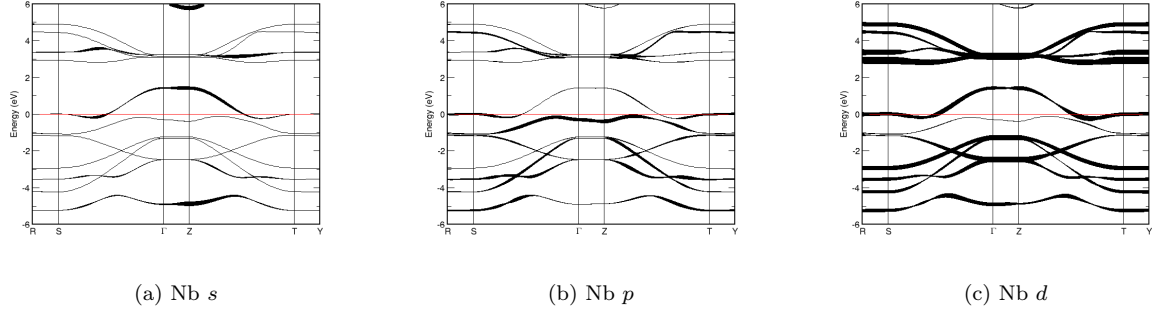


FIG. 116: Fat band representation of Nb in NbS₂

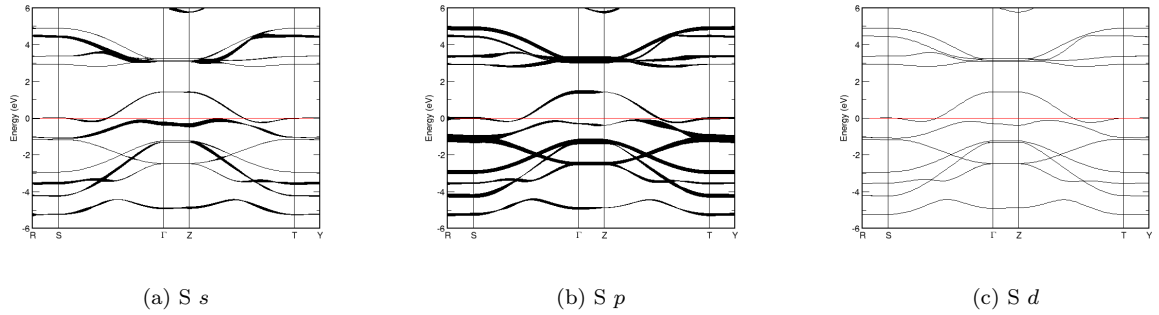


FIG. 117: Fat band representation of S in NbS₂

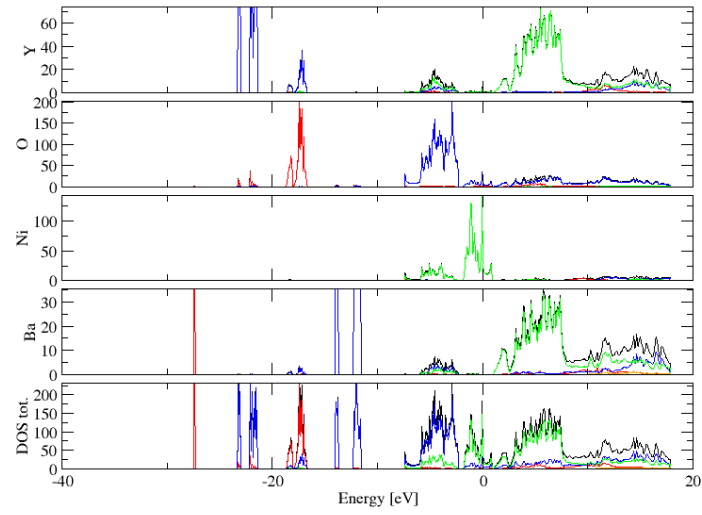


FIG. 118: (Color online) PDOS of BaNiY_2O_5 (ICSD #68795). The s -, p - and d -projected states are in red, blue and green, respectively. BaNiY_2O_5 crystallizes in space group I m m m (#71), in a orthorhombic body-centred structure.

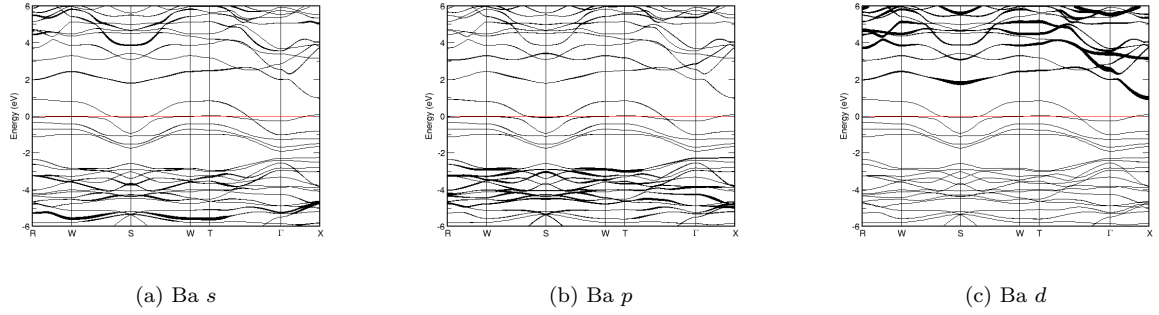


FIG. 119: Fat band representation of Ba in BaNiY_2O_5

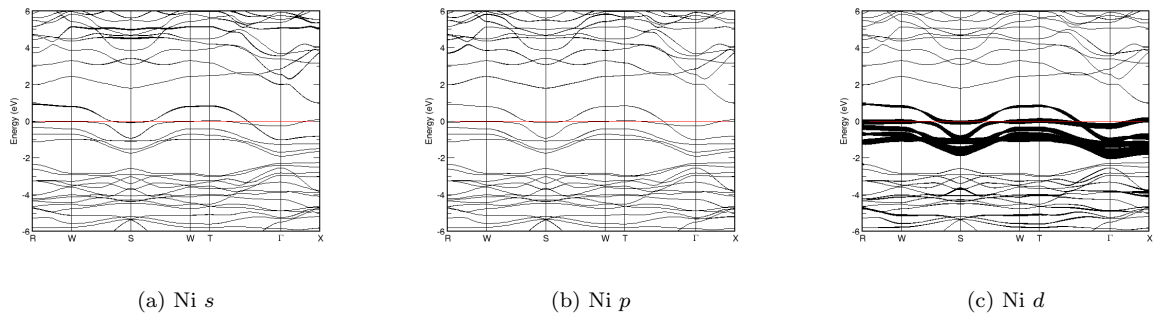
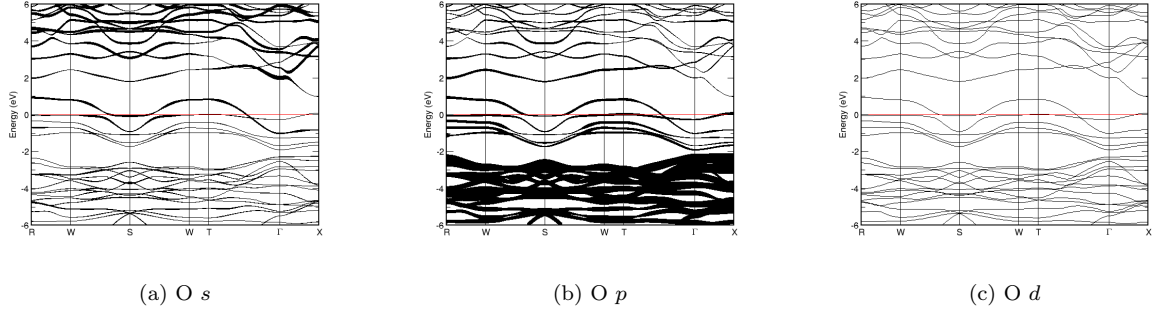
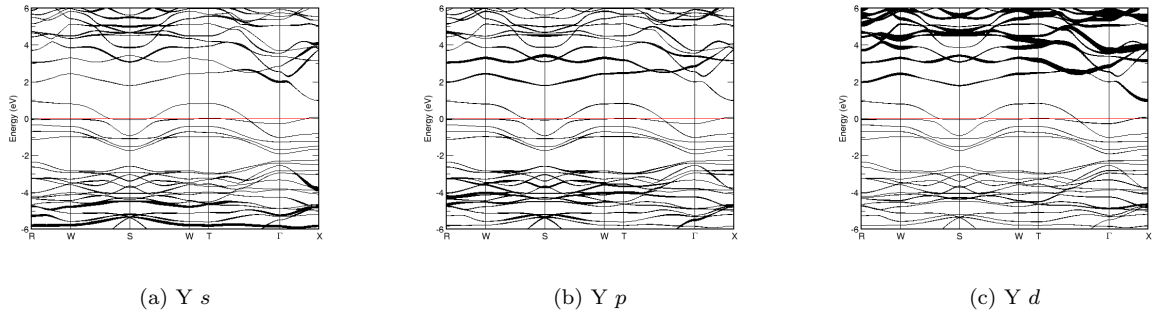
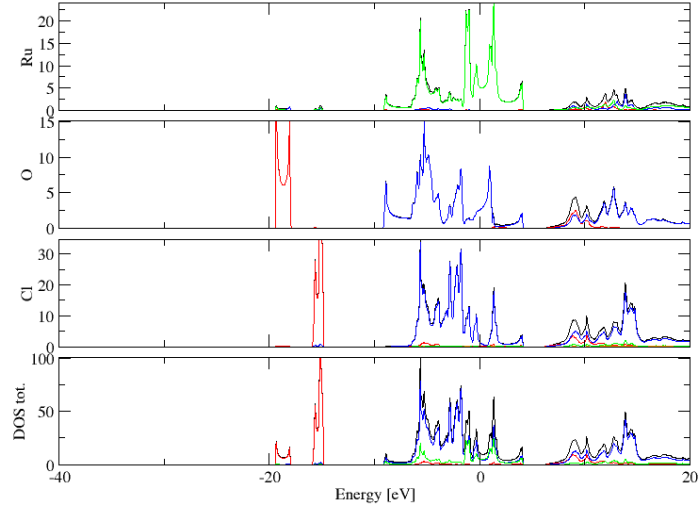
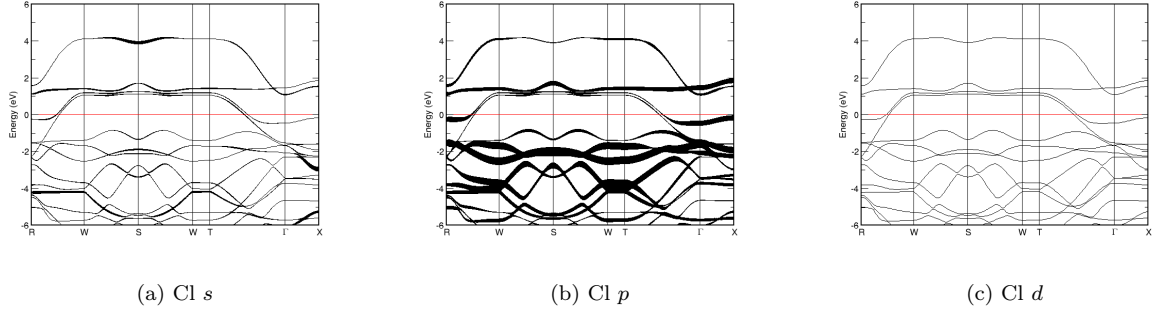
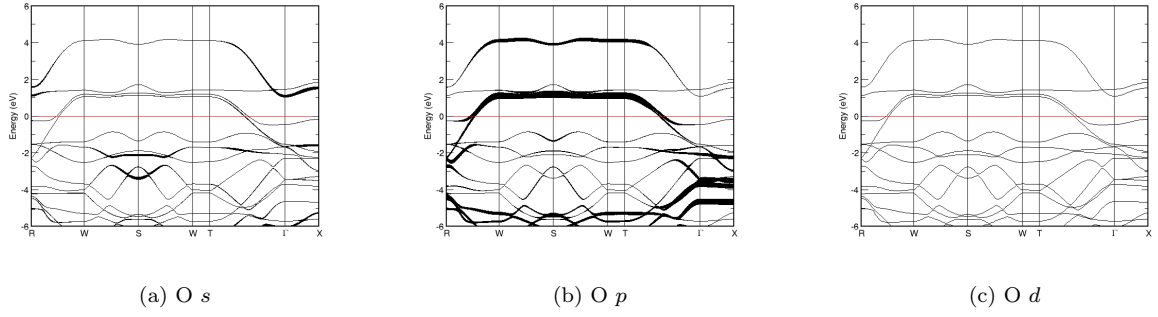
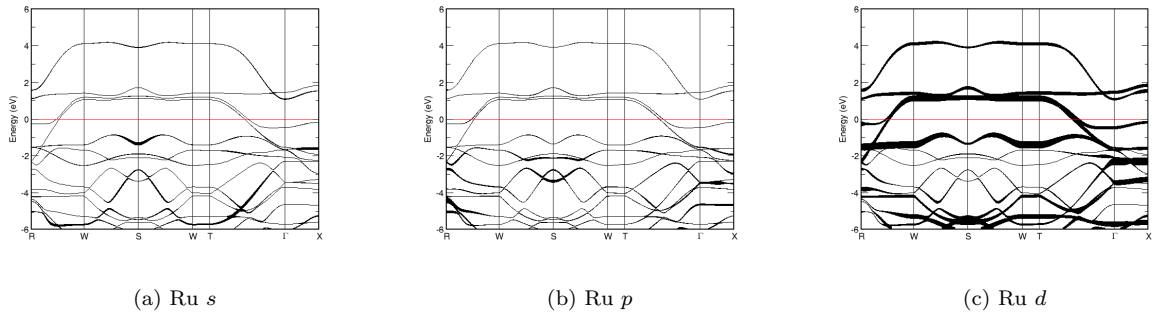


FIG. 120: Fat band representation of Ni in BaNiY_2O_5

FIG. 121: Fat band representation of O in BaNiY₂O₅FIG. 122: Fat band representation of Y in BaNiY₂O₅FIG. 123: (Color online) PDOS of RuOCl₂ (ICSD #83883). The *s*-, *p*- and *d*-projected states are in red, blue and green, respectively. RuOCl₂ crystallizes in space group I m m m (#71), in a orthorhombic body-centred structure.

FIG. 124: Fat band representation of Cl in RuOCl₂FIG. 125: Fat band representation of O in RuOCl₂FIG. 126: Fat band representation of Ru in RuOCl₂

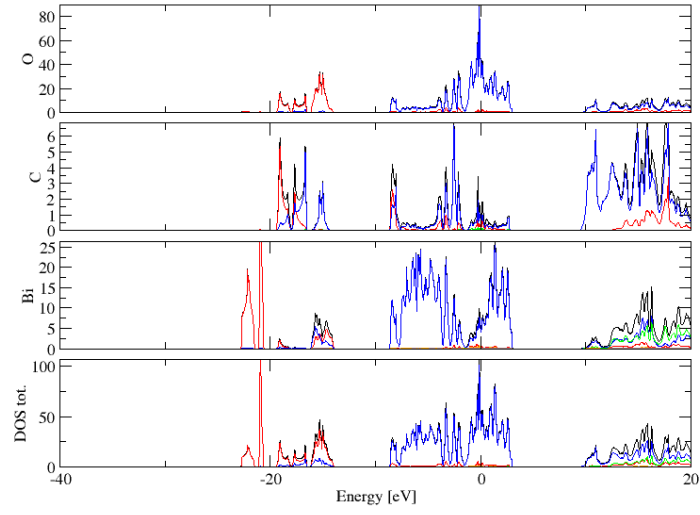


FIG. 127: (Color online) PDOS of $\text{Bi}_2(\text{CO}_3)\text{O}_2$ (ICSD #94740). The s -, p - and d -projected states are in red, blue and green, respectively. $\text{Bi}_2(\text{CO}_3)\text{O}_2$ crystallizes in space group $I m m 2$ (#44), in a orthorhombic body-centred structure.

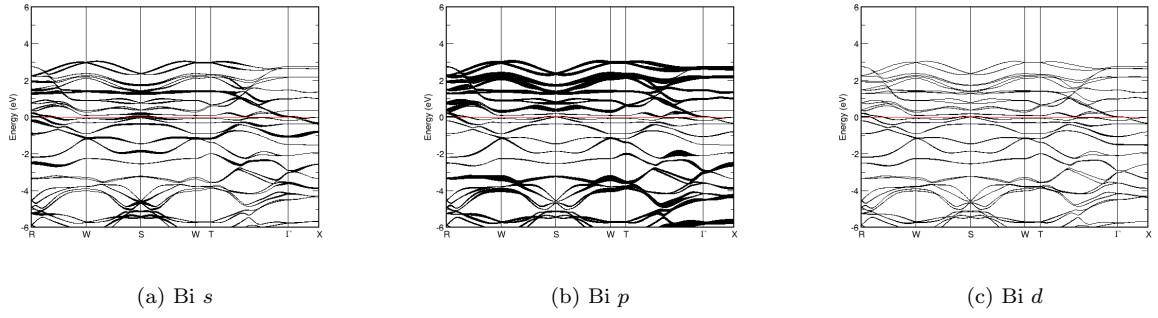


FIG. 128: Fat band representation of Bi in $\text{Bi}_2(\text{CO}_3)\text{O}_2$

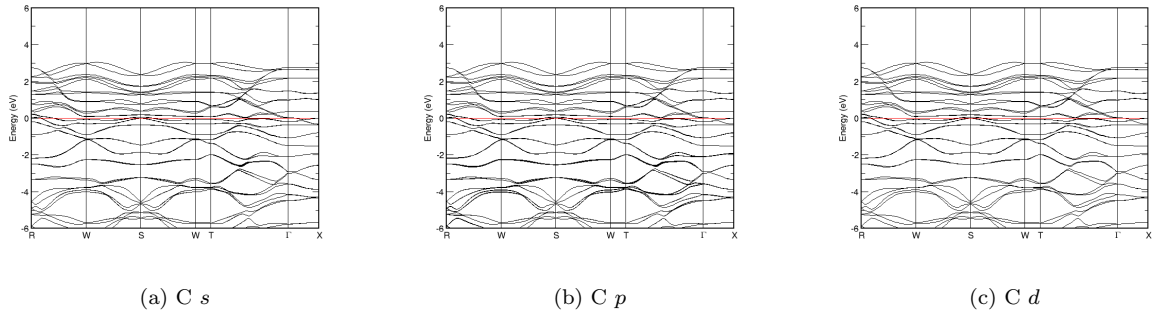
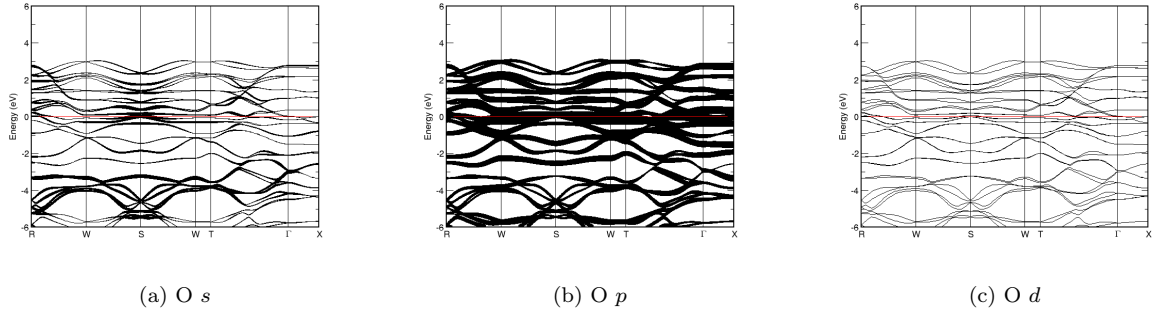
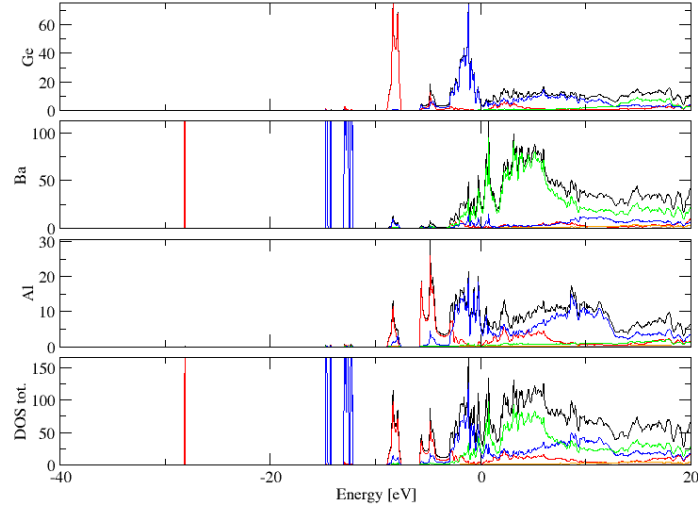
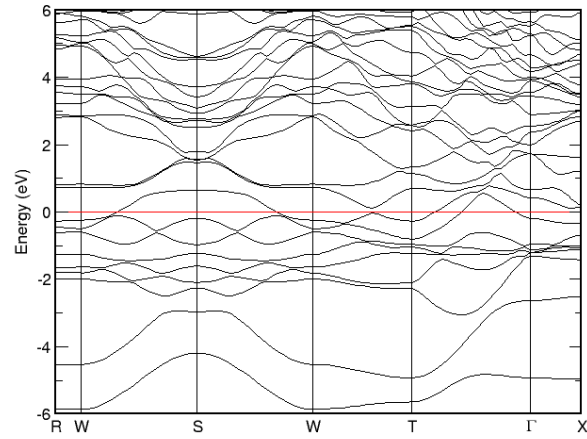


FIG. 129: Fat band representation of C in $\text{Bi}_2(\text{CO}_3)\text{O}_2$

FIG. 130: Fat band representation of O in $\text{Bi}_2(\text{CO}_3)\text{O}_2$ FIG. 131: (Color online) PDOS of $\text{Al}_2\text{Ba}_3\text{Ge}_2$ (ICSD #52612). The s -, p - and d -projected states are in red, blue and green, respectively. $\text{Al}_2\text{Ba}_3\text{Ge}_2$ crystallizes in space group $I m m m$ (#71), in a orthorhombic body-centred structure.(a) E vs. k FIG. 132: Band structure of $\text{Ba}_3\text{Al}_2\text{Sn}_2$

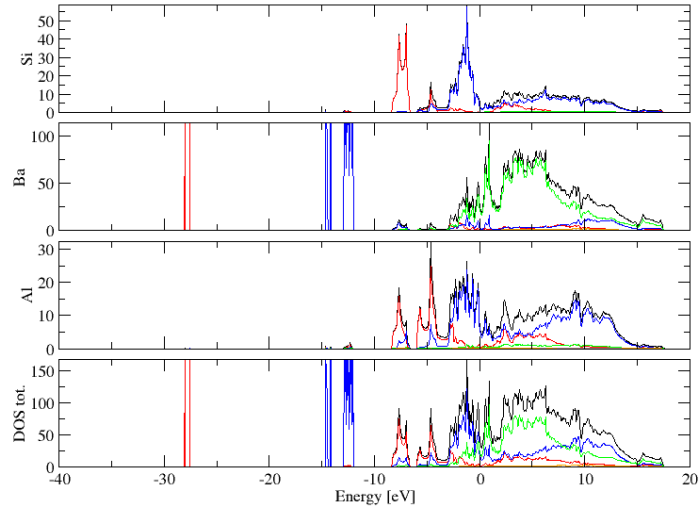


FIG. 133: (Color online) PDOS of $\text{Ba}_3\text{Al}_2\text{Si}_2$ (ICSD #100128). The s -, p - and d -projected states are in red, blue and green, respectively. $\text{Ba}_3\text{Al}_2\text{Si}_2$ crystallizes in space group $I m m m$ (#71), in a orthorhombic body-centred structure.

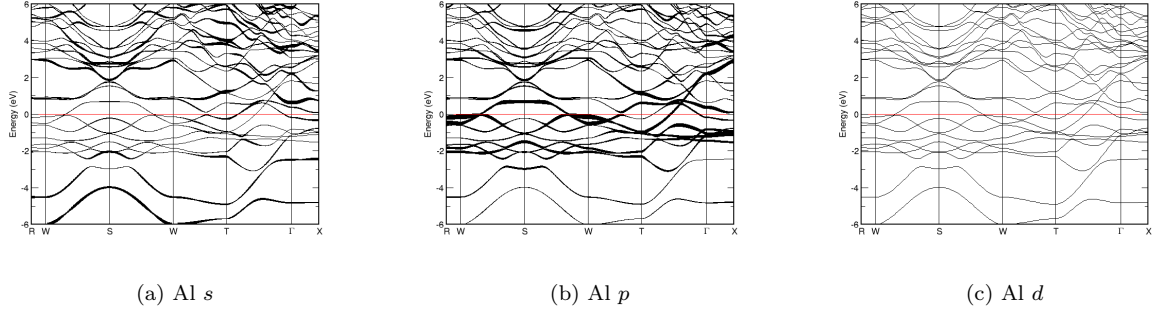


FIG. 134: Fat band representation of Al in $\text{Ba}_3\text{Al}_2\text{Si}_2$

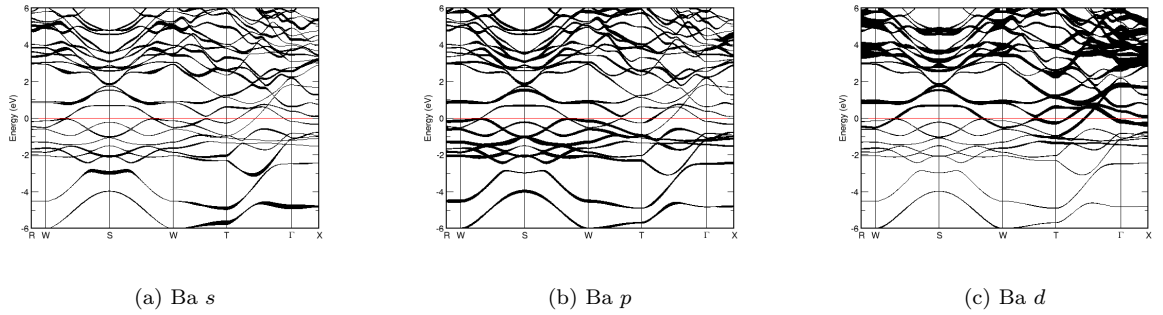
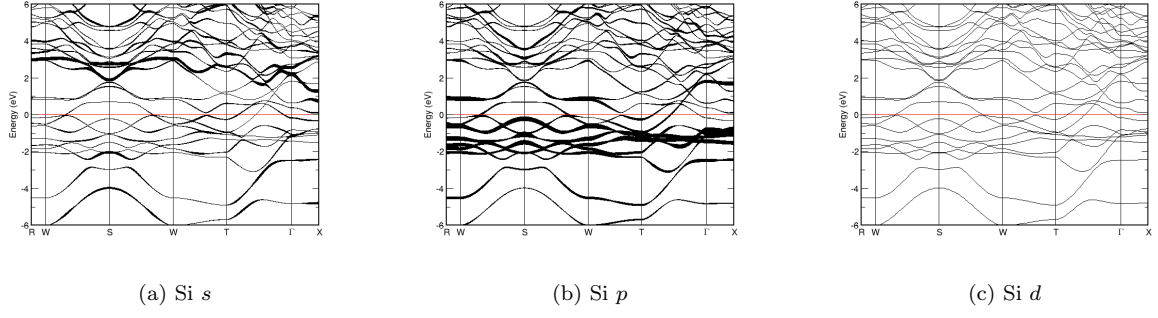
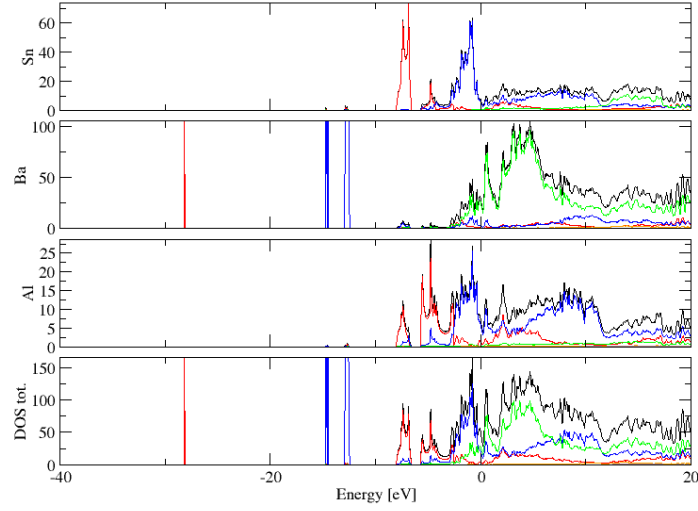
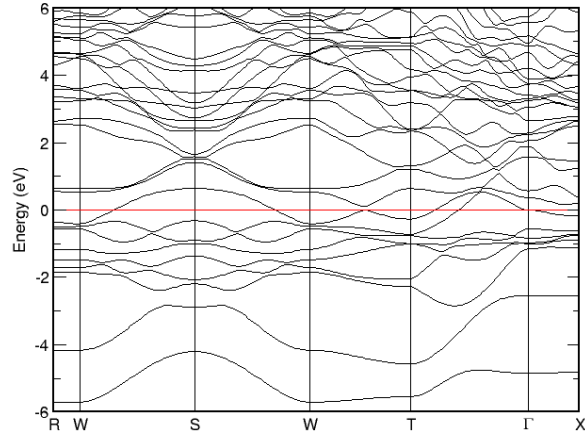


FIG. 135: Fat band representation of Ba in $\text{Ba}_3\text{Al}_2\text{Si}_2$

FIG. 136: Fat band representation of Si in $\text{Ba}_3\text{Al}_2\text{Si}_2$ FIG. 137: (Color online) PDOS of $\text{Ba}_3\text{Al}_2\text{Sn}_2$ (ICSD #9565). The *s*-, *p*- and *d*-projected states are in red, blue and green, respectively. $\text{Ba}_3\text{Al}_2\text{Sn}_2$ crystallizes in space group $I m m m$ (#71), in a orthorhombic body-centred structure.(a) *E vs. k*FIG. 138: Band structure of $\text{Ba}_3\text{Al}_2\text{Sn}_2$

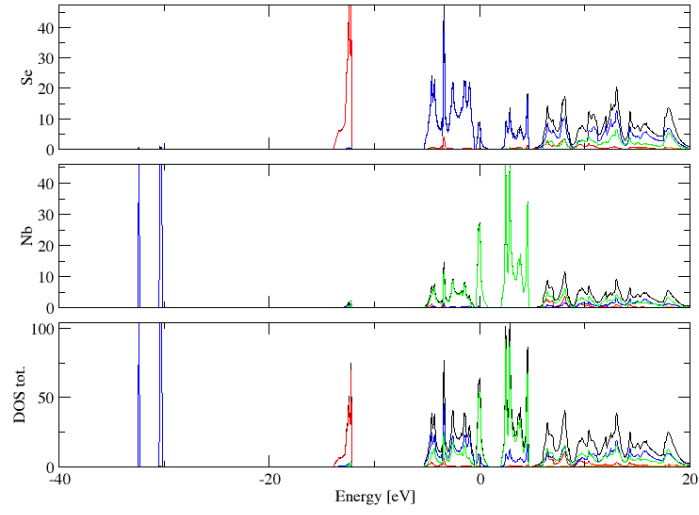


FIG. 139: (Color online) PDOS of NbSe₂ (ICSD #71339). The *s*-, *p*- and *d*-projected states are in red, blue and green, respectively. NbSe₂ crystallizes in space group *F m 2 m* (#42), in a orthorhombic face-centred structure.

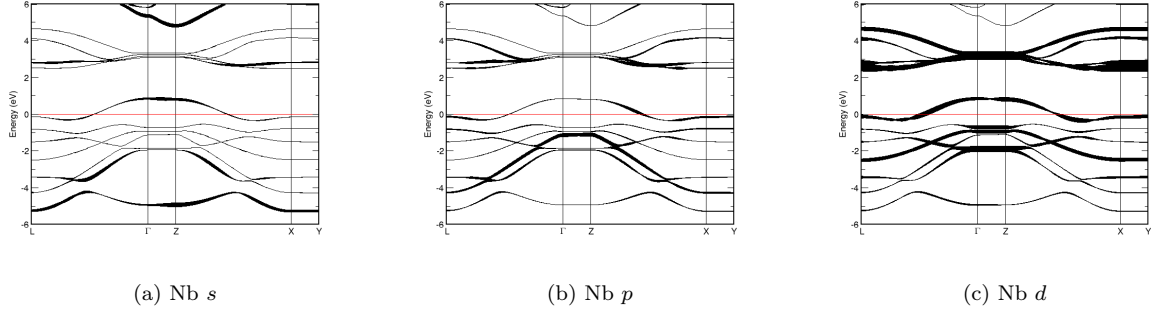


FIG. 140: Fat band representation of Nb in NbSe₂

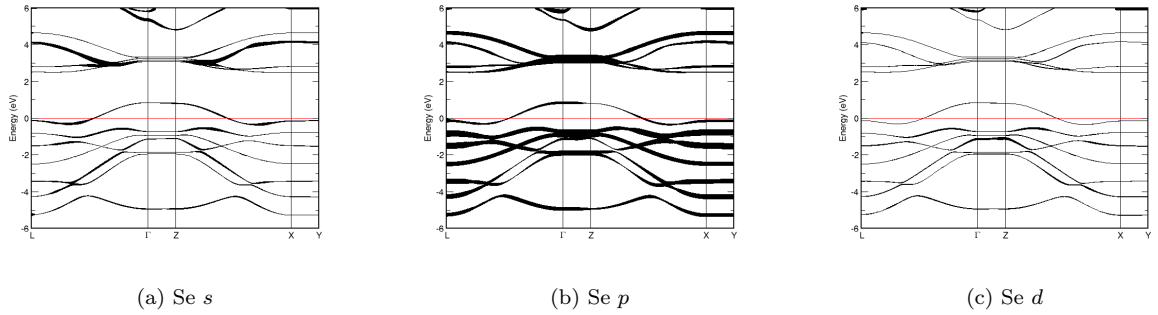


FIG. 141: Fat band representation of Se in NbSe₂

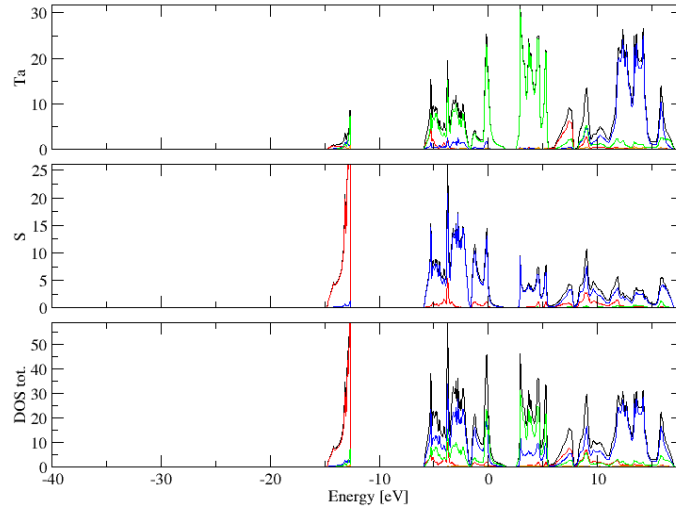


FIG. 142: (Color online) PDOS of TaS₂ (ICSD #280988). The *s*-, *p*- and *d*-projected states are in red, blue and green, respectively. TaS₂ crystallizes in space group F m 2 m (#42), in a orthorhombic face-centred structure.

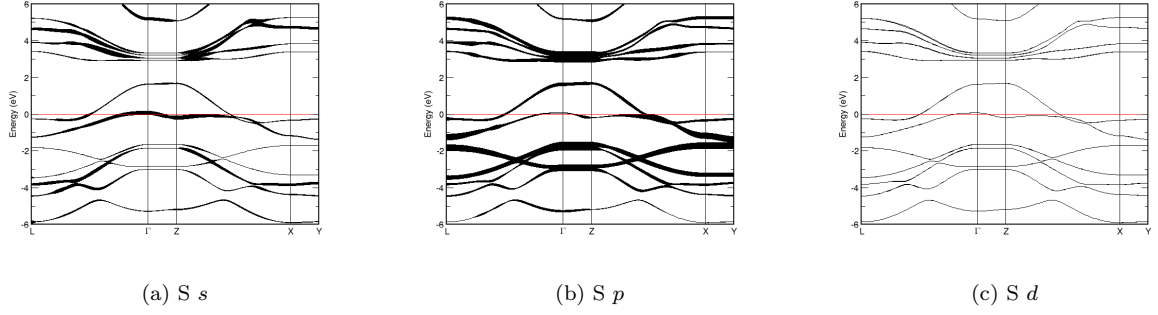


FIG. 143: Fat band representation of S in TaS₂

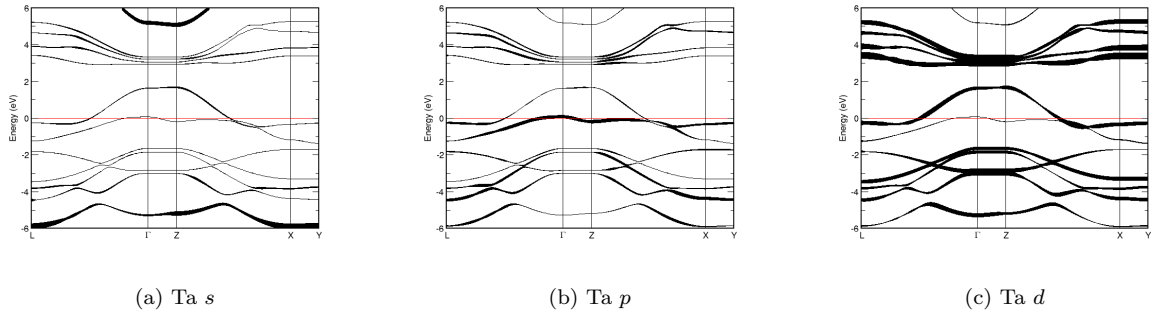


FIG. 144: Fat band representation of Ta in TaS₂

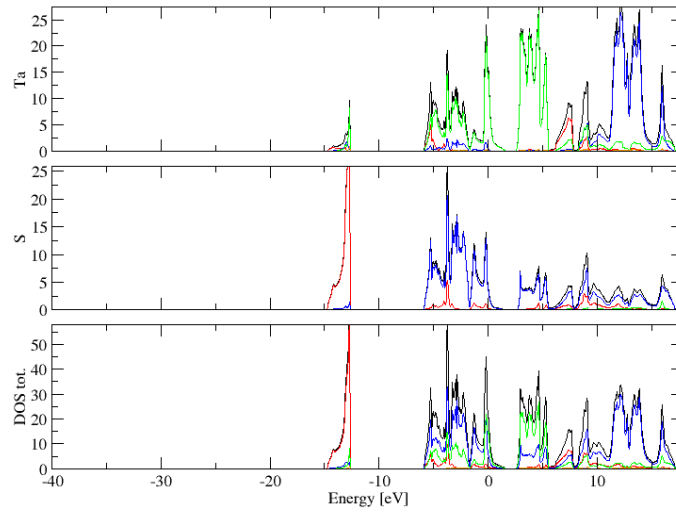


FIG. 145: (Color online) PDOS of TaS₂ (ICSD #67651). The *s*-, *p*- and *d*-projected states are in red, blue and green, respectively. TaS₂ crystallizes in space group *F* 2 *m* *m* (#42), in a orthorhombic face-centred structure.

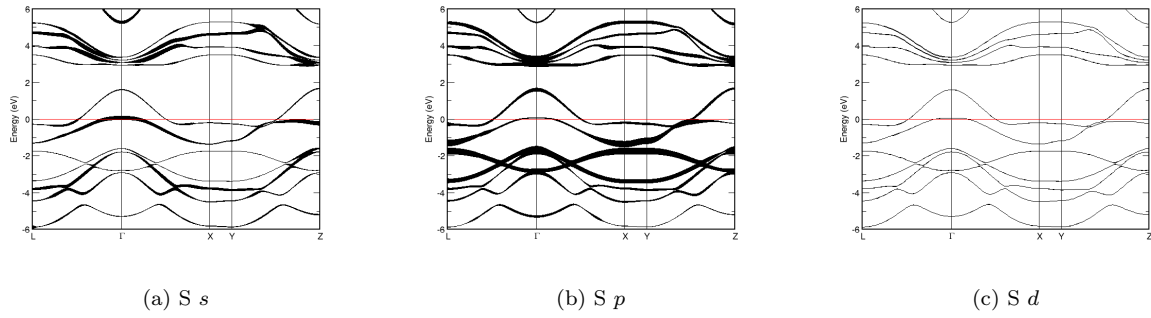


FIG. 146: Fat band representation of S in TaS₂

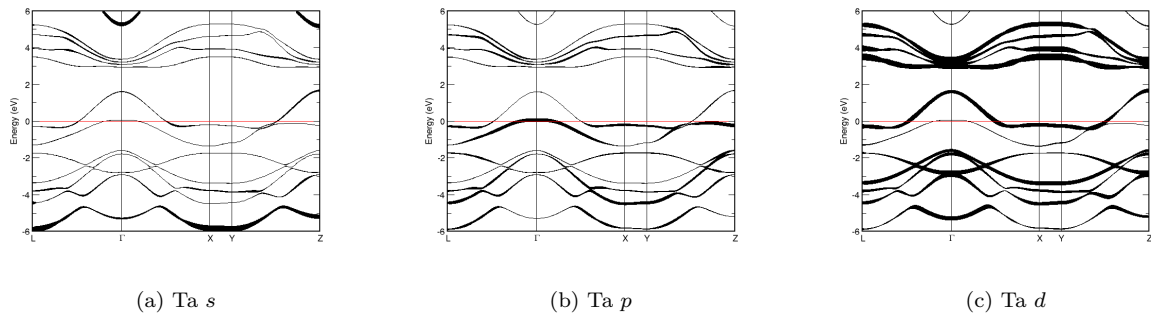


FIG. 147: Fat band representation of Ta in TaS₂

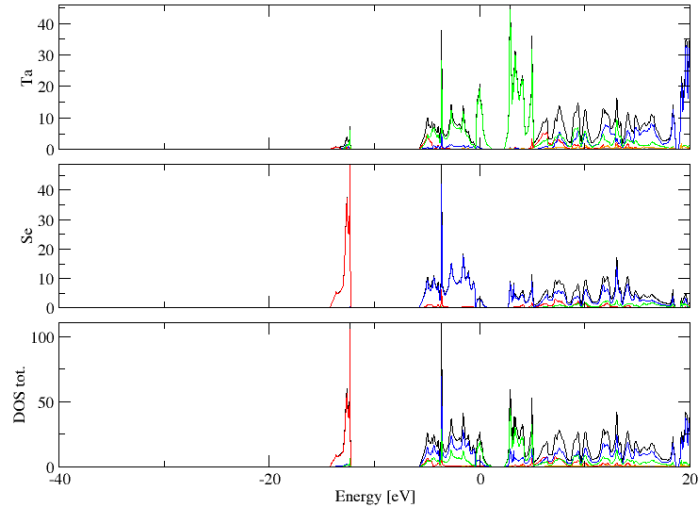


FIG. 148: (Color online) PDOS of TaSe₂ (ICSD #72198). The *s*-, *p*- and *d*-projected states are in red, blue and green, respectively. TaSe₂ crystallizes in space group *F m 2 m* (#42), in a orthorhombic face-centred structure.

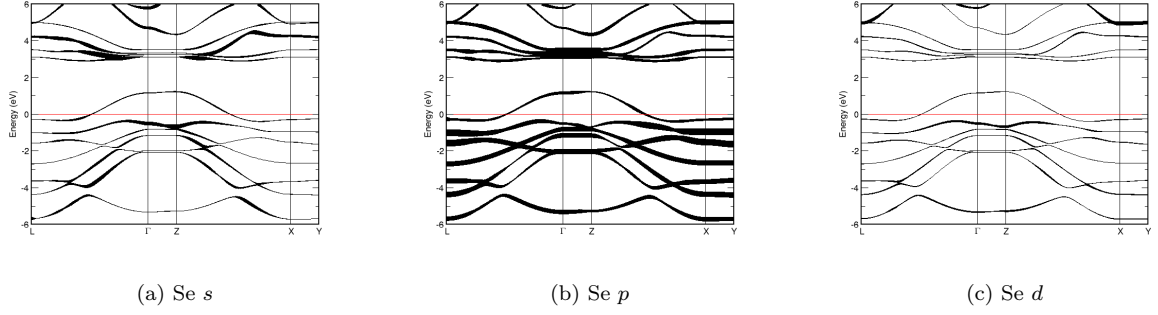


FIG. 149: Fat band representation of Se in TaSe₂

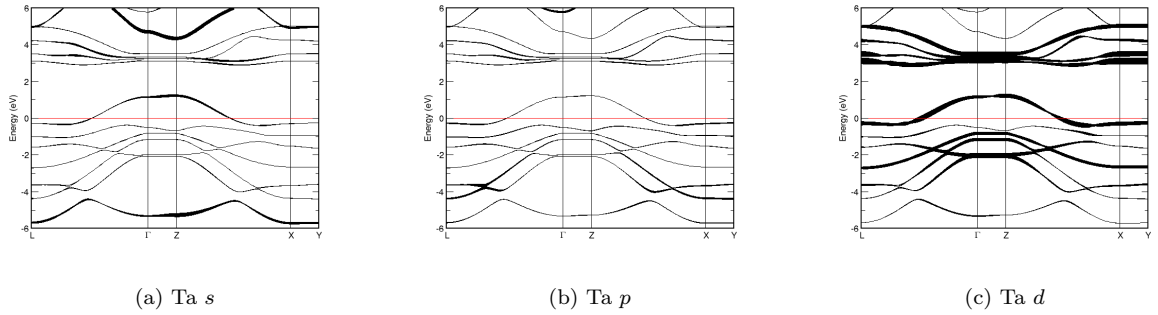


FIG. 150: Fat band representation of Ta in TaSe₂

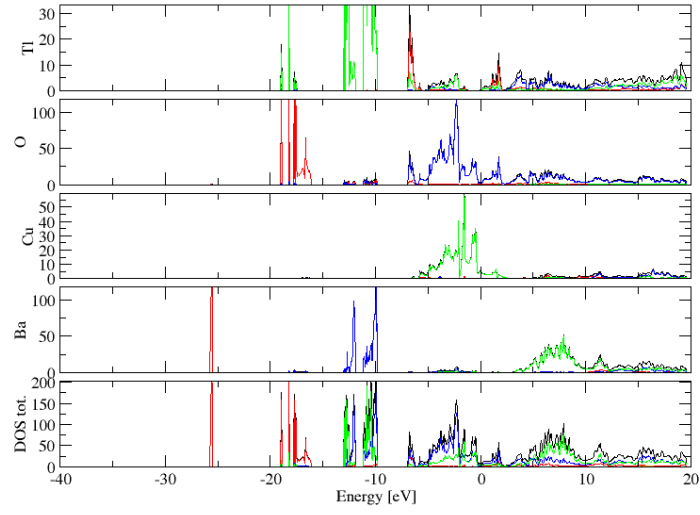


FIG. 151: (Color online) PDOS of $\text{Tl}_2\text{Ba}_2\text{CuO}_6$ (ICSD #41569). The s -, p - and d -projected states are in red, blue and green, respectively. $\text{Tl}_2\text{Ba}_2\text{CuO}_6$ crystallizes in space group $F m m m$ (#69), in a orthorhombic face-centred structure.

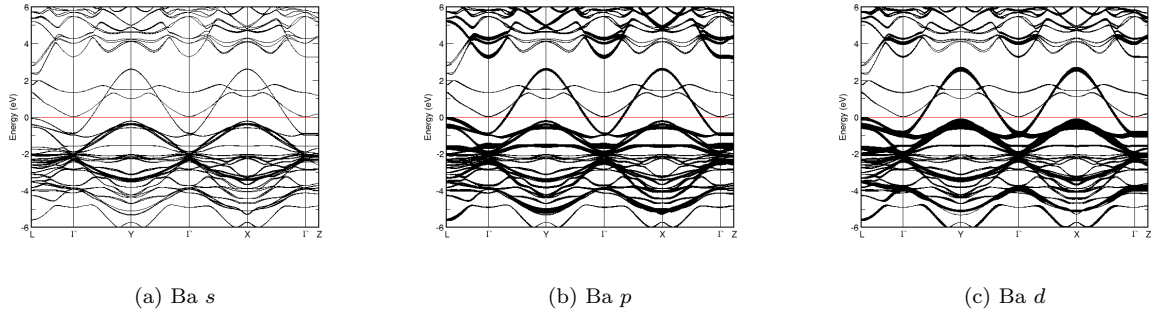


FIG. 152: Fat band representation of Ba in $\text{Tl}_2\text{Ba}_2\text{CuO}_6$

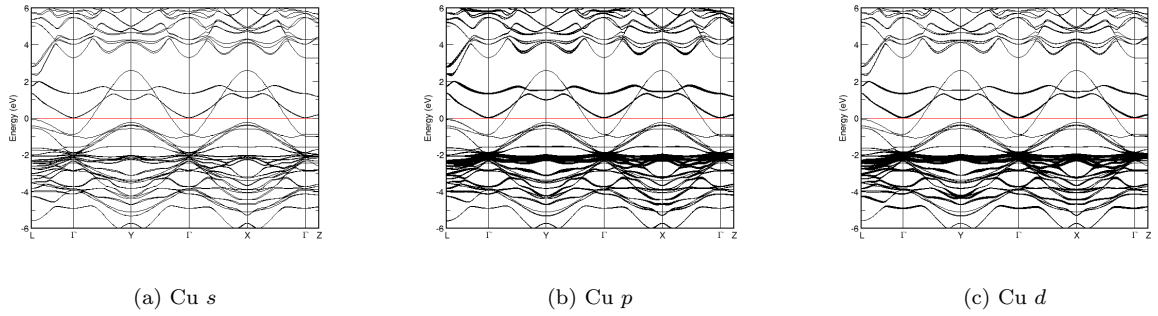
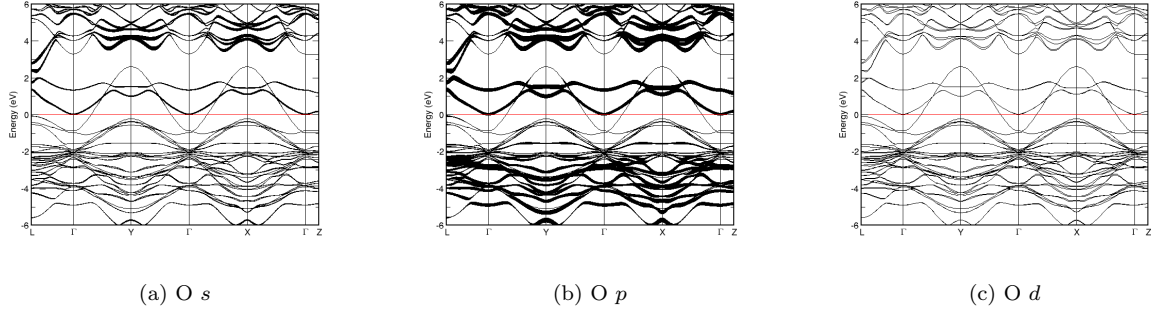
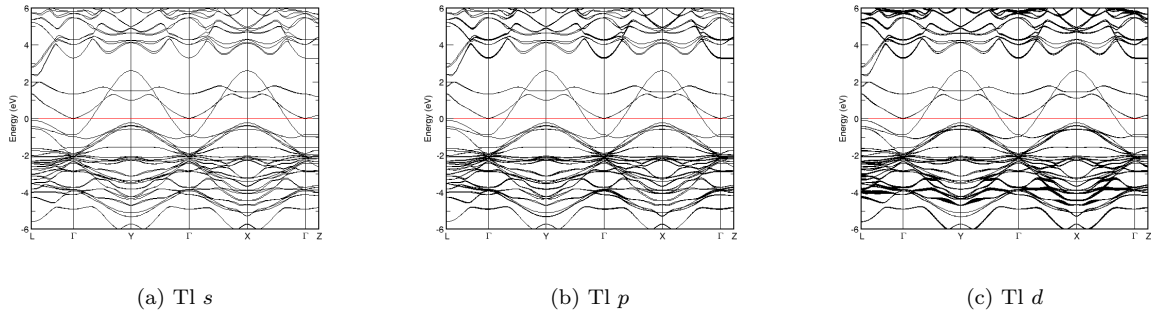
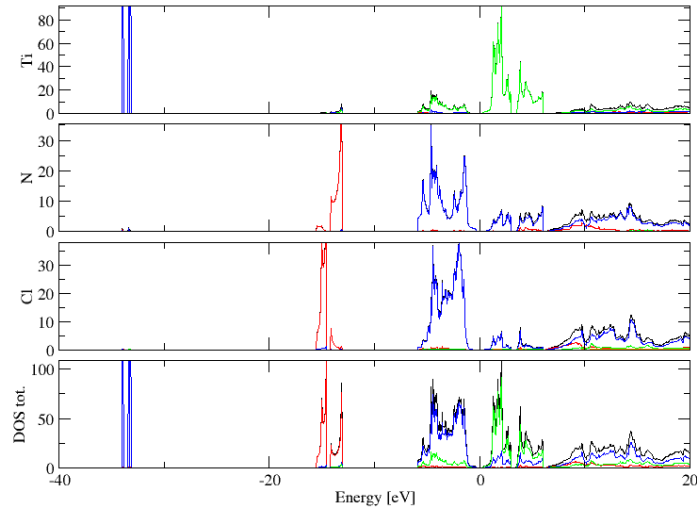


FIG. 153: Fat band representation of Cu in $\text{Tl}_2\text{Ba}_2\text{CuO}_6$

FIG. 154: Fat band representation of O in $\text{Tl}_2\text{Ba}_2\text{CuO}_6$ FIG. 155: Fat band representation of Tl in $\text{Tl}_2\text{Ba}_2\text{CuO}_6$ FIG. 156: (Color online) PDOS of TiNCI (ICSD #27396). The *s*-, *p*- and *d*-projected states are in red, blue and green, respectively. TiNCI crystallizes in space group $P m m n$ (#59), in a orthorhombic primitive structure.

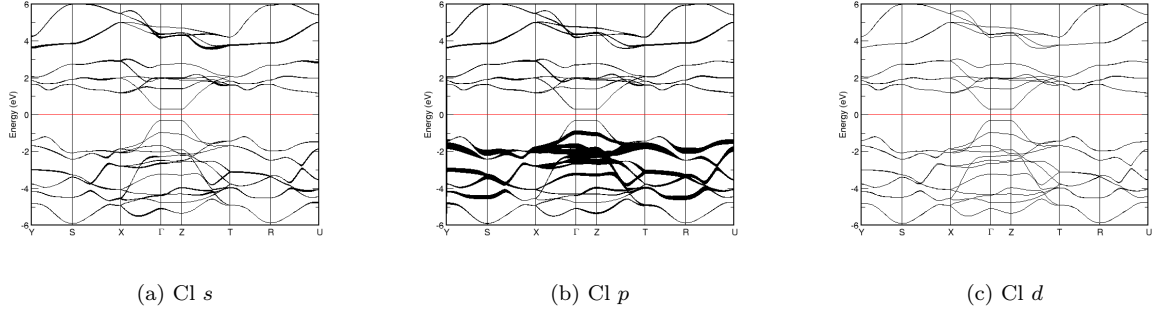


FIG. 157: Fat band representation of Cl in TiNCl

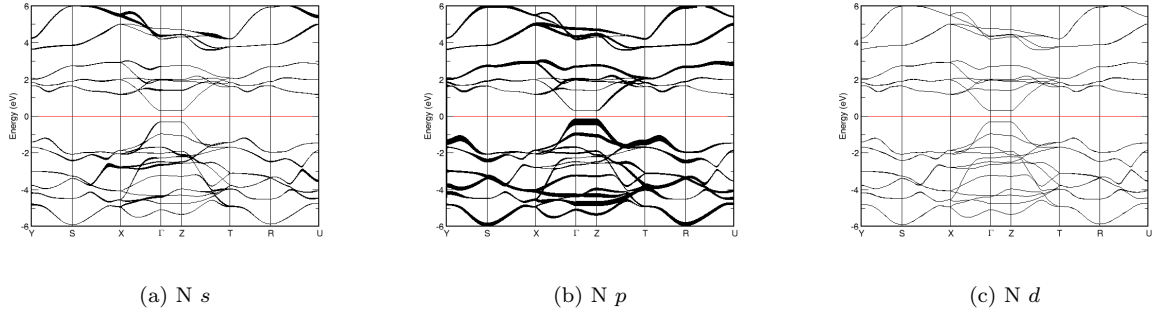


FIG. 158: Fat band representation of N in TiNCl

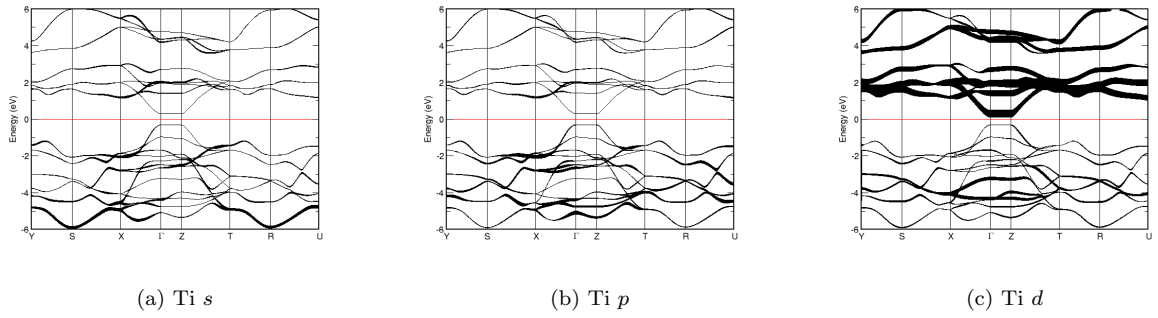


FIG. 159: Fat band representation of Ti in TiNCl

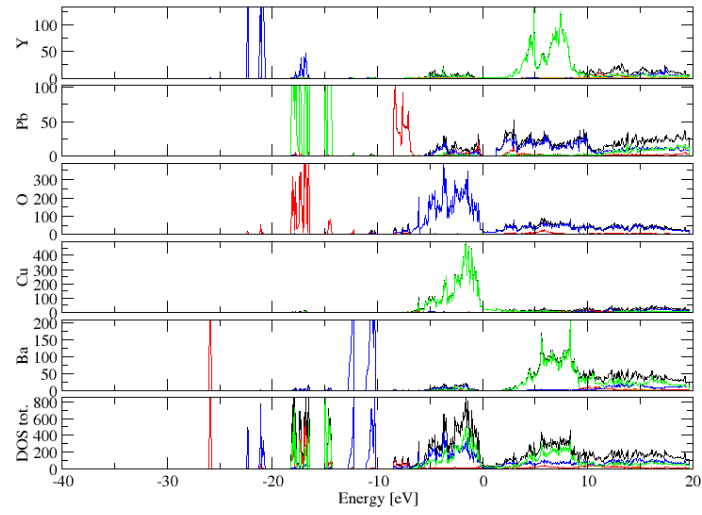
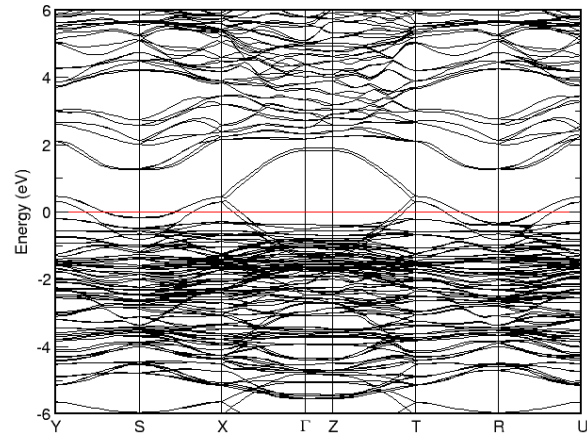


FIG. 160: (Color online) PDOS of $\text{Pb}_2\text{Ba}_2\text{YCuCu}_2\text{O}_8$ (ICSD #66088). The s -, p - and d -projected states are in red, blue and green, respectively. $\text{Pb}_2\text{Ba}_2\text{YCuCu}_2\text{O}_8$ crystallizes in space group $P 2_1 2_1 2$ (#17), in a orthorhombic primitive structure.



(a) E vs. k

FIG. 161: Band structure of $\text{Pb}_2\text{Ba}_2\text{YCuCu}_2\text{O}_8$

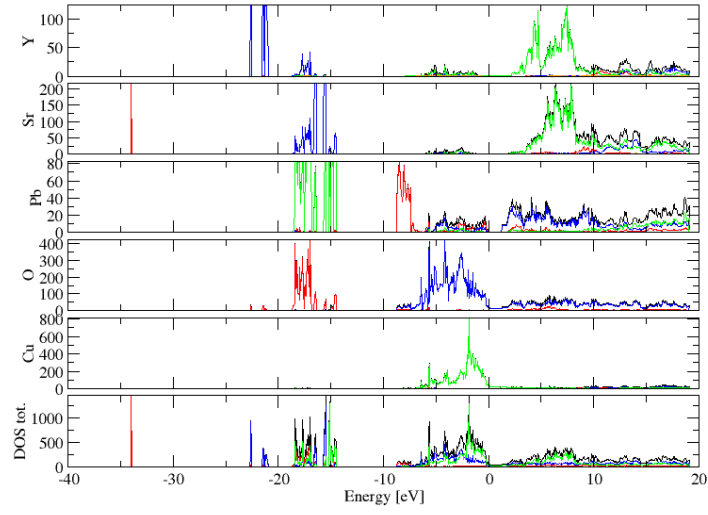
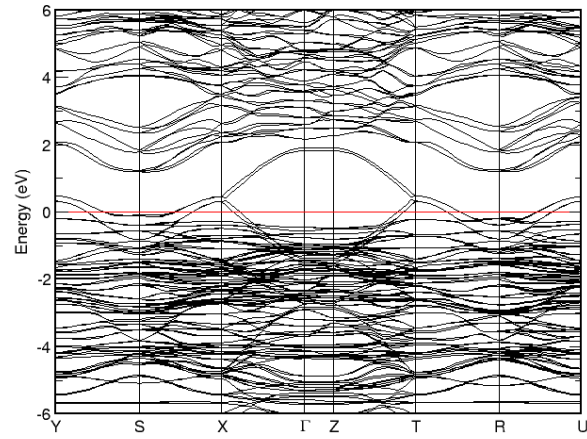


FIG. 162: (Color online) PDOS of $\text{Pb}_2\text{Sr}_2\text{YCu}_3\text{O}_8$ (ICSD #66587). The s -, p - and d -projected states are in red, blue and green, respectively. $\text{Pb}_2\text{Sr}_2\text{YCu}_3\text{O}_8$ crystallizes in space group $P 2_1 2$ (#17), in a orthorhombic primitive structure.



(a) E vs. k

FIG. 163: Band structure of $\text{Pb}_2\text{Sr}_2\text{YCu}_3\text{O}_8$

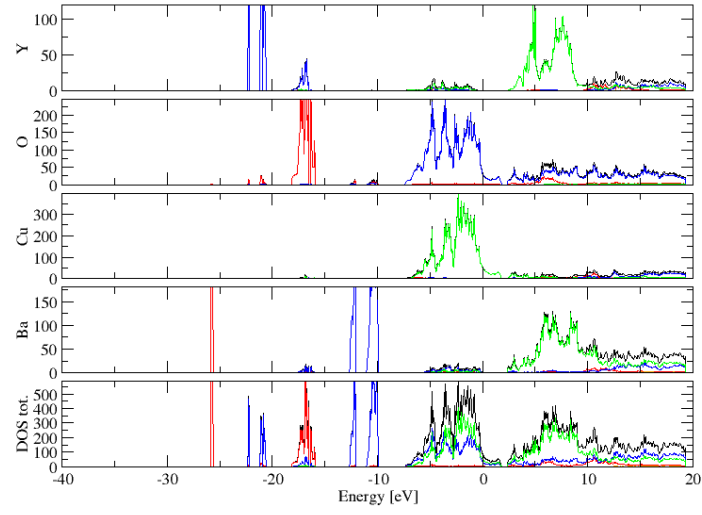
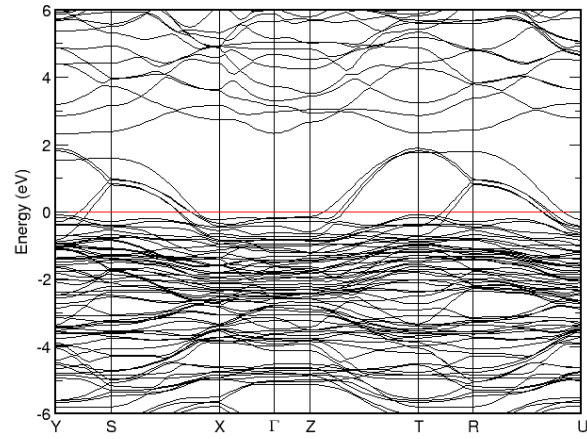


FIG. 164: (Color online) PDOS of $\text{YBa}_2\text{Cu}_3\text{O}_{6.5}$ (ICSD #75697). The s -, p - and d -projected states are in red, blue and green, respectively. $\text{YBa}_2\text{Cu}_3\text{O}_{6.5}$ crystallizes in space group $P m m m$ (#47), in a orthorhombic primitive structure.



(a) E vs. k

FIG. 165: Band structure of $\text{YBa}_2\text{Cu}_3\text{O}_{6.5}$

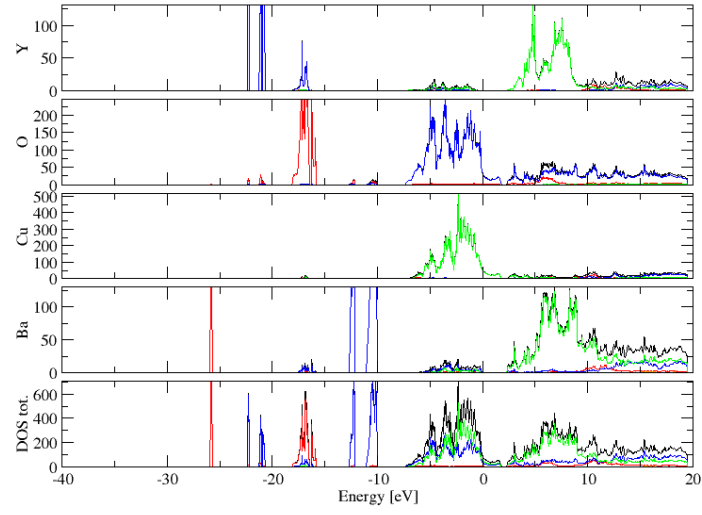
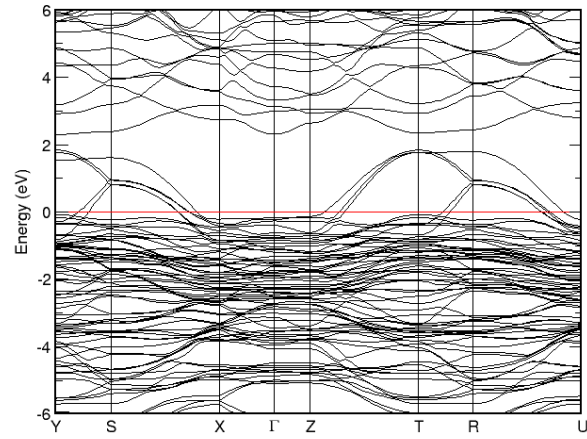


FIG. 166: (Color online) PDOS of $\text{YBa}_2\text{Cu}_3\text{O}_{6.5}$ (ICSD #96016). The s -, p - and d -projected states are in red, blue and green, respectively. $\text{YBa}_2\text{Cu}_3\text{O}_{6.5}$ crystallizes in space group $P m m m$ (#47), in a orthorhombic primitive structure.



(a) E vs. k

FIG. 167: Band structure of $\text{YBa}_2\text{Cu}_3\text{O}_{6.5}$

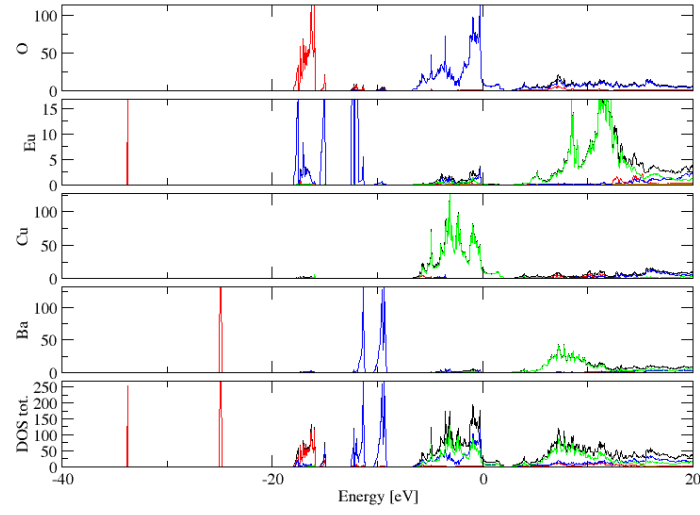


FIG. 168: (Color online) PDOS of $\text{EuBa}_2\text{Cu}_3\text{O}_7$ (ICSD #81171). The s -, p - and d -projected states are in red, blue and green, respectively. $\text{EuBa}_2\text{Cu}_3\text{O}_7$ crystallizes in space group $P m m m$ (#47), in a orthorhombic primitive structure.

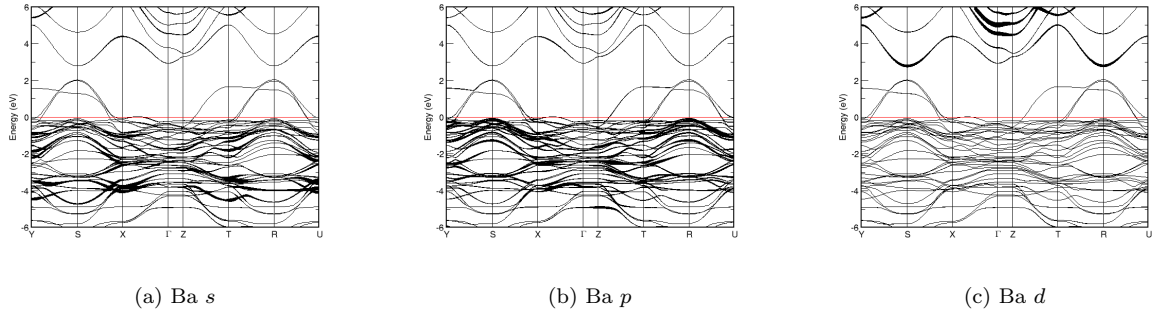


FIG. 169: Fat band representation of Ba in $\text{EuBa}_2\text{Cu}_3\text{O}_7$

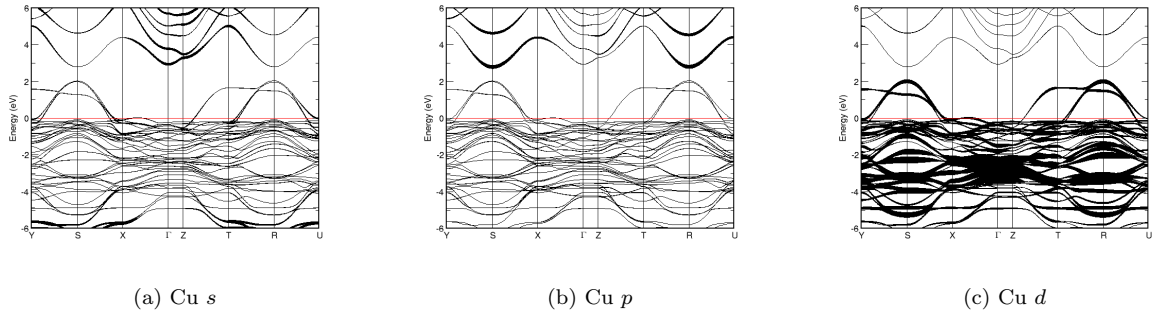


FIG. 170: Fat band representation of Cu in $\text{EuBa}_2\text{Cu}_3\text{O}_7$

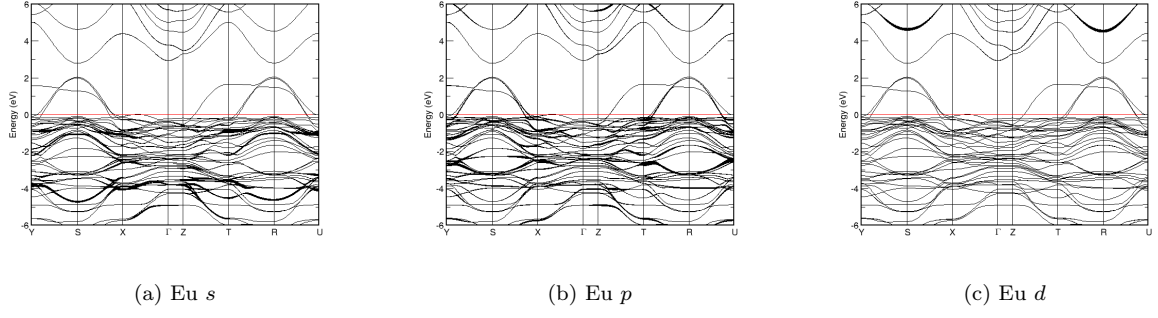
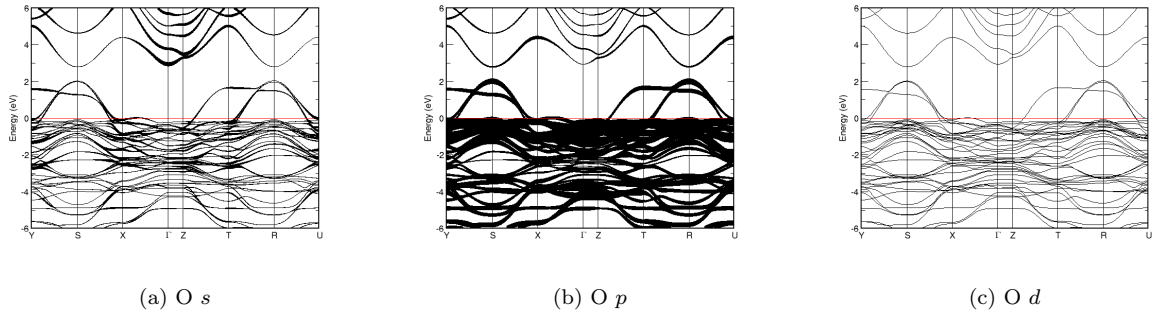
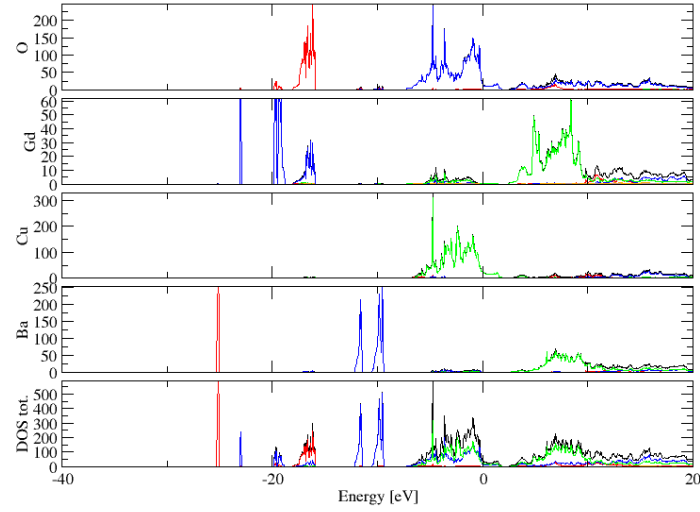
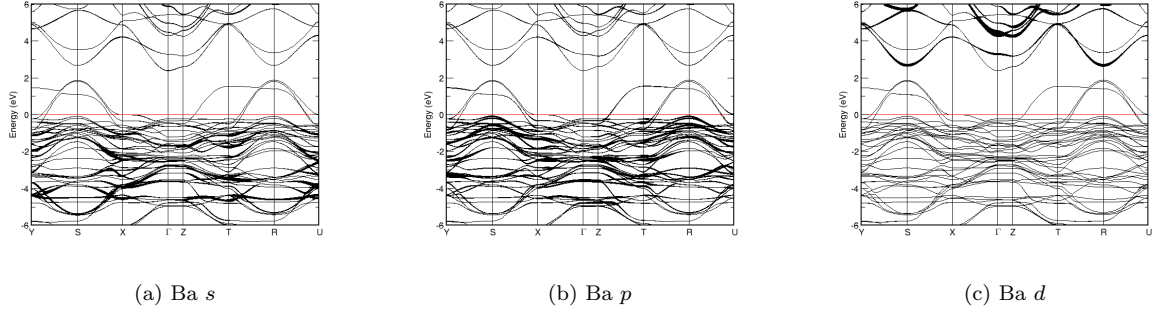
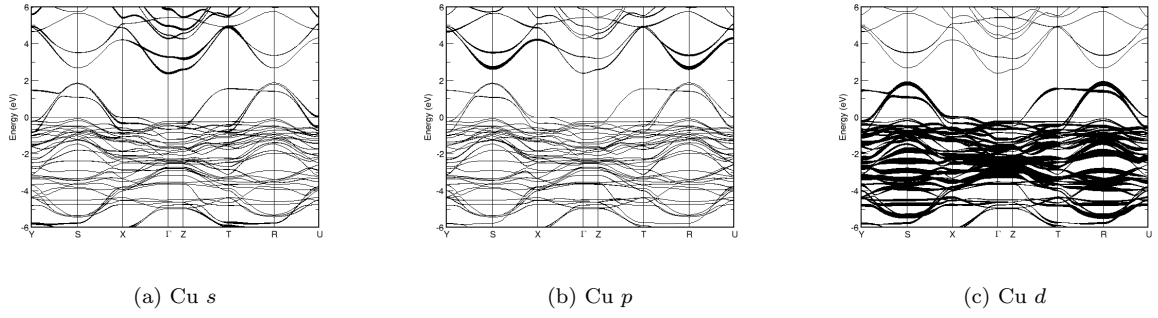
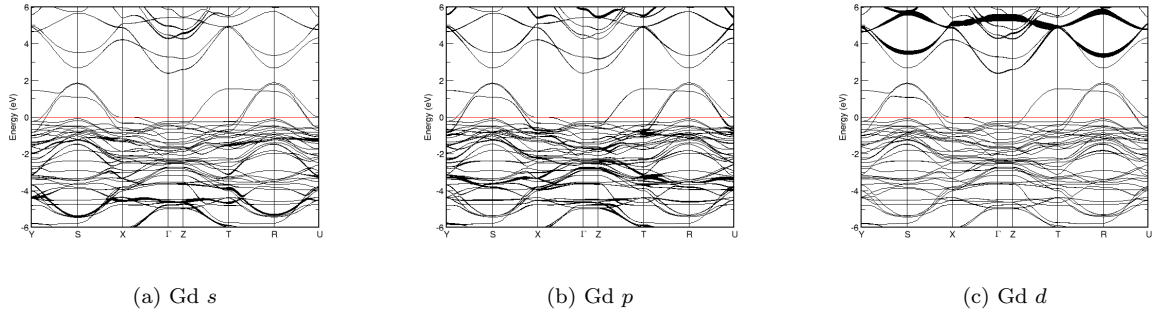
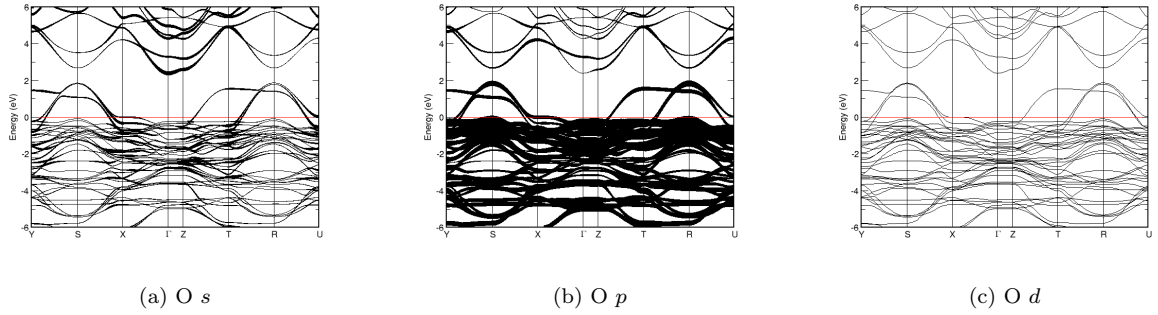
FIG. 171: Fat band representation of Eu in $\text{EuBa}_2\text{Cu}_3\text{O}_7$ FIG. 172: Fat band representation of O in $\text{EuBa}_2\text{Cu}_3\text{O}_7$ 

FIG. 173: (Color online) PDOS of $\text{Ba}_2\text{GdCu}_3\text{O}_7$ (ICSD #56514). The *s*-, *p*- and *d*-projected states are in red, blue and green, respectively. $\text{Ba}_2\text{GdCu}_3\text{O}_7$ crystallizes in space group $P m m m$ (#47), in a orthorhombic primitive structure.

FIG. 174: Fat band representation of Ba in $\text{Ba}_2\text{GdCu}_3\text{O}_7$ FIG. 175: Fat band representation of Cu in $\text{Ba}_2\text{GdCu}_3\text{O}_7$ FIG. 176: Fat band representation of Gd in $\text{Ba}_2\text{GdCu}_3\text{O}_7$ FIG. 177: Fat band representation of O in $\text{Ba}_2\text{GdCu}_3\text{O}_7$

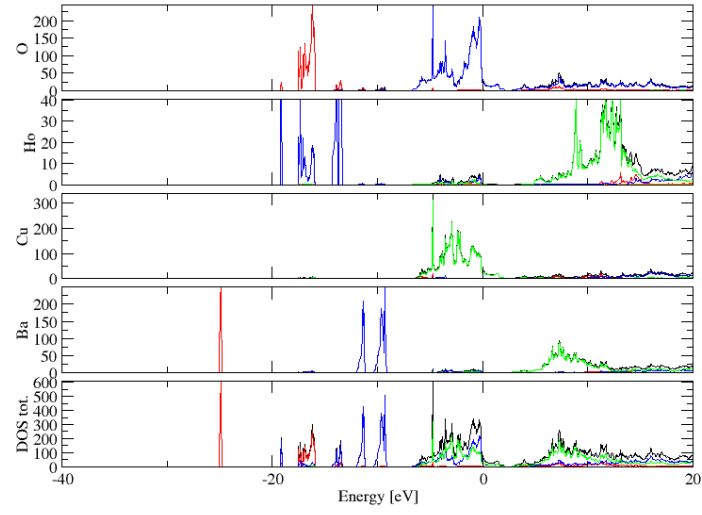


FIG. 178: (Color online) PDOS of $\text{HoBa}_2\text{Cu}_3\text{O}_7$ (ICSD #68044). The s -, p - and d -projected states are in red, blue and green, respectively. $\text{HoBa}_2\text{Cu}_3\text{O}_7$ crystallizes in space group $P m m m$ (#47), in a orthorhombic primitive structure.

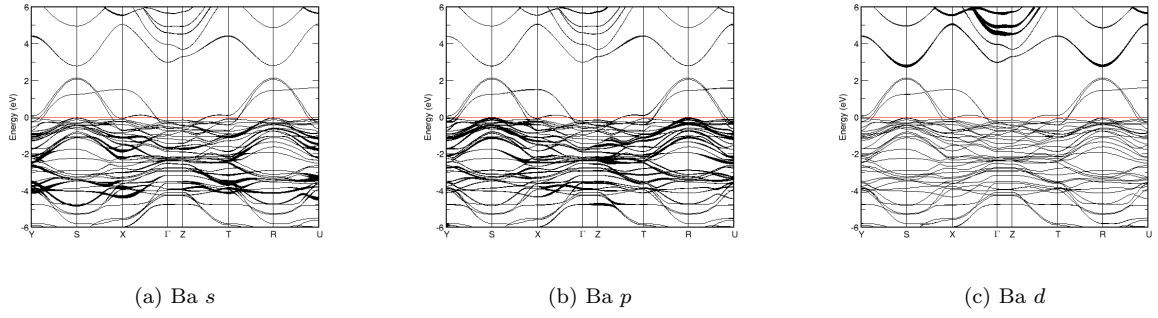


FIG. 179: Fat band representation of Ba in $\text{HoBa}_2\text{Cu}_3\text{O}_7$

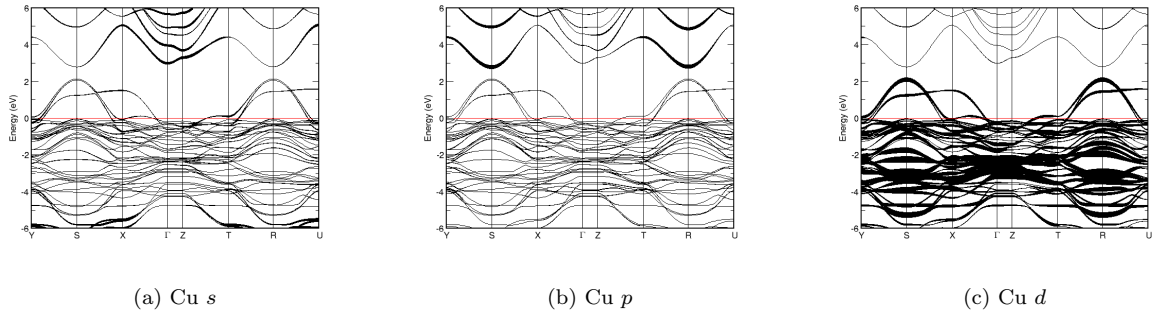
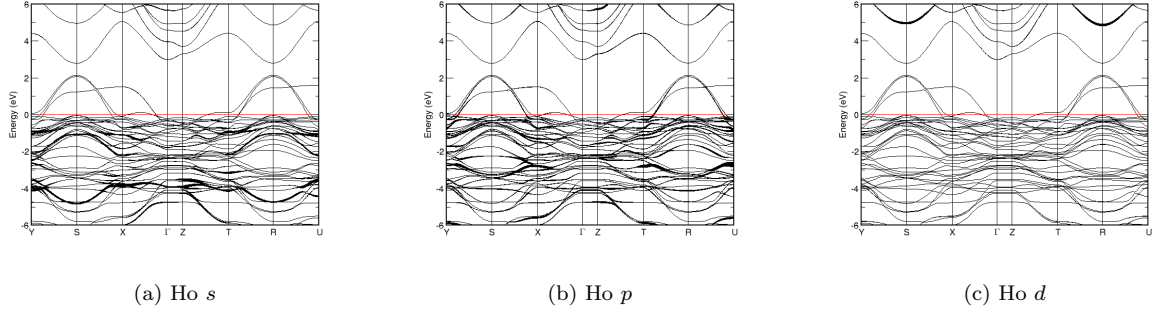
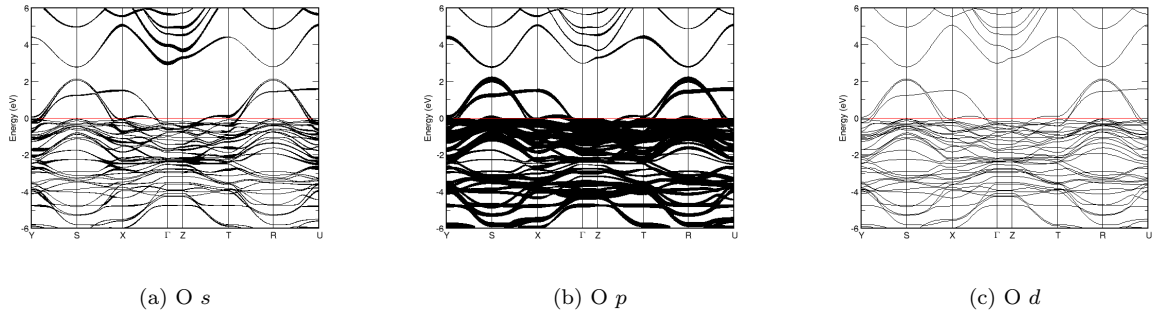
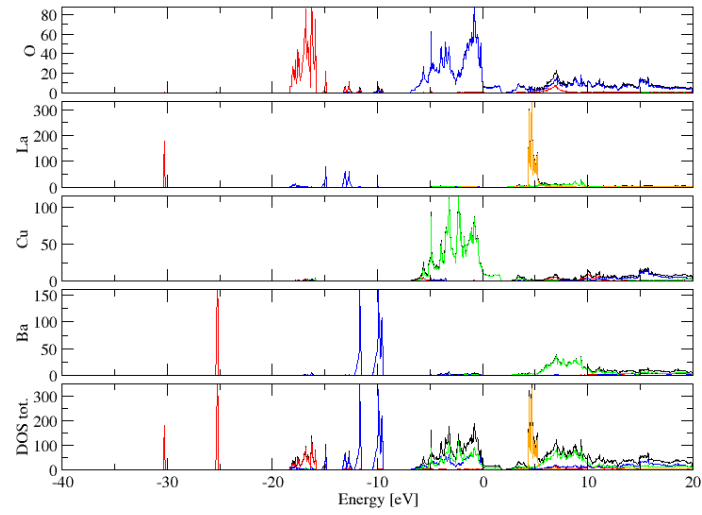


FIG. 180: Fat band representation of Cu in $\text{HoBa}_2\text{Cu}_3\text{O}_7$

FIG. 181: Fat band representation of Ho in $\text{HoBa}_2\text{Cu}_3\text{O}_7$ FIG. 182: Fat band representation of O in $\text{HoBa}_2\text{Cu}_3\text{O}_7$ FIG. 183: (Color online) PDOS of $\text{LaBa}_2\text{Cu}_3\text{O}_7$ (ICSD #81167). The *s*-, *p*- and *d*-projected states are in red, blue and green, respectively. $\text{LaBa}_2\text{Cu}_3\text{O}_7$ crystallizes in space group $P m m m$ (#47), in a orthorhombic primitive structure.

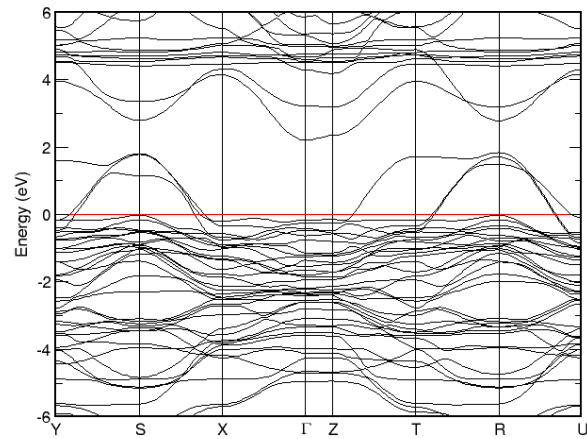
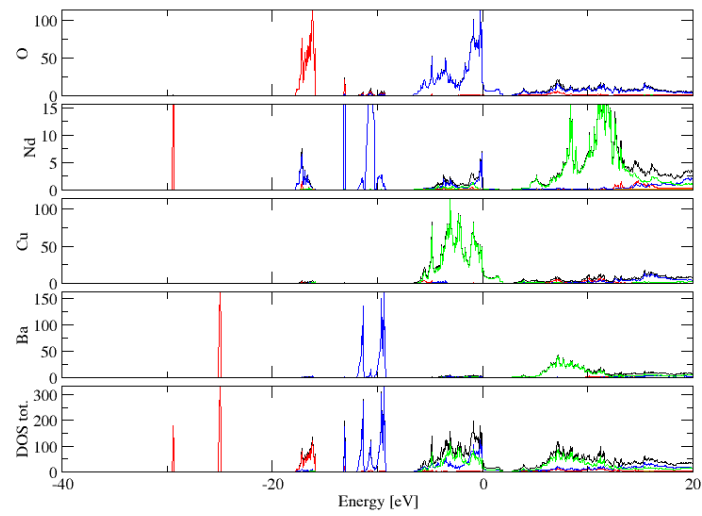
(a) E vs. k FIG. 184: Band structure of $\text{LaBa}_2\text{Cu}_3\text{O}_7$ 

FIG. 185: (Color online) PDOS of $\text{NdBa}_2\text{Cu}_3\text{O}_7$ (ICSD #81169). The s -, p - and d -projected states are in red, blue and green, respectively. $\text{NdBa}_2\text{Cu}_3\text{O}_7$ crystallizes in space group $P m m m$ (#47), in a orthorhombic primitive structure.

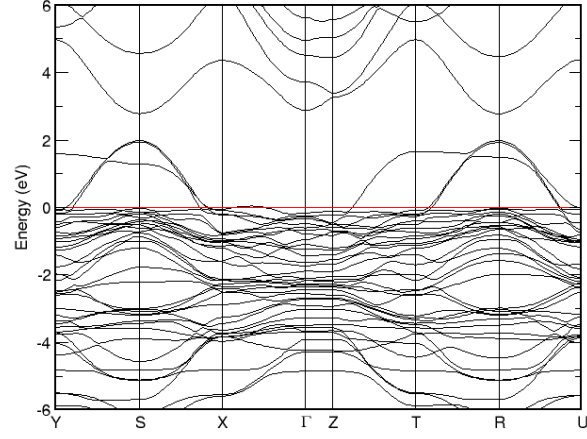
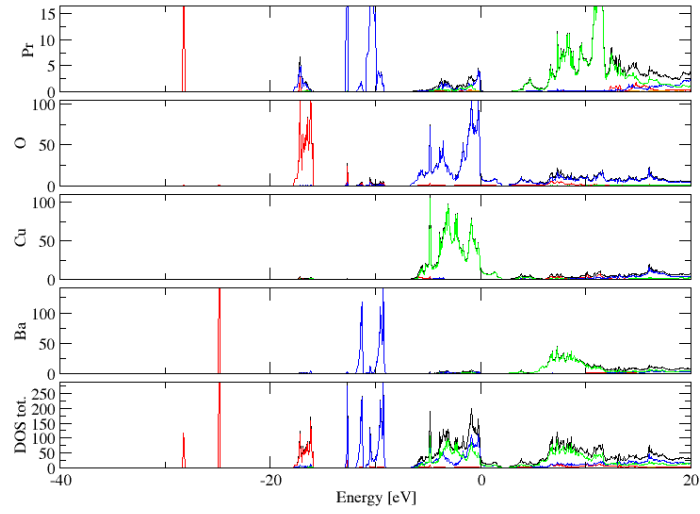
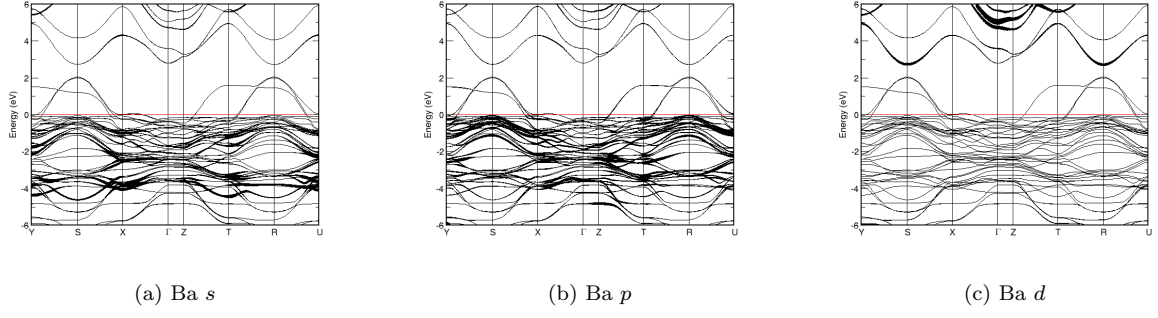
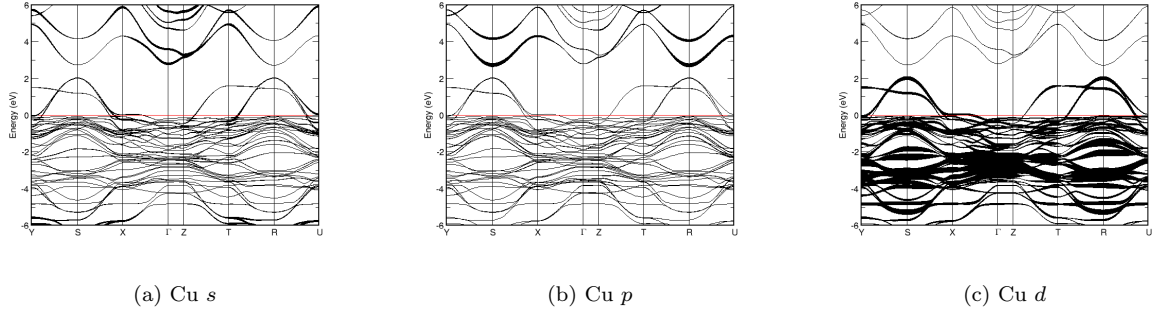
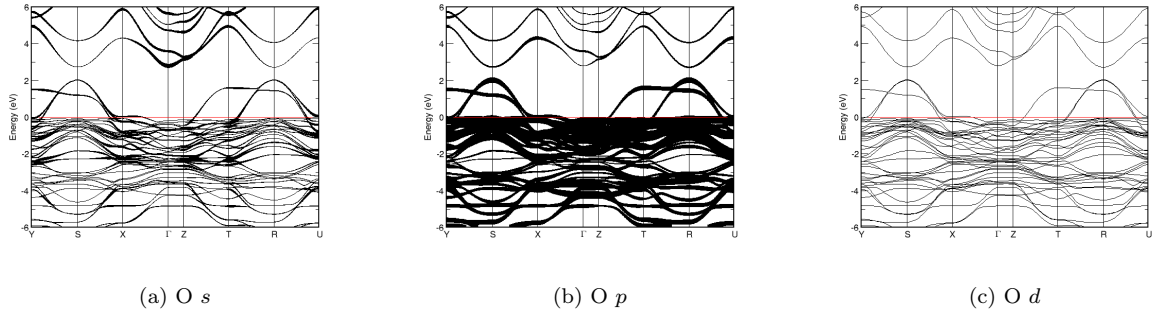
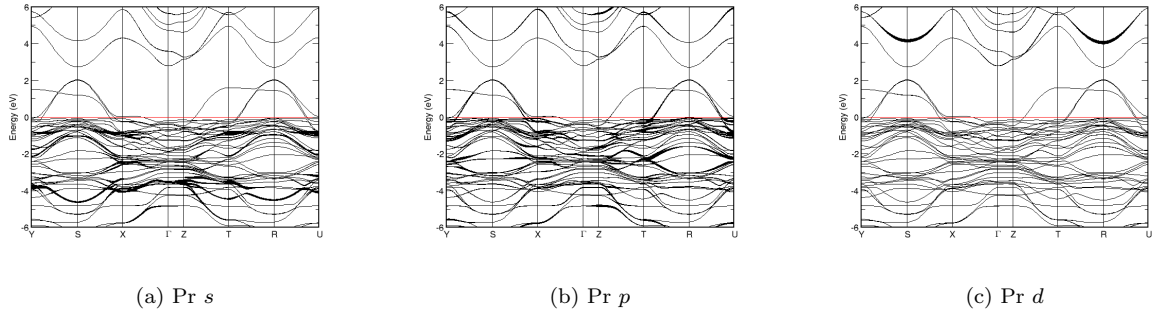
(a) E vs. k FIG. 186: Band structure of NdBa₂Cu₃O₇

FIG. 187: (Color online) PDOS of PrBa₂Cu₃O₇ (ICSD #81168). The s -, p - and d -projected states are in red, blue and green, respectively. PrBa₂Cu₃O₇ crystallizes in space group P m m m (#47), in a orthorhombic primitive structure.

FIG. 188: Fat band representation of Ba in $\text{PrBa}_2\text{Cu}_3\text{O}_7$ FIG. 189: Fat band representation of Cu in $\text{PrBa}_2\text{Cu}_3\text{O}_7$ FIG. 190: Fat band representation of O in $\text{PrBa}_2\text{Cu}_3\text{O}_7$ FIG. 191: Fat band representation of Pr in $\text{PrBa}_2\text{Cu}_3\text{O}_7$

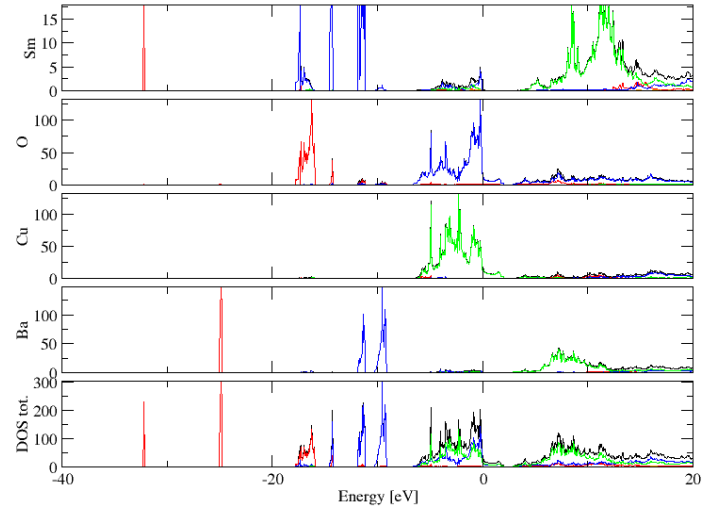


FIG. 192: (Color online) PDOS of $\text{SmBa}_2\text{Cu}_3\text{O}_7$ (ICSD #71705). The s -, p - and d -projected states are in red, blue and green, respectively. $\text{SmBa}_2\text{Cu}_3\text{O}_7$ crystallizes in space group $P m m m$ (#47), in a orthorhombic primitive structure.

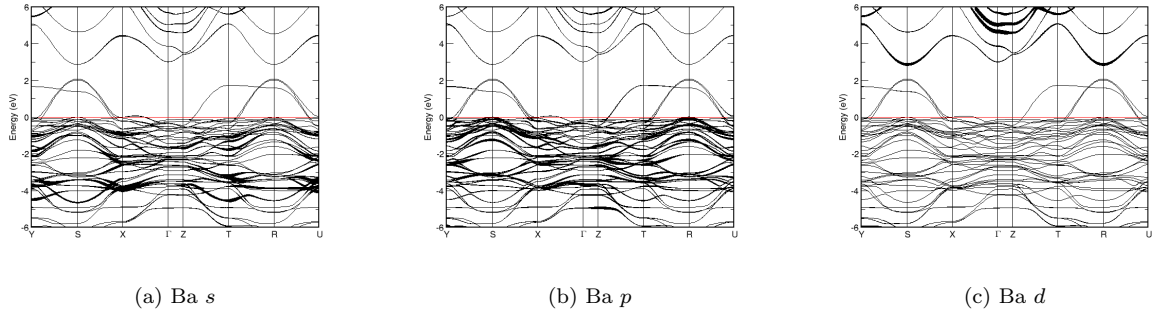


FIG. 193: Fat band representation of Ba in $\text{SmBa}_2\text{Cu}_3\text{O}_7$

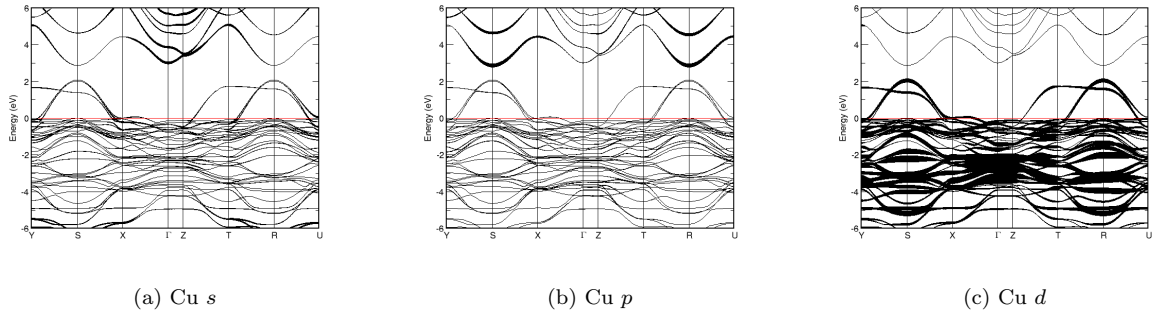


FIG. 194: Fat band representation of Cu in $\text{SmBa}_2\text{Cu}_3\text{O}_7$

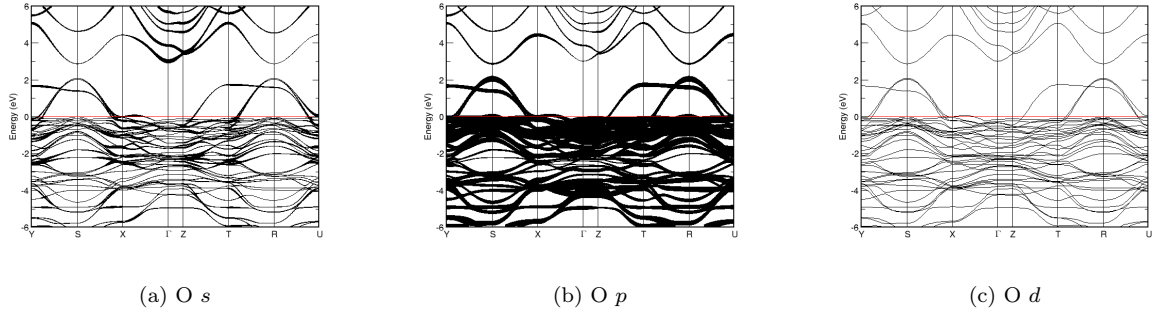
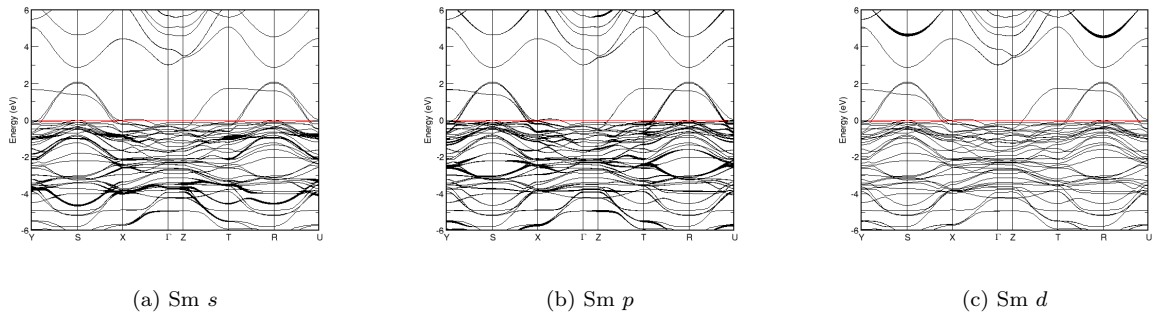
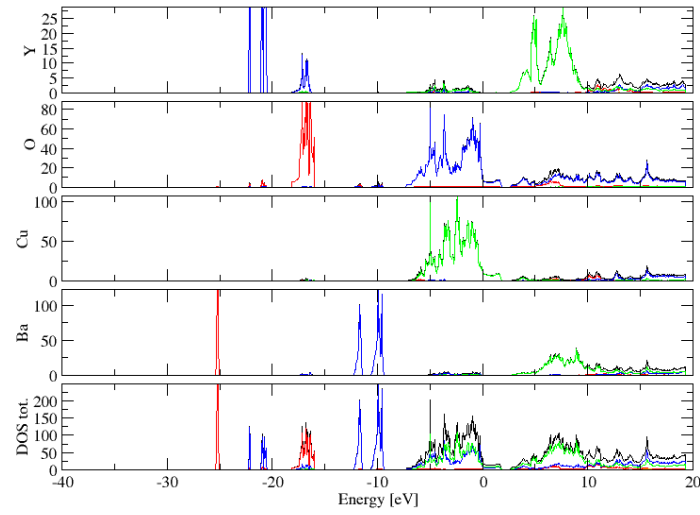
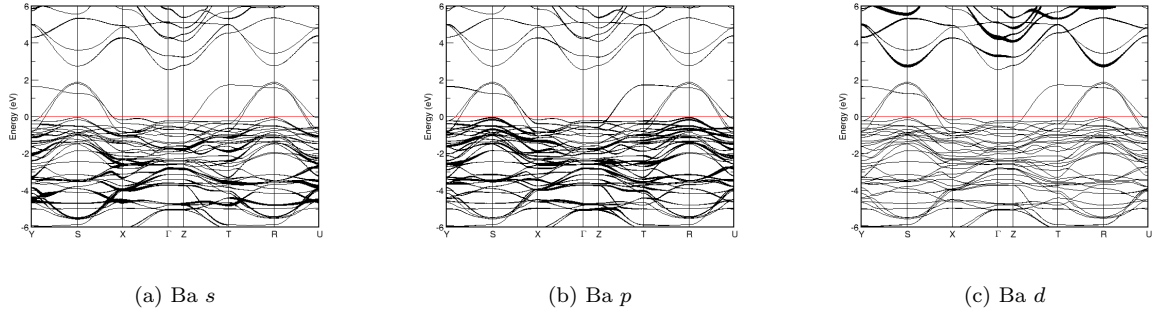
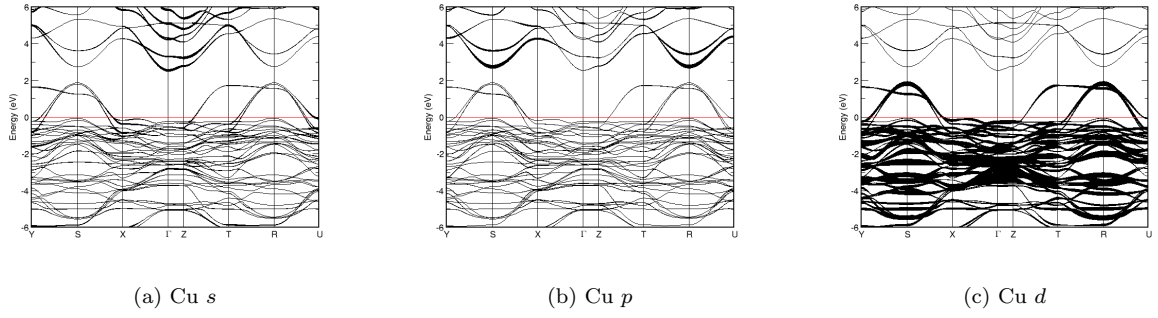
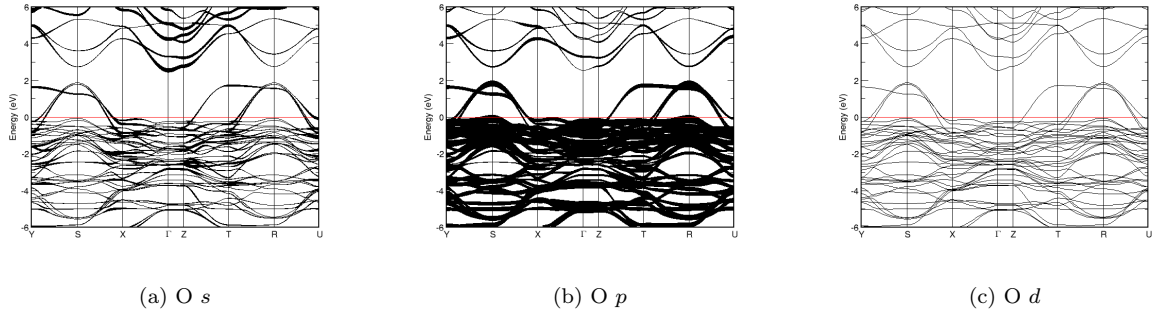
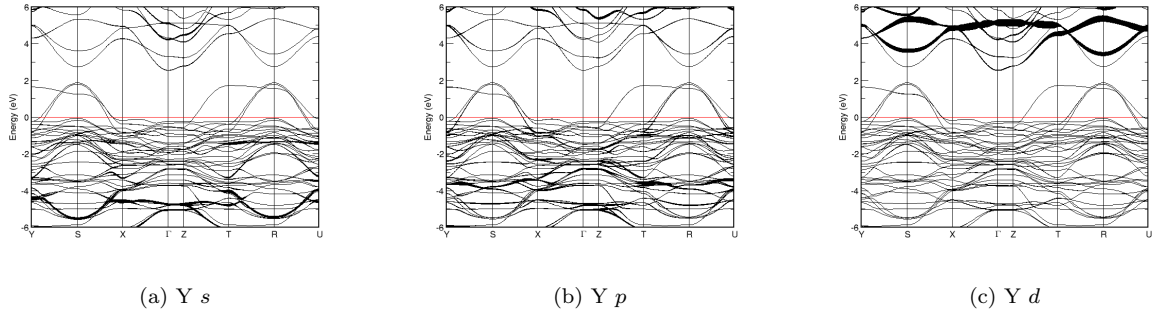
FIG. 195: Fat band representation of O in $\text{SmBa}_2\text{Cu}_3\text{O}_7$ FIG. 196: Fat band representation of Sm in $\text{SmBa}_2\text{Cu}_3\text{O}_7$ 

FIG. 197: (Color online) PDOS of $\text{Ba}_2\text{YCu}_3\text{O}_7$ (ICSD #202770). The *s*-, *p*- and *d*-projected states are in red, blue and green, respectively. $\text{Ba}_2\text{YCu}_3\text{O}_7$ crystallizes in space group $P m m m$ (#47), in a orthorhombic primitive structure.

FIG. 198: Fat band representation of Ba in $\text{Ba}_2\text{YCu}_3\text{O}_7$ FIG. 199: Fat band representation of Cu in $\text{Ba}_2\text{YCu}_3\text{O}_7$ FIG. 200: Fat band representation of O in $\text{Ba}_2\text{YCu}_3\text{O}_7$ FIG. 201: Fat band representation of Y in $\text{Ba}_2\text{YCu}_3\text{O}_7$

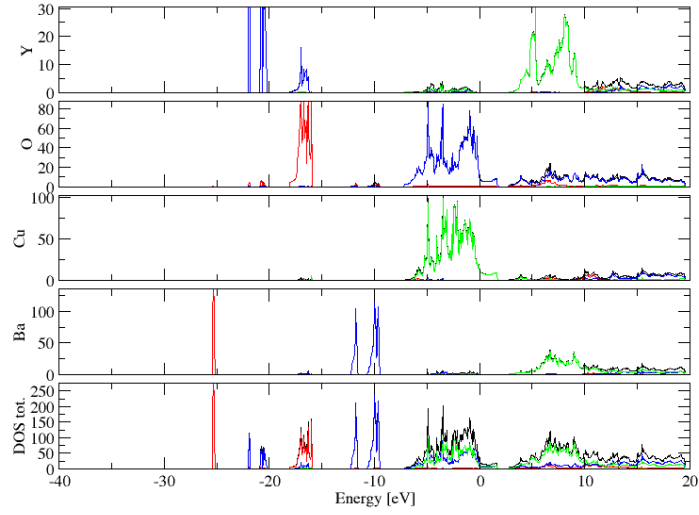


FIG. 202: (Color online) PDOS of $\text{Ba}_2\text{YCu}_3\text{O}_7$ (ICSD #77737). The s -, p - and d -projected states are in red, blue and green, respectively. $\text{Ba}_2\text{YCu}_3\text{O}_7$ crystallizes in space group $P m m m$ (#47), in a orthorhombic primitive structure.

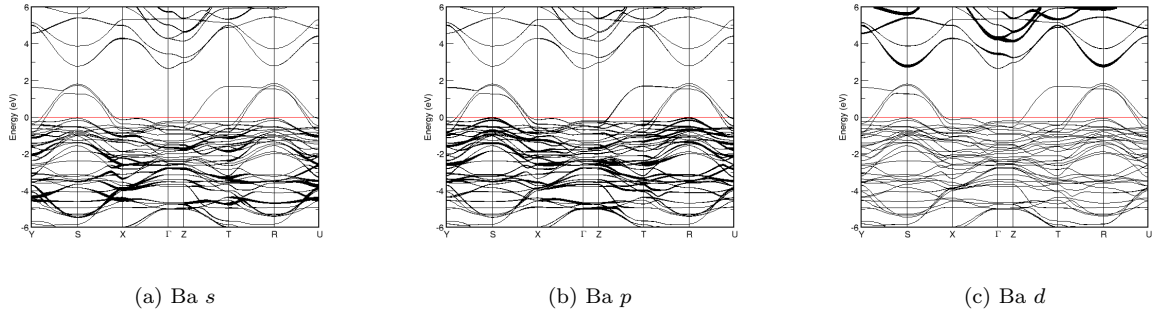


FIG. 203: Fat band representation of Ba in $\text{Ba}_2\text{YCu}_3\text{O}_7$

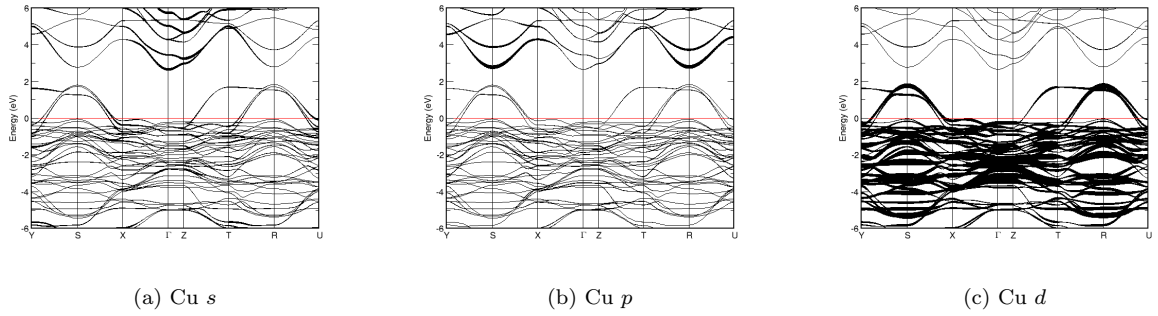


FIG. 204: Fat band representation of Cu in $\text{Ba}_2\text{YCu}_3\text{O}_7$

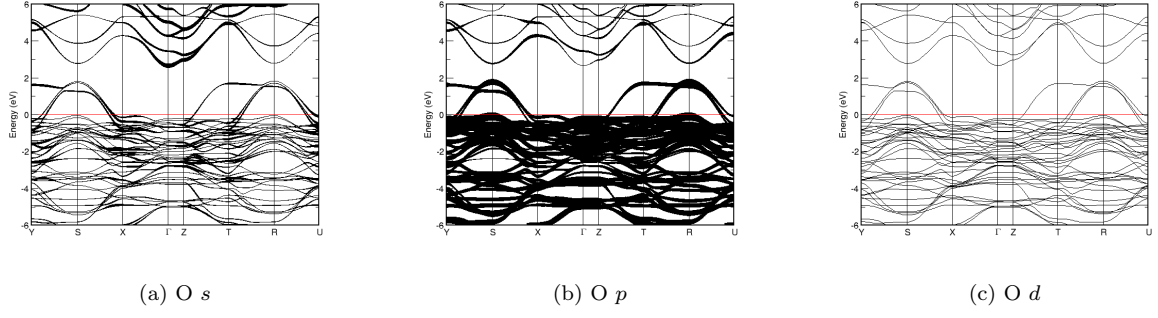
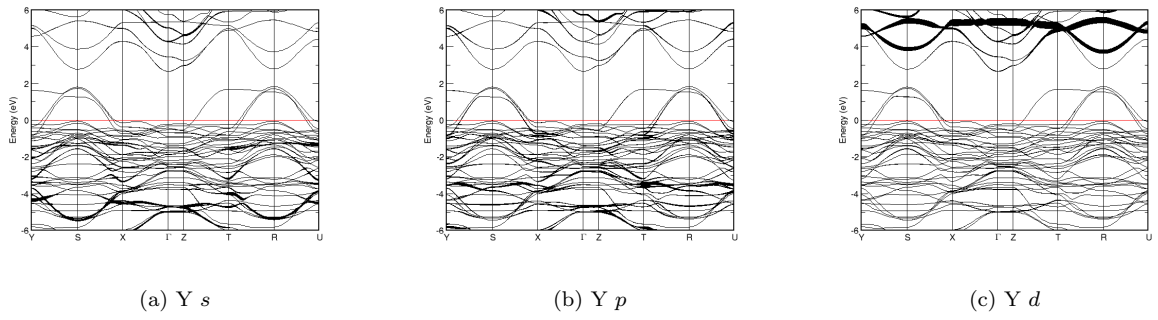
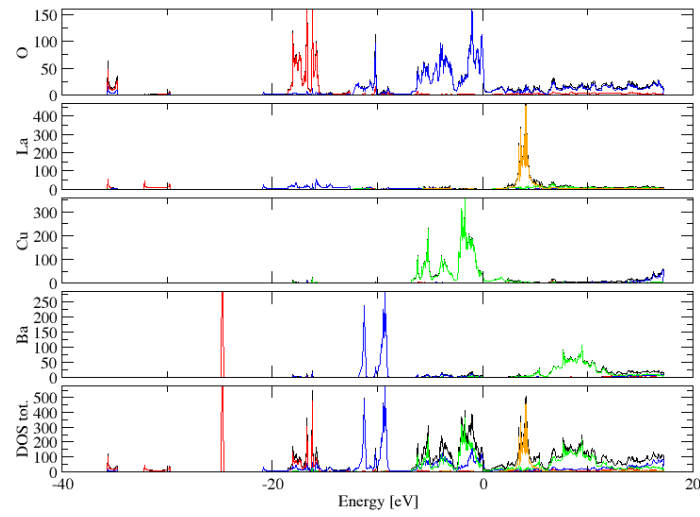
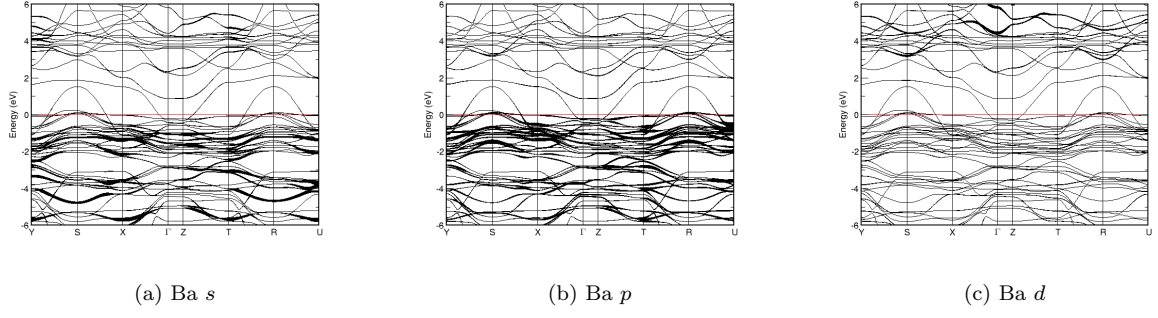
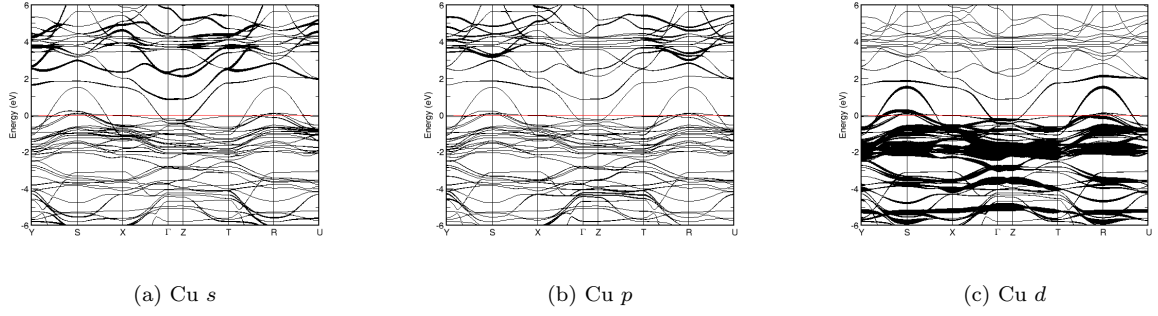
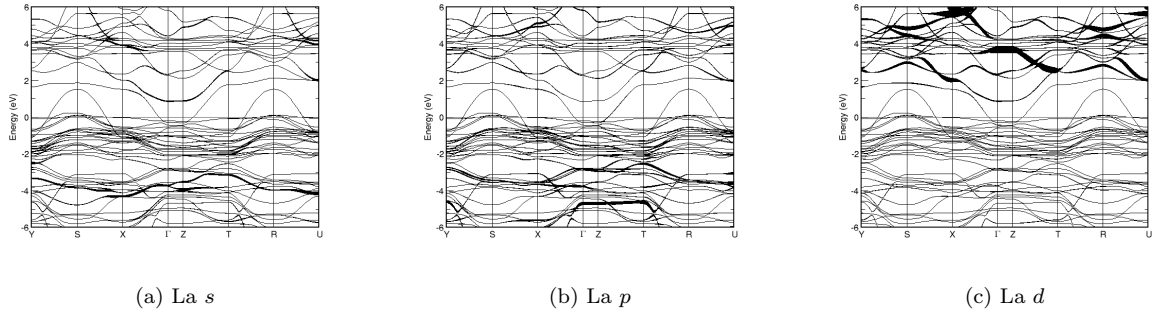
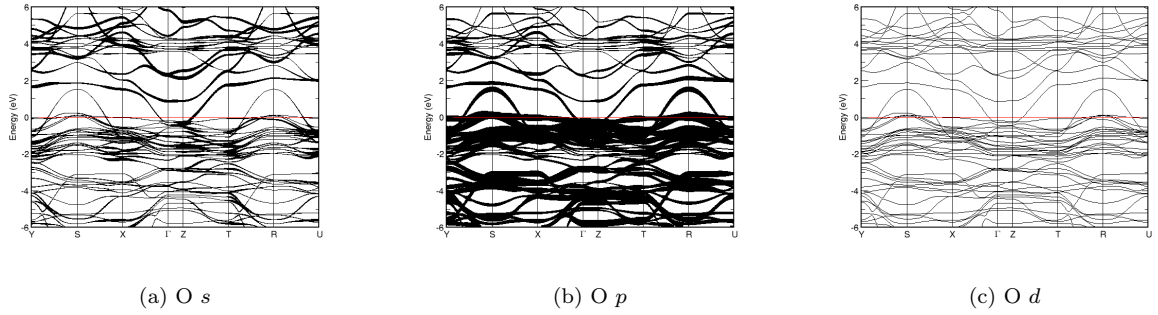
FIG. 205: Fat band representation of O in $\text{Ba}_2\text{YCu}_3\text{O}_7$ FIG. 206: Fat band representation of Y in $\text{Ba}_2\text{YCu}_3\text{O}_7$ 

FIG. 207: (Color online) PDOS of $\text{LaBa}_2\text{Cu}_3\text{O}_8$ (ICSD #85291). The *s*-, *p*- and *d*-projected states are in red, blue and green, respectively. $\text{LaBa}_2\text{Cu}_3\text{O}_8$ crystallizes in space group $P m m m$ (#47), in a orthorhombic primitive structure.

FIG. 208: Fat band representation of Ba in $\text{LaBa}_2\text{Cu}_3\text{O}_8$ FIG. 209: Fat band representation of Cu in $\text{LaBa}_2\text{Cu}_3\text{O}_8$ FIG. 210: Fat band representation of La in $\text{LaBa}_2\text{Cu}_3\text{O}_8$ FIG. 211: Fat band representation of O in $\text{LaBa}_2\text{Cu}_3\text{O}_8$

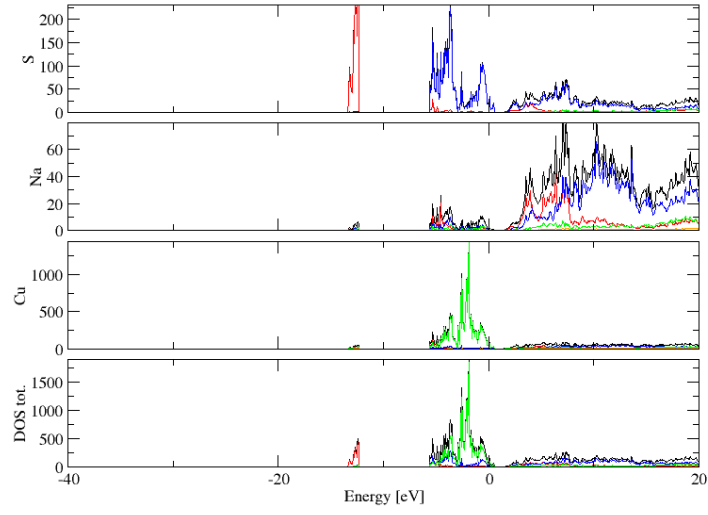


FIG. 212: (Color online) PDOS of $\text{Na}_3\text{Cu}_4\text{S}_4$ (ICSD #10004). The s -, p - and d -projected states are in red, blue and green, respectively. $\text{Na}_3\text{Cu}_4\text{S}_4$ crystallizes in space group $P b a m$ (#55), in a orthorhombic primitive structure.

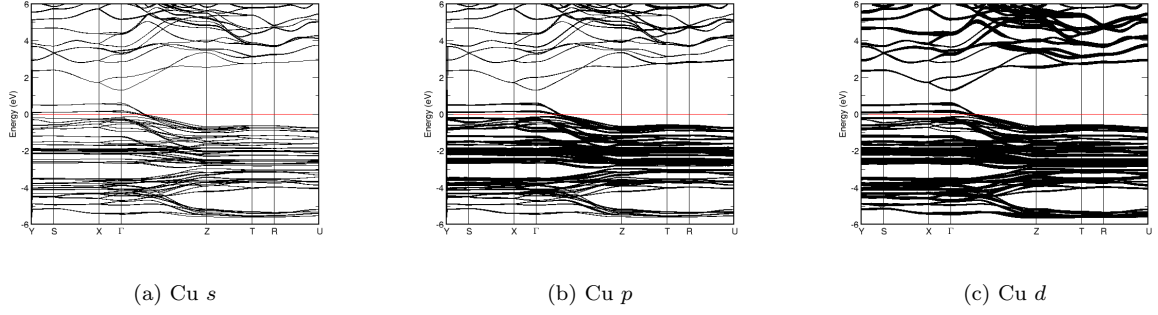


FIG. 213: Fat band representation of Cu in $\text{Na}_3\text{Cu}_4\text{S}_4$

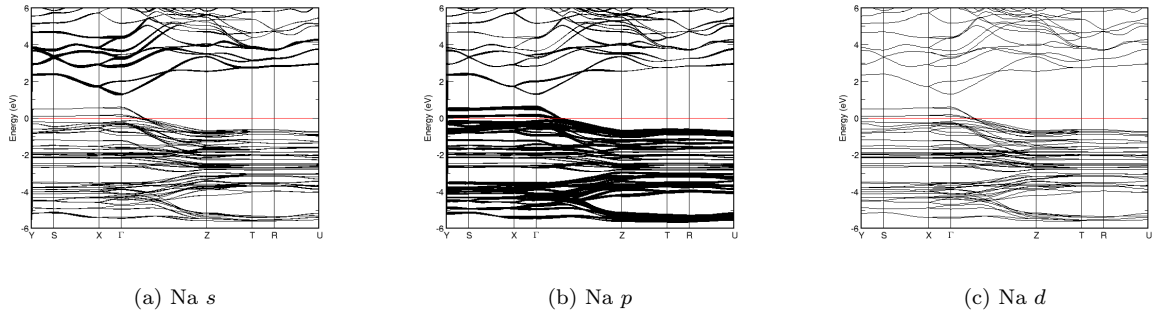
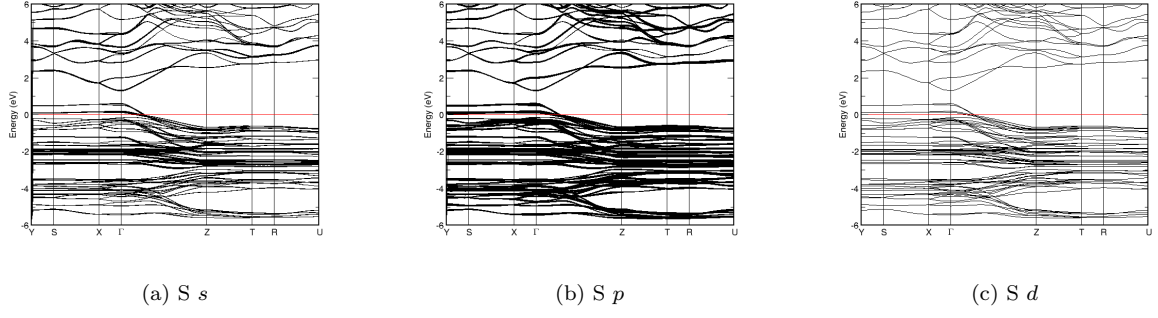
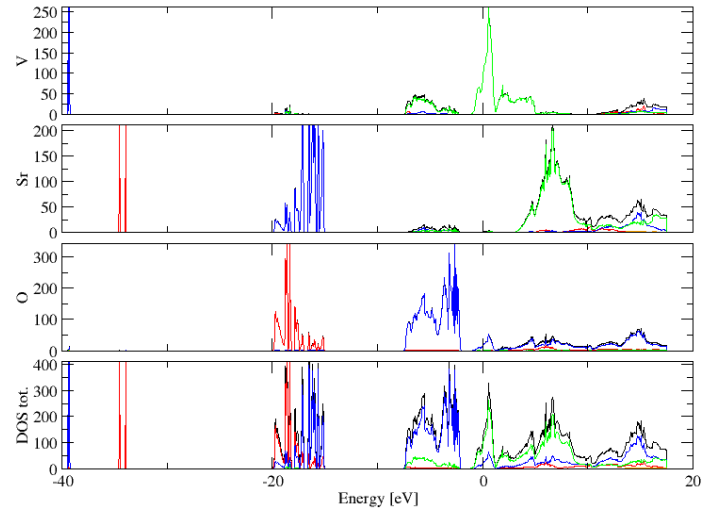
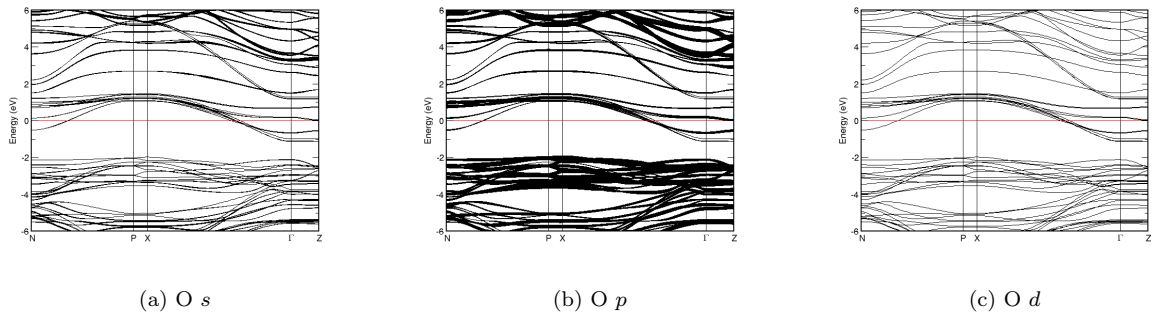
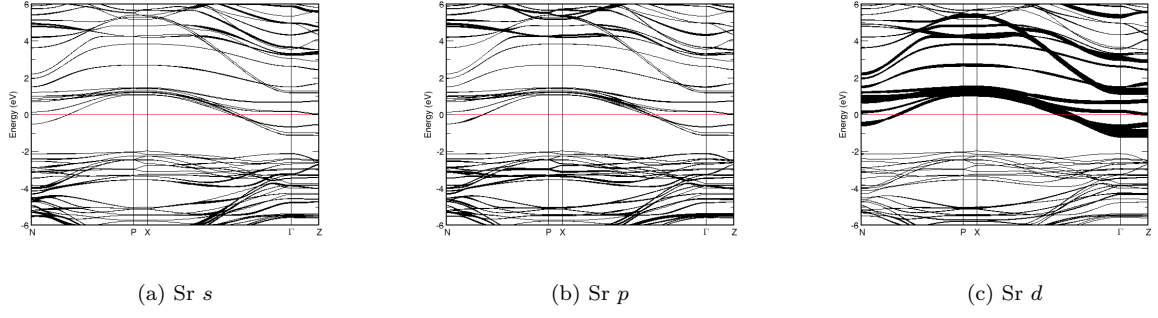
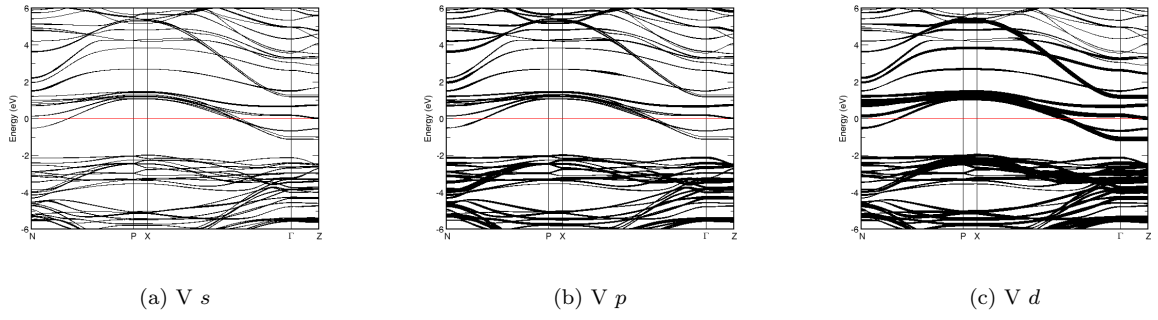
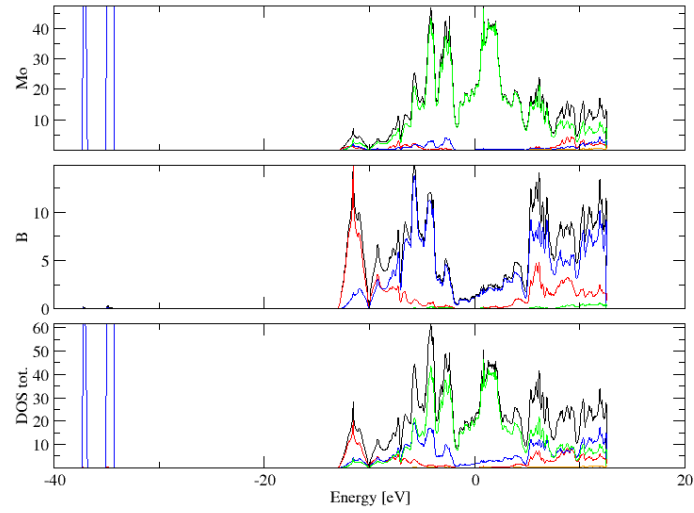


FIG. 214: Fat band representation of Na in $\text{Na}_3\text{Cu}_4\text{S}_4$

FIG. 215: Fat band representation of S in $\text{Na}_3\text{Cu}_4\text{S}_4$ FIG. 216: (Color online) PDOS of $\text{Sr}_4\text{V}_3\text{O}_{10}$ (ICSD #73698). The *s*-, *p*- and *d*-projected states are in red, blue and green, respectively. $\text{Sr}_4\text{V}_3\text{O}_{10}$ crystallizes in space group $I 4/m m m$ (#139), in a tetragonal body-centred structure.FIG. 217: Fat band representation of O in $\text{Sr}_4\text{V}_3\text{O}_{10}$

FIG. 218: Fat band representation of Sr in $\text{Sr}_4\text{V}_3\text{O}_{10}$ FIG. 219: Fat band representation of V in $\text{Sr}_4\text{V}_3\text{O}_{10}$ FIG. 220: (Color online) PDOS of MoB (ICSD #24280). The *s*-, *p*- and *d*-projected states are in red, blue and green, respectively. MoB crystallizes in space group $I 41/a m d S$ (#141), in a tetragonal body-centred structure.

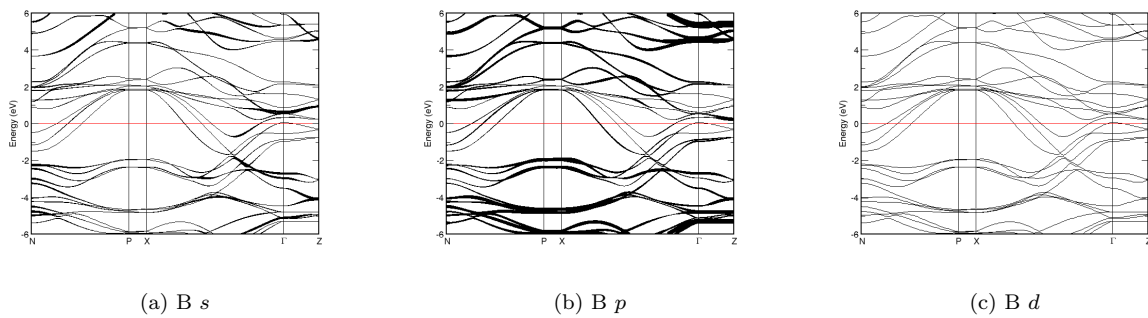


FIG. 221: Fat band representation of B in MoB

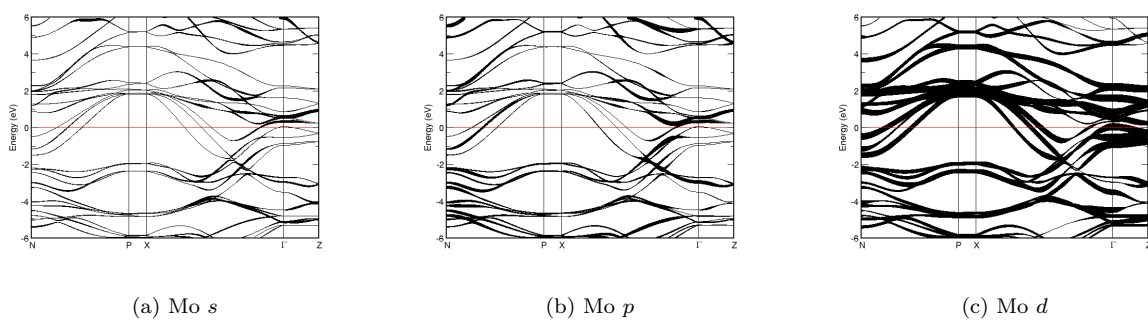
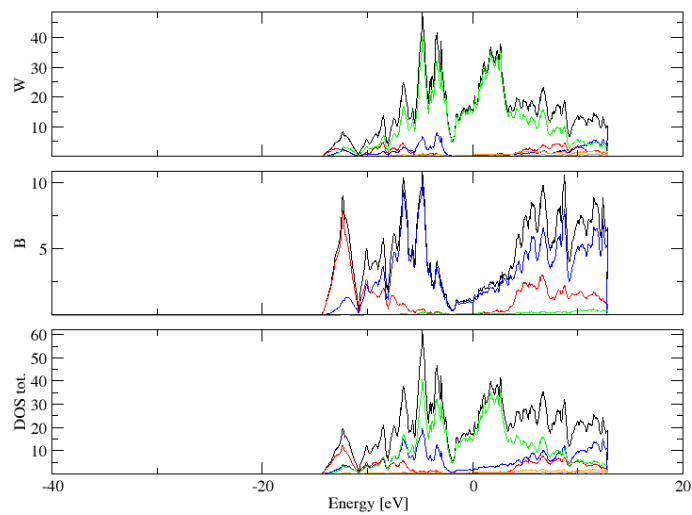


FIG. 222: Fat band representation of Mo in MoB

FIG. 223: (Color online) PDOS of WB (ICSD #24281). The *s*-, *p*- and *d*-projected states are in red, blue and green, respectively. WB crystallizes in space group $I 41/a m d S$ (#141), in a tetragonal body-centred structure.

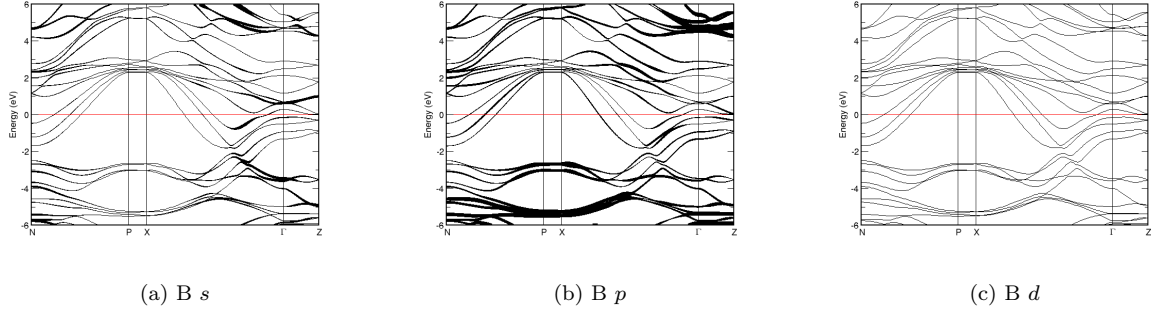


FIG. 224: Fat band representation of B in WB

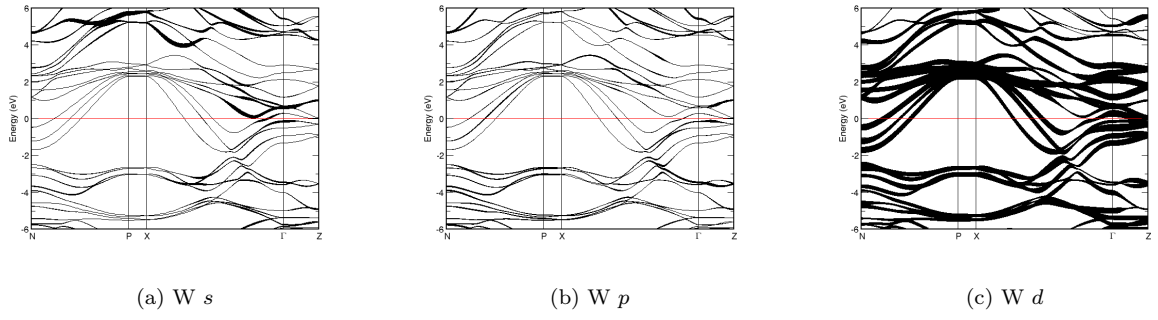


FIG. 225: Fat band representation of W in WB

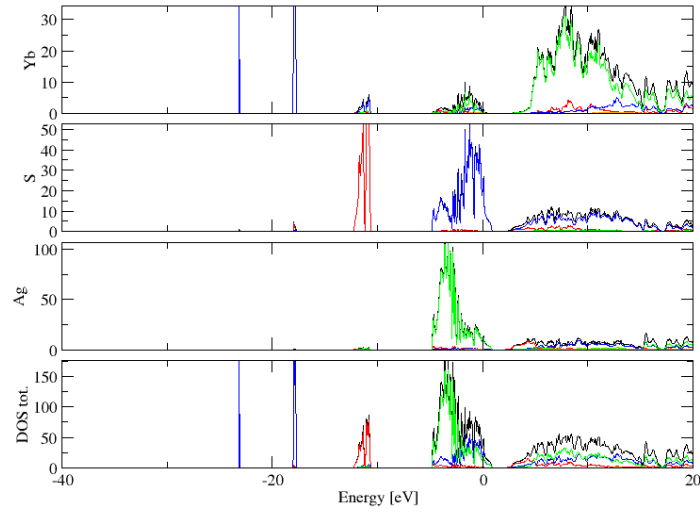


FIG. 226: (Color online) PDOS of $\text{Yb}(\text{AgS}_2)$ (ICSD #27091). The s -, p - and d -projected states are in red, blue and green, respectively. $\text{Yb}(\text{AgS}_2)$ crystallizes in space group $I 41 m d$ (#109), in a tetragonal body-centred structure.

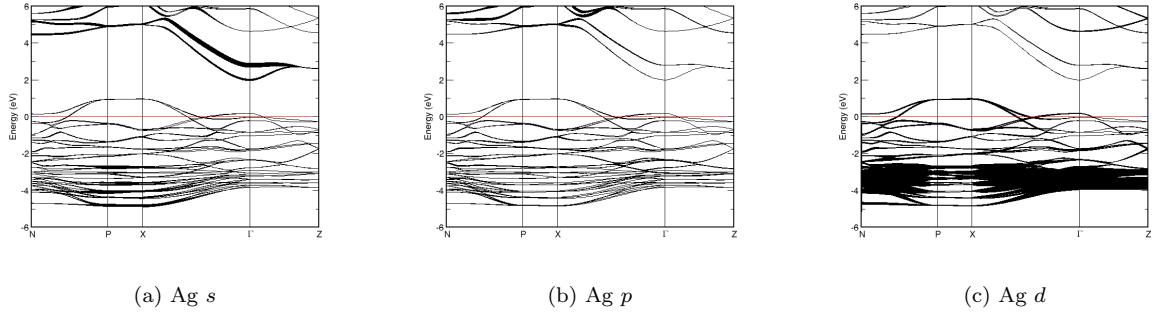


FIG. 227: Fat band representation of Ag in Yb(AgS₂)

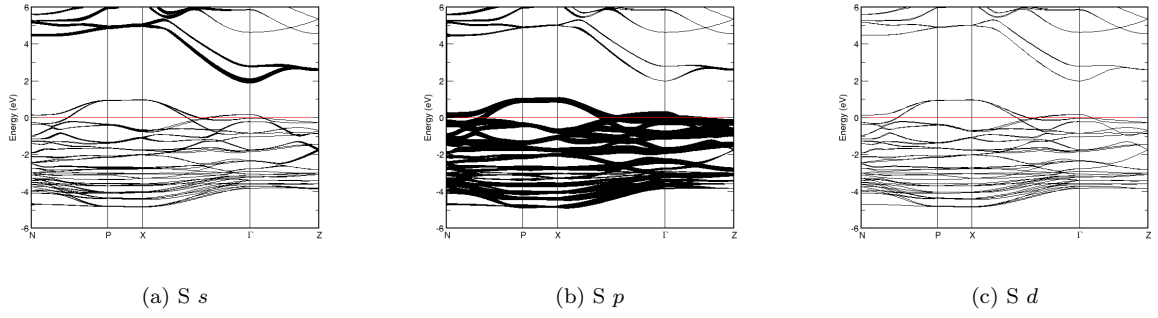


FIG. 228: Fat band representation of S in Yb(AgS₂)

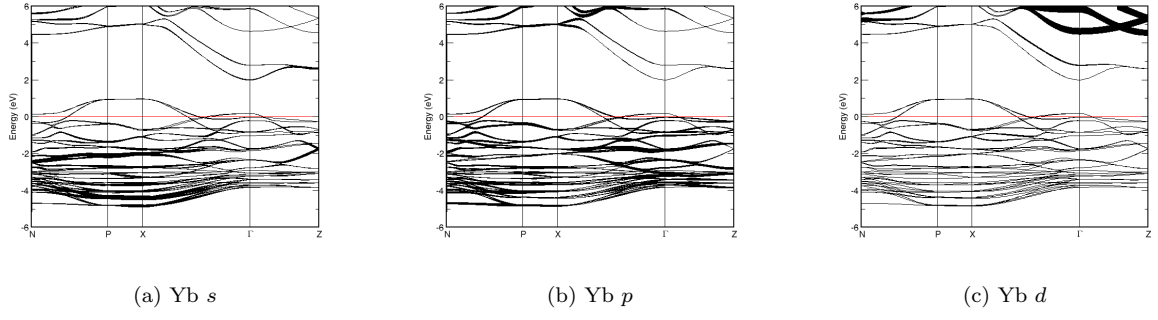


FIG. 229: Fat band representation of Yb in Yb(AgS₂)

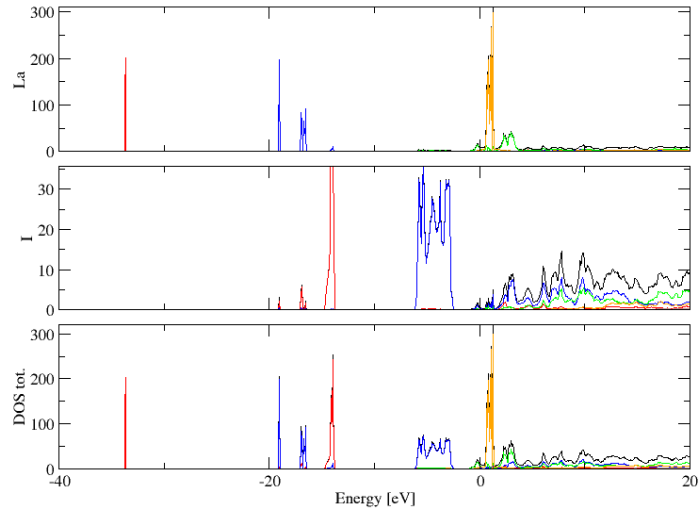


FIG. 230: (Color online) PDOS of LaI₂ (ICSD #202452). The *s*-, *p*- and *d*-projected states are in red, blue and green, respectively. LaI₂ crystallizes in space group I 4/m m m (#139), in a tetragonal body-centred structure.

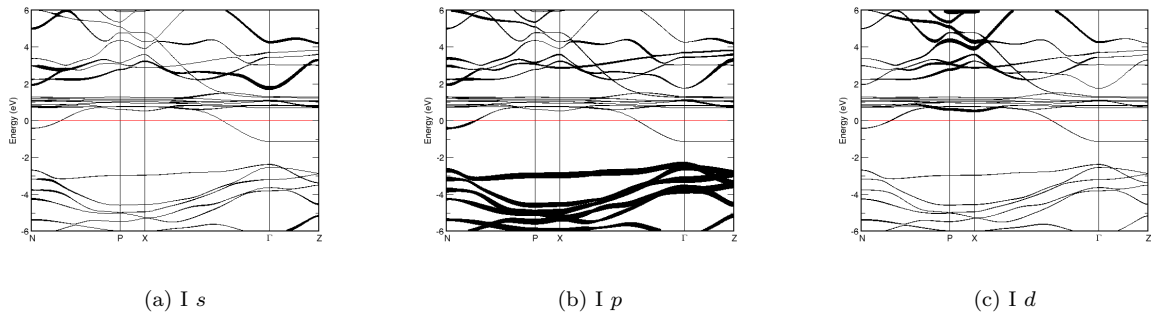
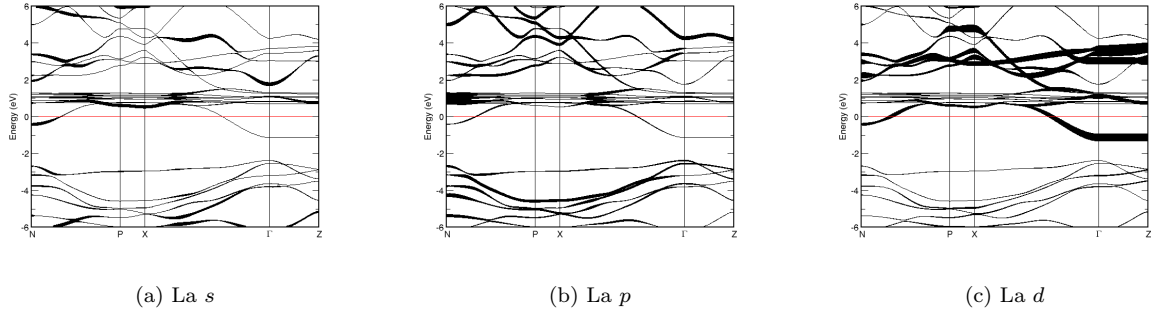
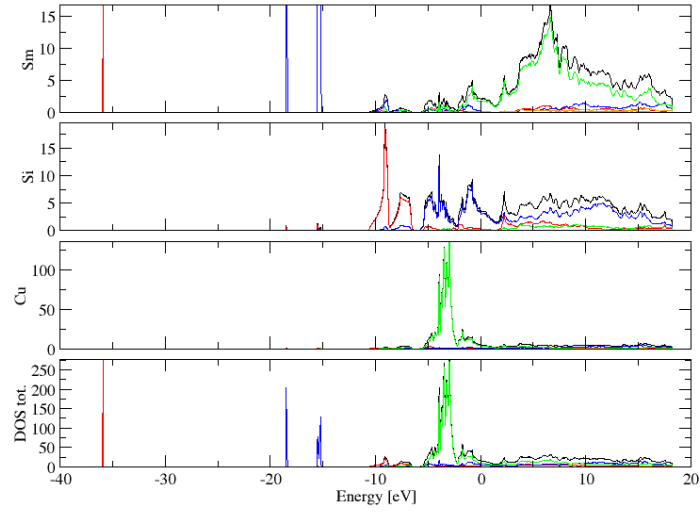
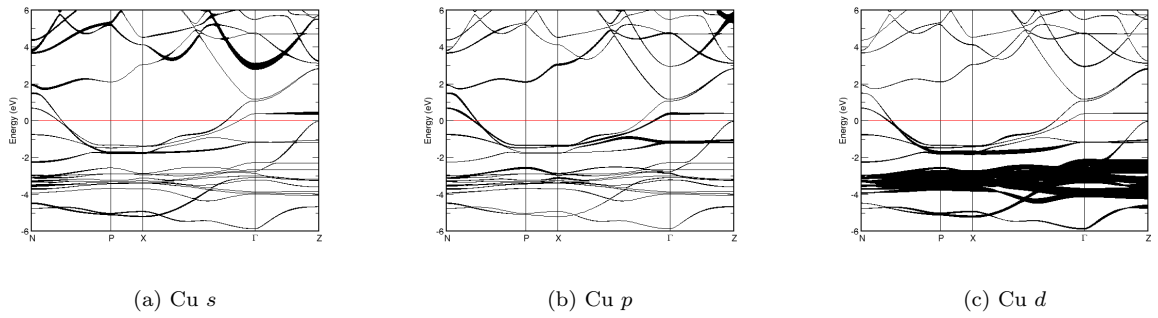
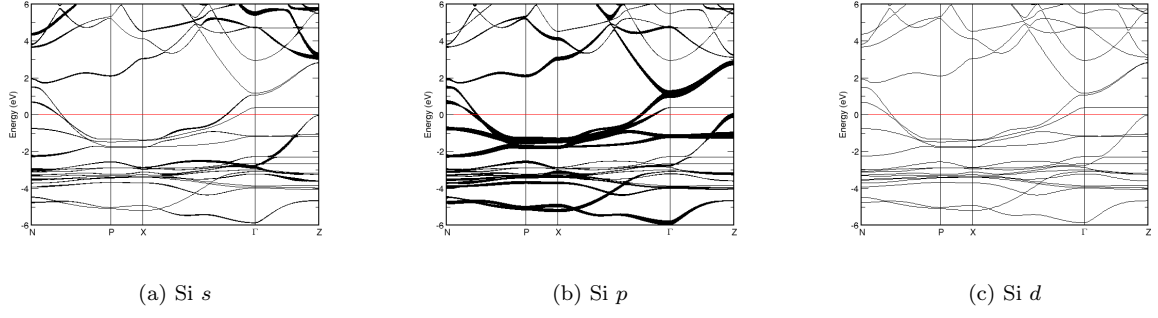
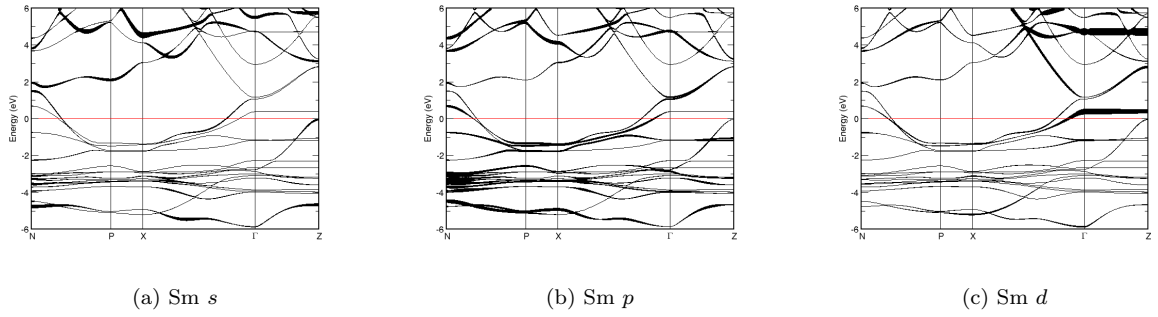
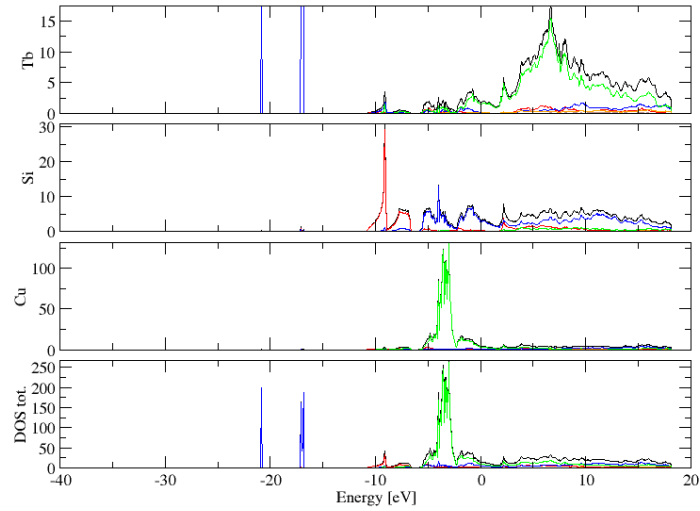
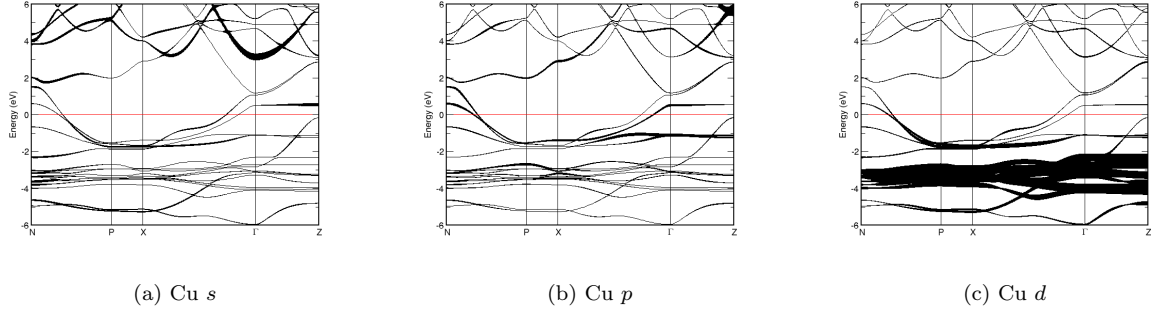
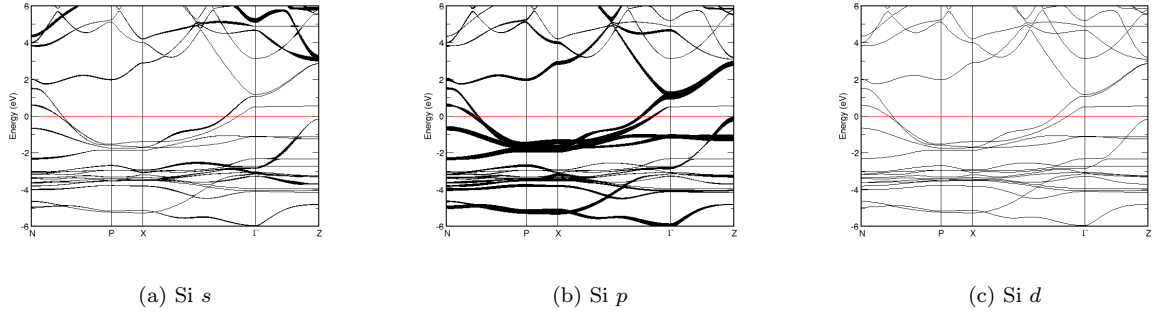
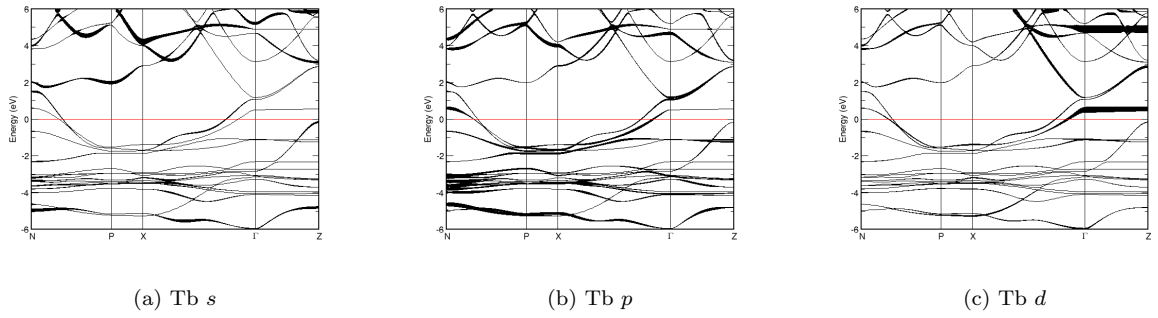


FIG. 231: Fat band representation of I in LaI₂

FIG. 232: Fat band representation of La in LaI_2 FIG. 233: (Color online) PDOS of SmCu_2Si_2 (ICSD #106843). The s -, p - and d -projected states are in red, blue and green, respectively. SmCu_2Si_2 crystallizes in space group $I 4/m m m$ (#139), in a tetragonal body-centred structure.FIG. 234: Fat band representation of Cu in SmCu_2Si_2

FIG. 235: Fat band representation of Si in SmCu_2Si_2 FIG. 236: Fat band representation of Sm in SmCu_2Si_2 FIG. 237: (Color online) PDOS of TbCu_2Si_2 (ICSD #106844). The s -, p - and d -projected states are in red, blue and green, respectively. TbCu_2Si_2 crystallizes in space group $I 4/m m m$ (#139), in a tetragonal body-centred structure.

FIG. 238: Fat band representation of Cu in TbCu_2Si_2 FIG. 239: Fat band representation of Si in TbCu_2Si_2 FIG. 240: Fat band representation of Tb in TbCu_2Si_2

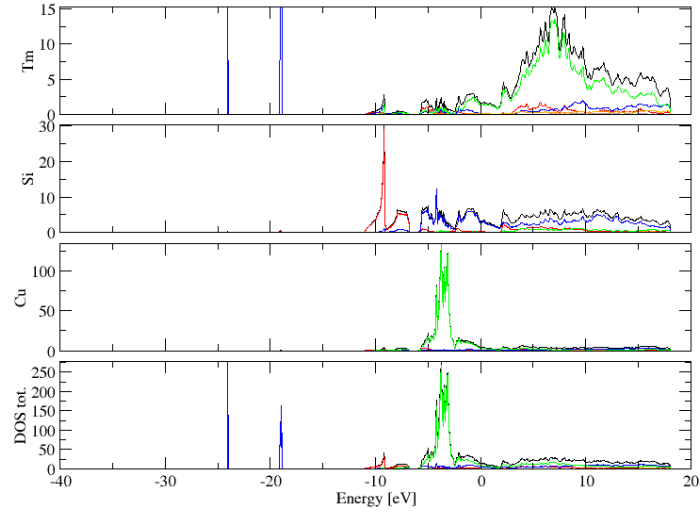


FIG. 241: (Color online) PDOS of Cu_2TmSi_2 (ICSD #53349). The s -, p - and d -projected states are in red, blue and green, respectively. Cu_2TmSi_2 crystallizes in space group $I 4/m m m$ (#139), in a tetragonal body-centred structure.

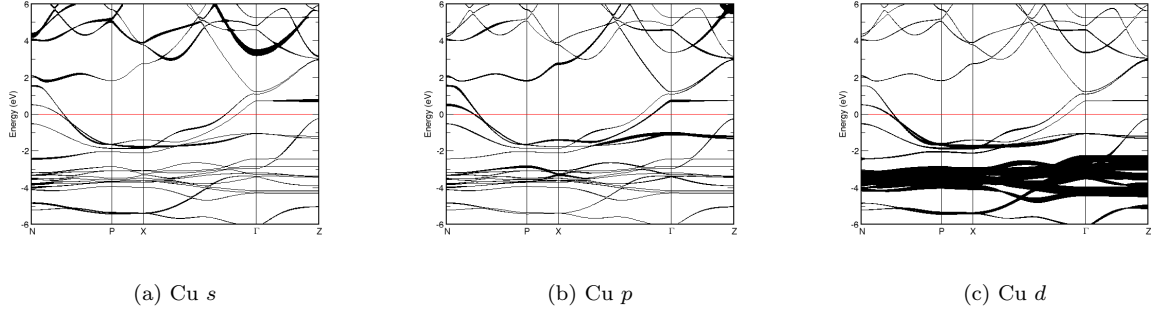


FIG. 242: Fat band representation of Cu in Cu_2TmSi_2

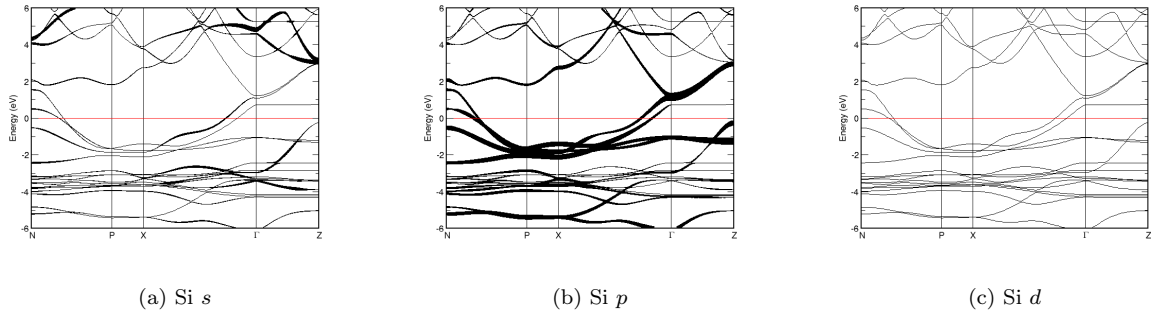
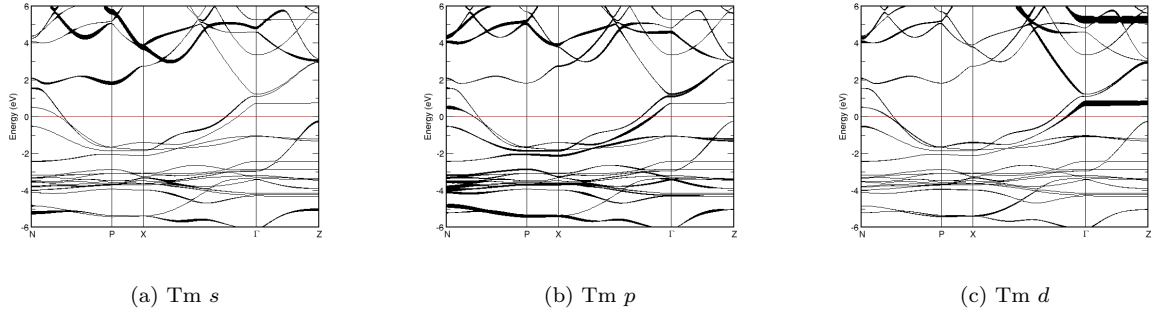
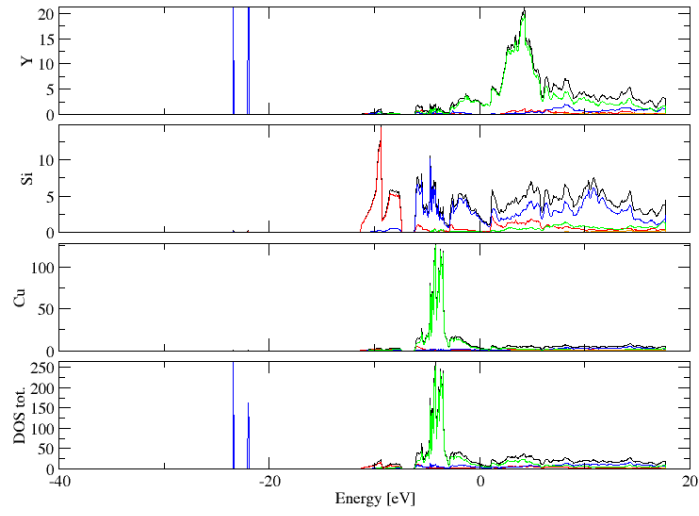
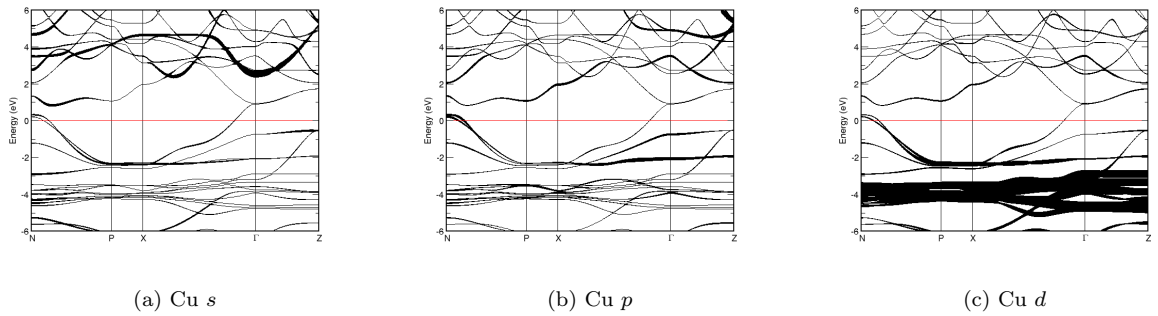
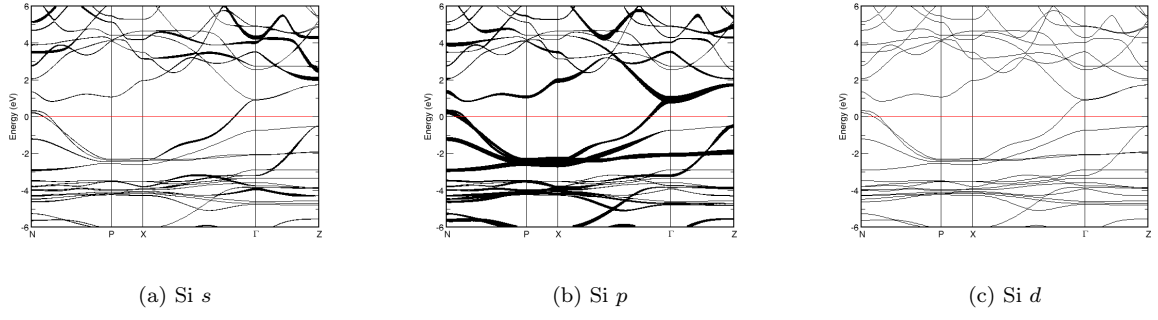
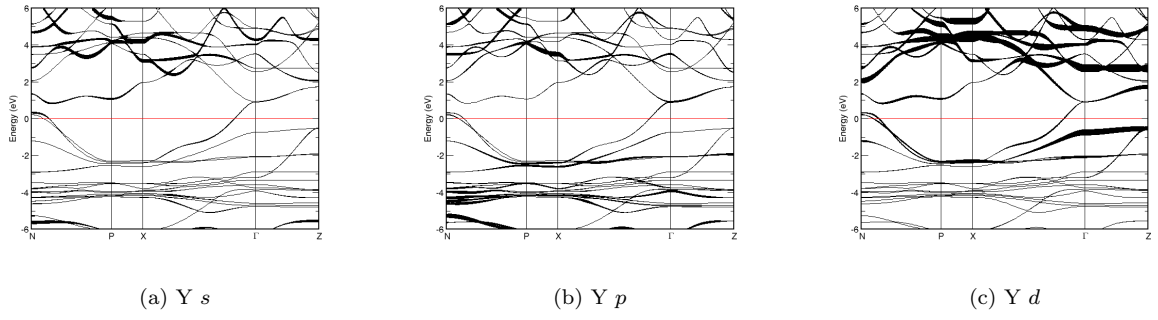
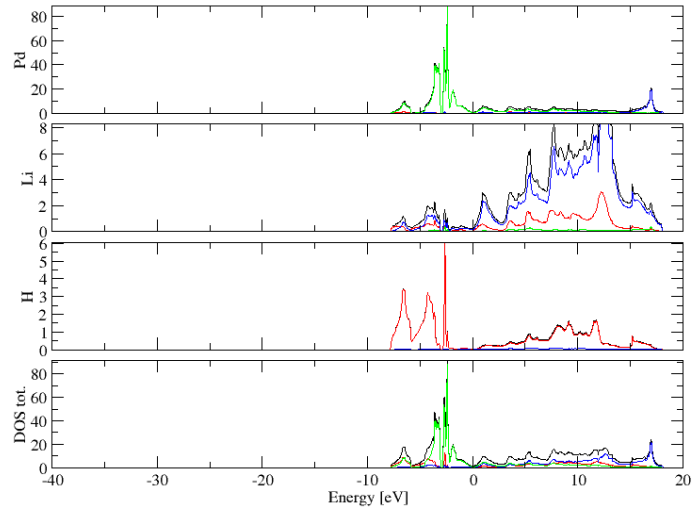
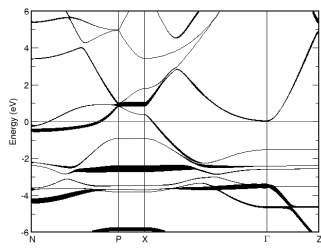
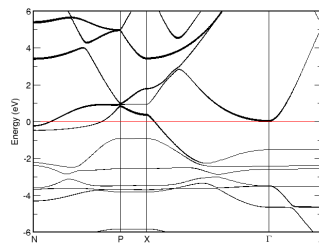
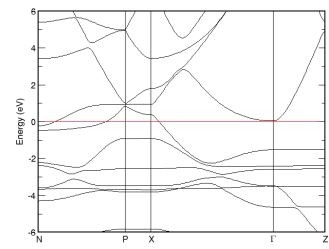
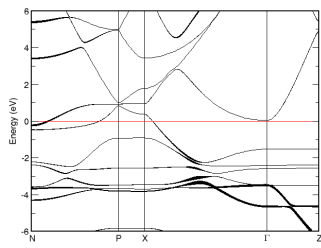
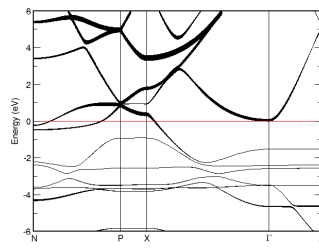
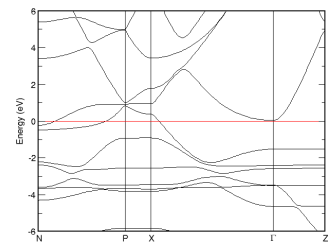
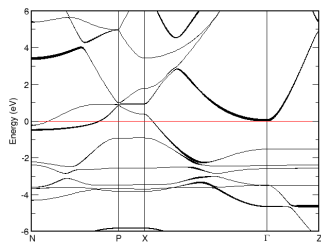
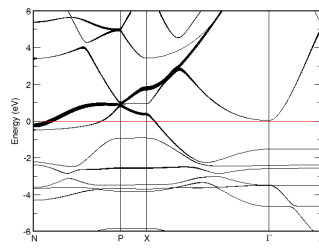
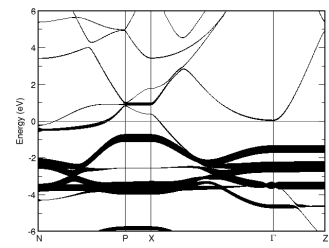


FIG. 243: Fat band representation of Si in Cu_2TmSi_2

FIG. 244: Fat band representation of Tm in Cu_2TmSi_2 FIG. 245: (Color online) PDOS of Cu_2YSi_2 (ICSD #23551). The *s*-, *p*- and *d*-projected states are in red, blue and green, respectively. Cu_2YSi_2 crystallizes in space group I $4/m\ m\ m$ (#139), in a tetragonal body-centred structure.FIG. 246: Fat band representation of Cu in Cu_2YSi_2

FIG. 247: Fat band representation of Si in Cu_2YSi_2 FIG. 248: Fat band representation of Y in Cu_2YSi_2 FIG. 249: (Color online) PDOS of Li_2PdH_2 (ICSD #108534). The *s*-, *p*- and *d*-projected states are in red, blue and green, respectively. Li_2PdH_2 crystallizes in space group $I 4/m m m$ (#139), in a tetragonal body-centred structure.

(a) H *s*(b) H *p*(c) H *d*FIG. 250: Fat band representation of H in Li_2PdH_2 (a) Li *s*(b) Li *p*(c) Li *d*FIG. 251: Fat band representation of Li in Li_2PdH_2 (a) Pd *s*(b) Pd *p*(c) Pd *d*FIG. 252: Fat band representation of Pd in Li_2PdH_2

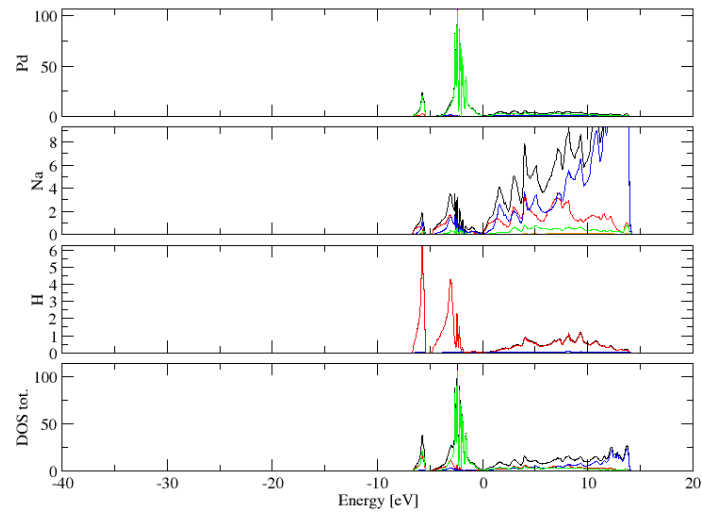


FIG. 253: (Color online) PDOS of Na_2PdH_2 (ICSD #68071). The s -, p - and d -projected states are in red, blue and green, respectively. Na_2PdH_2 crystallizes in space group $I 4/m m m$ (#139), in a tetragonal body-centred structure.

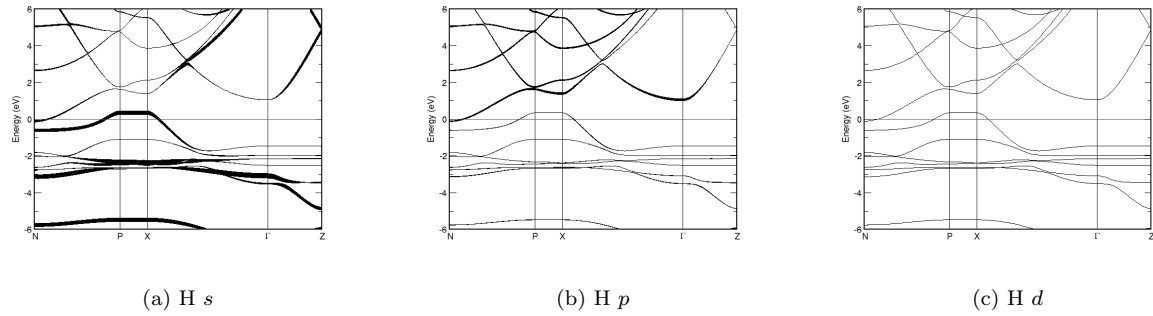


FIG. 254: Fat band representation of H in Na_2PdH_2

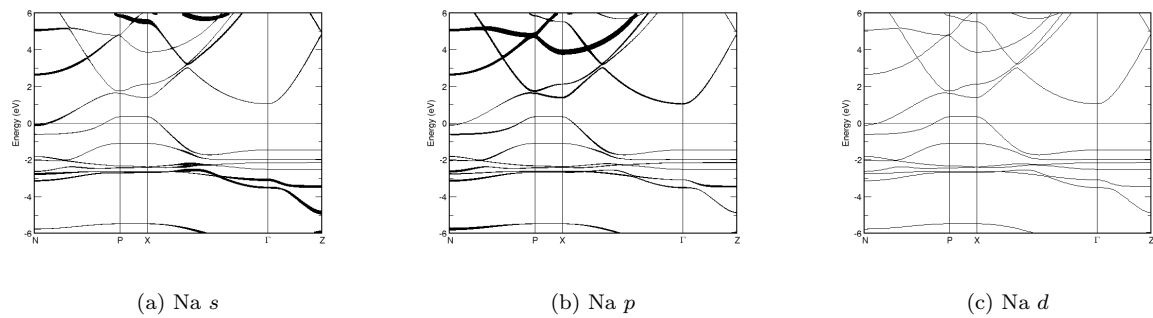
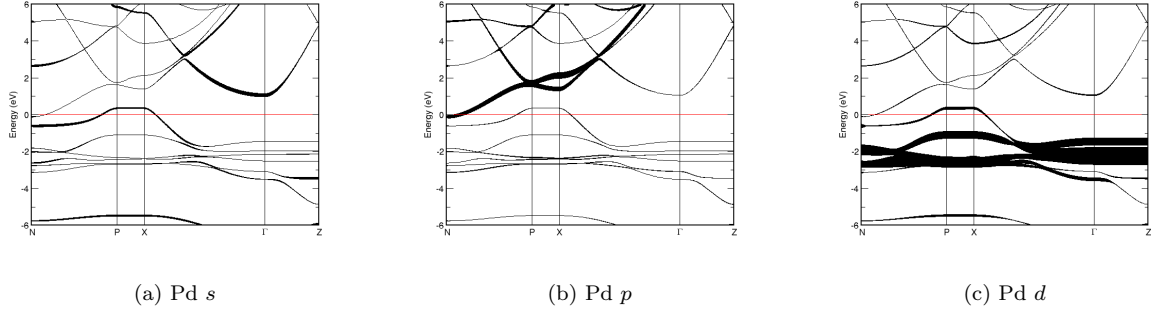
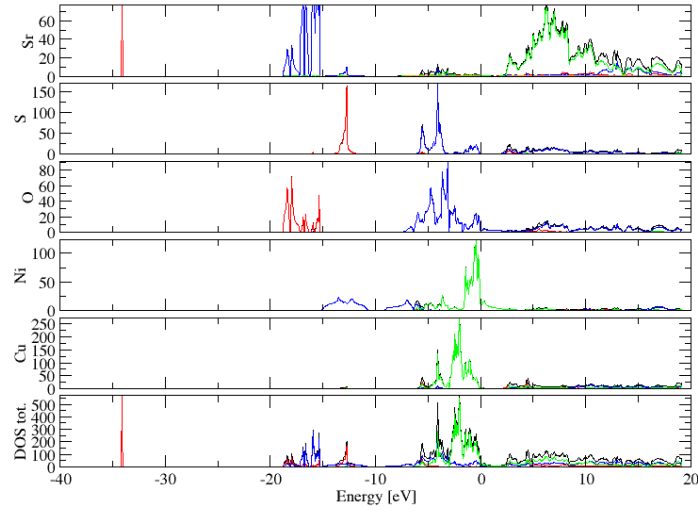
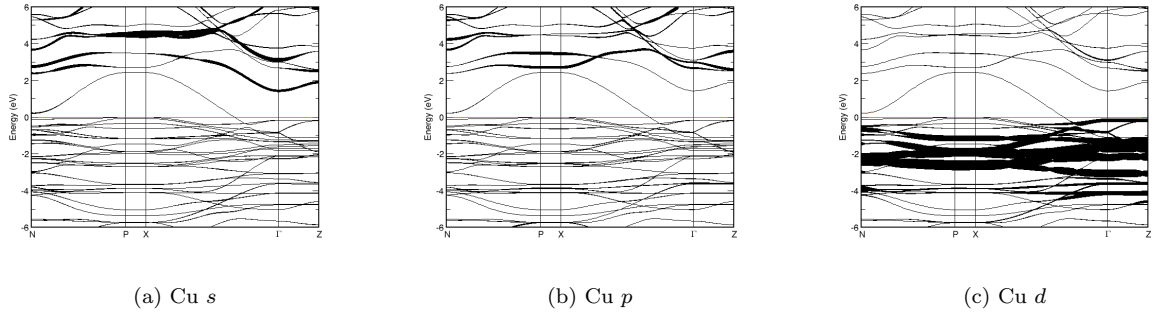
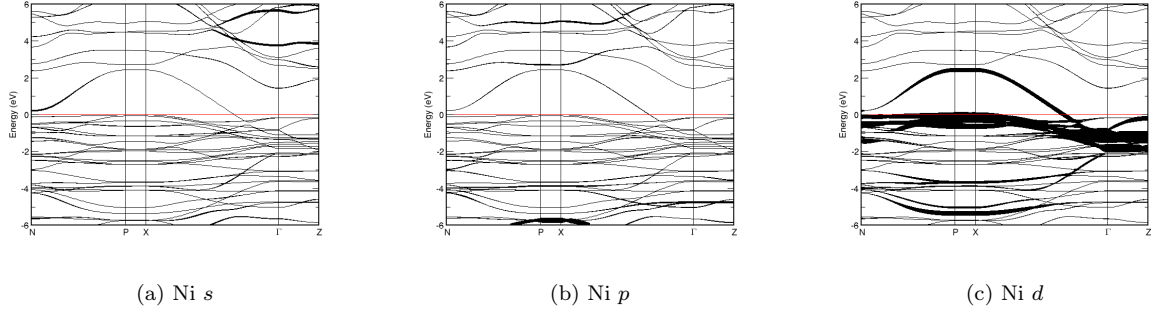
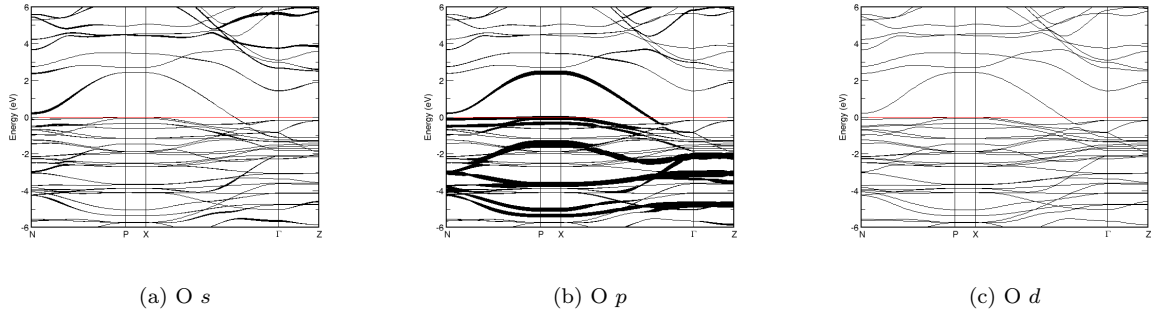
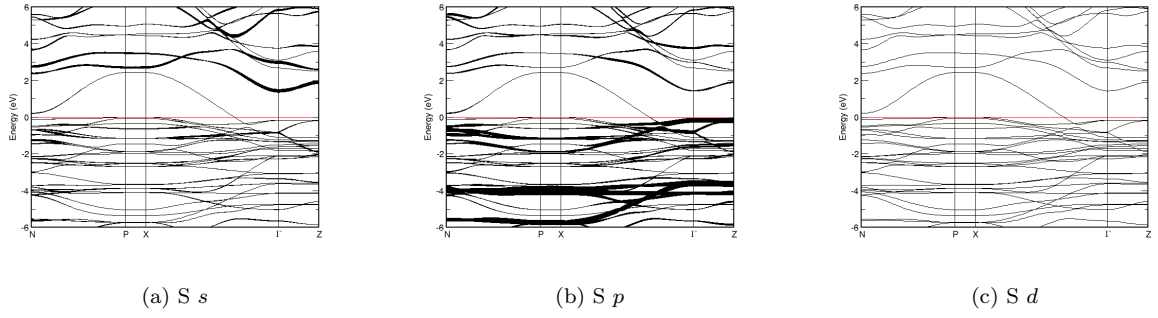
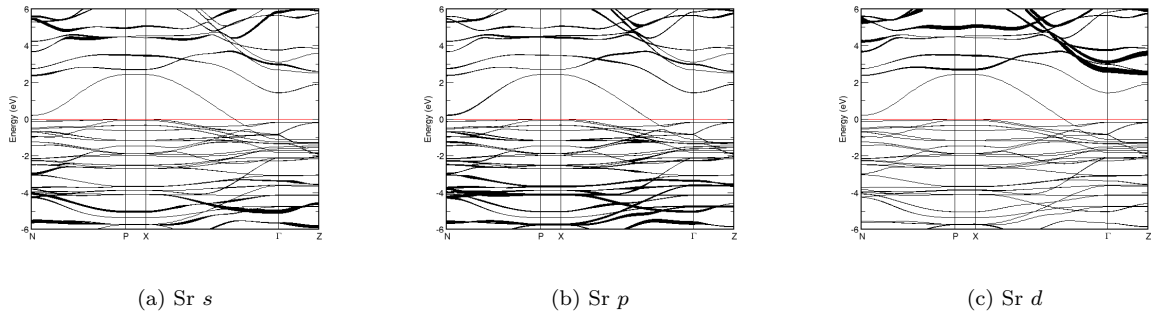


FIG. 255: Fat band representation of Na in Na_2PdH_2

FIG. 256: Fat band representation of Pd in Na_2PdH_2 FIG. 257: (Color online) PDOS of $(\text{Cu}_2\text{S}_2)(\text{Sr}_2\text{NiO}_2)$ (ICSD #88424). The *s*-, *p*- and *d*-projected states are in red, blue and green, respectively. $(\text{Cu}_2\text{S}_2)(\text{Sr}_2\text{NiO}_2)$ crystallizes in space group $I 4/m m m$ (#139), in a tetragonal body-centred structure.FIG. 258: Fat band representation of Cu in $(\text{Cu}_2\text{S}_2)(\text{Sr}_2\text{NiO}_2)$

FIG. 259: Fat band representation of Ni in $(\text{Cu}_2\text{S}_2)(\text{Sr}_2\text{NiO}_2)$ FIG. 260: Fat band representation of O in $(\text{Cu}_2\text{S}_2)(\text{Sr}_2\text{NiO}_2)$ FIG. 261: Fat band representation of S in $(\text{Cu}_2\text{S}_2)(\text{Sr}_2\text{NiO}_2)$ FIG. 262: Fat band representation of Sr in $(\text{Cu}_2\text{S}_2)(\text{Sr}_2\text{NiO}_2)$

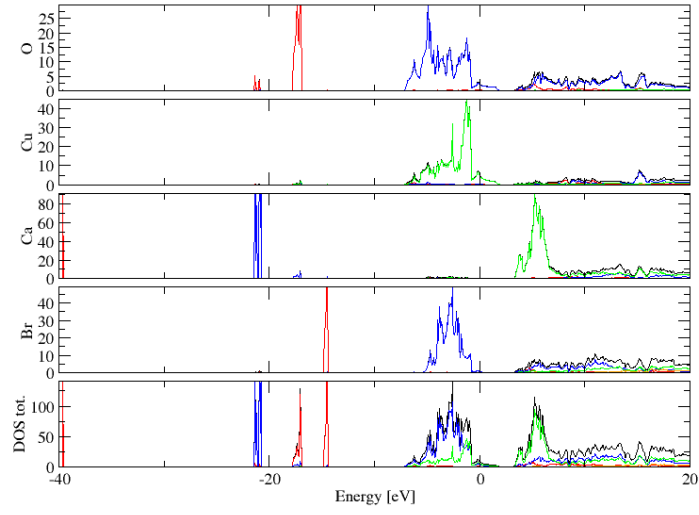


FIG. 263: (Color online) PDOS of $\text{Ca}_2(\text{CuBr}_2\text{O}_2)$ (ICSD #1028). The s -, p - and d -projected states are in red, blue and green, respectively. $\text{Ca}_2(\text{CuBr}_2\text{O}_2)$ crystallizes in space group $I 4/m m m$ (#139), in a tetragonal body-centred structure.

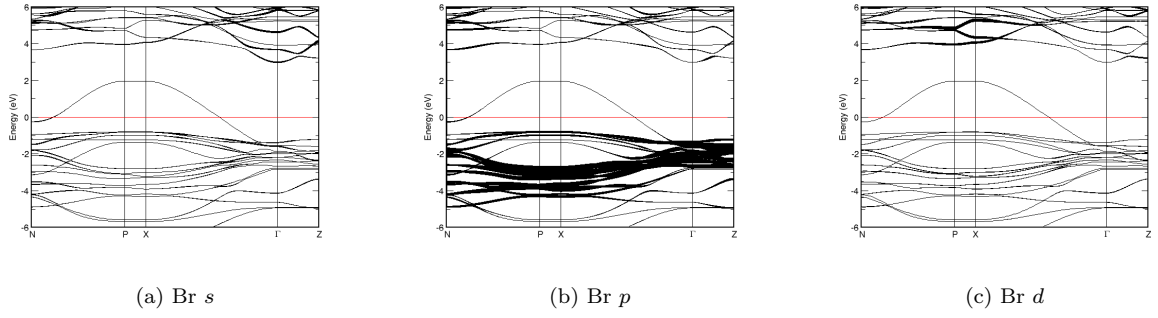


FIG. 264: Fat band representation of Br in $\text{Ca}_2(\text{CuBr}_2\text{O}_2)$

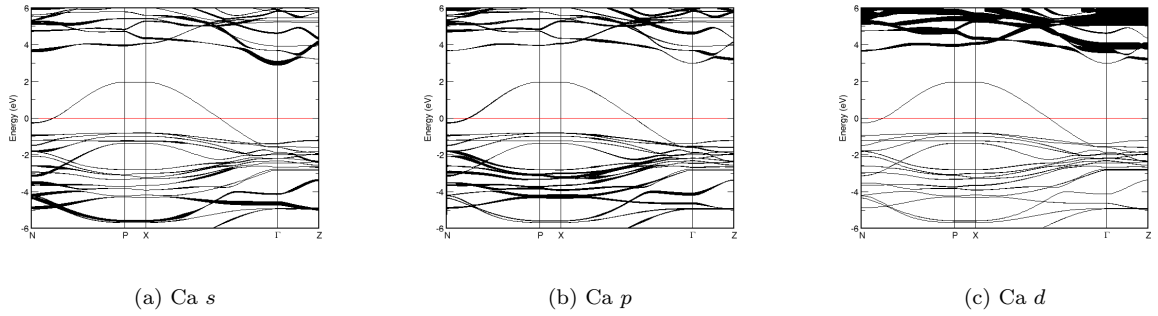


FIG. 265: Fat band representation of Ca in $\text{Ca}_2(\text{CuBr}_2\text{O}_2)$

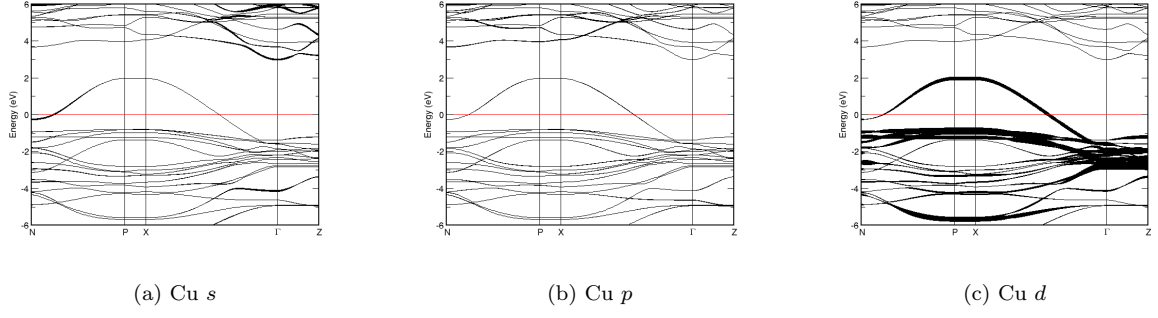


FIG. 266: Fat band representation of Cu in $\text{Ca}_2(\text{CuBr}_2\text{O}_2)$

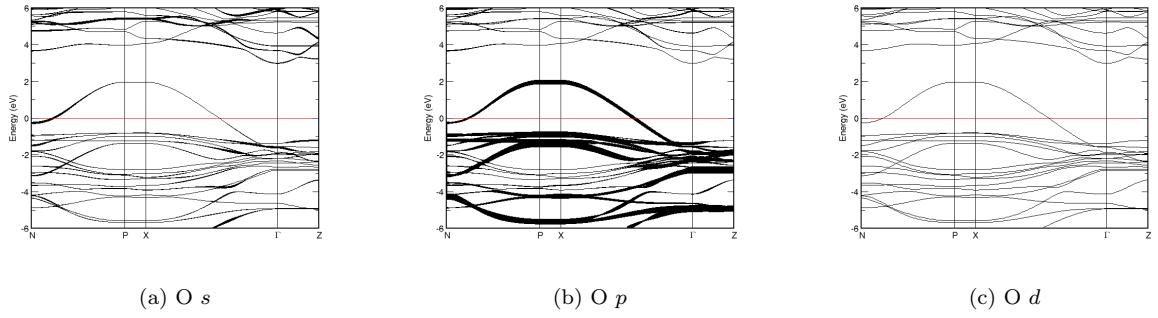


FIG. 267: Fat band representation of O in $\text{Ca}_2(\text{CuBr}_2\text{O}_2)$

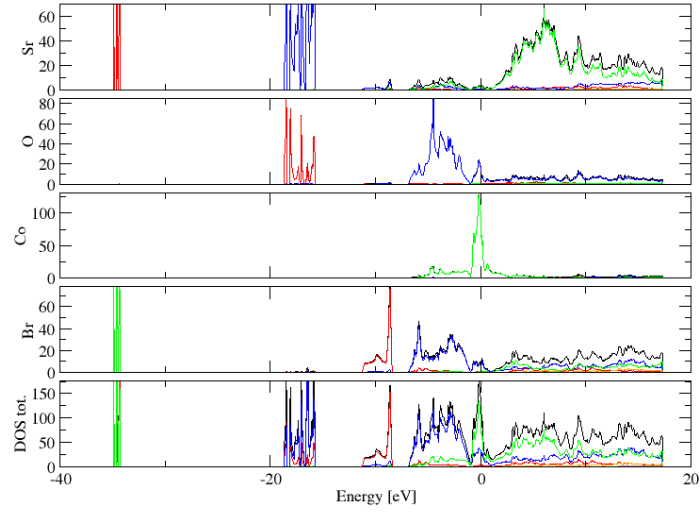
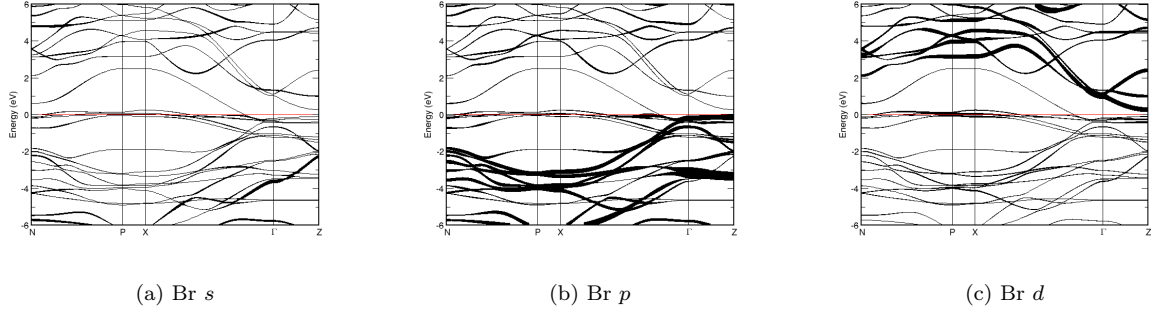
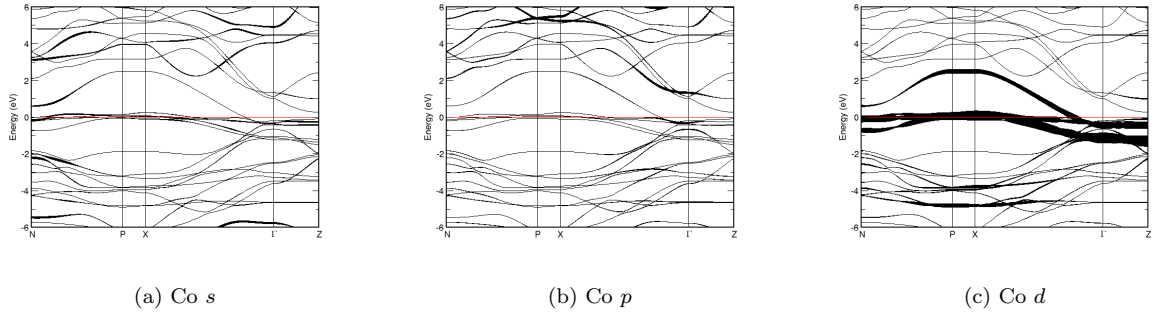
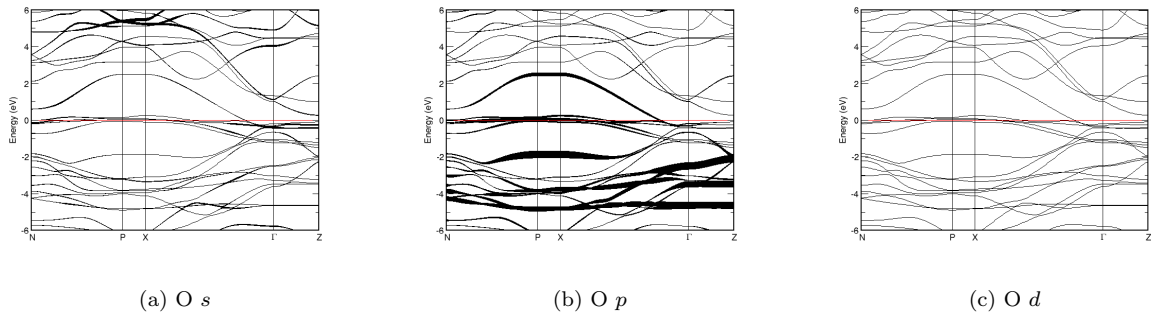
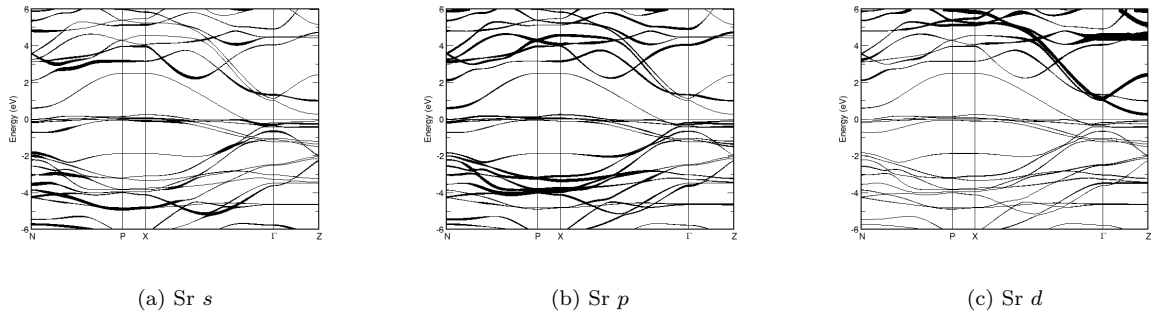


FIG. 268: (Color online) PDOS of $\text{Sr}_2\text{CoO}_2\text{Br}_2$ (ICSD #151789). The s -, p - and d -projected states are in red, blue and green, respectively. $\text{Sr}_2\text{CoO}_2\text{Br}_2$ crystallizes in space group $I 4/m m m$ (#139), in a tetragonal body-centred structure.

FIG. 269: Fat band representation of Br in $\text{Sr}_2\text{CoO}_2\text{Br}_2$ FIG. 270: Fat band representation of Co in $\text{Sr}_2\text{CoO}_2\text{Br}_2$ FIG. 271: Fat band representation of O in $\text{Sr}_2\text{CoO}_2\text{Br}_2$ FIG. 272: Fat band representation of Sr in $\text{Sr}_2\text{CoO}_2\text{Br}_2$

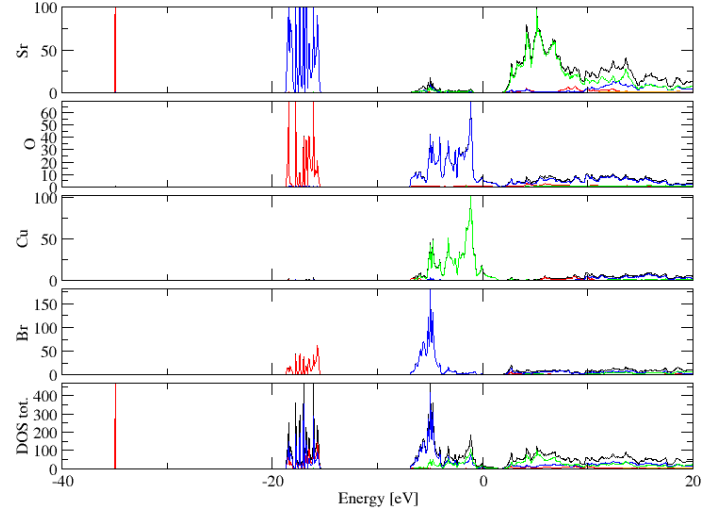


FIG. 273: (Color online) PDOS of $\text{CuSr}_2\text{Br}_2\text{O}_2$ (ICSD #1178). The s -, p - and d -projected states are in red, blue and green, respectively. $\text{CuSr}_2\text{Br}_2\text{O}_2$ crystallizes in space group $I 4/m m m$ (#139), in a tetragonal body-centred structure.

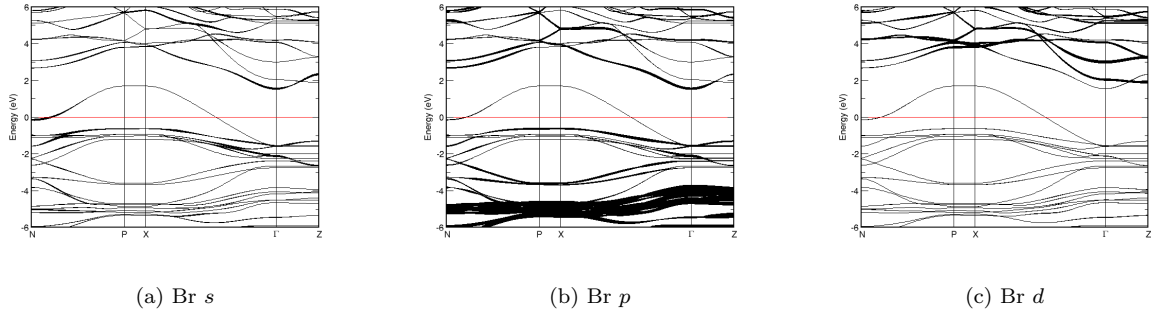


FIG. 274: Fat band representation of Br in $\text{CuSr}_2\text{Br}_2\text{O}_2$

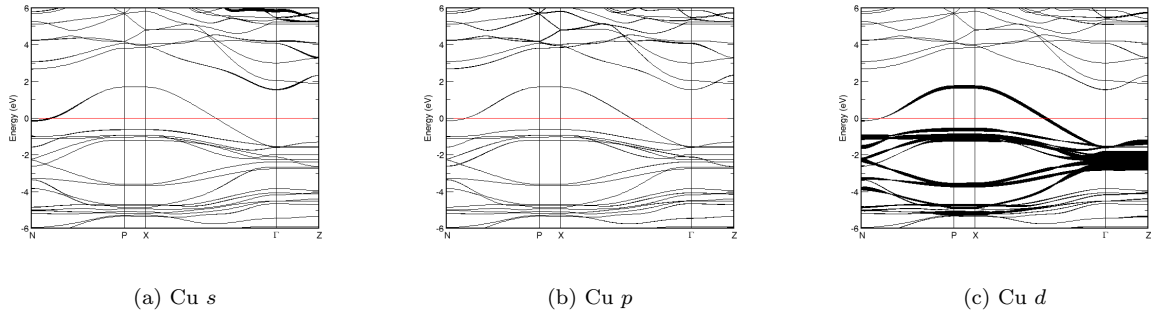


FIG. 275: Fat band representation of Cu in $\text{CuSr}_2\text{Br}_2\text{O}_2$

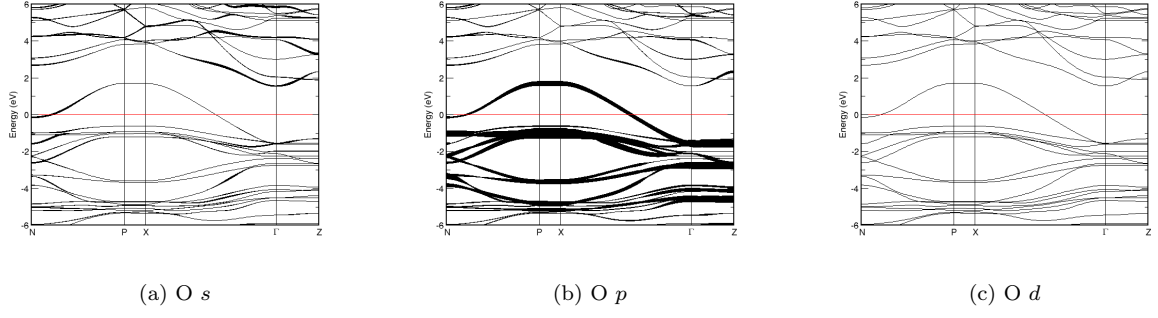
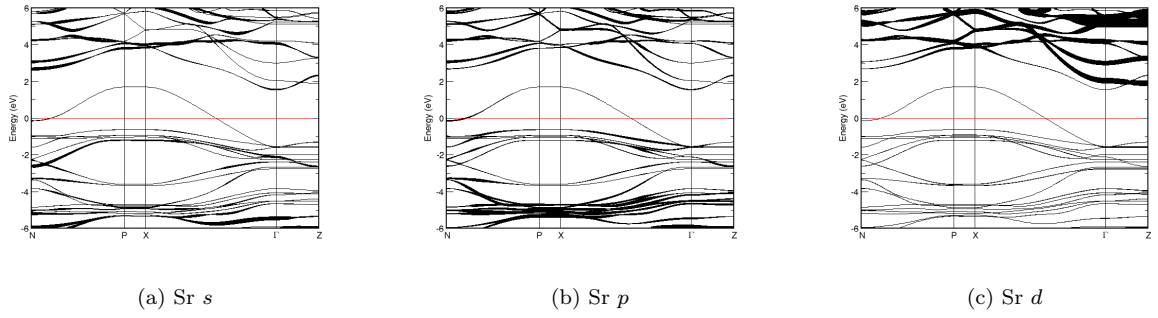
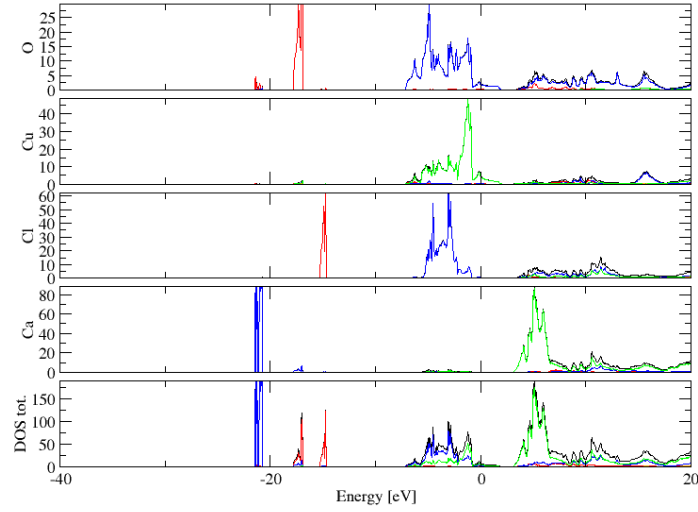
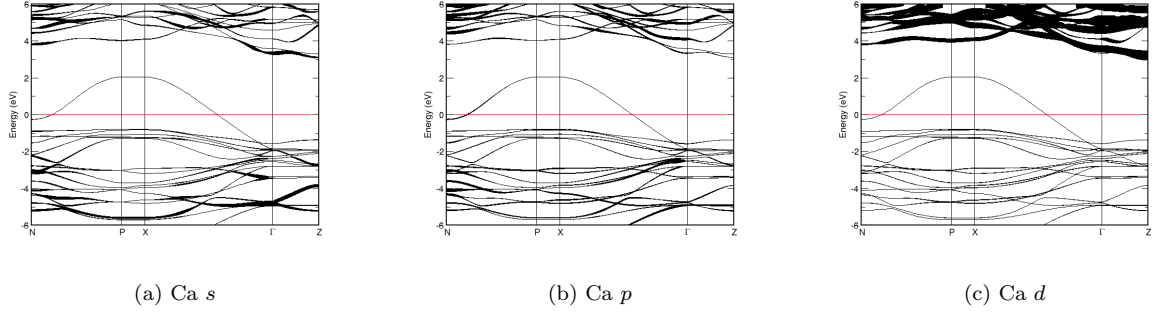
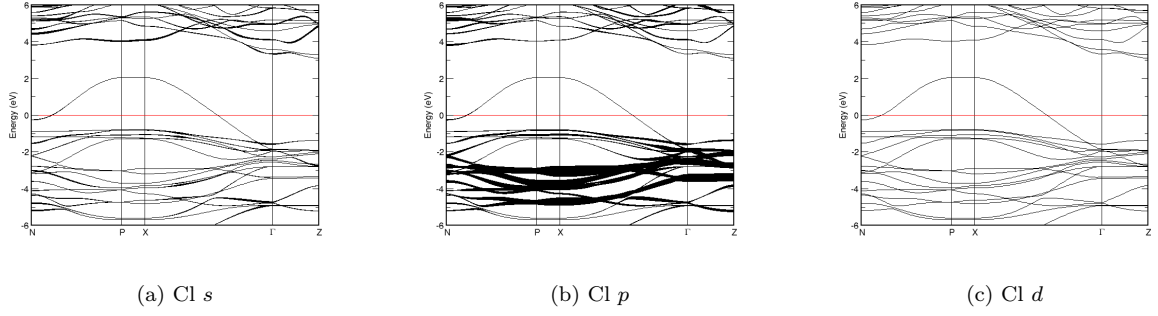
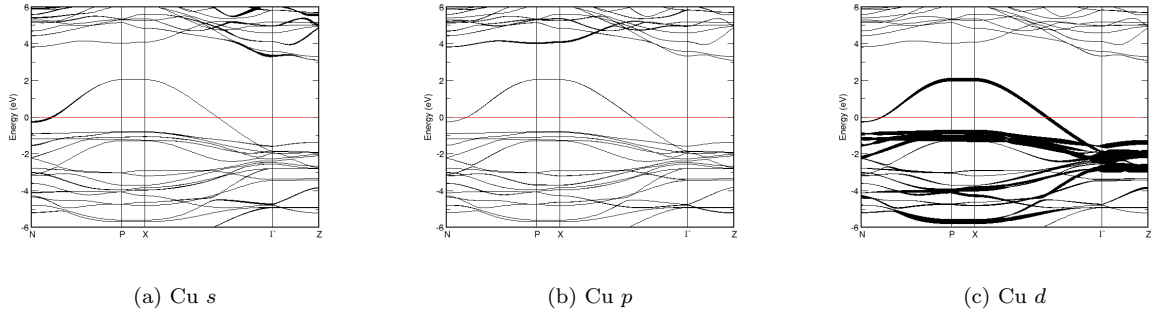
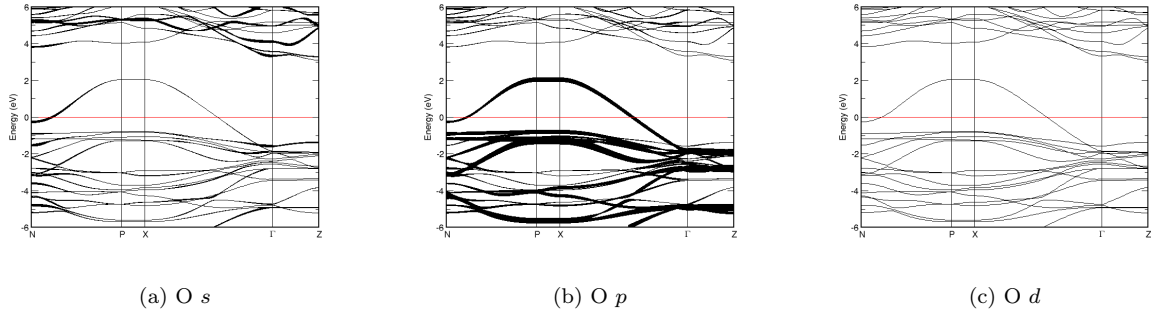
FIG. 276: Fat band representation of O in $\text{CuSr}_2\text{Br}_2\text{O}_2$ FIG. 277: Fat band representation of Sr in $\text{CuSr}_2\text{Br}_2\text{O}_2$ 

FIG. 278: (Color online) PDOS of $\text{Ca}_2(\text{CuCl}_2\text{O}_2)$ (ICSD #1027). The *s*-, *p*- and *d*-projected states are in red, blue and green, respectively. $\text{Ca}_2(\text{CuCl}_2\text{O}_2)$ crystallizes in space group $I 4/m m m$ (#139), in a tetragonal body-centred structure.

FIG. 279: Fat band representation of Ca in $\text{Ca}_2(\text{CuCl}_2\text{O}_2)$ FIG. 280: Fat band representation of Cl in $\text{Ca}_2(\text{CuCl}_2\text{O}_2)$ FIG. 281: Fat band representation of Cu in $\text{Ca}_2(\text{CuCl}_2\text{O}_2)$ FIG. 282: Fat band representation of O in $\text{Ca}_2(\text{CuCl}_2\text{O}_2)$

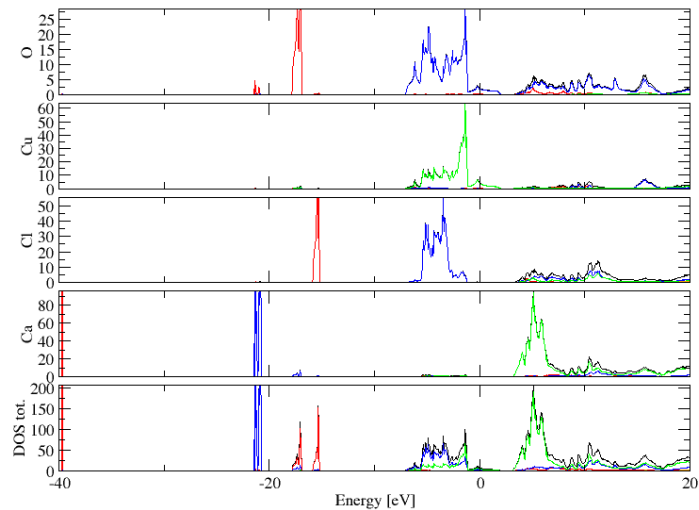


FIG. 283: (Color online) PDOS of $\text{Ca}_2\text{CuO}_2\text{Cl}_2$ (ICSD #83117). The s -, p - and d -projected states are in red, blue and green, respectively. $\text{Ca}_2\text{CuO}_2\text{Cl}_2$ crystallizes in space group $I 4/m m m$ (#139), in a tetragonal body-centred structure.

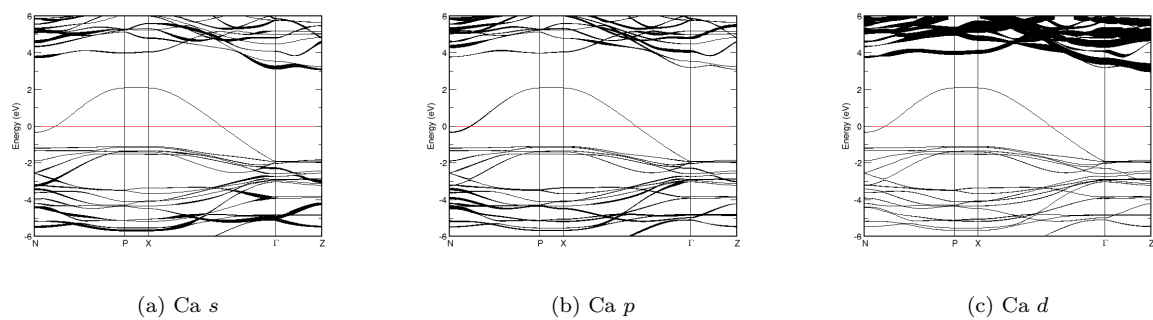


FIG. 284: Fat band representation of Ca in $\text{Ca}_2\text{CuO}_2\text{Cl}_2$

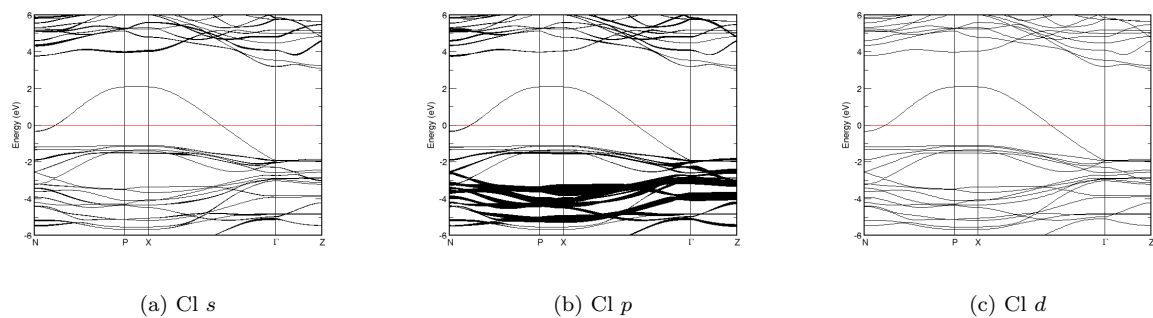


FIG. 285: Fat band representation of Cl in $\text{Ca}_2\text{CuO}_2\text{Cl}_2$

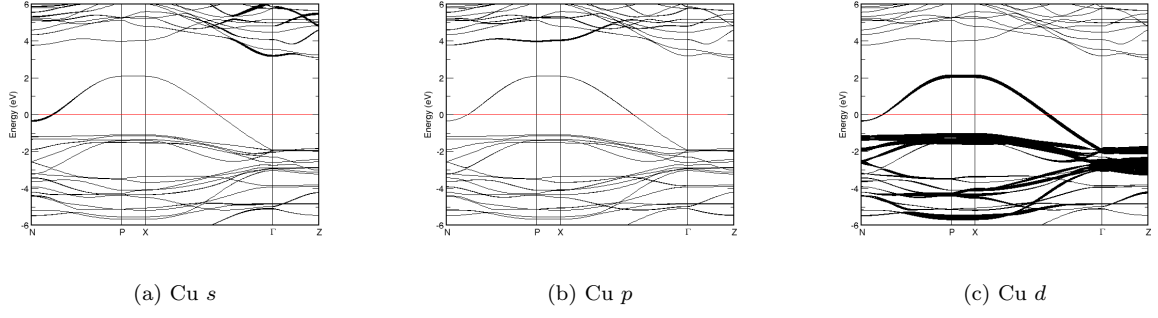
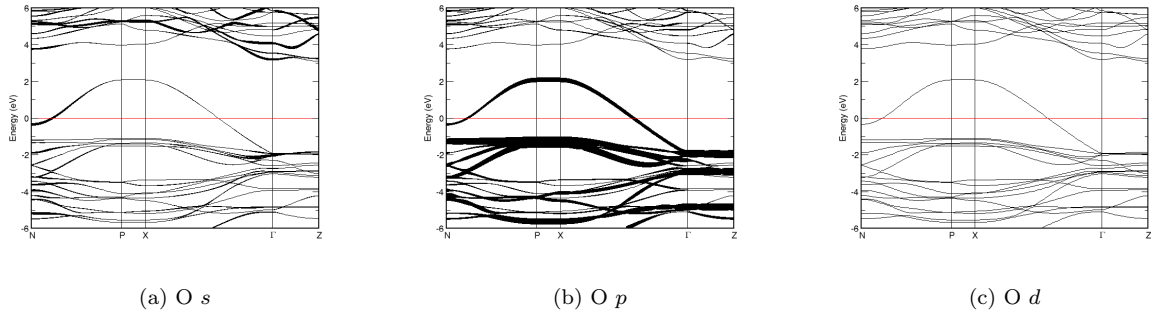
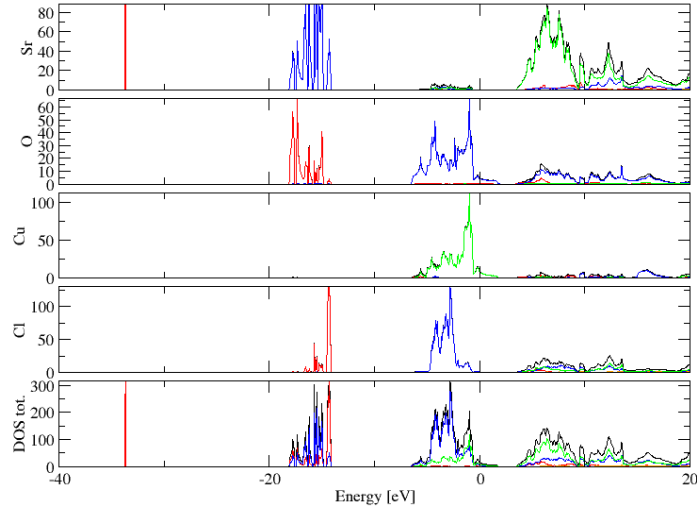
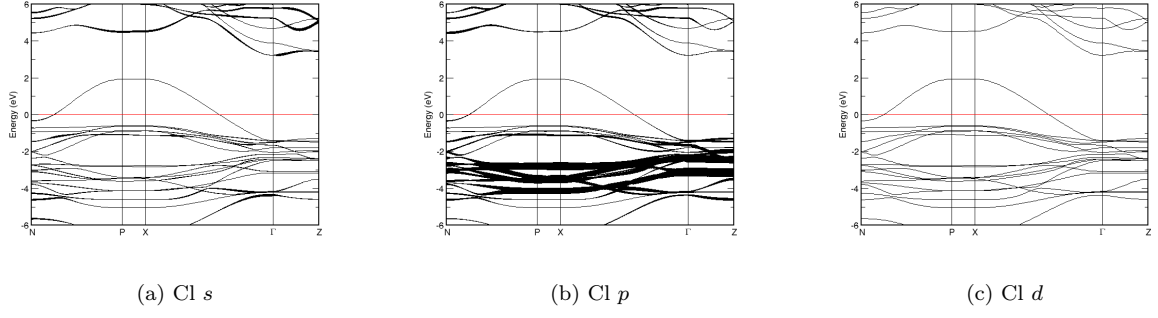
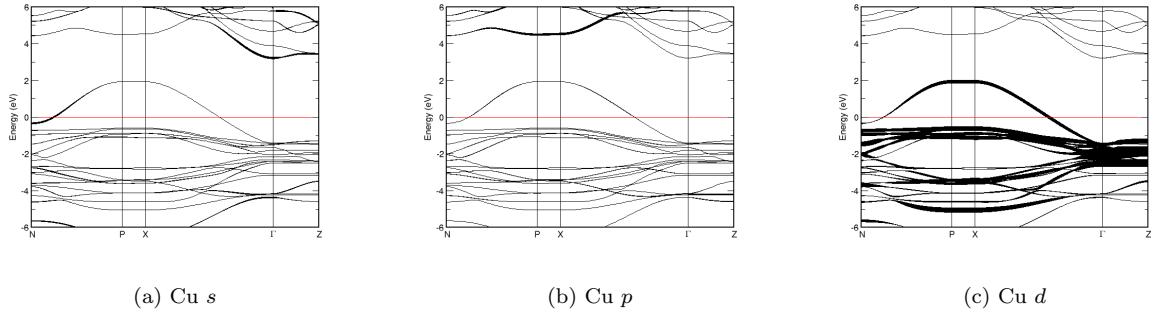
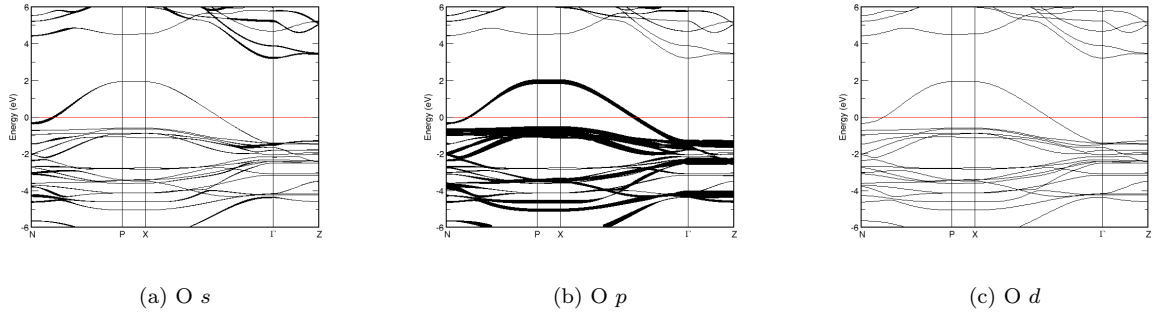
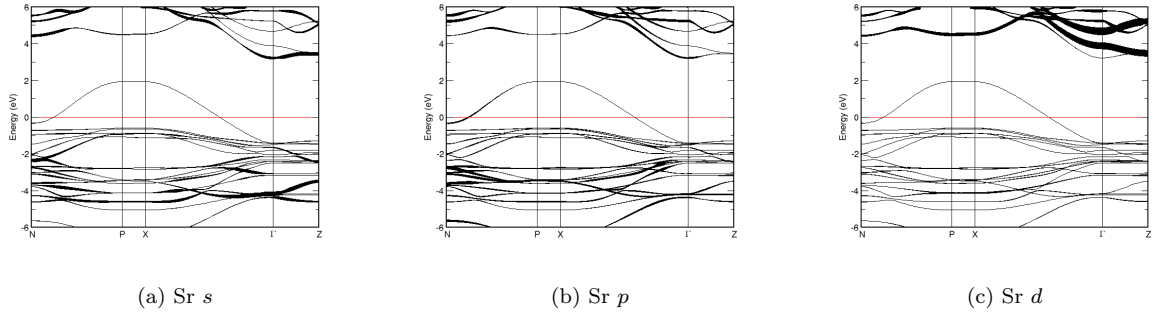
FIG. 286: Fat band representation of Cu in $\text{Ca}_2\text{CuO}_2\text{Cl}_2$ FIG. 287: Fat band representation of O in $\text{Ca}_2\text{CuO}_2\text{Cl}_2$ 

FIG. 288: (Color online) PDOS of $\text{Sr}_2\text{CuO}_2\text{Cl}_2$ (ICSD #4087). The *s*-, *p*- and *d*-projected states are in red, blue and green, respectively. $\text{Sr}_2\text{CuO}_2\text{Cl}_2$ crystallizes in space group $I 4/m m m$ (#139), in a tetragonal body-centred structure.

FIG. 289: Fat band representation of Cl in $\text{Sr}_2\text{CuO}_2\text{Cl}_2$ FIG. 290: Fat band representation of Cu in $\text{Sr}_2\text{CuO}_2\text{Cl}_2$ FIG. 291: Fat band representation of O in $\text{Sr}_2\text{CuO}_2\text{Cl}_2$ FIG. 292: Fat band representation of Sr in $\text{Sr}_2\text{CuO}_2\text{Cl}_2$

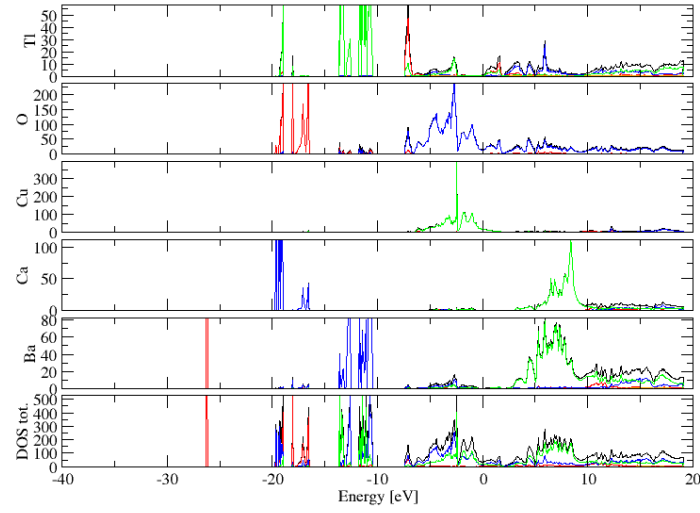


FIG. 293: (Color online) PDOS of $\text{Tl}_2\text{Ba}_2\text{CaCu}_2\text{O}_8$ (ICSD #78592). The s -, p - and d -projected states are in red, blue and green, respectively. $\text{Tl}_2\text{Ba}_2\text{CaCu}_2\text{O}_8$ crystallizes in space group $I 4/m m m$ (#139), in a tetragonal body-centred structure.

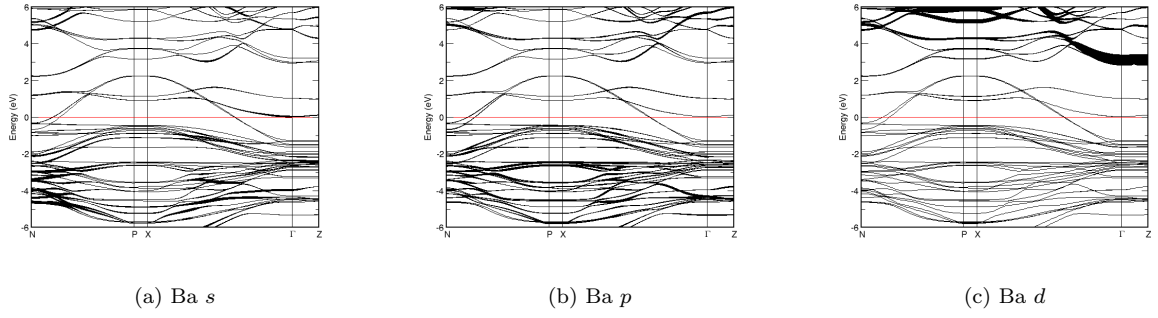


FIG. 294: Fat band representation of Ba in $\text{Tl}_2\text{Ba}_2\text{CaCu}_2\text{O}_8$

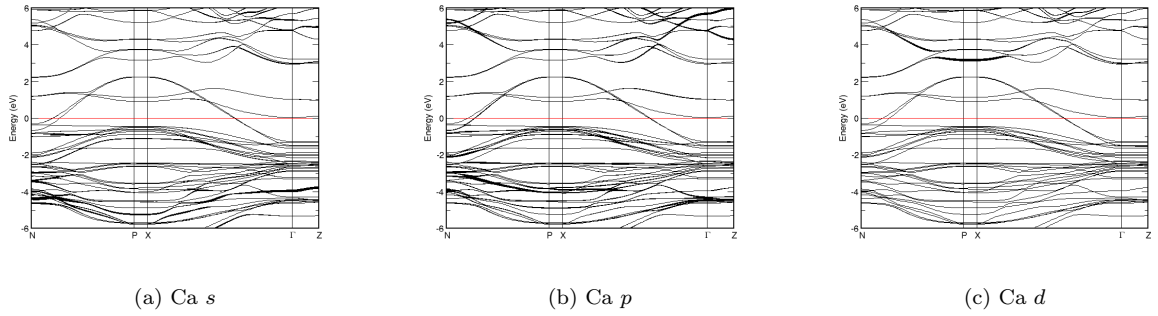
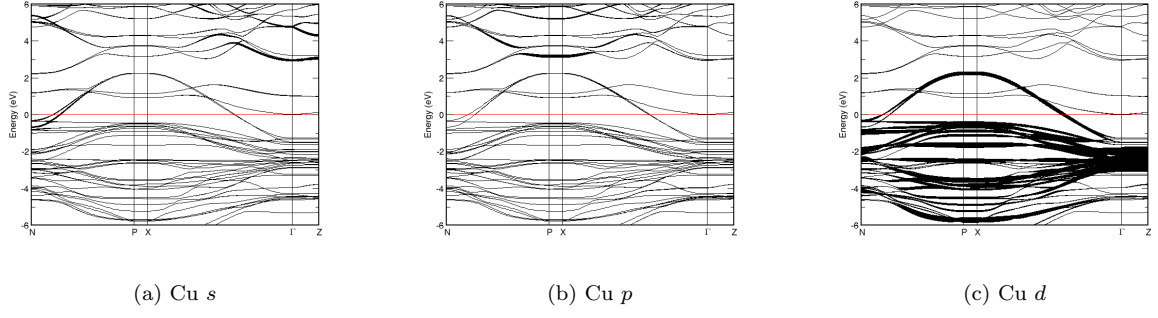
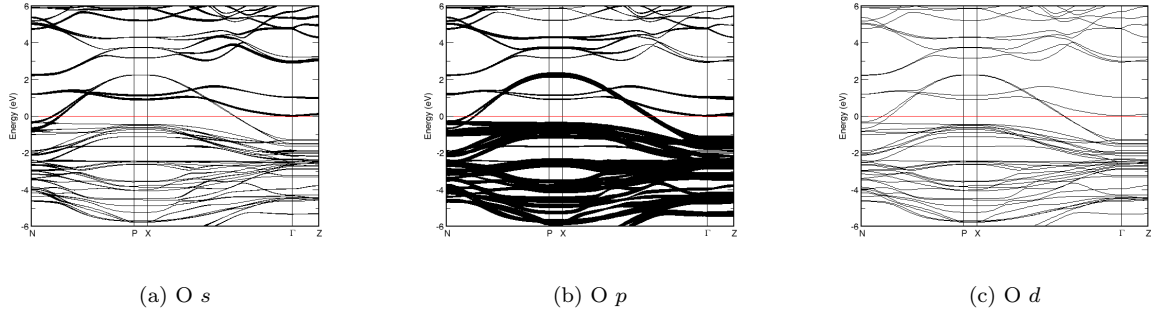
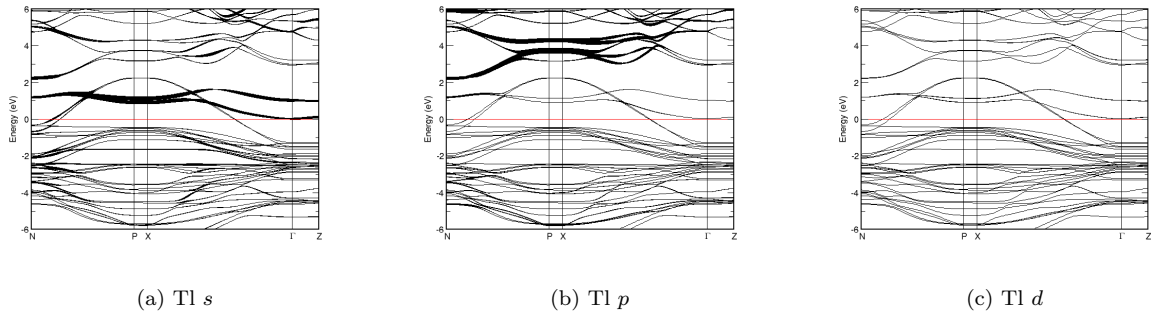


FIG. 295: Fat band representation of Ca in $\text{Tl}_2\text{Ba}_2\text{CaCu}_2\text{O}_8$

FIG. 296: Fat band representation of Cu in $\text{Tl}_2\text{Ba}_2\text{CaCu}_2\text{O}_8$ FIG. 297: Fat band representation of O in $\text{Tl}_2\text{Ba}_2\text{CaCu}_2\text{O}_8$ FIG. 298: Fat band representation of Tl in $\text{Tl}_2\text{Ba}_2\text{CaCu}_2\text{O}_8$

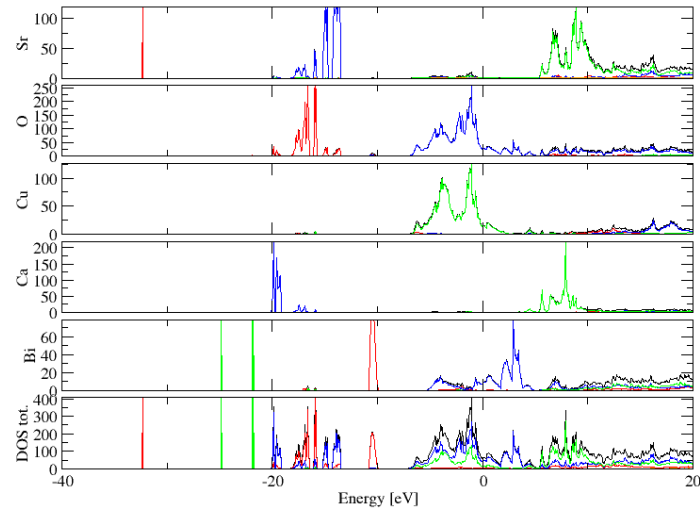


FIG. 299: (Color online) PDOS of $\text{Bi}_2\text{Sr}_2\text{CaCu}_2\text{O}_8$ (ICSD #68188). The s -, p - and d -projected states are in red, blue and green, respectively. $\text{Bi}_2\text{Sr}_2\text{CaCu}_2\text{O}_8$ crystallizes in space group $I 4/m m m$ (#139), in a tetragonal body-centred structure.

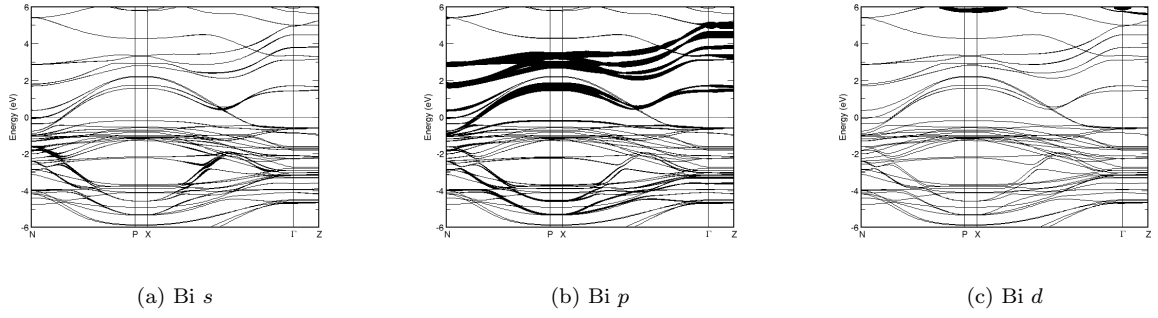


FIG. 300: Fat band representation of Bi in $\text{Bi}_2\text{Sr}_2\text{CaCu}_2\text{O}_8$

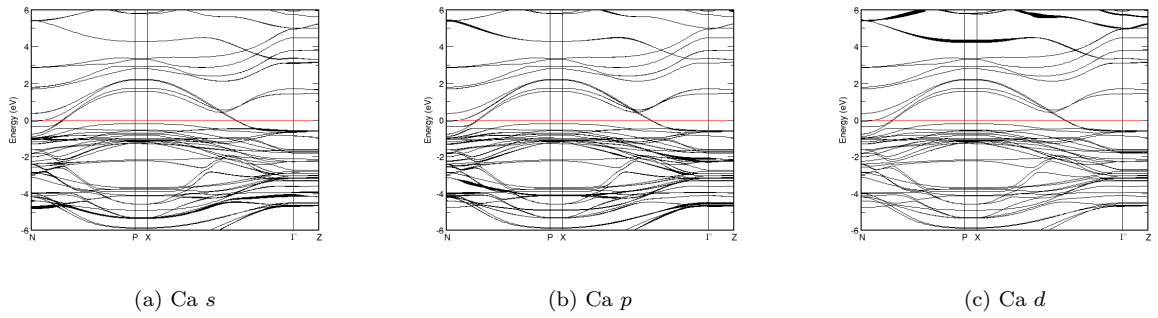
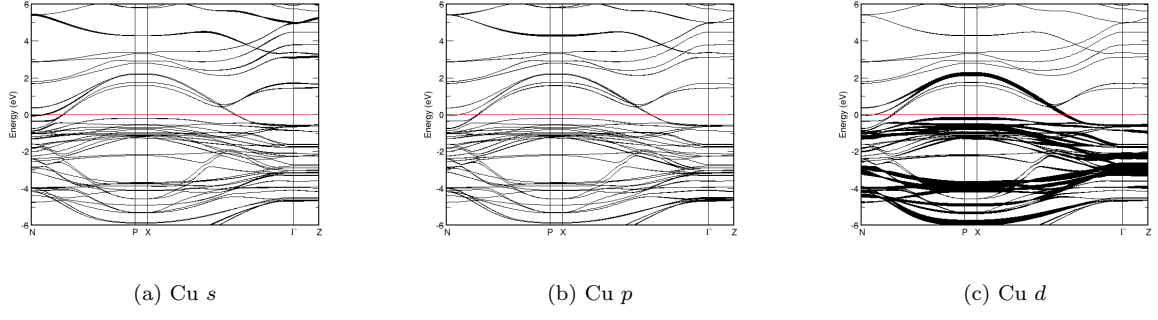
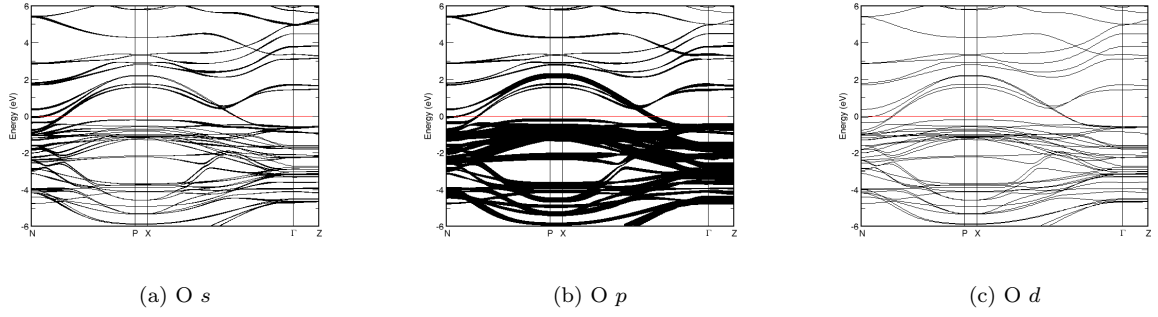
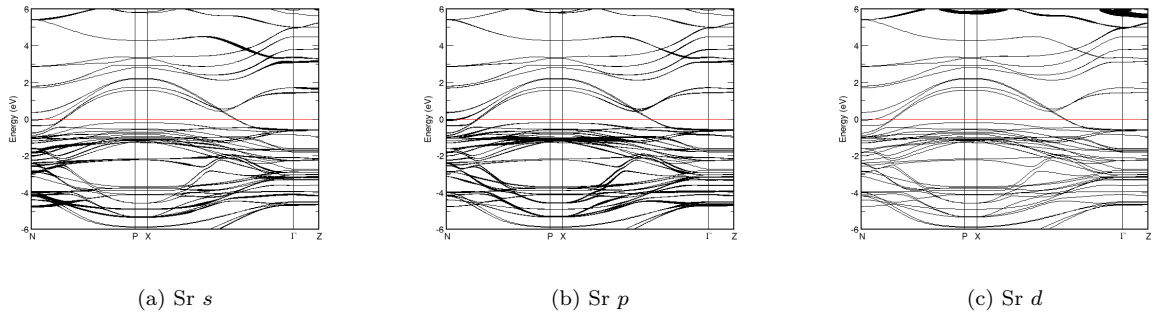


FIG. 301: Fat band representation of Ca in $\text{Bi}_2\text{Sr}_2\text{CaCu}_2\text{O}_8$

FIG. 302: Fat band representation of Cu in $\text{Bi}_2\text{Sr}_2\text{CaCu}_2\text{O}_8$ FIG. 303: Fat band representation of O in $\text{Bi}_2\text{Sr}_2\text{CaCu}_2\text{O}_8$ FIG. 304: Fat band representation of Sr in $\text{Bi}_2\text{Sr}_2\text{CaCu}_2\text{O}_8$

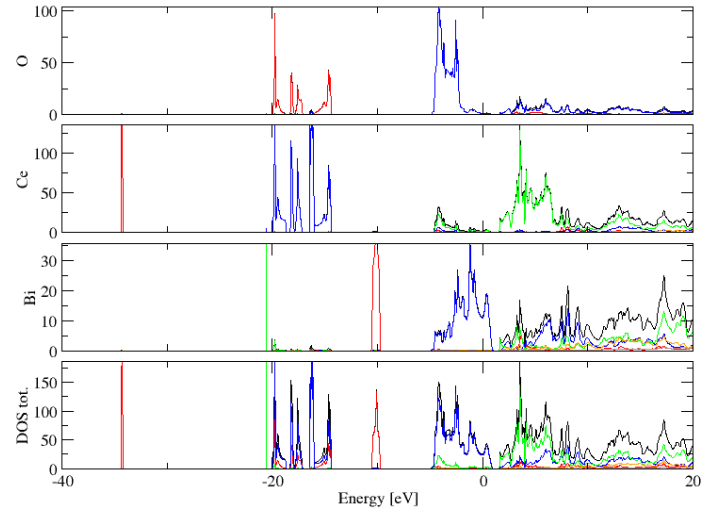


FIG. 305: (Color online) PDOS of Ce_2BiO_2 (ICSD #9099). The s -, p - and d -projected states are in red, blue and green, respectively. Ce_2BiO_2 crystallizes in space group $I 4/m m m$ (#139), in a tetragonal body-centred structure.

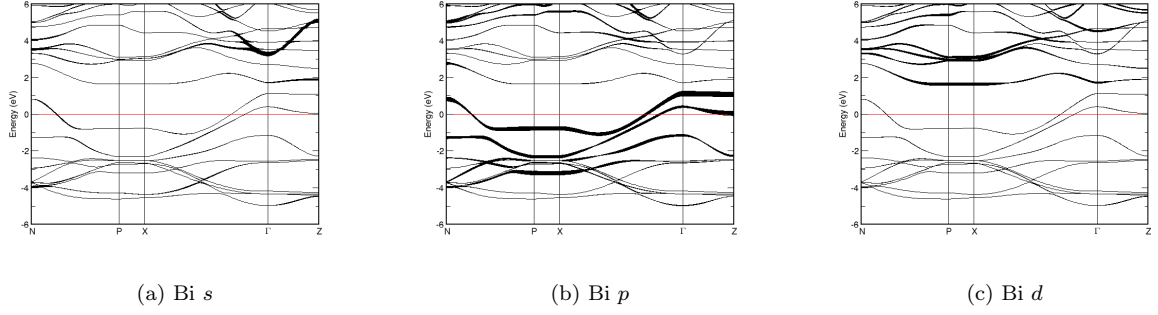


FIG. 306: Fat band representation of Bi in Ce_2BiO_2

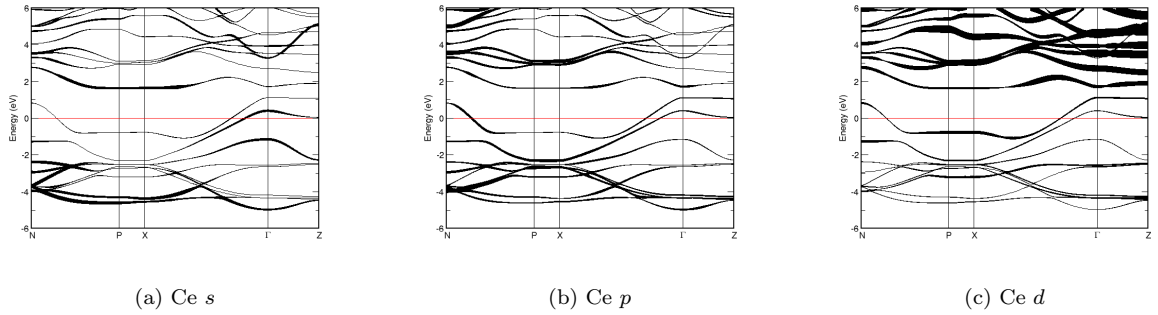
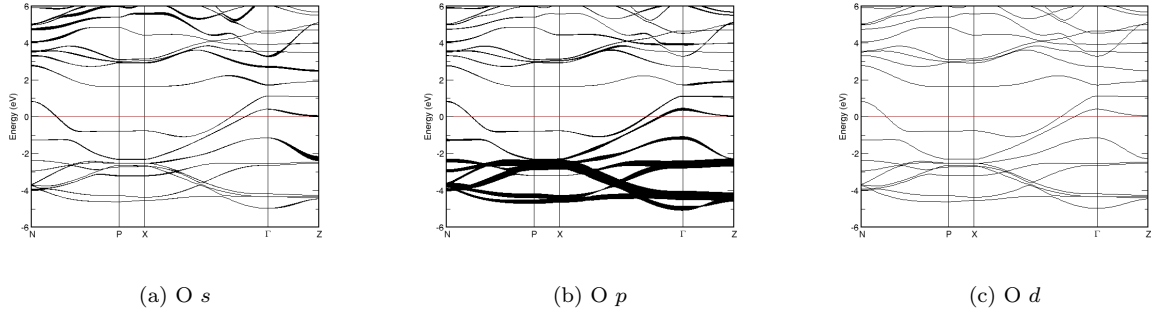
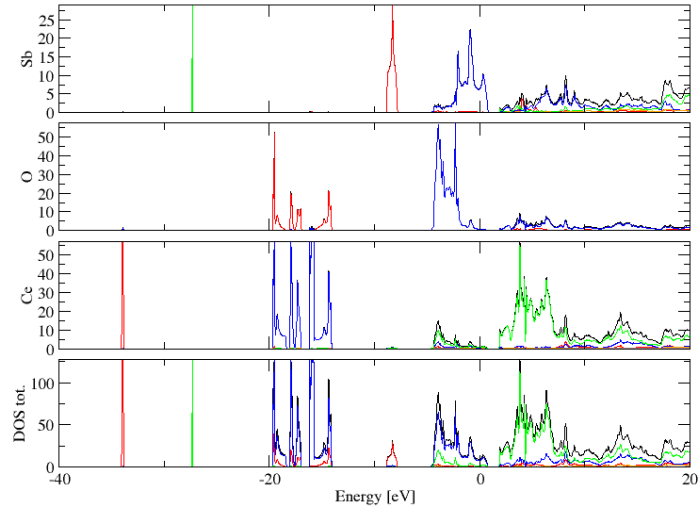
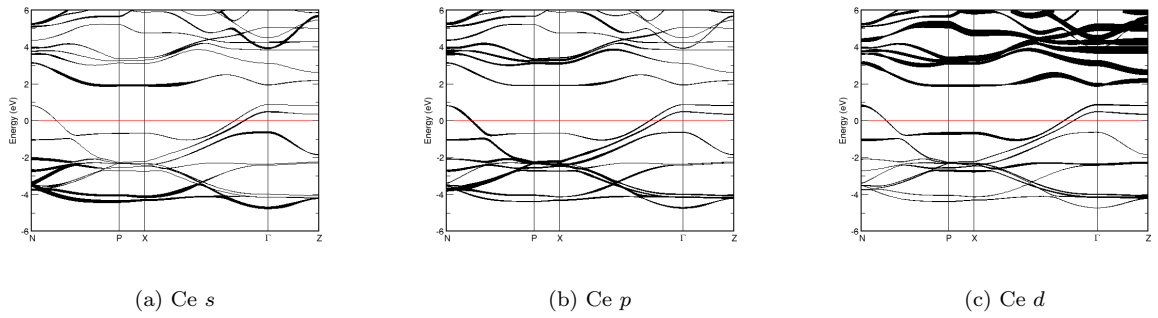
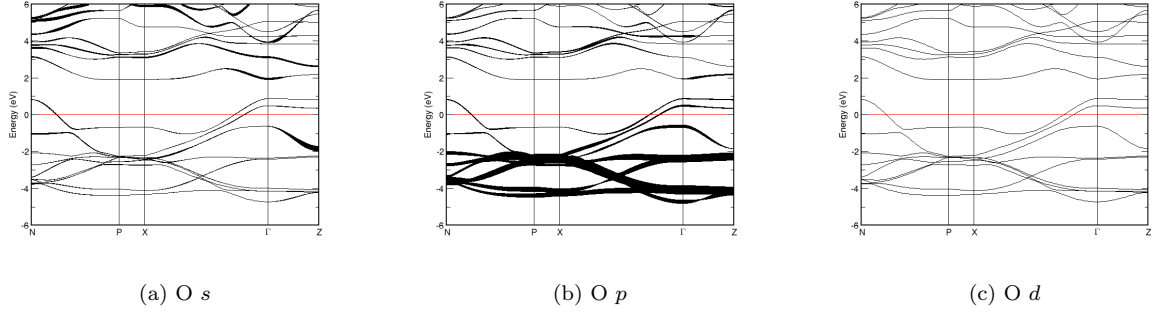
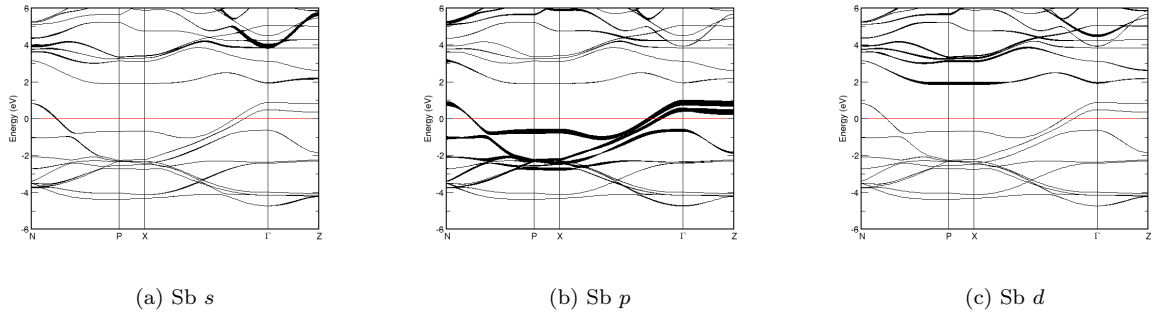
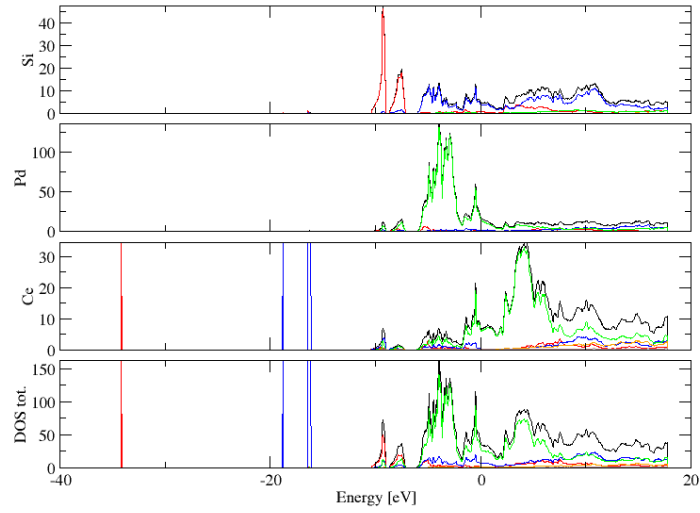
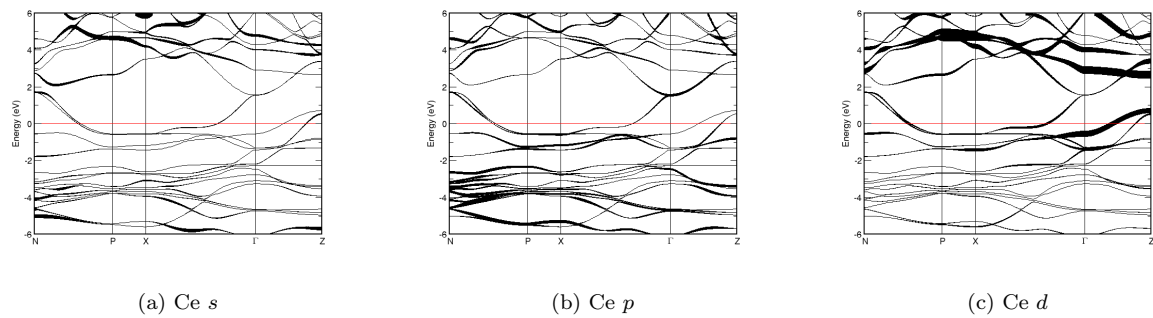
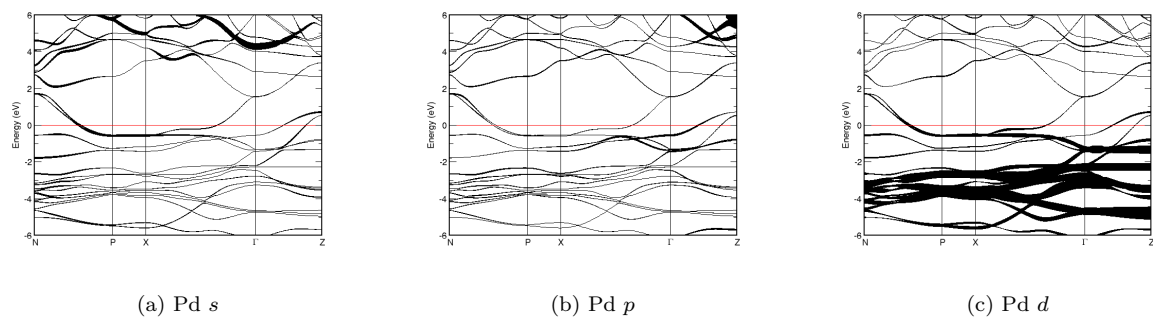
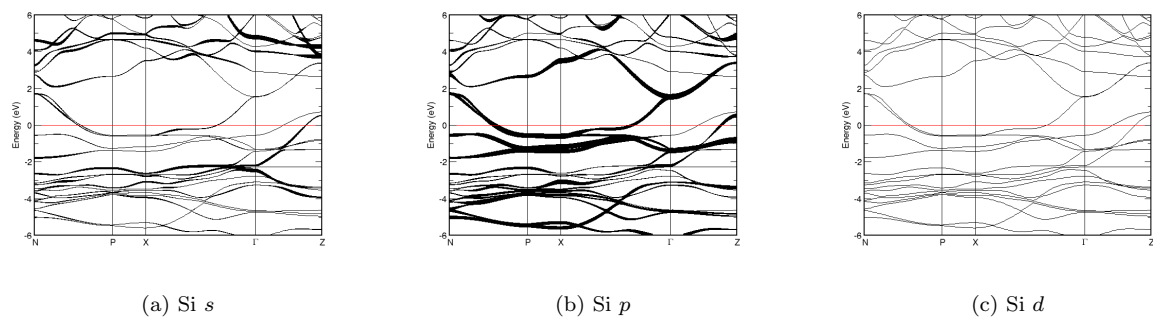


FIG. 307: Fat band representation of Ce in Ce_2BiO_2

FIG. 308: Fat band representation of O in Ce_2BiO_2 FIG. 309: (Color online) PDOS of Ce_2SbO_2 (ICSD #9100). The *s*-, *p*- and *d*-projected states are in red, blue and green, respectively. Ce_2SbO_2 crystallizes in space group $I 4/m m m$ (#139), in a tetragonal body-centred structure.FIG. 310: Fat band representation of Ce in Ce_2SbO_2

FIG. 311: Fat band representation of O in Ce_2SbO_2 FIG. 312: Fat band representation of Sb in Ce_2SbO_2 FIG. 313: (Color online) PDOS of CePd_2Si_2 (ICSD #621852). The s -, p - and d -projected states are in red, blue and green, respectively. CePd_2Si_2 crystallizes in space group $I 4/m m m$ (#139), in a tetragonal body-centred structure.

FIG. 314: Fat band representation of Ce in CePd_2Si_2 FIG. 315: Fat band representation of Pd in CePd_2Si_2 FIG. 316: Fat band representation of Si in CePd_2Si_2

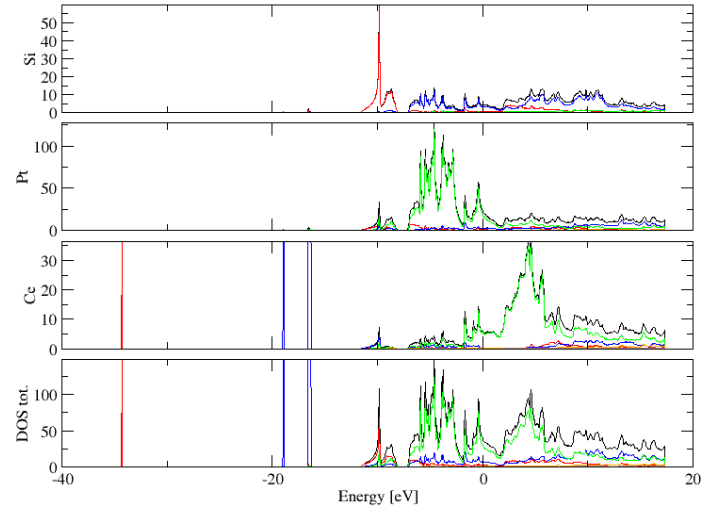


FIG. 317: (Color online) PDOS of CePt_2Si_2 (ICSD #52895). The s -, p - and d -projected states are in red, blue and green, respectively. CePt_2Si_2 crystallizes in space group $I 4/m m m$ (#139), in a tetragonal body-centred structure.

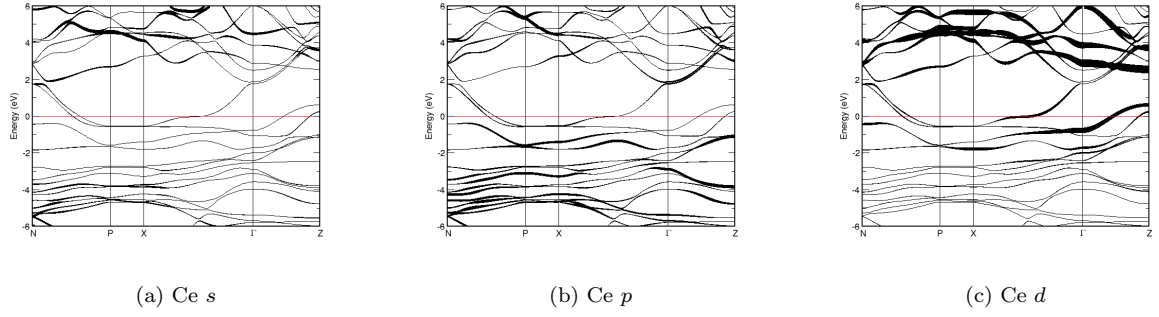


FIG. 318: Fat band representation of Ce in CePt_2Si_2

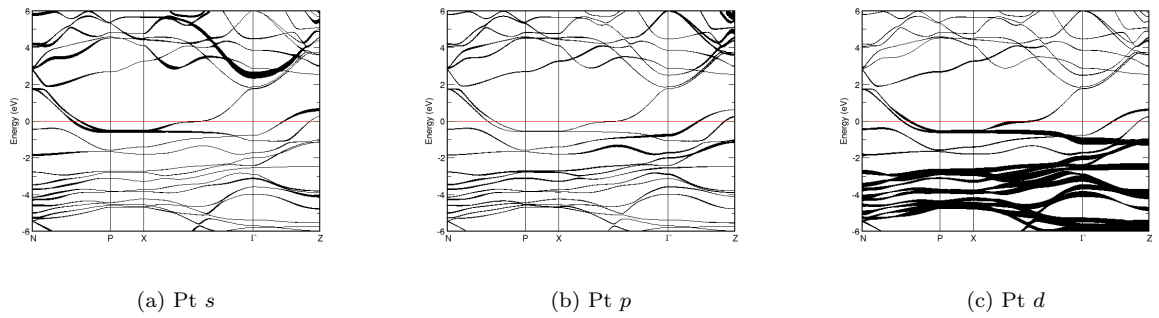
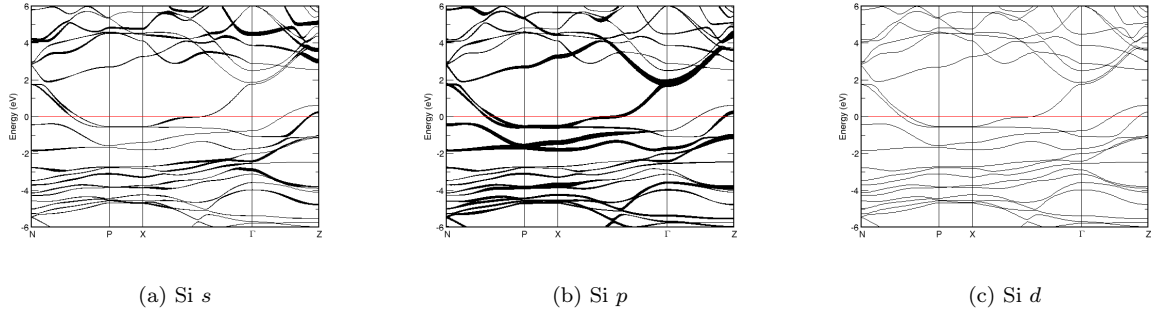
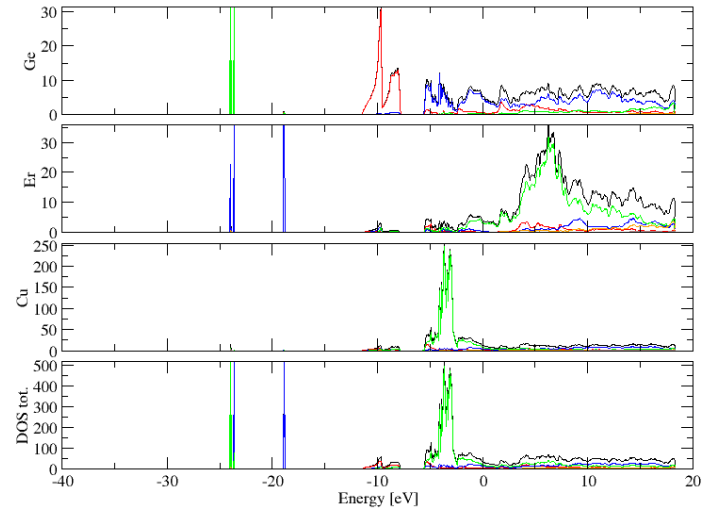
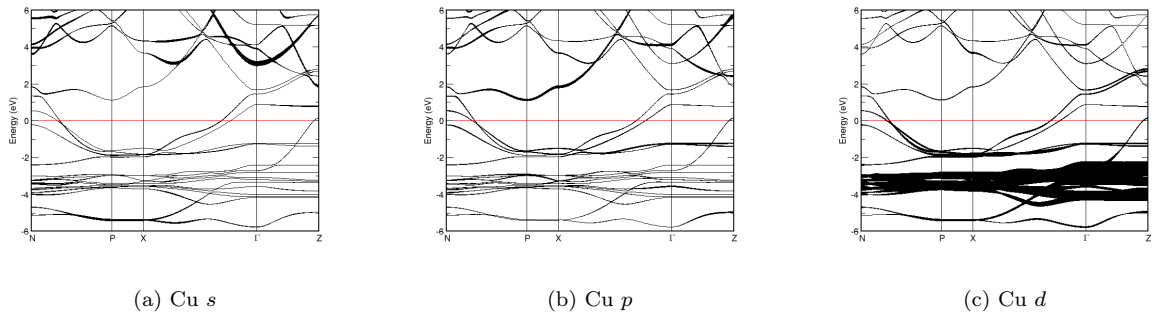
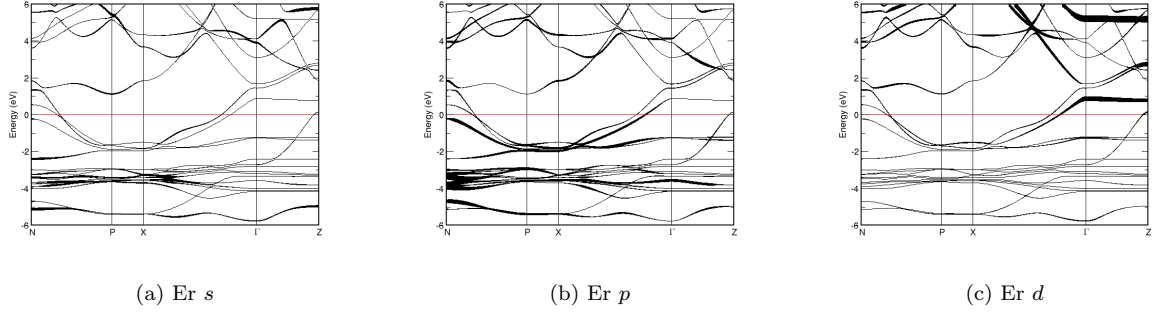
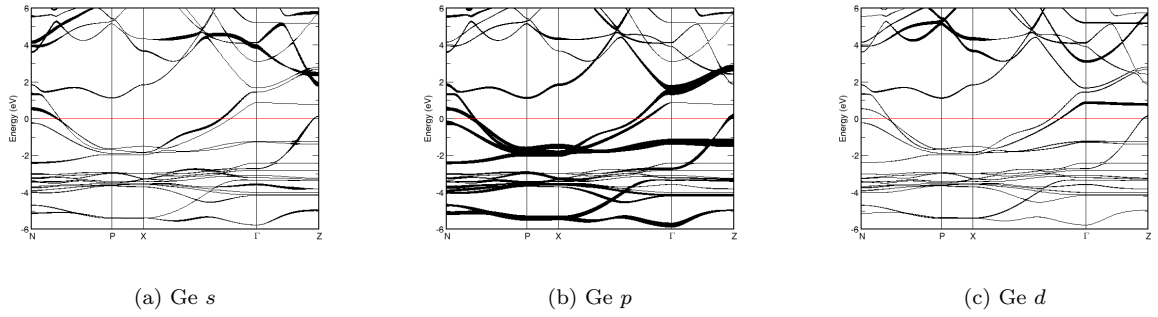
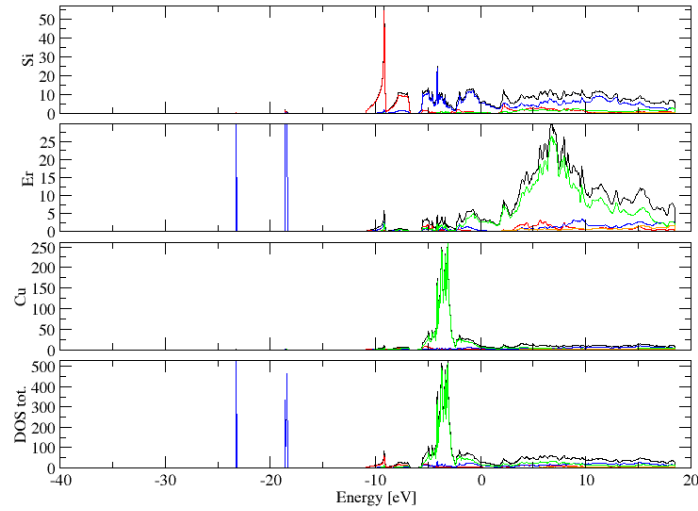
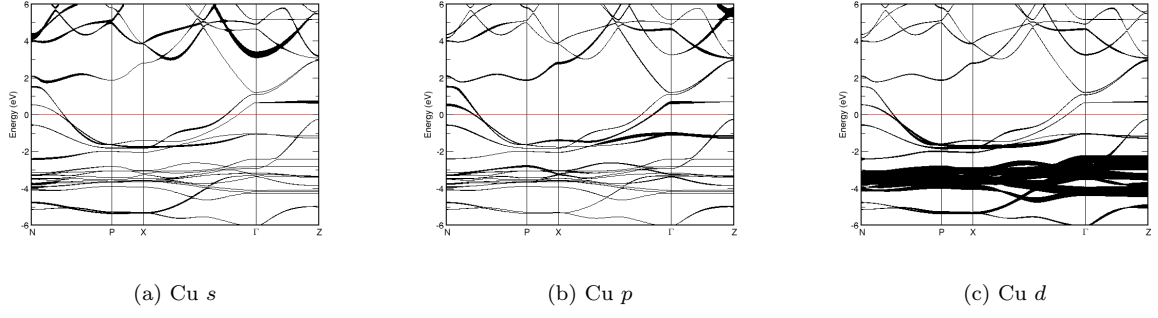
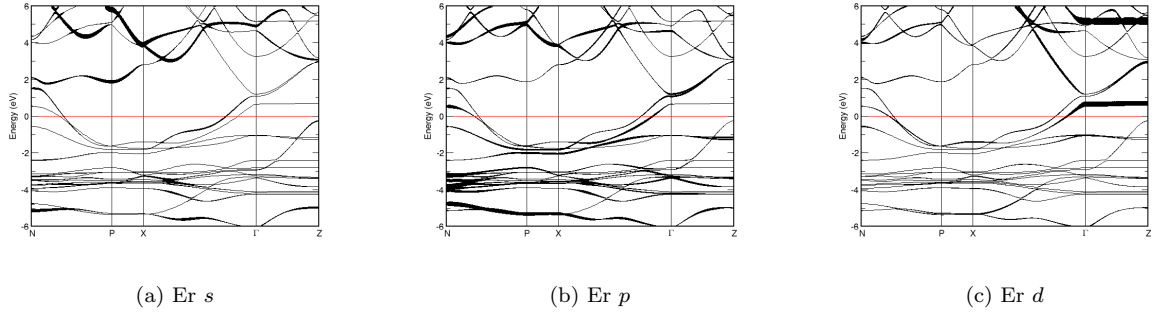
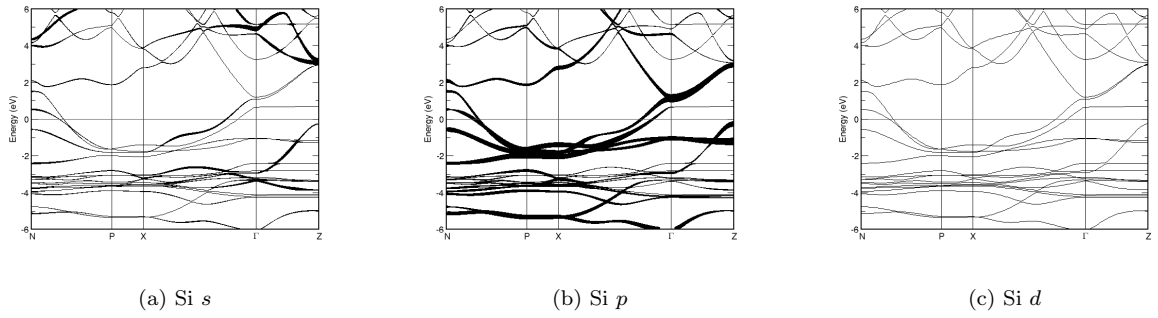


FIG. 319: Fat band representation of Pt in CePt_2Si_2

FIG. 320: Fat band representation of Si in CePt_2Si_2 FIG. 321: (Color online) PDOS of Cu_2ErGe_2 (ICSD #53251). The *s*-, *p*- and *d*-projected states are in red, blue and green, respectively. Cu_2ErGe_2 crystallizes in space group $I 4/m m m$ (#139), in a tetragonal body-centred structure.FIG. 322: Fat band representation of Cu in Cu_2ErGe_2

FIG. 323: Fat band representation of Er in Cu_2ErGe_2 FIG. 324: Fat band representation of Ge in Cu_2ErGe_2 FIG. 325: (Color online) PDOS of ErCu_2Si_2 (ICSD #106845). The *s*-, *p*- and *d*-projected states are in red, blue and green, respectively. ErCu_2Si_2 crystallizes in space group $I 4/m m m$ (#139), in a tetragonal body-centred structure.

FIG. 326: Fat band representation of Cu in ErCu_2Si_2 FIG. 327: Fat band representation of Er in ErCu_2Si_2 FIG. 328: Fat band representation of Si in ErCu_2Si_2

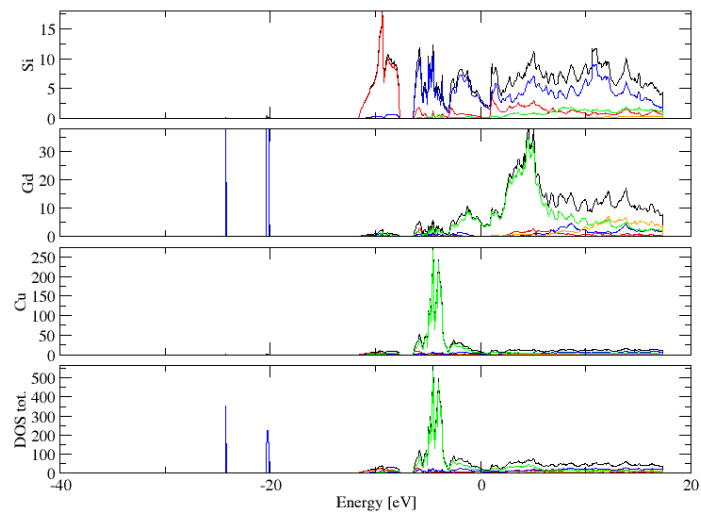


FIG. 329: (Color online) PDOS of Cu_2GdSi_2 (ICSD #64825). The s -, p - and d -projected states are in red, blue and green, respectively. Cu_2GdSi_2 crystallizes in space group $I 4/m m m$ (#139), in a tetragonal body-centred structure.

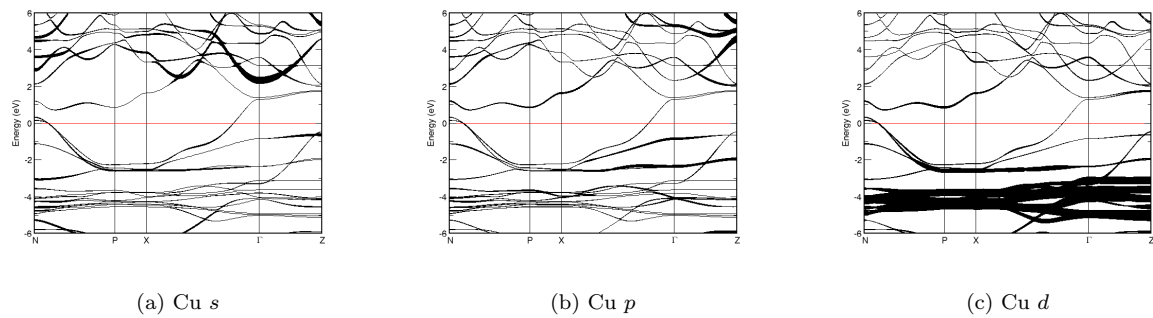


FIG. 330: Fat band representation of Cu in Cu_2GdSi_2

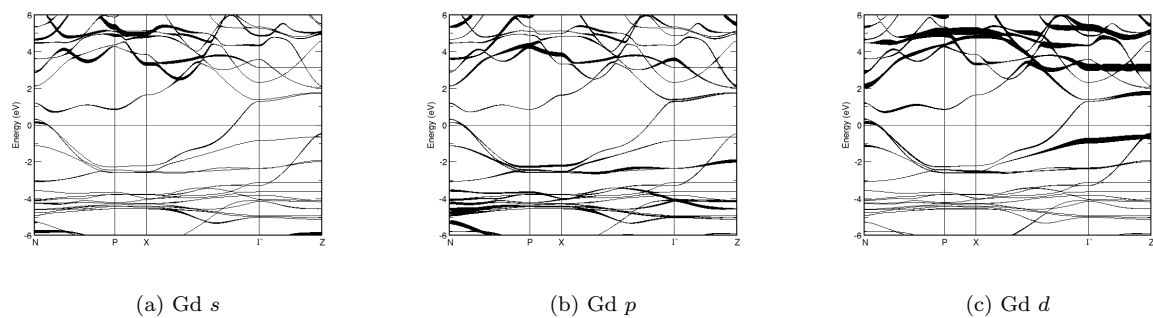
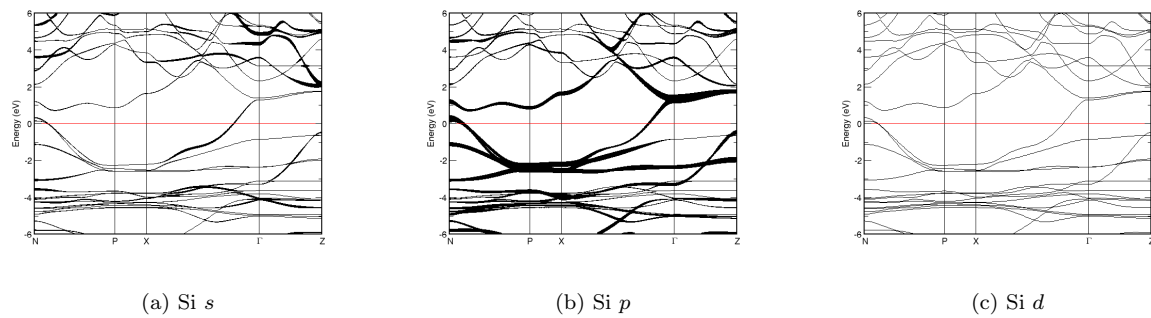
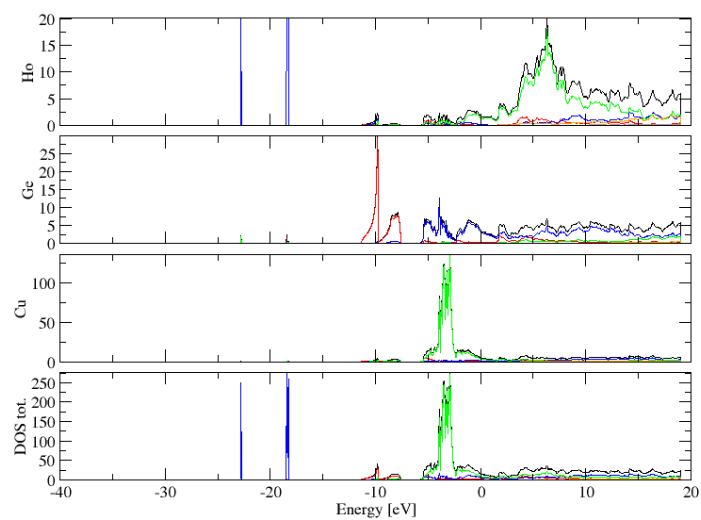
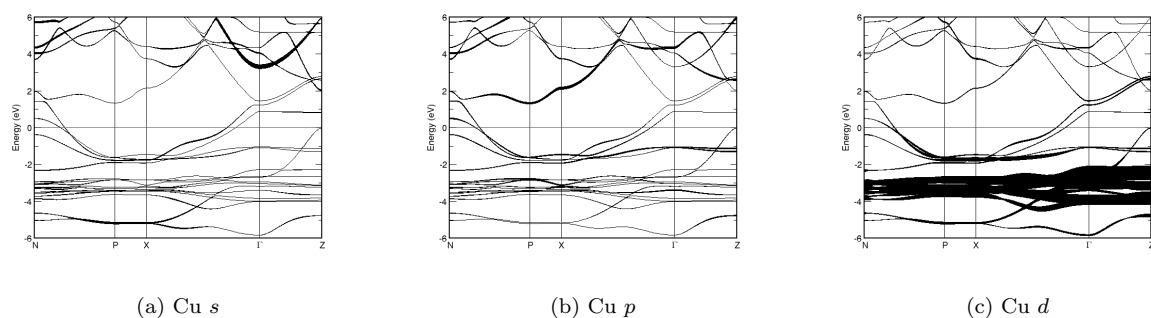
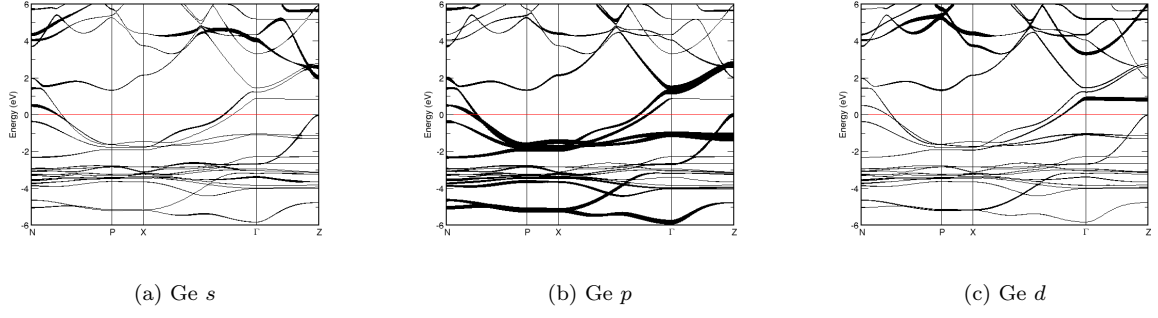
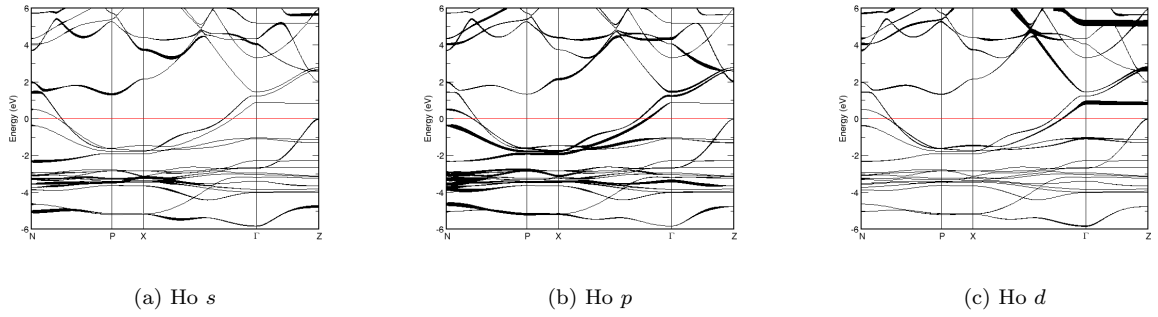
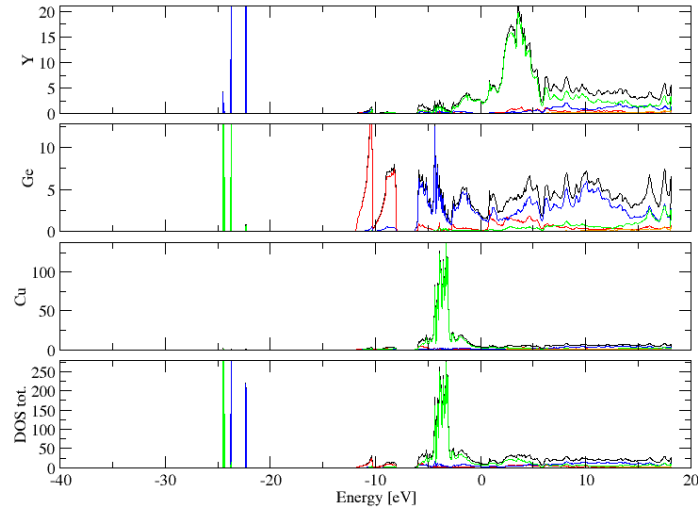
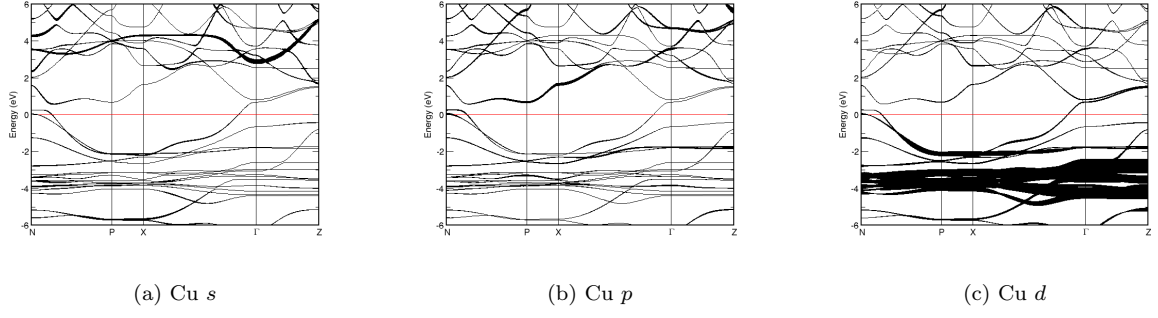
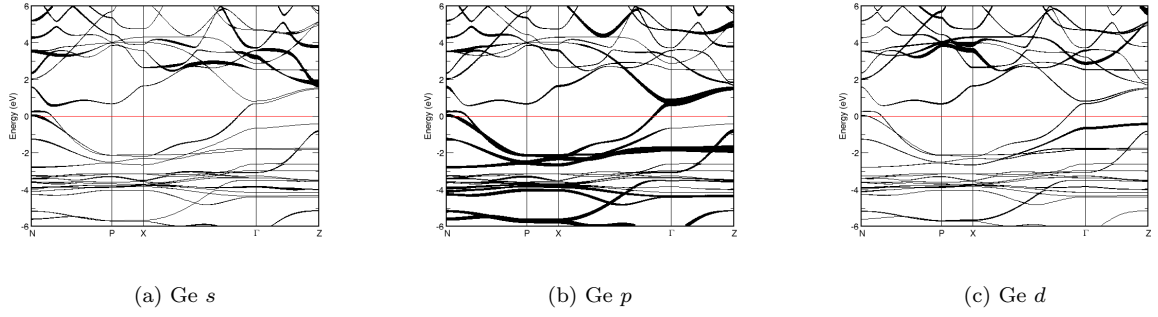
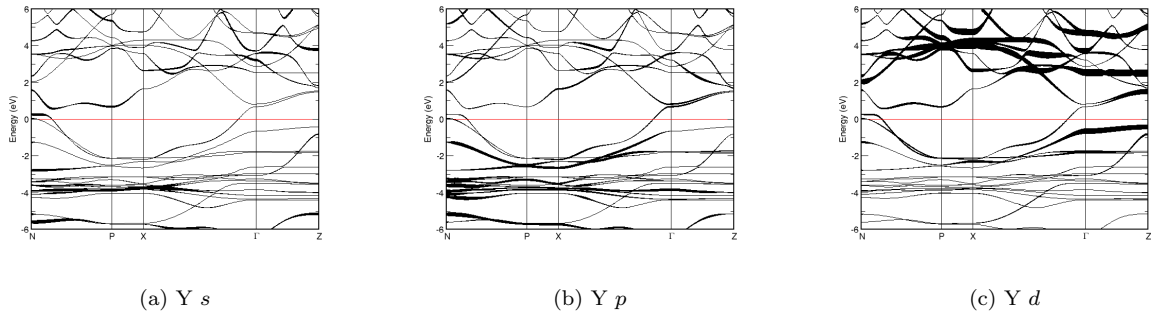


FIG. 331: Fat band representation of Gd in Cu_2GdSi_2

FIG. 332: Fat band representation of Si in Cu_2GdSi_2 FIG. 333: (Color online) PDOS of Cu_2HoGe_2 (ICSD #53270). The s -, p - and d -projected states are in red, blue and green, respectively. Cu_2HoGe_2 crystallizes in space group $I 4/m m m$ (#139), in a tetragonal body-centred structure.FIG. 334: Fat band representation of Cu in Cu_2HoGe_2

FIG. 335: Fat band representation of Ge in Cu_2HoGe_2 FIG. 336: Fat band representation of Ho in Cu_2HoGe_2 FIG. 337: (Color online) PDOS of YCu_2Ge_2 (ICSD #52764). The *s*-, *p*- and *d*-projected states are in red, blue and green, respectively. YCu_2Ge_2 crystallizes in space group $I 4/m m m$ (#139), in a tetragonal body-centred structure.

FIG. 338: Fat band representation of Cu in YCu_2Ge_2 FIG. 339: Fat band representation of Ge in YCu_2Ge_2 FIG. 340: Fat band representation of Y in YCu_2Ge_2

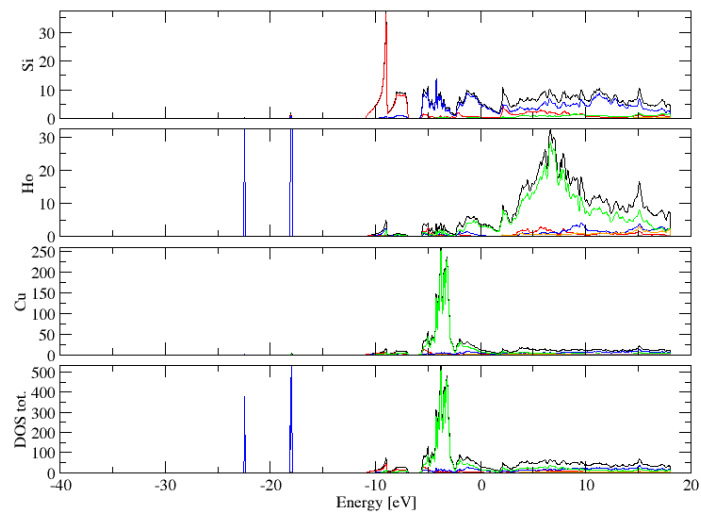


FIG. 341: (Color online) PDOS of Cu_2HoSi_2 (ICSD #53289). The s -, p - and d -projected states are in red, blue and green, respectively. Cu_2HoSi_2 crystallizes in space group $I 4/m m m$ (#139), in a tetragonal body-centred structure.

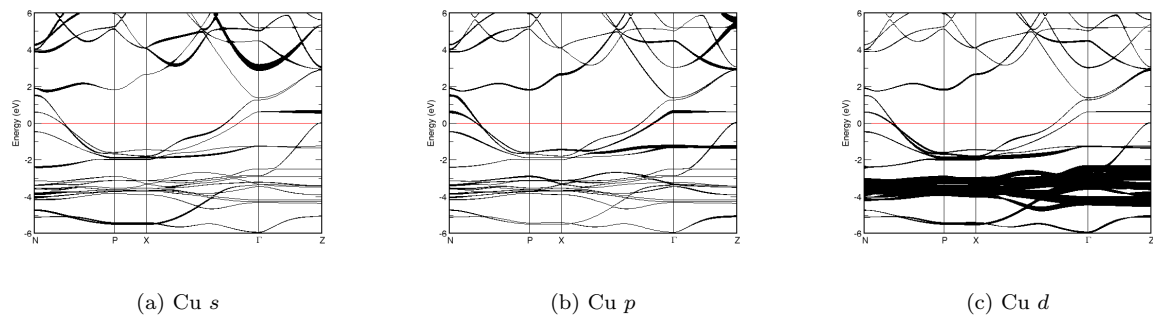


FIG. 342: Fat band representation of Cu in Cu_2HoSi_2

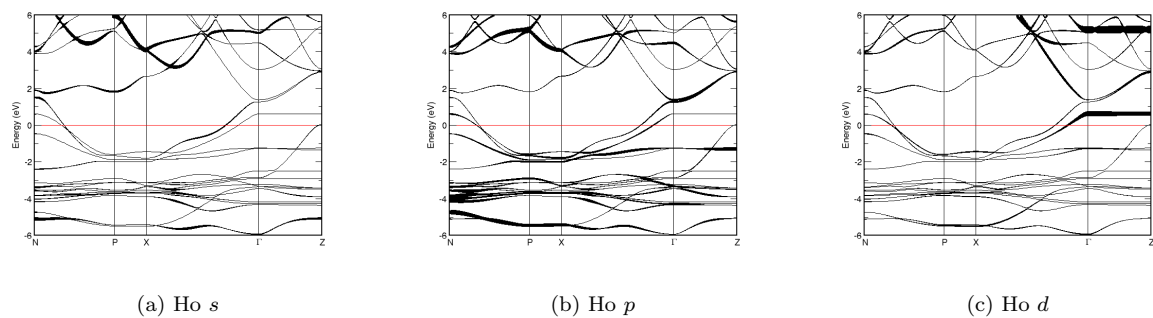
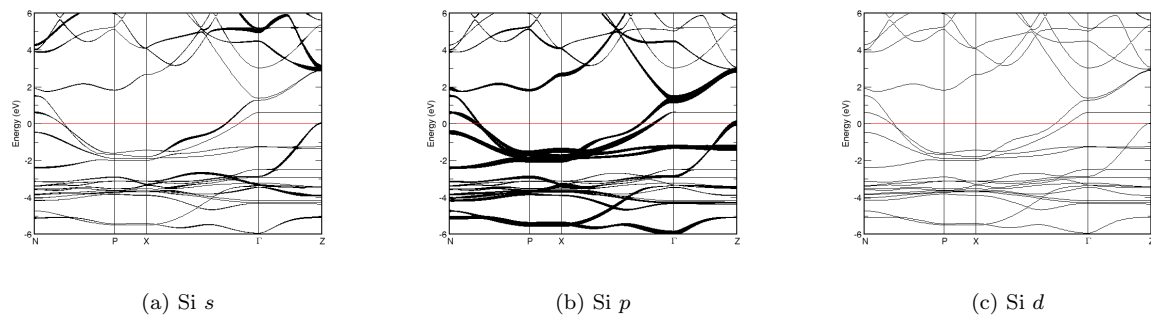
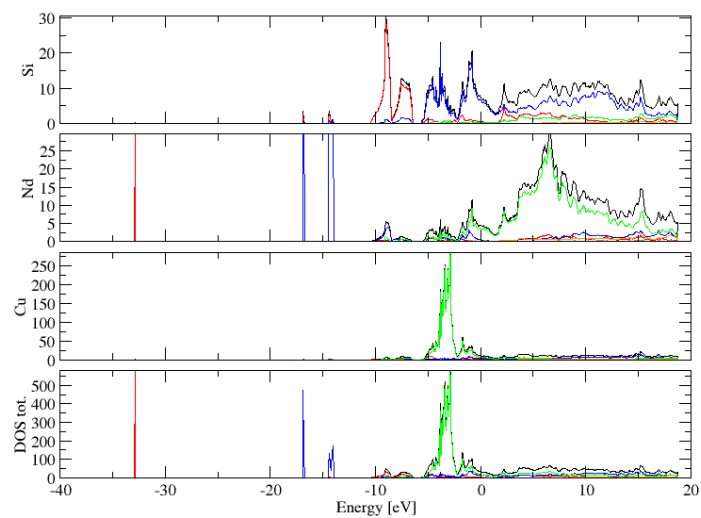
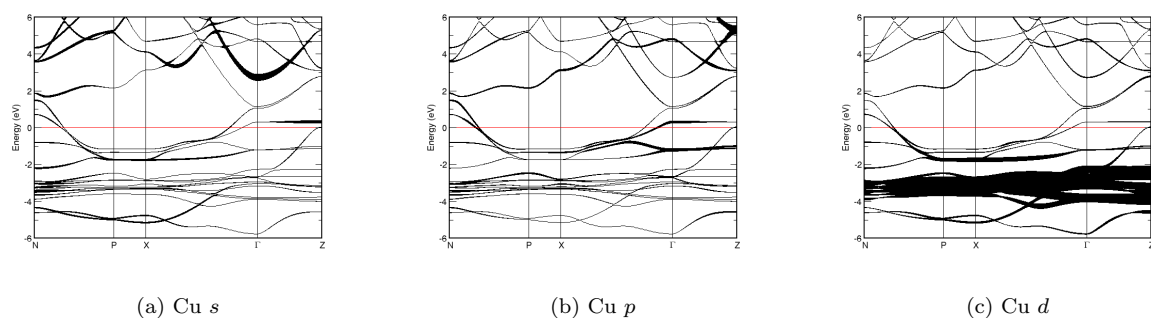
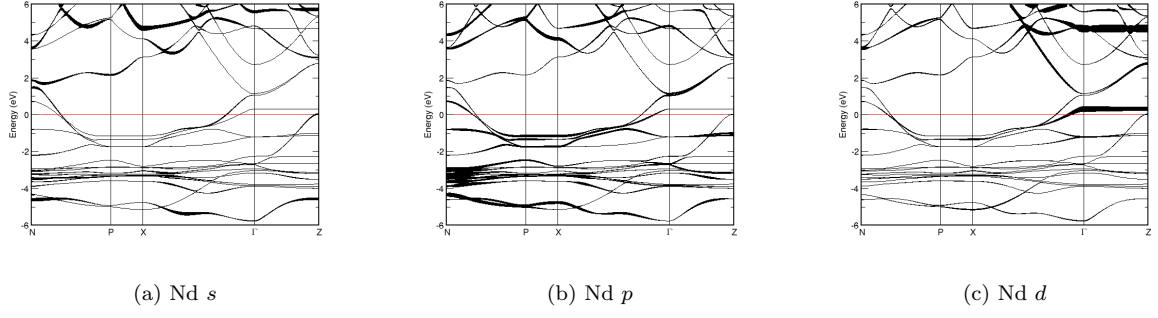
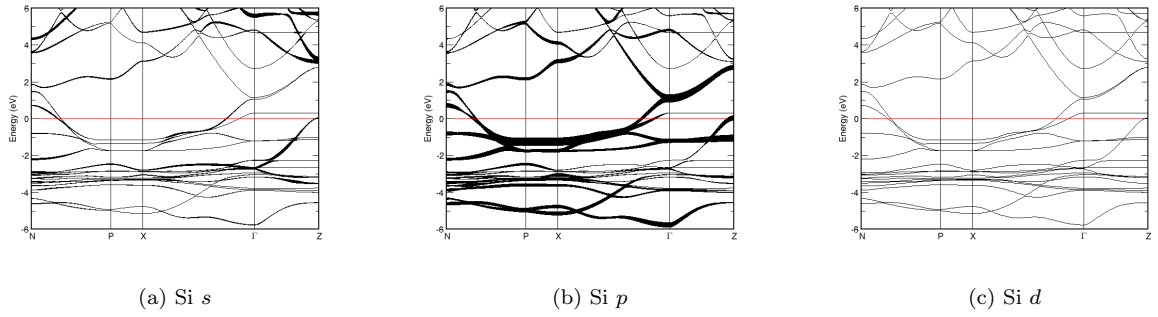
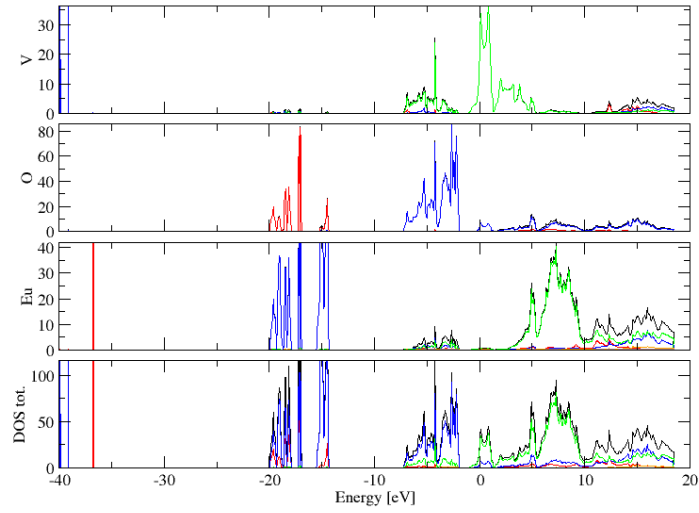
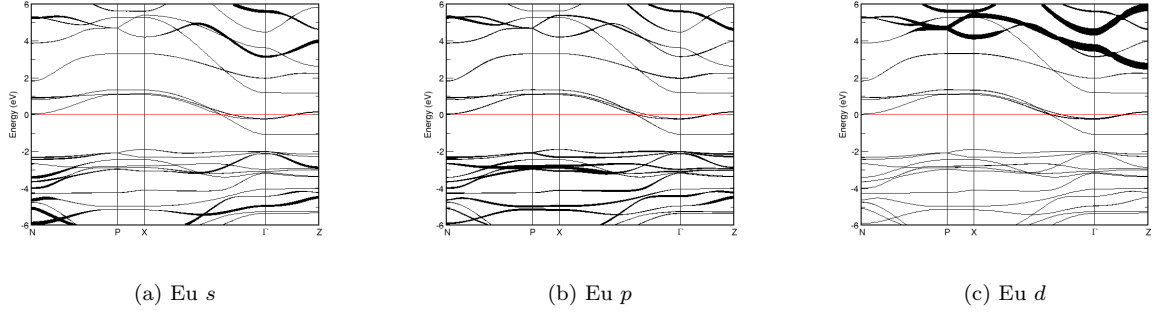
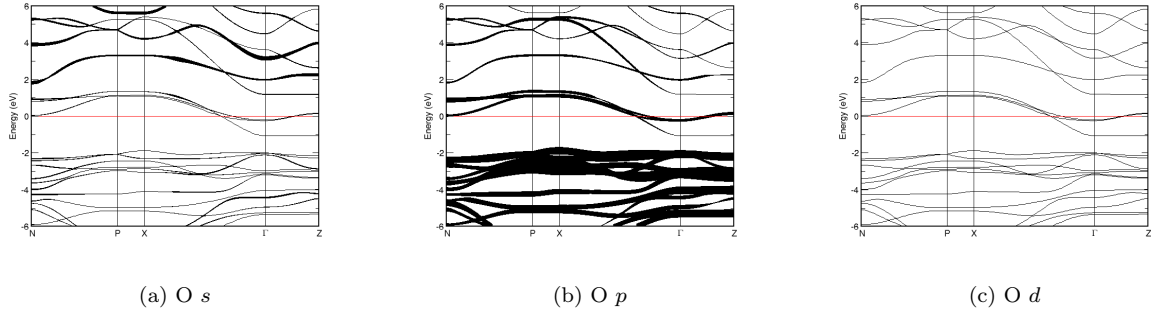
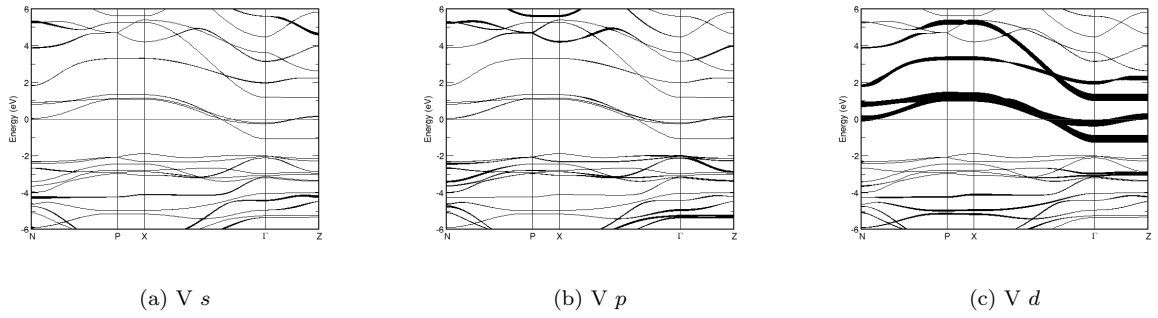


FIG. 343: Fat band representation of Ho in Cu_2HoSi_2

FIG. 344: Fat band representation of Si in Cu_2HoSi_2 FIG. 345: (Color online) PDOS of NdCu_2Si_2 (ICSD #106842). The *s*-, *p*- and *d*-projected states are in red, blue and green, respectively. NdCu_2Si_2 crystallizes in space group $I 4/m m m$ (#139), in a tetragonal body-centred structure.FIG. 346: Fat band representation of Cu in NdCu_2Si_2

FIG. 347: Fat band representation of Nd in NdCu₂Si₂FIG. 348: Fat band representation of Si in NdCu₂Si₂FIG. 349: (Color online) PDOS of Eu₂(VO₄) (ICSD #89000). The *s*-, *p*- and *d*-projected states are in red, blue and green, respectively. Eu₂(VO₄) crystallizes in space group I 4/m m m (#139), in a tetragonal body-centred structure.

FIG. 350: Fat band representation of Eu in $\text{Eu}_2(\text{VO}_4)$ FIG. 351: Fat band representation of O in $\text{Eu}_2(\text{VO}_4)$ FIG. 352: Fat band representation of V in $\text{Eu}_2(\text{VO}_4)$

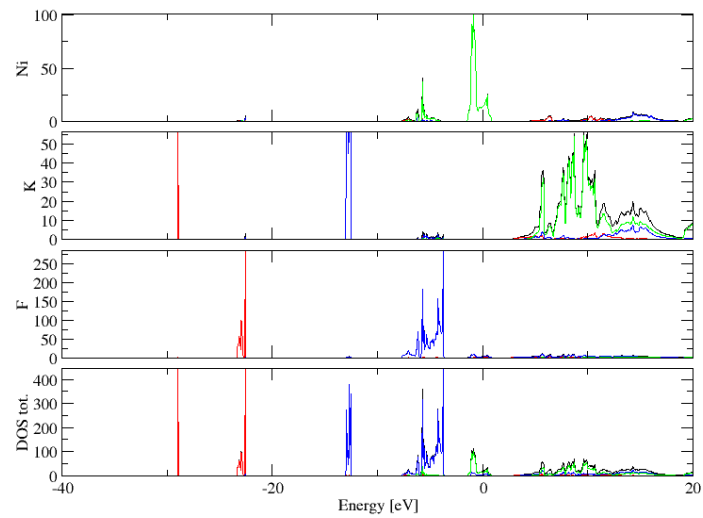


FIG. 353: (Color online) PDOS of $K_2(NiF_4)$ (ICSD #15576). The s -, p - and d -projected states are in red, blue and green, respectively. $K_2(NiF_4)$ crystallizes in space group $I 4/m m m$ (#139), in a tetragonal body-centred structure.

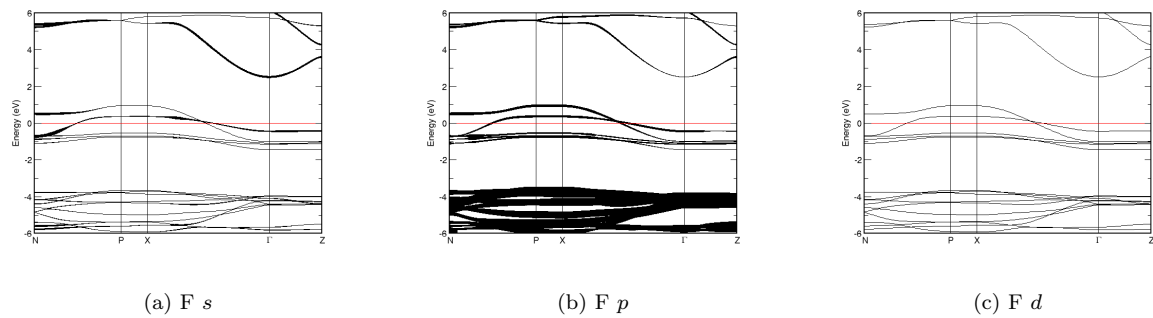


FIG. 354: Fat band representation of F in $K_2(NiF_4)$

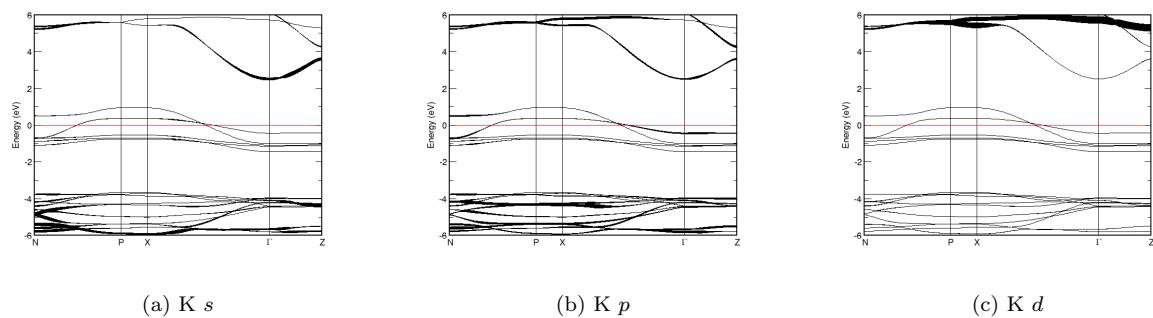
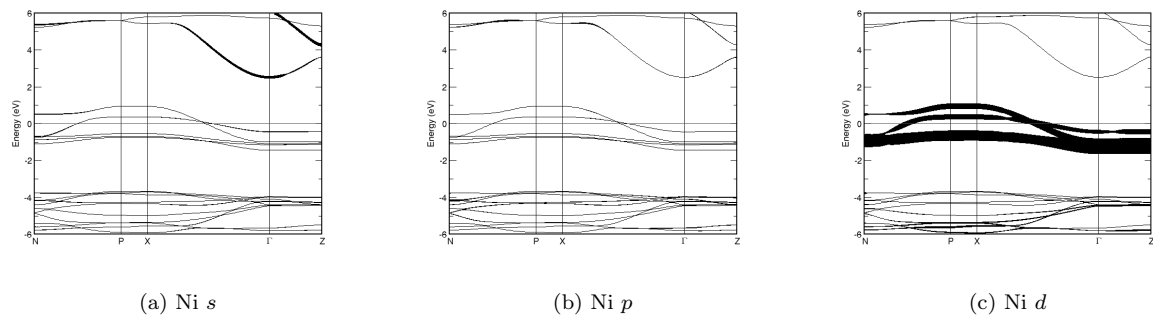
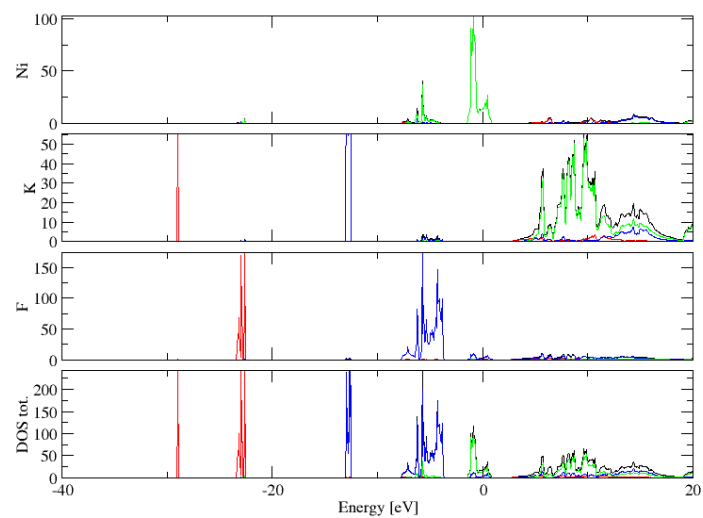
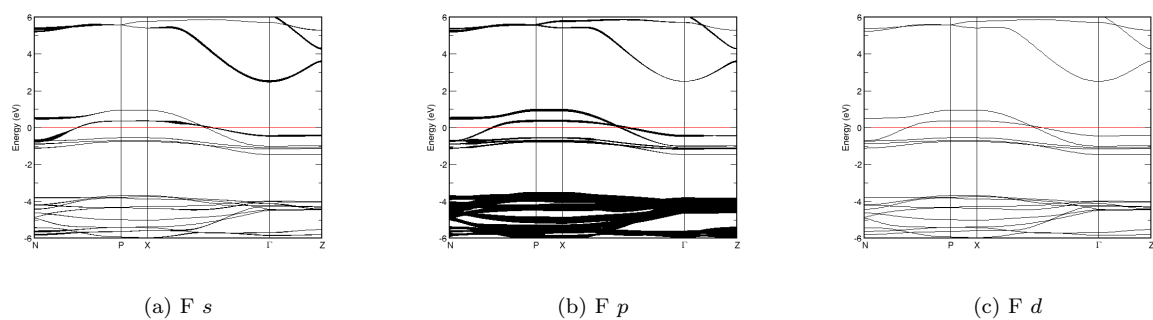
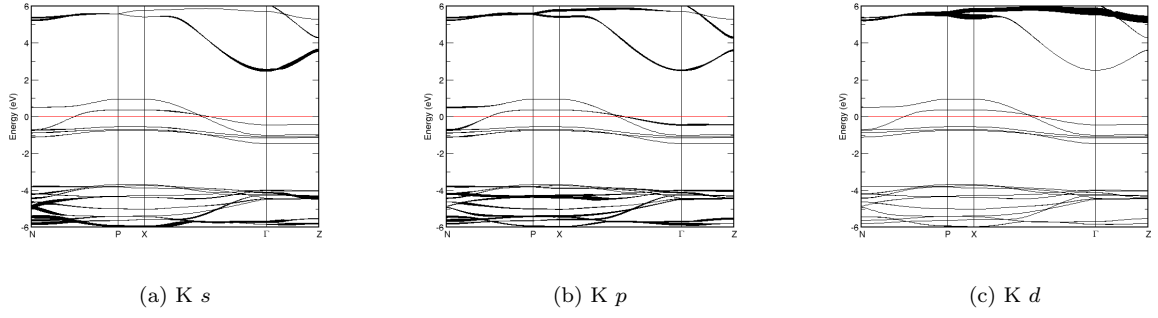
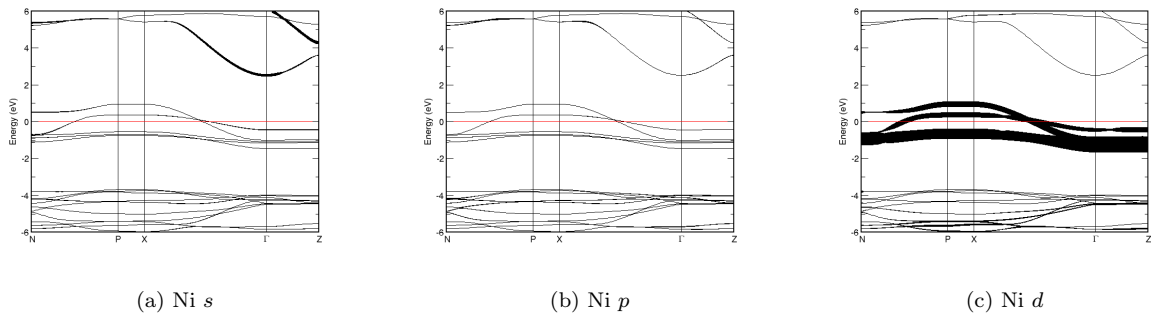
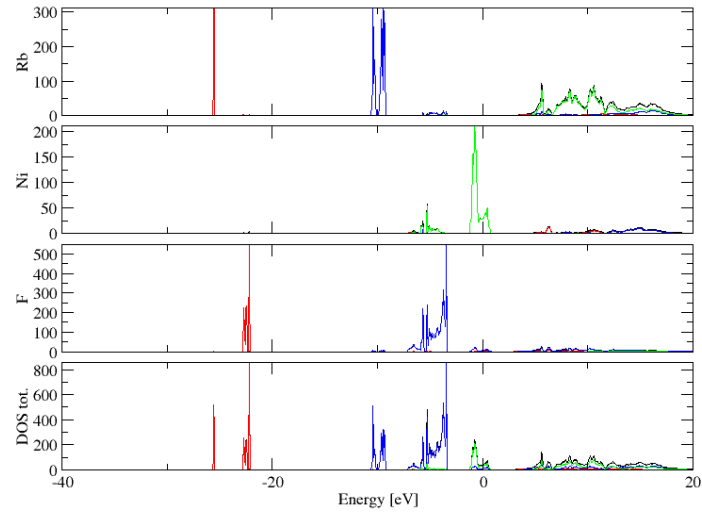
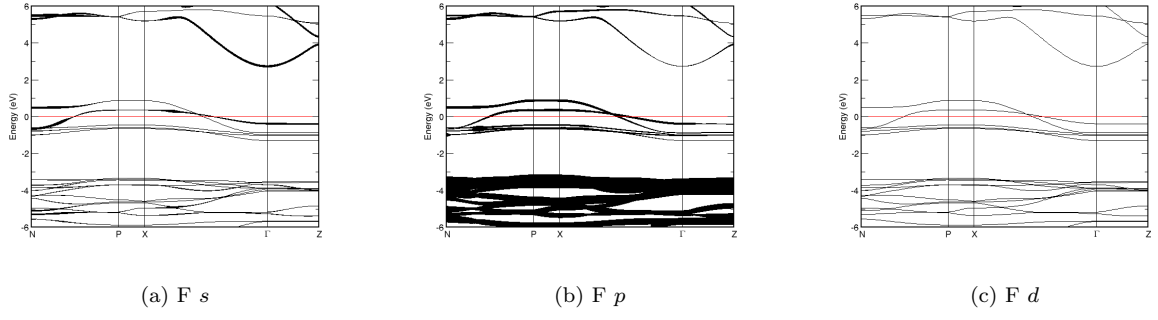
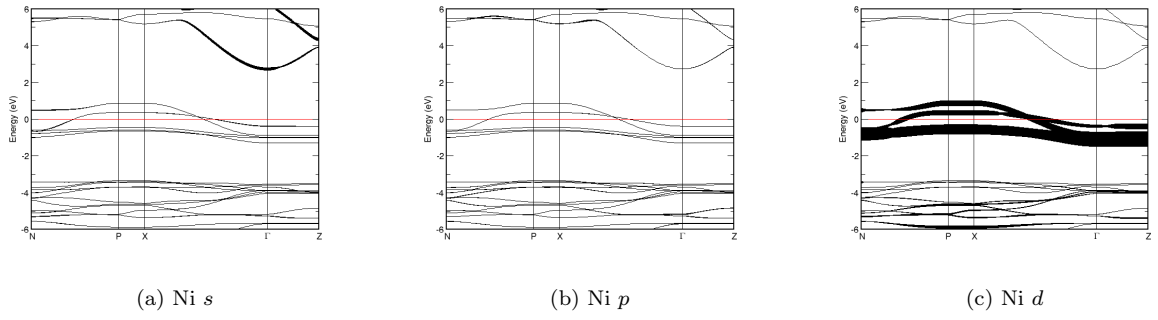
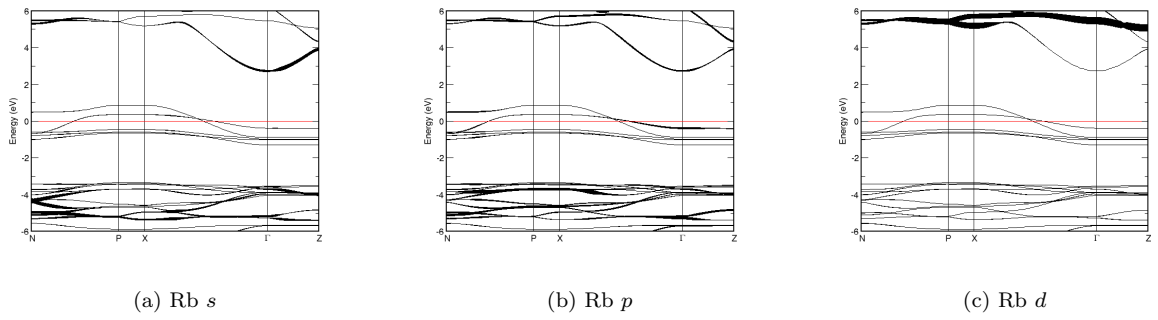


FIG. 355: Fat band representation of K in $K_2(NiF_4)$

FIG. 356: Fat band representation of Ni in $K_2(NiF_4)$ FIG. 357: (Color online) PDOS of $K_2(NiF_4)$ (ICSD #631720). The *s*-, *p*- and *d*-projected states are in red, blue and green, respectively. $K_2(NiF_4)$ crystallizes in space group $I 4/m m m$ (#139), in a tetragonal body-centred structure.FIG. 358: Fat band representation of F in $K_2(NiF_4)$

FIG. 359: Fat band representation of K in $K_2(NiF_4)$ FIG. 360: Fat band representation of Ni in $K_2(NiF_4)$ FIG. 361: (Color online) PDOS of $Rb_2(NiF_4)$ (ICSD #69682). The *s*-, *p*- and *d*-projected states are in red, blue and green, respectively. $Rb_2(NiF_4)$ crystallizes in space group $I 4/m m m$ (#139), in a tetragonal body-centred structure.

FIG. 362: Fat band representation of F in $\text{Rb}_2(\text{NiF}_4)$ FIG. 363: Fat band representation of Ni in $\text{Rb}_2(\text{NiF}_4)$ FIG. 364: Fat band representation of Rb in $\text{Rb}_2(\text{NiF}_4)$

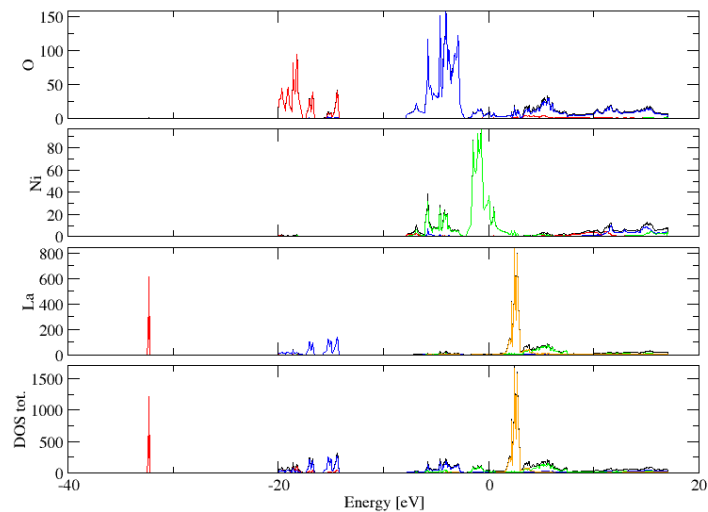


FIG. 365: (Color online) PDOS of $\text{La}_2(\text{NiO}_4)$ (ICSD #1179). The s -, p - and d -projected states are in red, blue and green, respectively. $\text{La}_2(\text{NiO}_4)$ crystallizes in space group $I 4/m m m$ (#139), in a tetragonal body-centred structure.

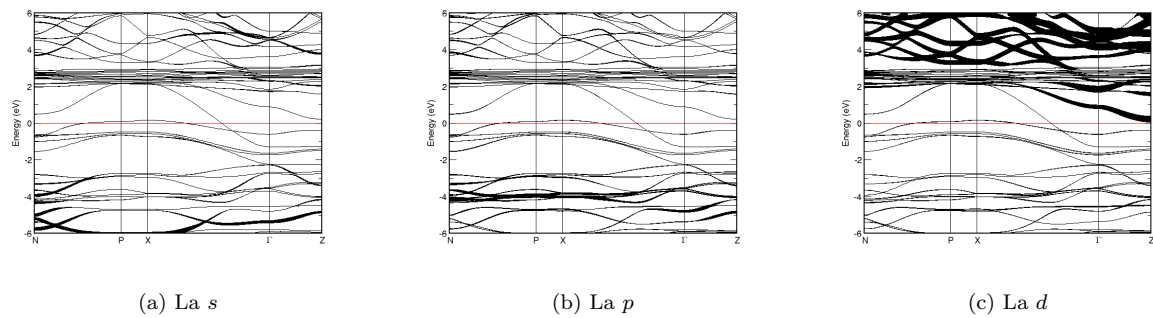


FIG. 366: Fat band representation of La in $\text{La}_2(\text{NiO}_4)$

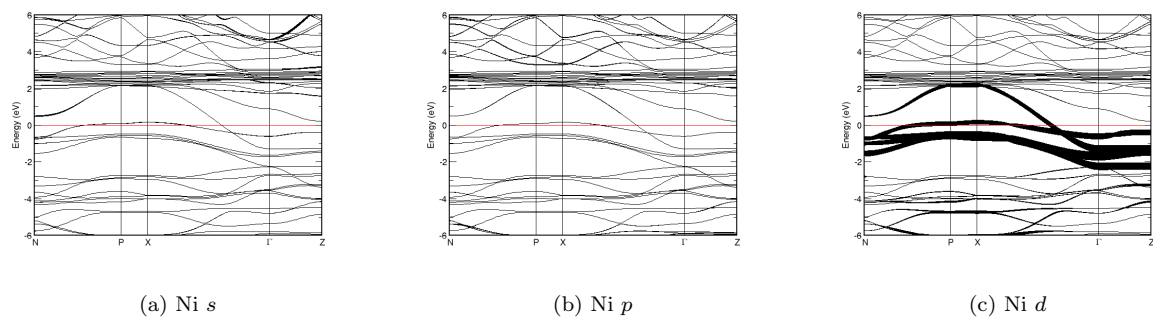
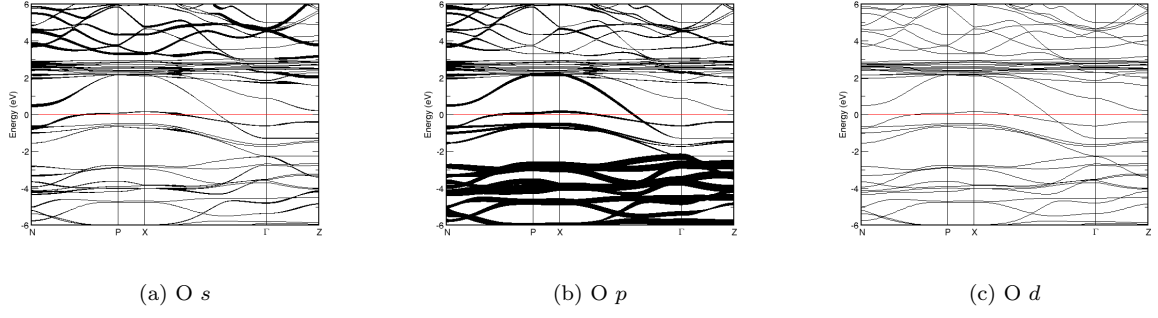
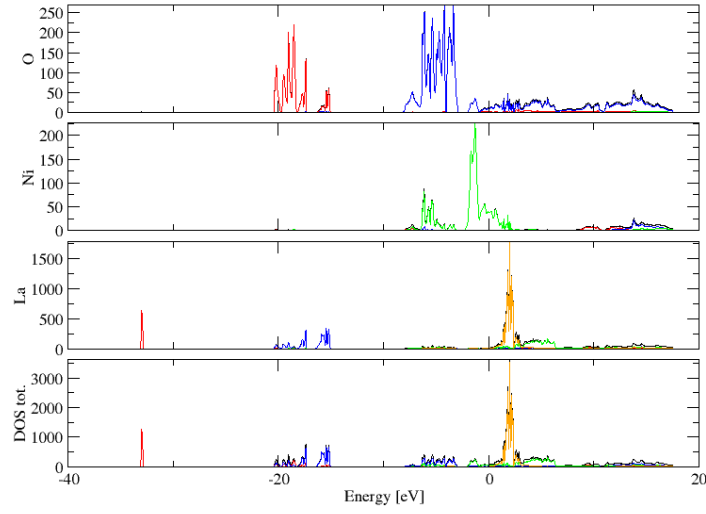
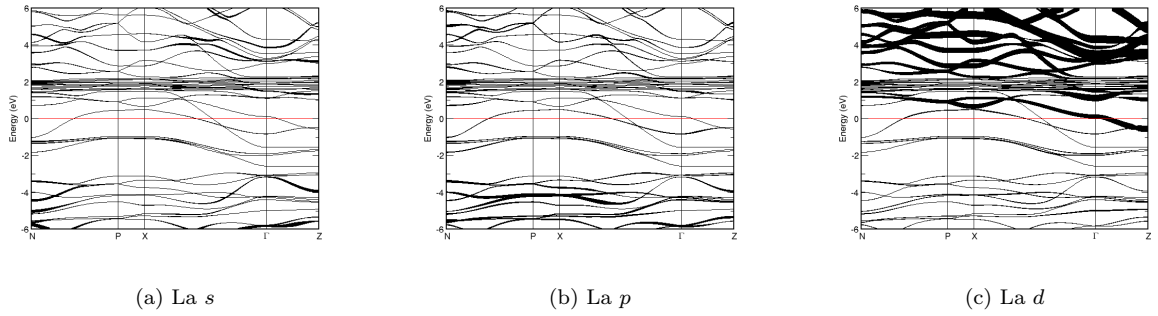
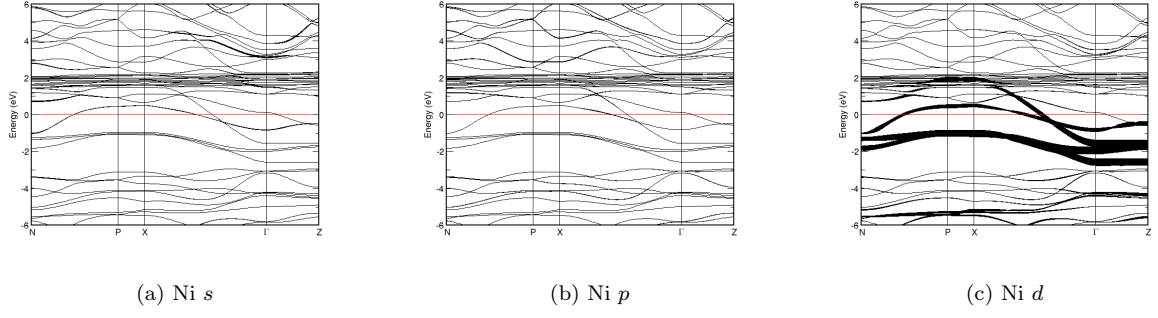
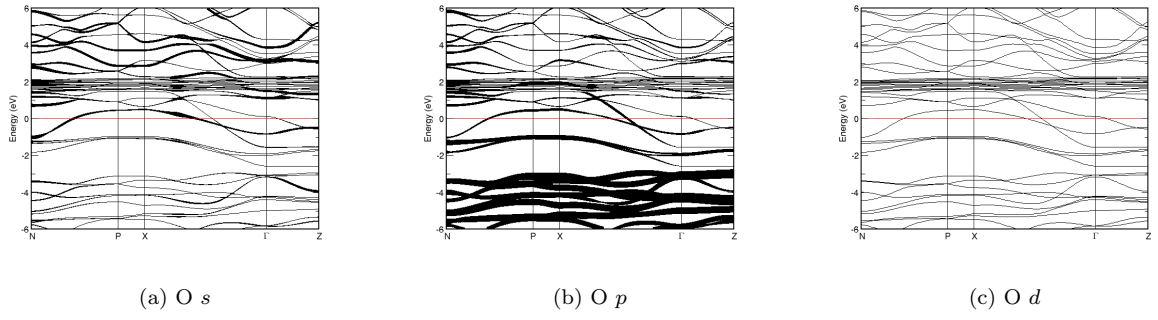
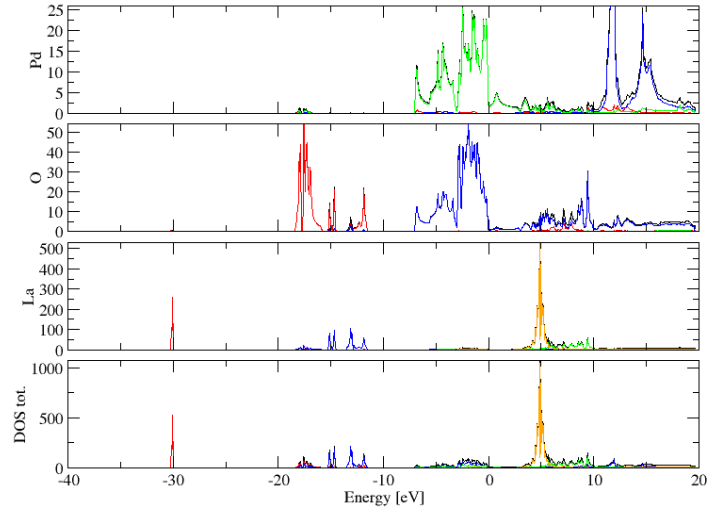
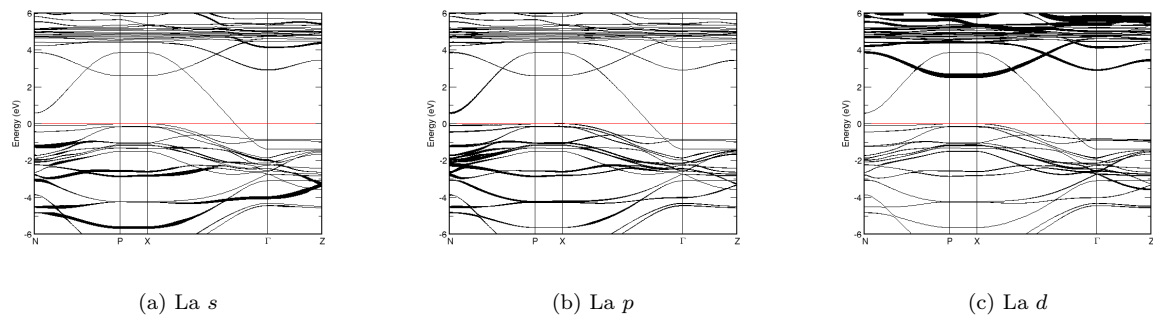
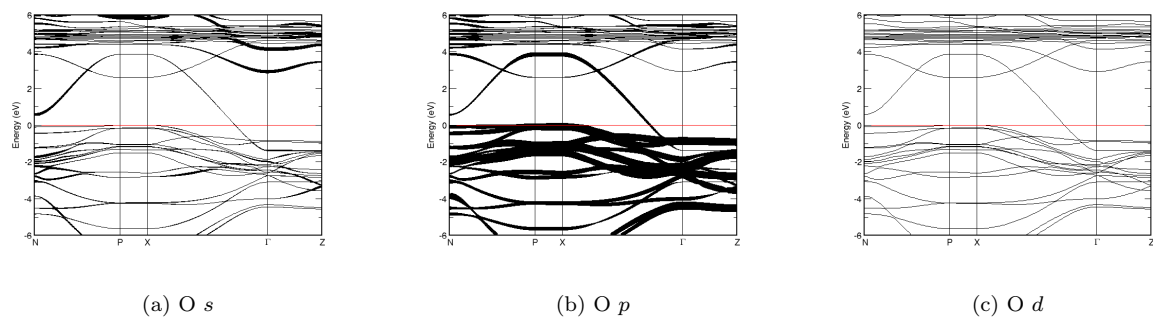
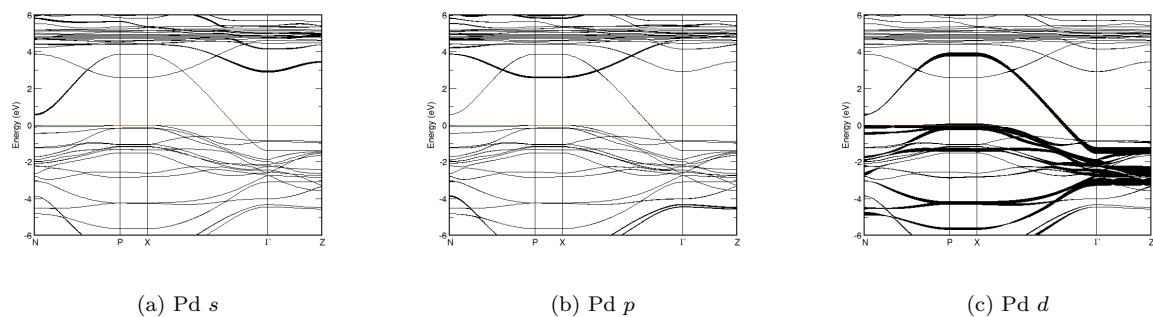


FIG. 367: Fat band representation of Ni in $\text{La}_2(\text{NiO}_4)$

FIG. 368: Fat band representation of O in $\text{La}_2(\text{NiO}_4)$ FIG. 369: (Color online) PDOS of $\text{La}_2(\text{NiO}_4)$ (ICSD #33536). The s -, p - and d -projected states are in red, blue and green, respectively. $\text{La}_2(\text{NiO}_4)$ crystallizes in space group $I 4/m m m$ (#139), in a tetragonal body-centred structure.FIG. 370: Fat band representation of La in $\text{La}_2(\text{NiO}_4)$

FIG. 371: Fat band representation of Ni in $\text{La}_2(\text{NiO}_4)$ FIG. 372: Fat band representation of O in $\text{La}_2(\text{NiO}_4)$ FIG. 373: (Color online) PDOS of La_2PdO_4 (ICSD #40262). The s -, p - and d -projected states are in red, blue and green, respectively. La_2PdO_4 crystallizes in space group $I 4/m m m$ (#139), in a tetragonal body-centred structure.

FIG. 374: Fat band representation of La in La_2PdO_4 FIG. 375: Fat band representation of O in La_2PdO_4 FIG. 376: Fat band representation of Pd in La_2PdO_4

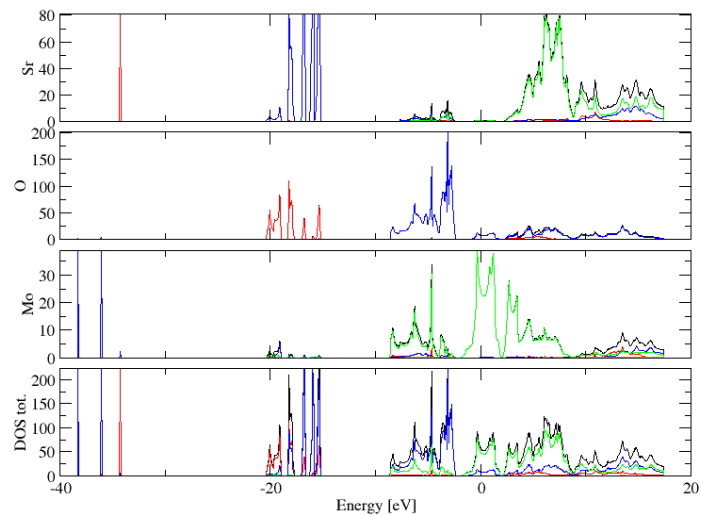


FIG. 377: (Color online) PDOS of $\text{Sr}_2(\text{MoO}_4)$ (ICSD #152123). The s -, p - and d -projected states are in red, blue and green, respectively. $\text{Sr}_2(\text{MoO}_4)$ crystallizes in space group $I 4/m m m$ (#139), in a tetragonal body-centred structure.

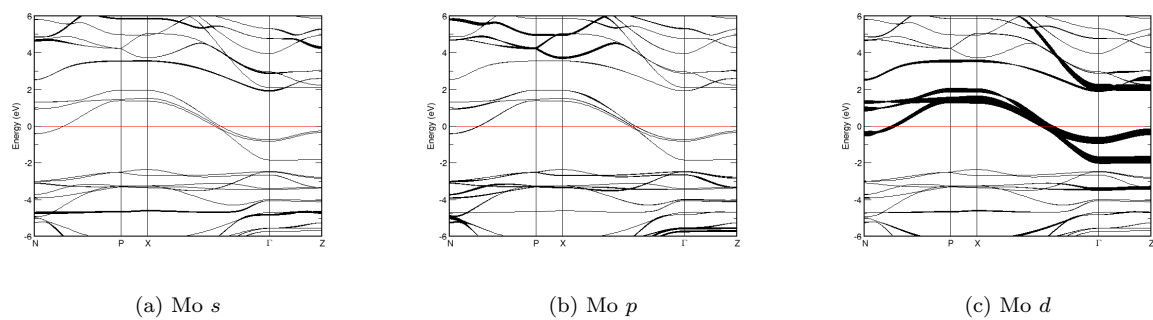


FIG. 378: Fat band representation of Mo in $\text{Sr}_2(\text{MoO}_4)$

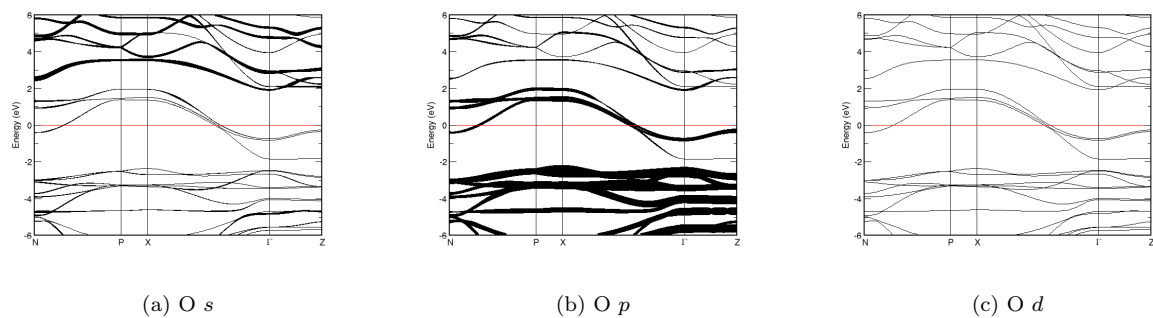


FIG. 379: Fat band representation of O in $\text{Sr}_2(\text{MoO}_4)$

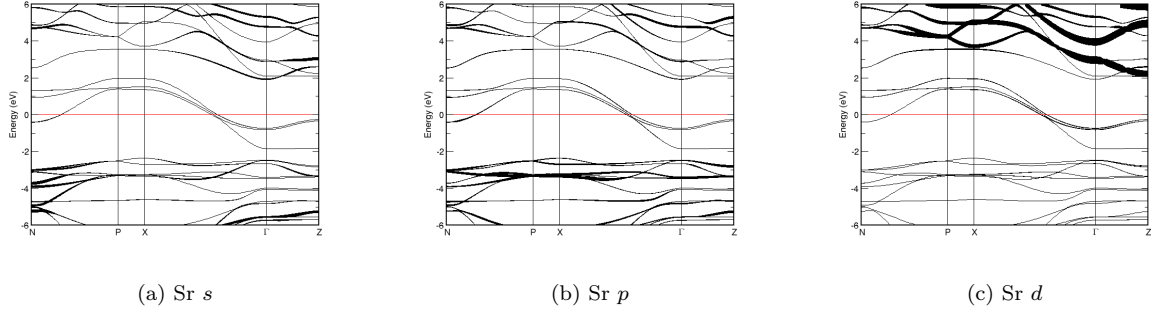


FIG. 380: Fat band representation of Sr in $\text{Sr}_2(\text{MoO}_4)$

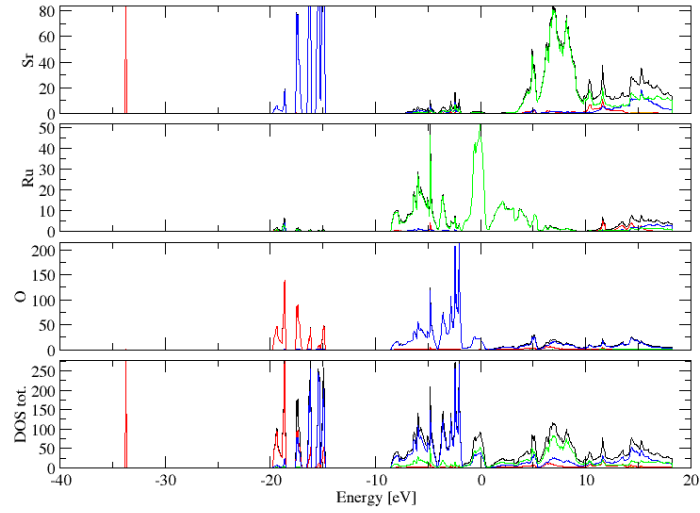


FIG. 381: (Color online) PDOS of $\text{Sr}_2(\text{RuO}_4)$ (ICSD #157401). The *s*-, *p*- and *d*-projected states are in red, blue and green, respectively. $\text{Sr}_2(\text{RuO}_4)$ crystallizes in space group $I 4/m m m$ (#139), in a tetragonal body-centred structure.

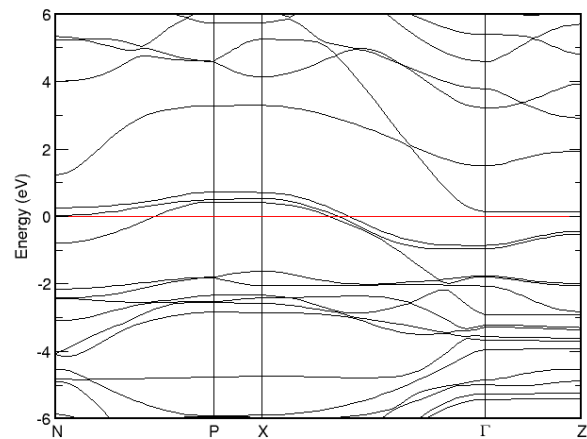
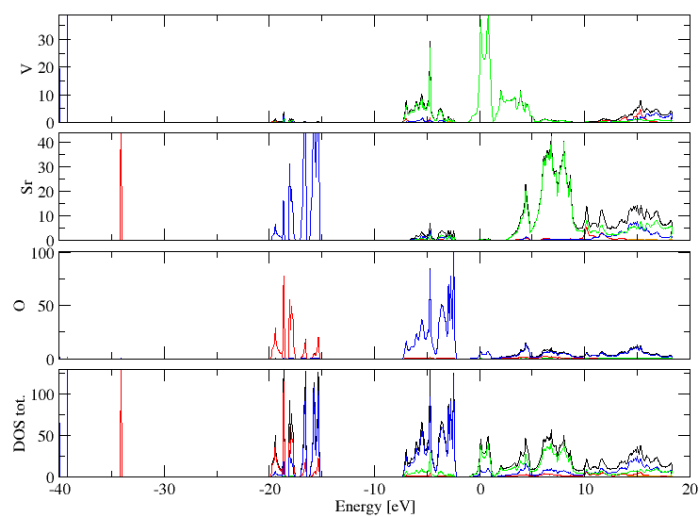
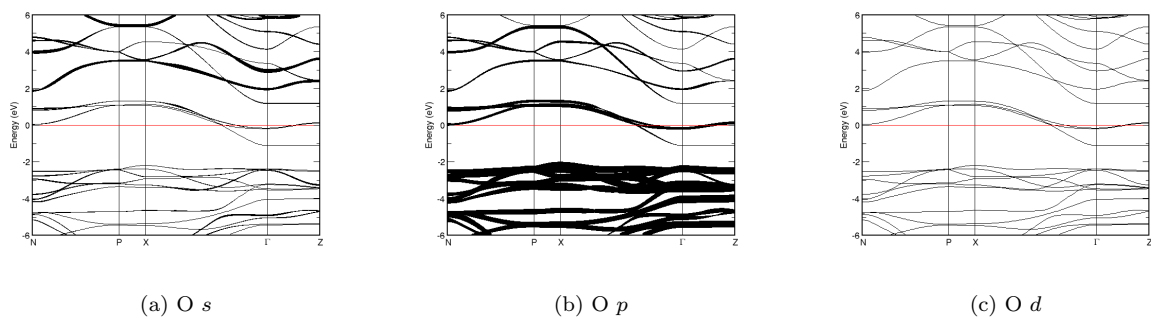
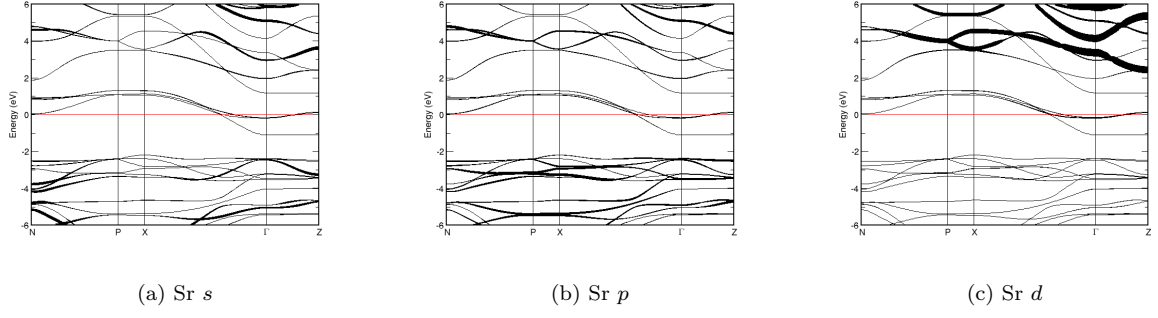
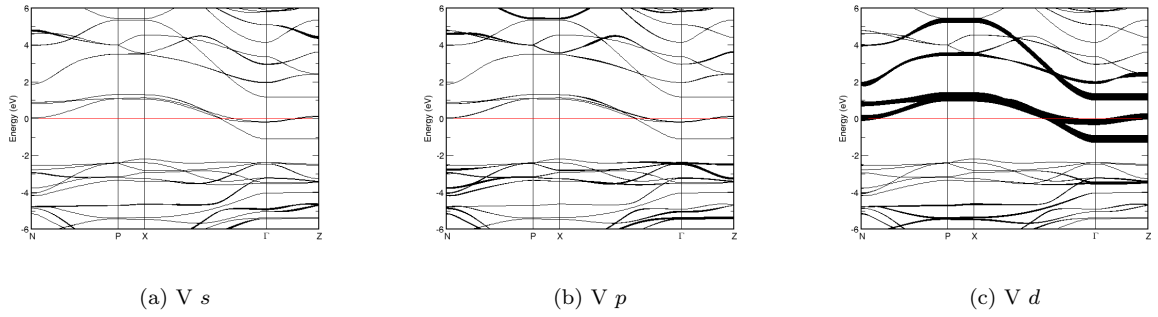
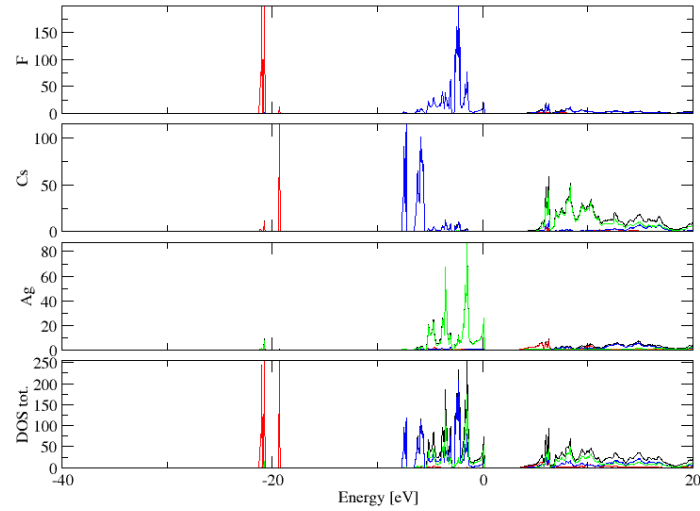
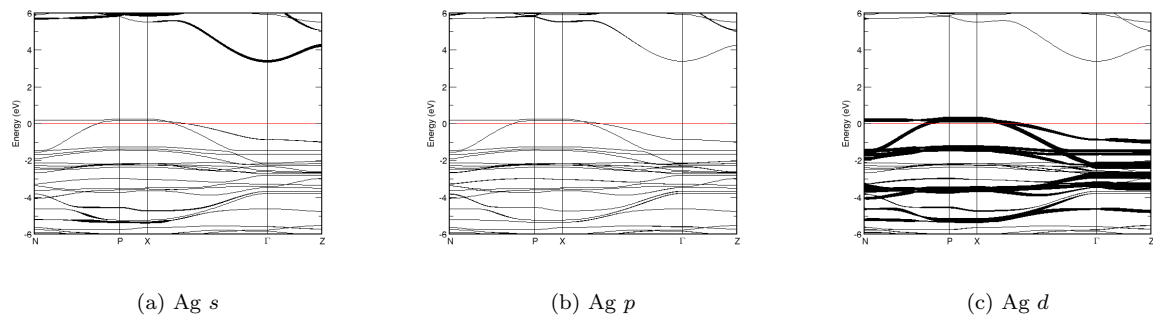
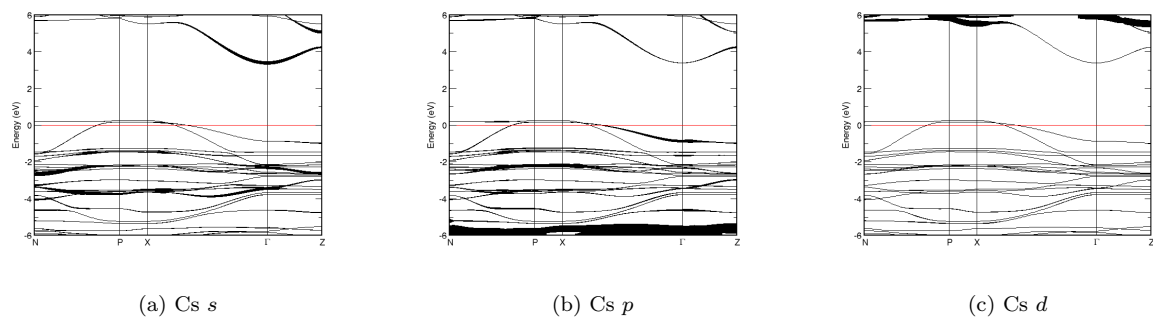
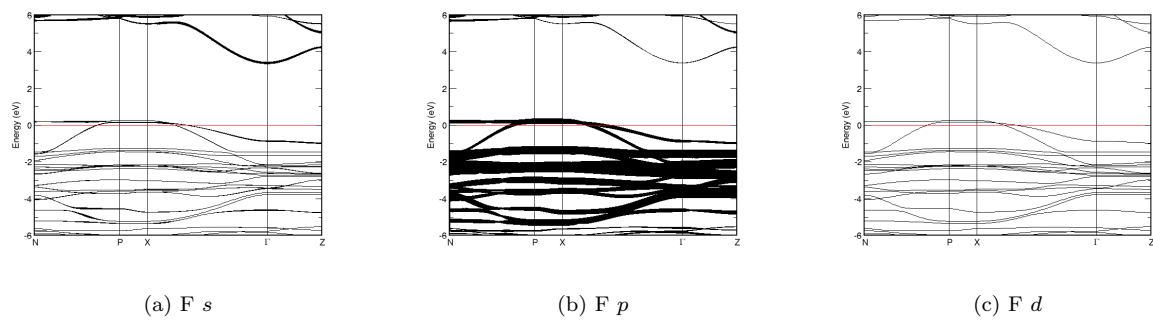
(a) E vs. k FIG. 382: Band structure of $\text{Sr}_2(\text{RuO}_4)$ 

FIG. 383: (Color online) PDOS of Sr_2VO_4 (ICSD #72219). The s -, p - and d -projected states are in red, blue and green, respectively. Sr_2VO_4 crystallizes in space group $I 4/m m m$ (#139), in a tetragonal body-centred structure.

(a) O s (b) O p (c) O d FIG. 384: Fat band representation of O in Sr_2VO_4

FIG. 385: Fat band representation of Sr in Sr_2VO_4 FIG. 386: Fat band representation of V in Sr_2VO_4 FIG. 387: (Color online) PDOS of Cs_2AgF_4 (ICSD #16254). The *s*-, *p*- and *d*-projected states are in red, blue and green, respectively. Cs_2AgF_4 crystallizes in space group $I 4/m m m$ (#139), in a tetragonal body-centred structure.

FIG. 388: Fat band representation of Ag in Cs_2AgF_4 FIG. 389: Fat band representation of Cs in Cs_2AgF_4 FIG. 390: Fat band representation of F in Cs_2AgF_4

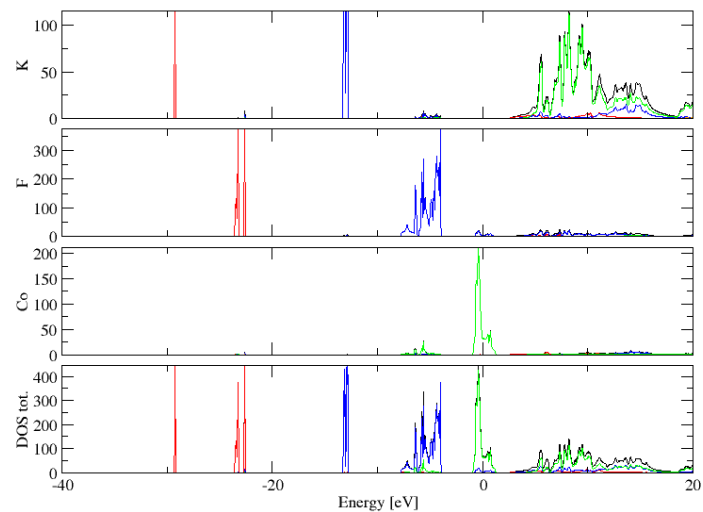


FIG. 391: (Color online) PDOS of K_2CoF_4 (ICSD #33522). The s -, p - and d -projected states are in red, blue and green, respectively. K_2CoF_4 crystallizes in space group $I 4/m m m$ (#139), in a tetragonal body-centred structure.

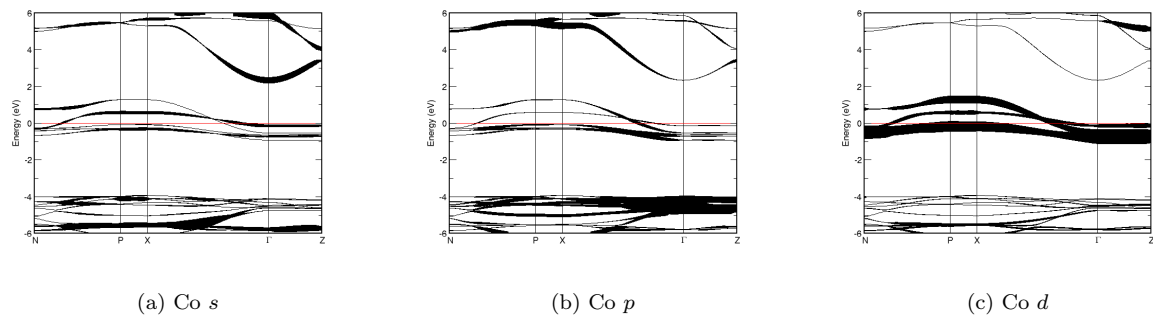


FIG. 392: Fat band representation of Co in K_2CoF_4

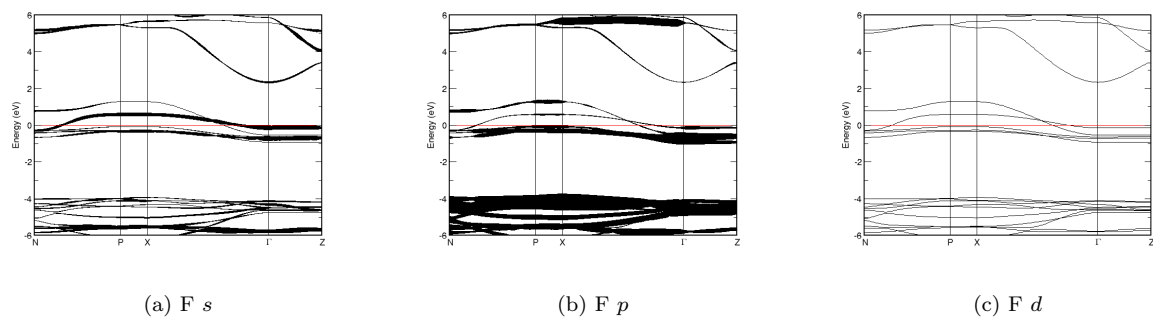
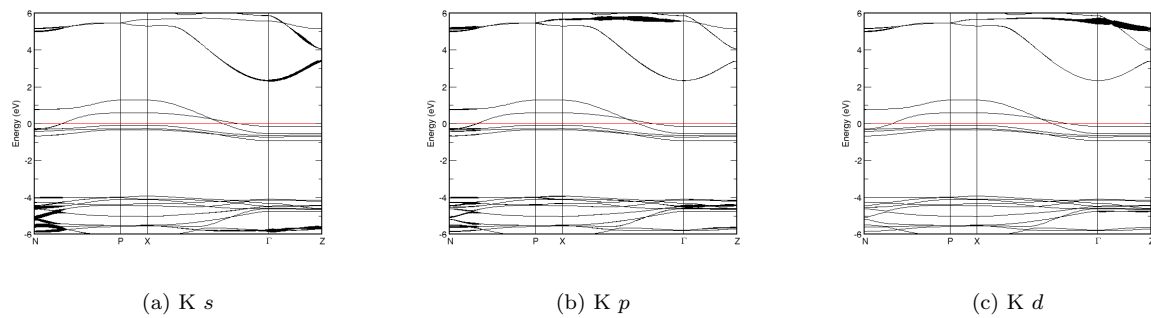
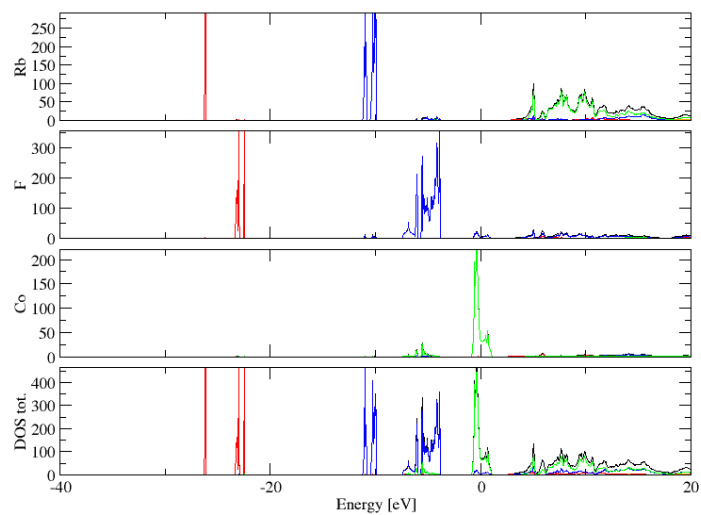
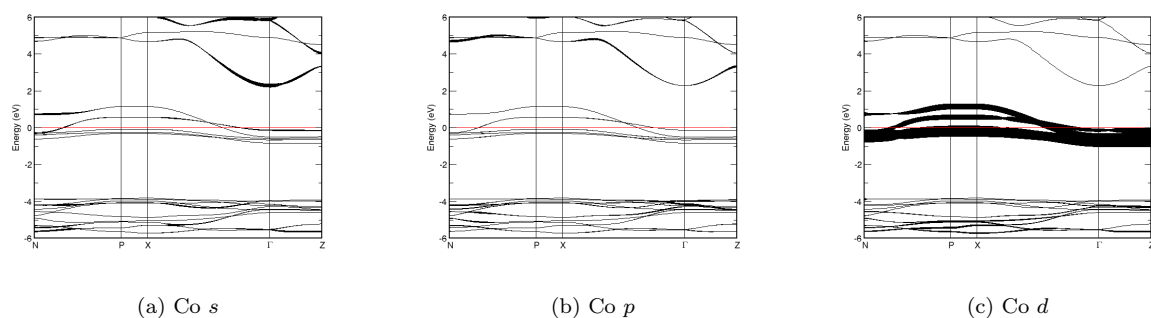


FIG. 393: Fat band representation of F in K_2CoF_4

FIG. 394: Fat band representation of K in K_2CoF_4 FIG. 395: (Color online) PDOS of Rb_2CoF_4 (ICSD #69683). The *s*-, *p*- and *d*-projected states are in red, blue and green, respectively. Rb_2CoF_4 crystallizes in space group $I 4/m m m$ (#139), in a tetragonal body-centred structure.FIG. 396: Fat band representation of Co in Rb_2CoF_4

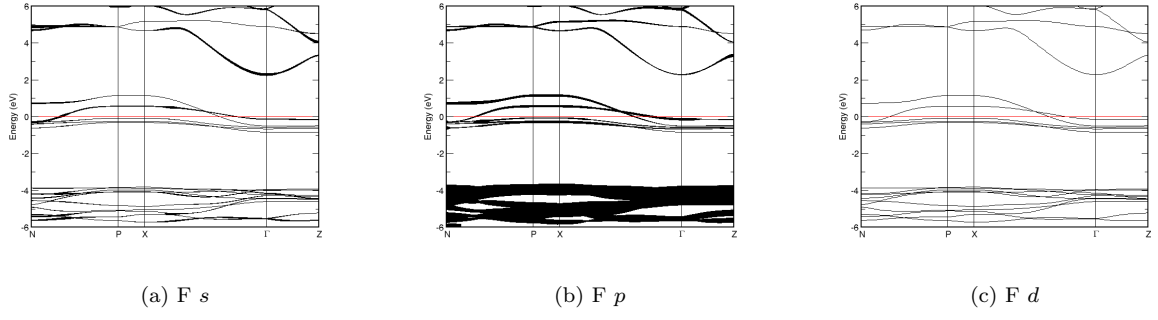
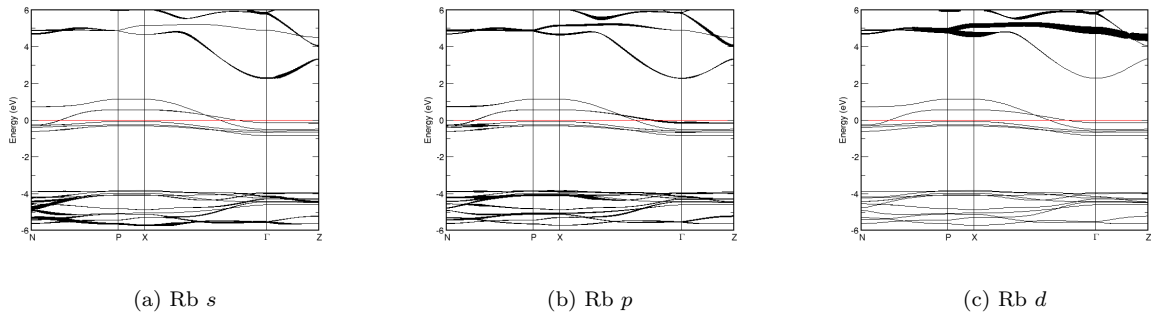
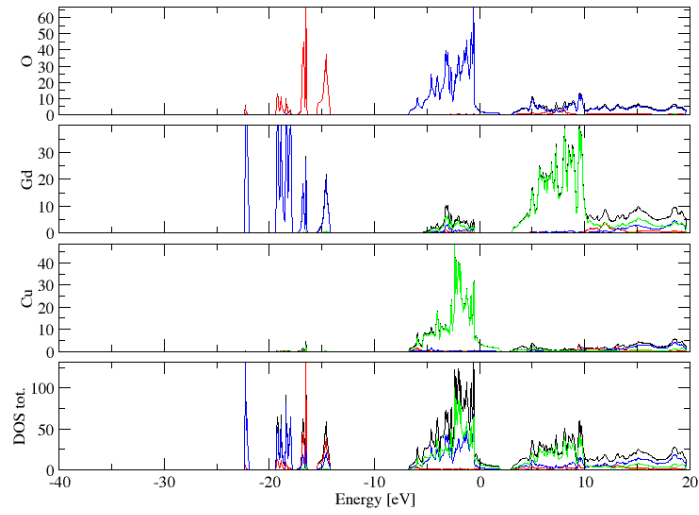
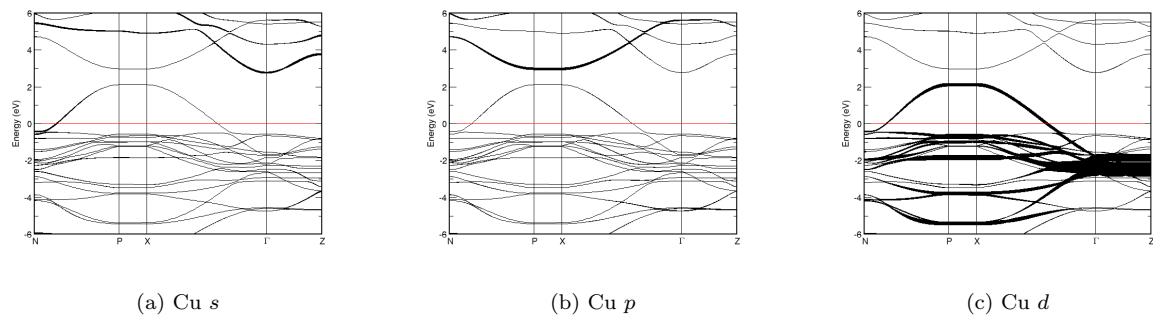
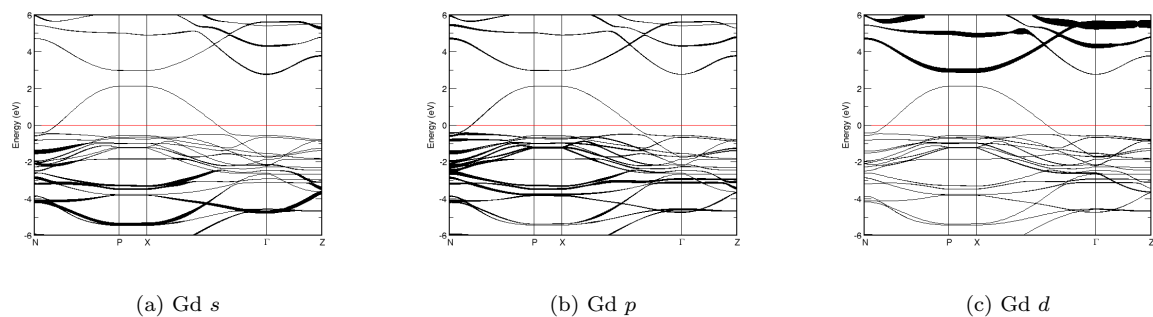
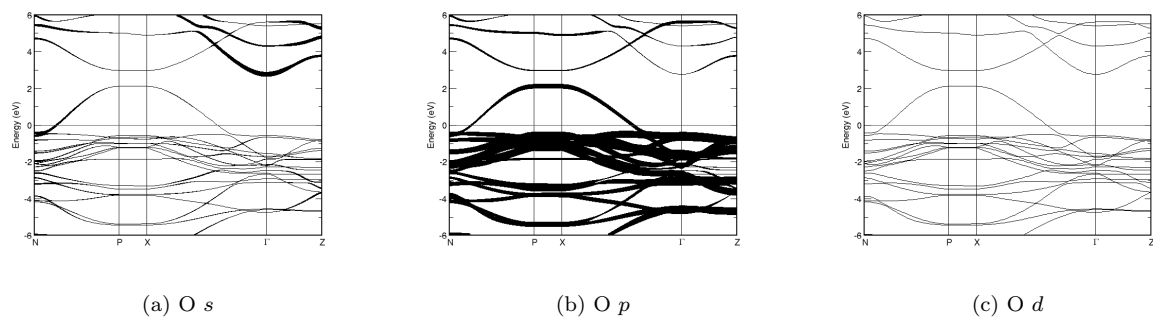
FIG. 397: Fat band representation of F in Rb_2CoF_4 FIG. 398: Fat band representation of Rb in Rb_2CoF_4 

FIG. 399: (Color online) PDOS of $\text{Gd}_2(\text{CuO}_4)$ (ICSD #41844). The *s*-, *p*- and *d*-projected states are in red, blue and green, respectively. $\text{Gd}_2(\text{CuO}_4)$ crystallizes in space group $I 4/m m m$ (#139), in a tetragonal body-centred structure.

FIG. 400: Fat band representation of Cu in $\text{Gd}_2(\text{CuO}_4)$ FIG. 401: Fat band representation of Gd in $\text{Gd}_2(\text{CuO}_4)$ FIG. 402: Fat band representation of O in $\text{Gd}_2(\text{CuO}_4)$

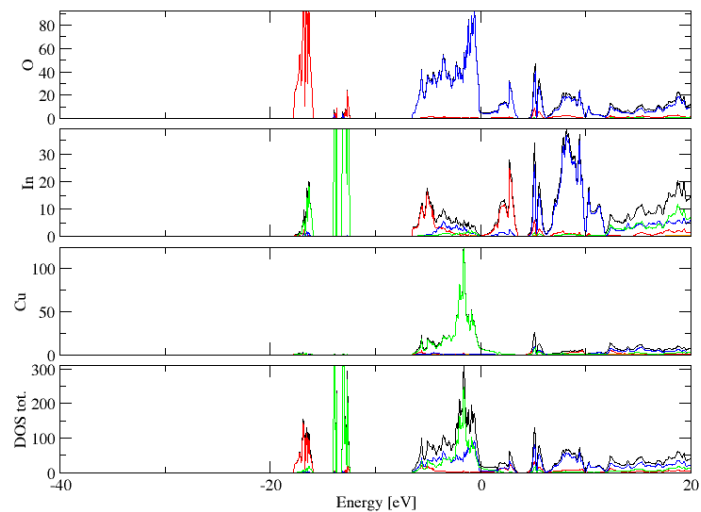


FIG. 403: (Color online) PDOS of In_2CuO_4 (ICSD #39475). The s -, p - and d -projected states are in red, blue and green, respectively. In_2CuO_4 crystallizes in space group $I 4/m m m$ (#139), in a tetragonal body-centred structure.

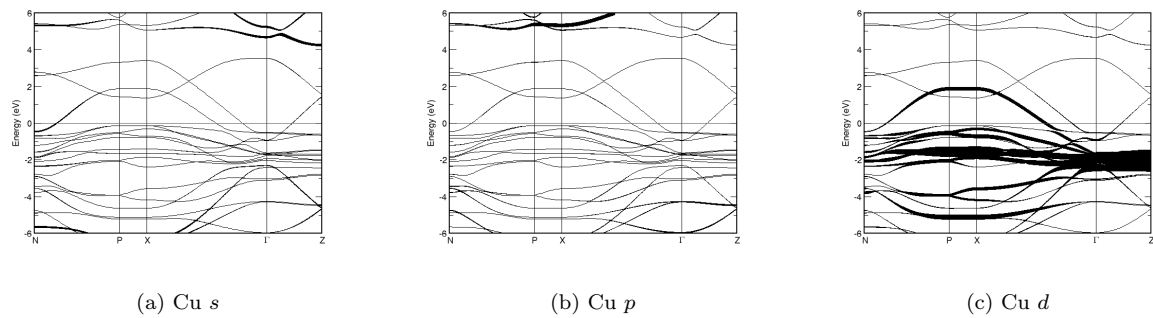


FIG. 404: Fat band representation of Cu in In_2CuO_4

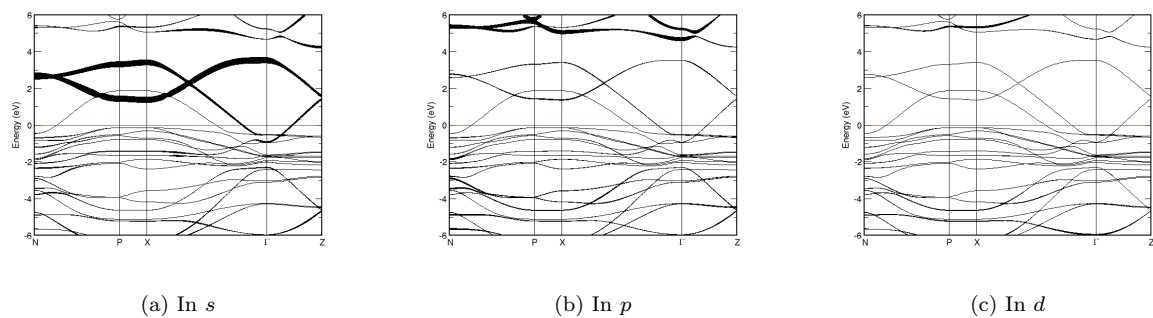
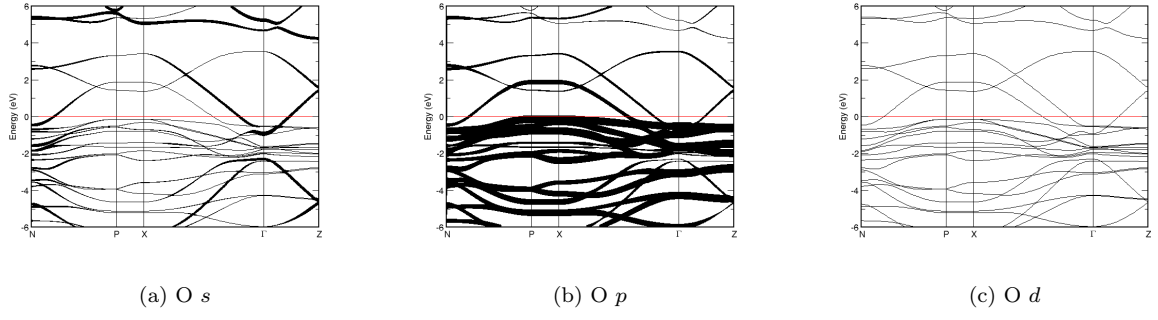
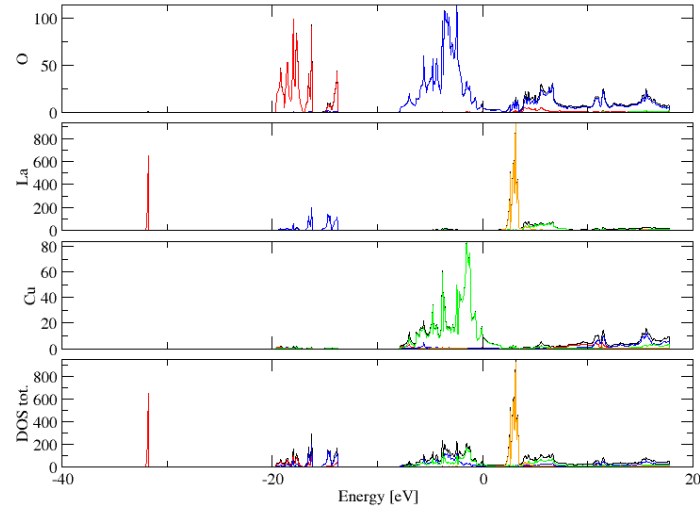
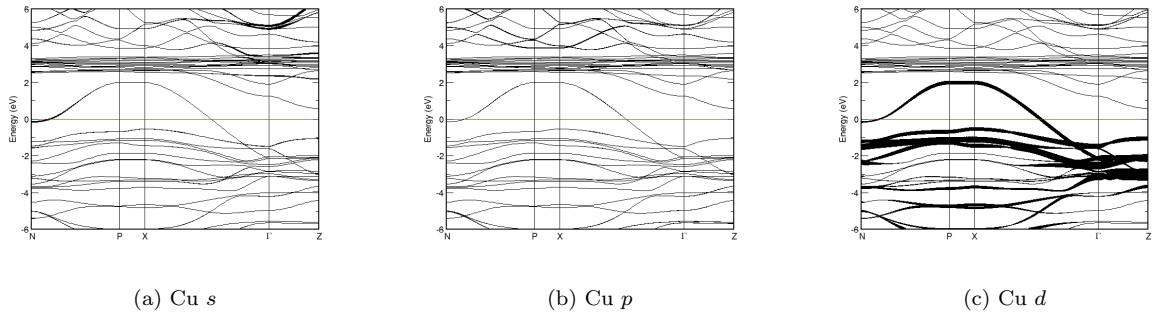
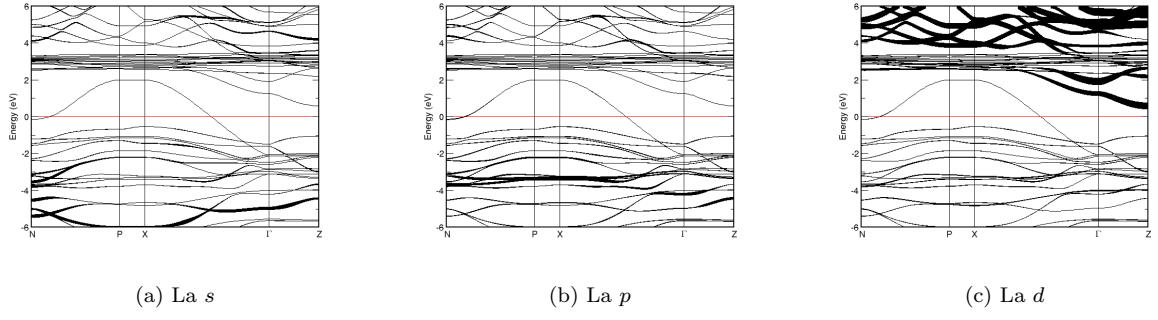
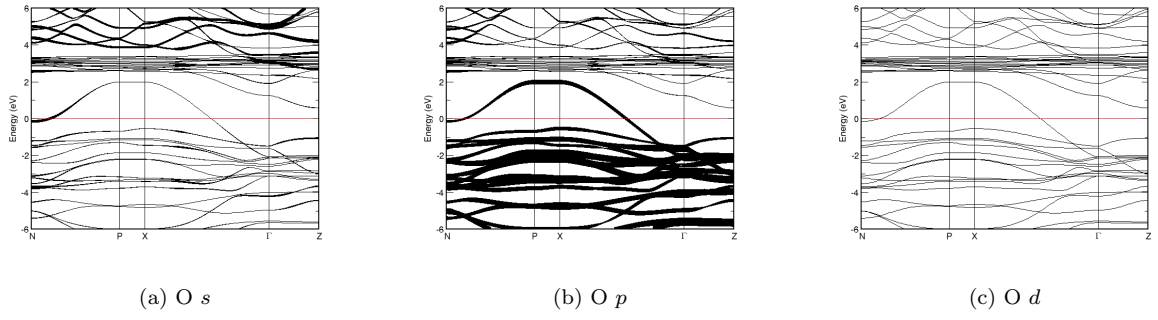
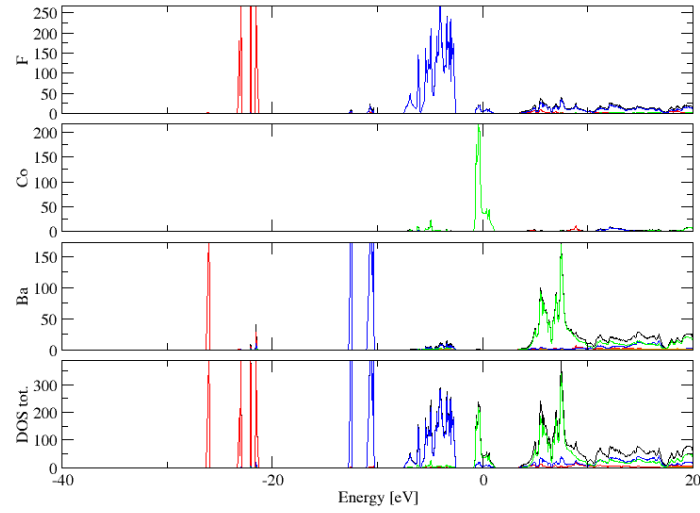
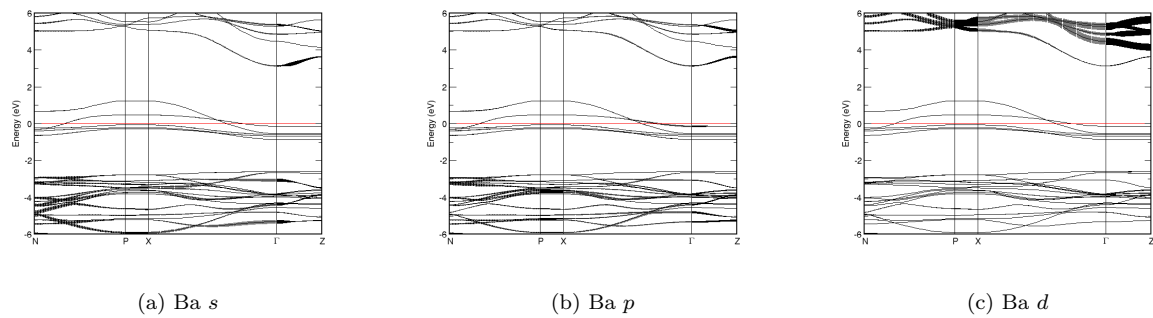
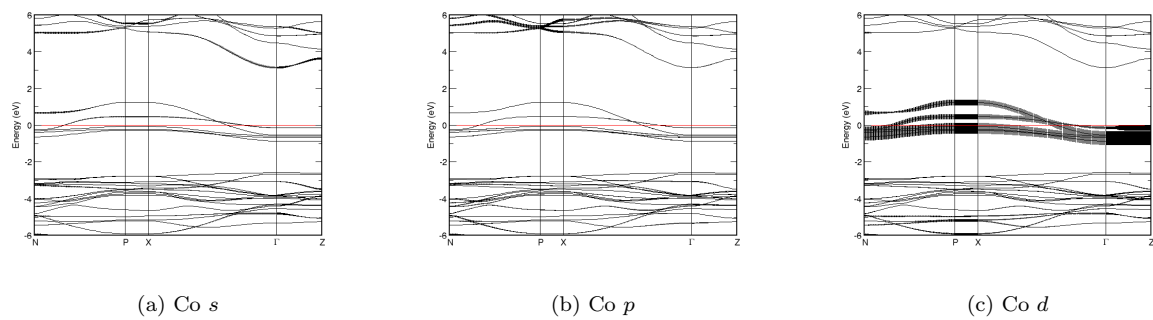
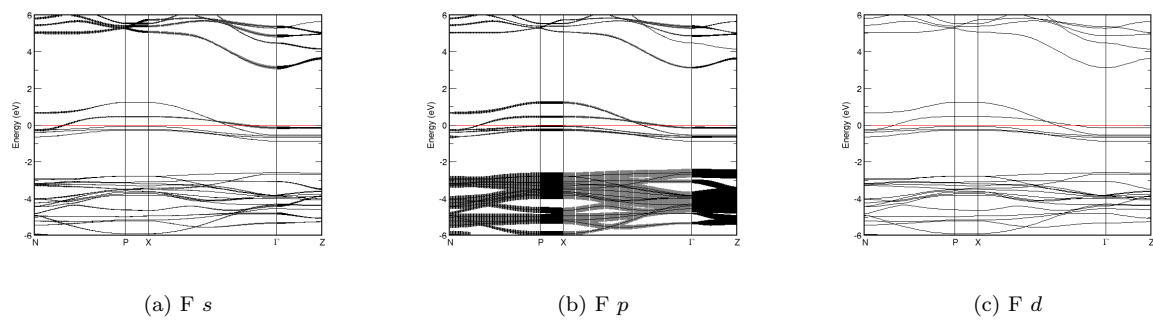


FIG. 405: Fat band representation of In in In_2CuO_4

FIG. 406: Fat band representation of O in In_2CuO_4 FIG. 407: (Color online) PDOS of $\text{La}_2(\text{CuO}_4)$ (ICSD #41643). The *s*-, *p*- and *d*-projected states are in red, blue and green, respectively. $\text{La}_2(\text{CuO}_4)$ crystallizes in space group $I 4/m m m$ (#139), in a tetragonal body-centred structure.FIG. 408: Fat band representation of Cu in $\text{La}_2(\text{CuO}_4)$

FIG. 409: Fat band representation of La in $\text{La}_2(\text{CuO}_4)$ FIG. 410: Fat band representation of O in $\text{La}_2(\text{CuO}_4)$ FIG. 411: (Color online) PDOS of Ba_2CoF_6 (ICSD #21057). The s -, p - and d -projected states are in red, blue and green, respectively. Ba_2CoF_6 crystallizes in space group $I 4/m m m$ (#139), in a tetragonal body-centred structure.

FIG. 412: Fat band representation of Ba in Ba_2CoF_6 FIG. 413: Fat band representation of Co in Ba_2CoF_6 FIG. 414: Fat band representation of F in Ba_2CoF_6

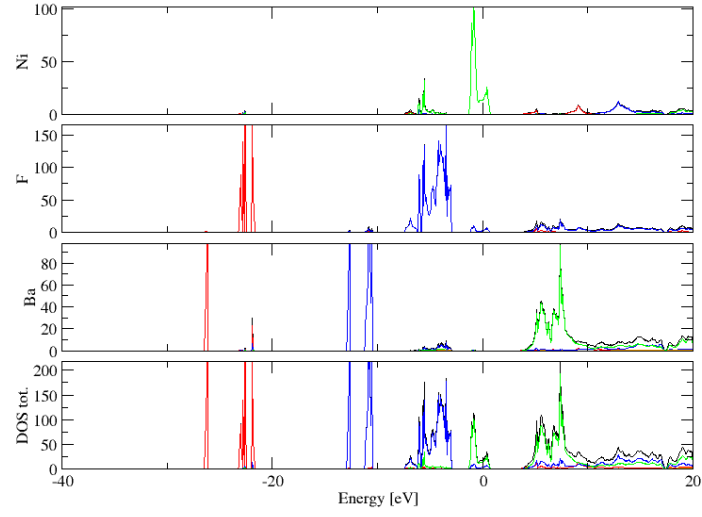


FIG. 415: (Color online) PDOS of Ba_2NiF_6 (ICSD #21056). The s -, p - and d -projected states are in red, blue and green, respectively. Ba_2NiF_6 crystallizes in space group $I 4/m m m$ (#139), in a tetragonal body-centred structure.

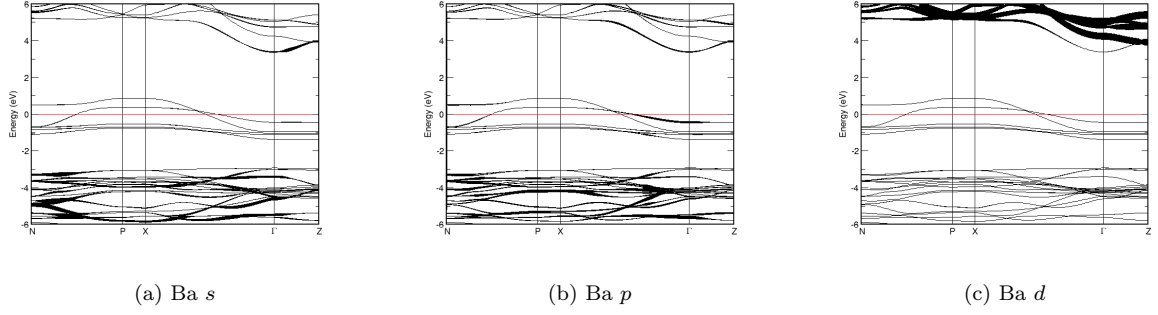


FIG. 416: Fat band representation of Ba in Ba_2NiF_6

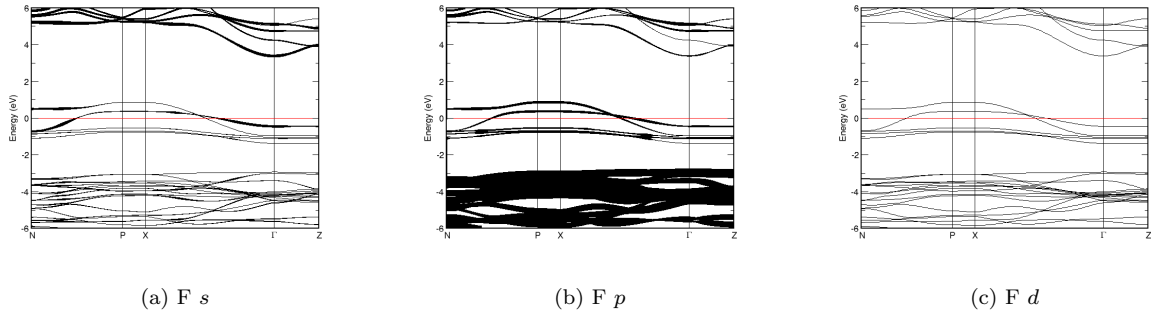
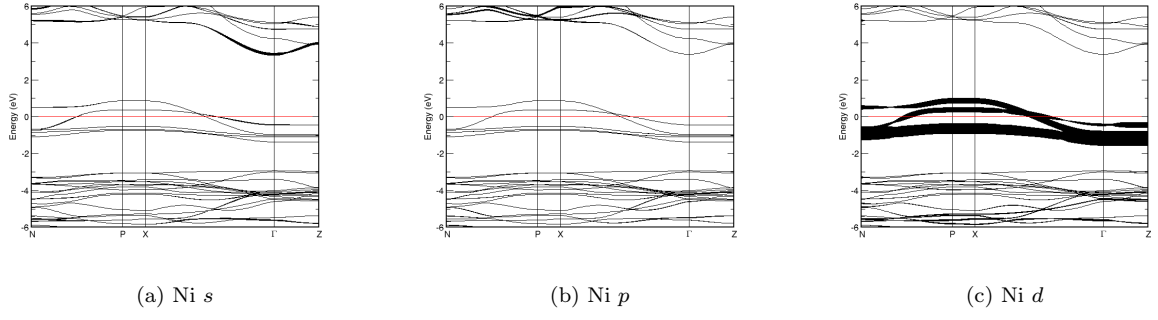
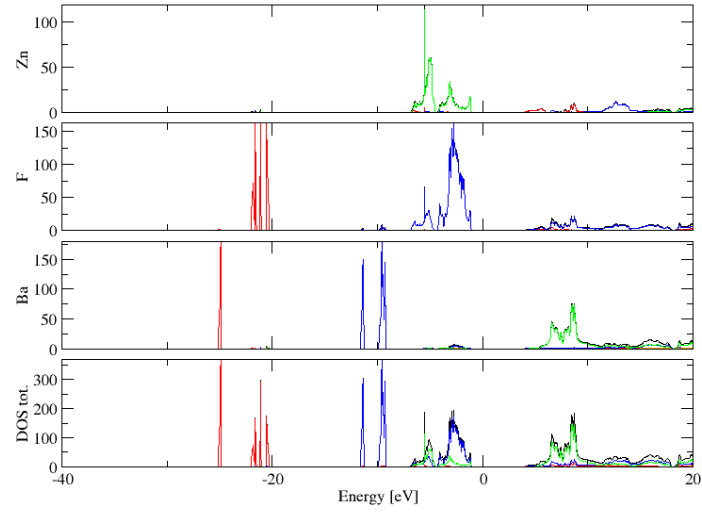
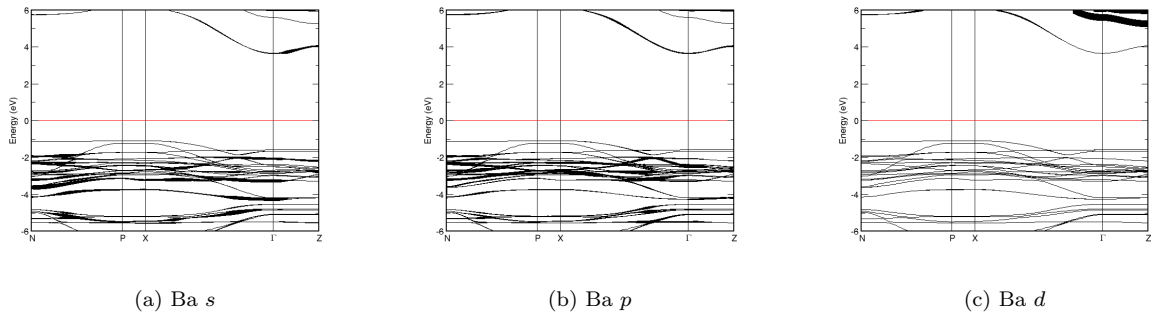


FIG. 417: Fat band representation of F in Ba_2NiF_6

FIG. 418: Fat band representation of Ni in Ba_2NiF_6 FIG. 419: (Color online) PDOS of $\text{Ba}_2(\text{ZnF}_6)$ (ICSD #21054). The *s*-, *p*- and *d*-projected states are in red, blue and green, respectively. $\text{Ba}_2(\text{ZnF}_6)$ crystallizes in space group $I 4/m m m$ (#139), in a tetragonal body-centred structure.FIG. 420: Fat band representation of Ba in $\text{Ba}_2(\text{ZnF}_6)$

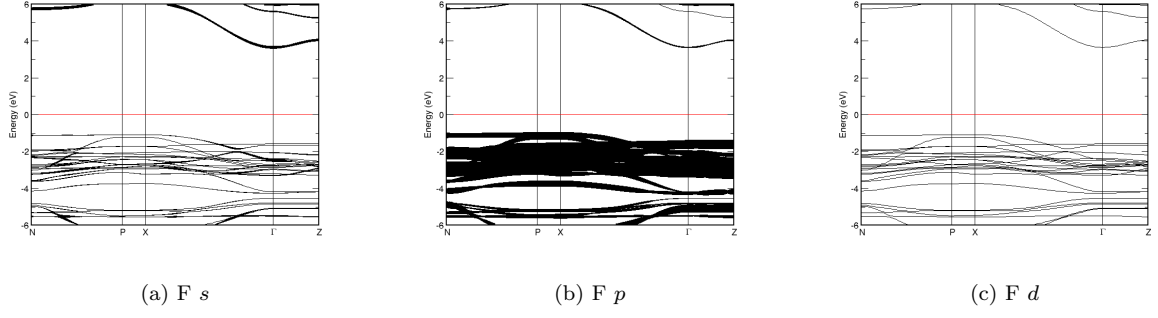
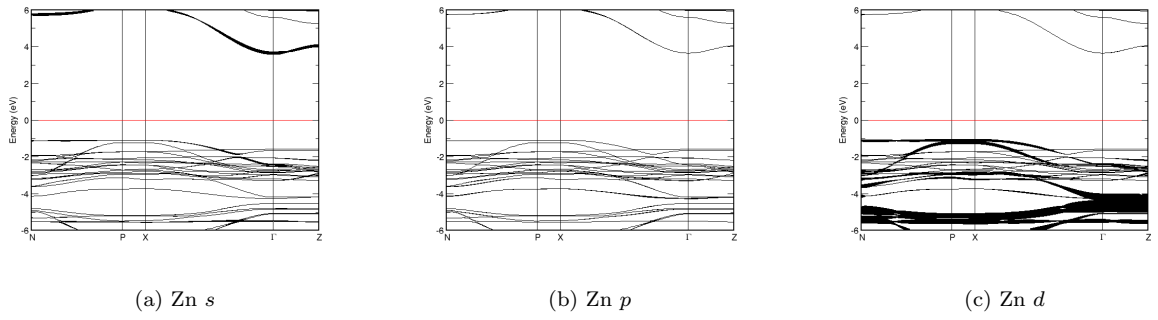
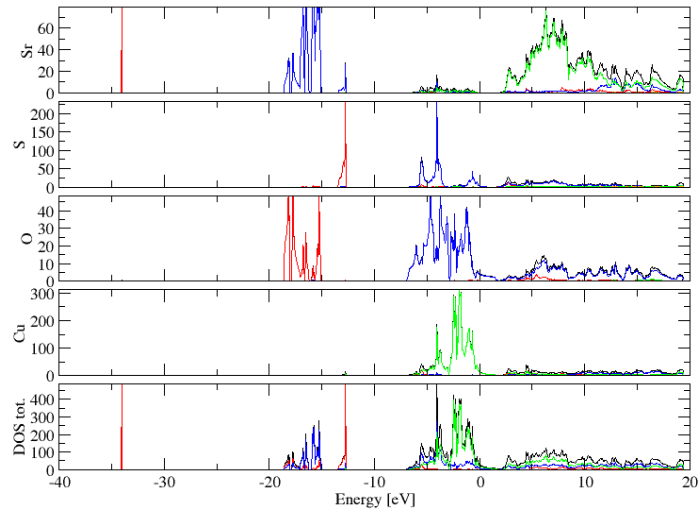
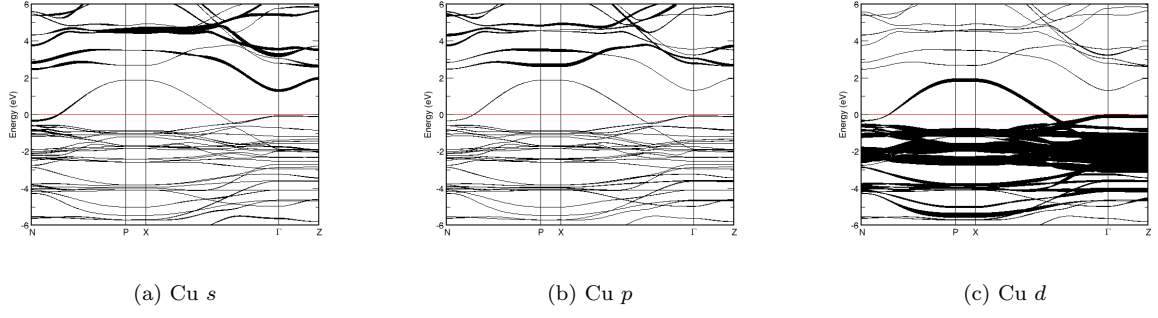
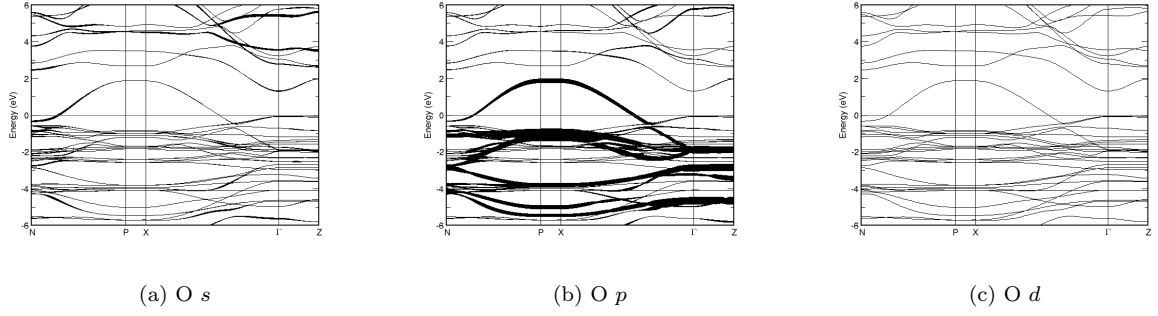
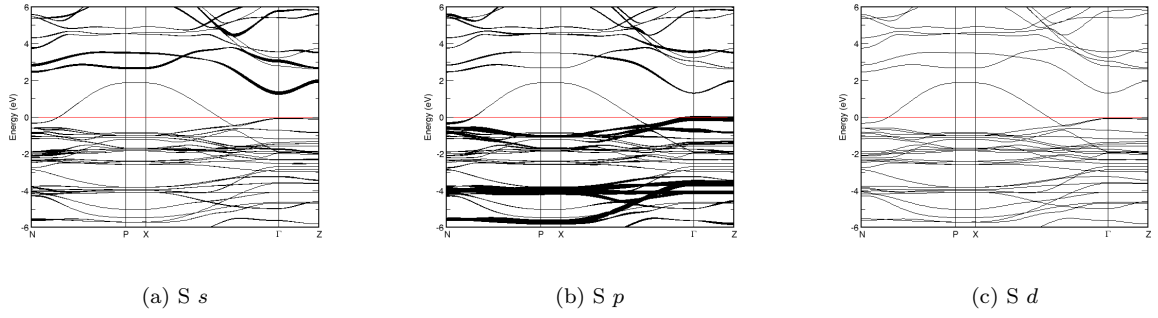
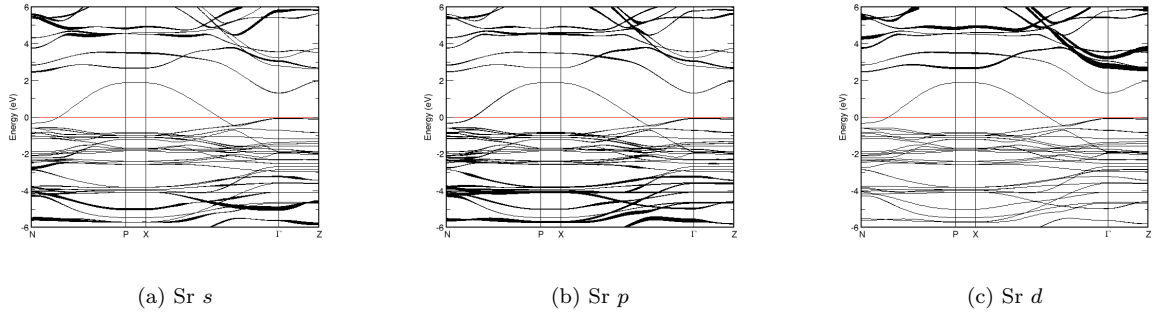
FIG. 421: Fat band representation of F in $\text{Ba}_2(\text{ZnF}_6)$ FIG. 422: Fat band representation of Zn in $\text{Ba}_2(\text{ZnF}_6)$ 

FIG. 423: (Color online) PDOS of $(\text{Cu}_2\text{S}_2)(\text{Sr}_2\text{CuO}_2)$ (ICSD #88423). The *s*-, *p*- and *d*-projected states are in red, blue and green, respectively. $(\text{Cu}_2\text{S}_2)(\text{Sr}_2\text{CuO}_2)$ crystallizes in space group $I 4/m m m$ (#139), in a tetragonal body-centred structure.

FIG. 424: Fat band representation of Cu in $(\text{Cu}_2\text{S}_2)(\text{Sr}_2\text{CuO}_2)$ FIG. 425: Fat band representation of O in $(\text{Cu}_2\text{S}_2)(\text{Sr}_2\text{CuO}_2)$ FIG. 426: Fat band representation of S in $(\text{Cu}_2\text{S}_2)(\text{Sr}_2\text{CuO}_2)$ FIG. 427: Fat band representation of Sr in $(\text{Cu}_2\text{S}_2)(\text{Sr}_2\text{CuO}_2)$

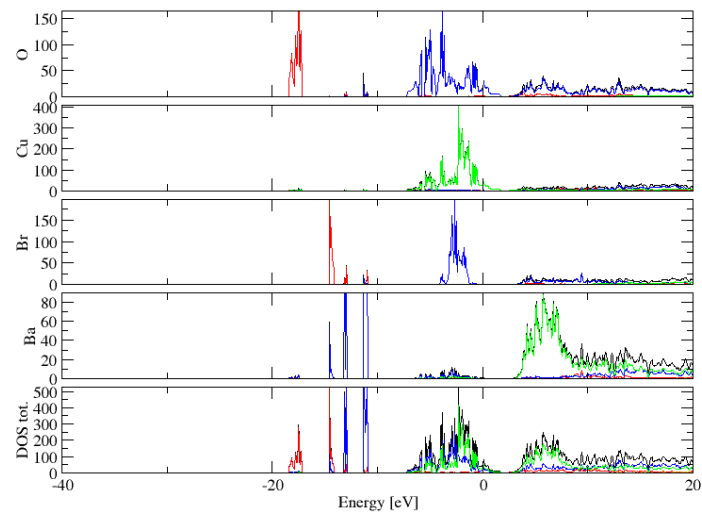


FIG. 428: (Color online) PDOS of $\text{Ba}_2\text{Cu}_3\text{O}_4\text{Br}_2$ (ICSD #36128). The s -, p - and d -projected states are in red, blue and green, respectively. $\text{Ba}_2\text{Cu}_3\text{O}_4\text{Br}_2$ crystallizes in space group $I\ 4/m\ m\ m$ (#139), in a tetragonal body-centred structure.

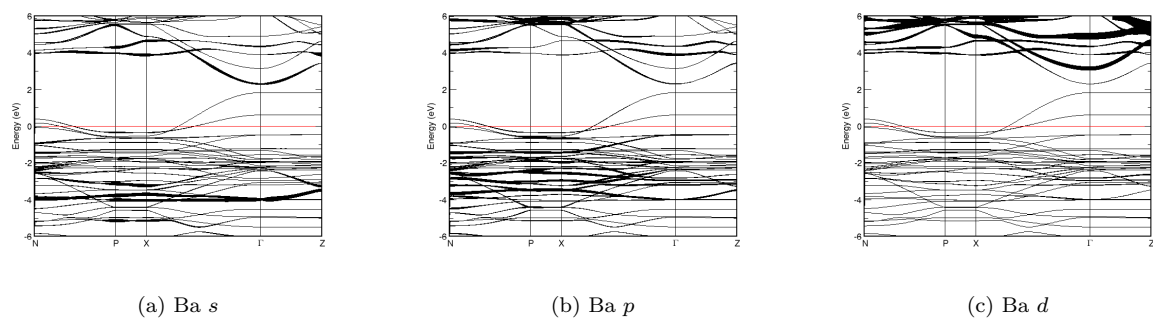


FIG. 429: Fat band representation of Ba in $\text{Ba}_2\text{Cu}_3\text{O}_4\text{Br}_2$

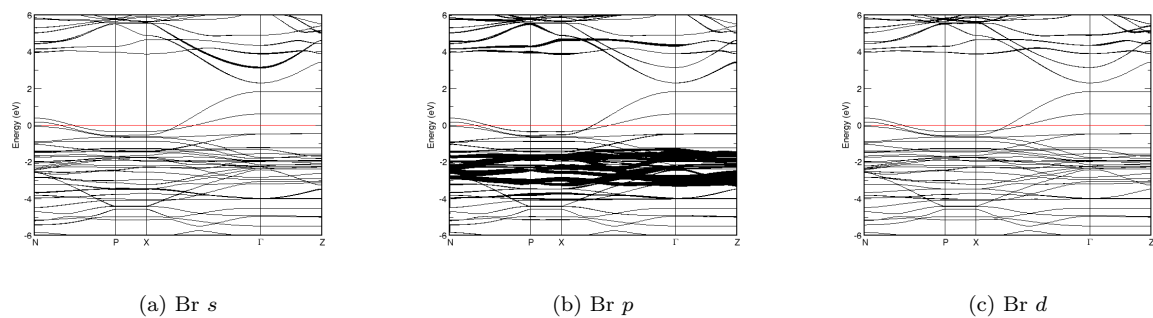


FIG. 430: Fat band representation of Br in $\text{Ba}_2\text{Cu}_3\text{O}_4\text{Br}_2$

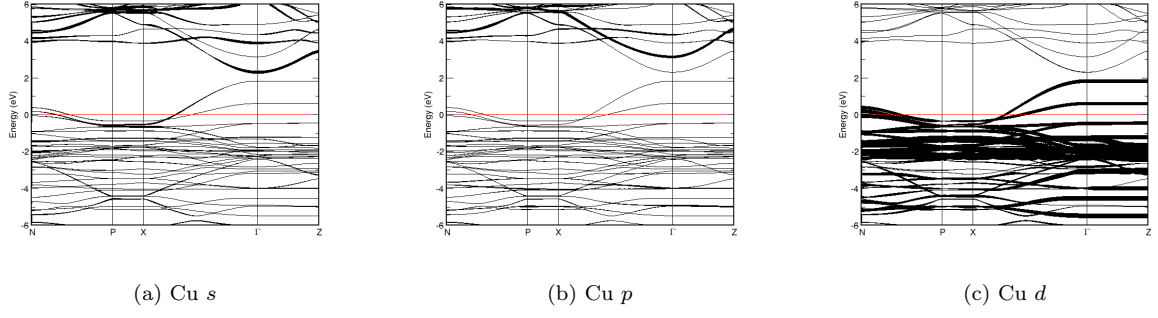
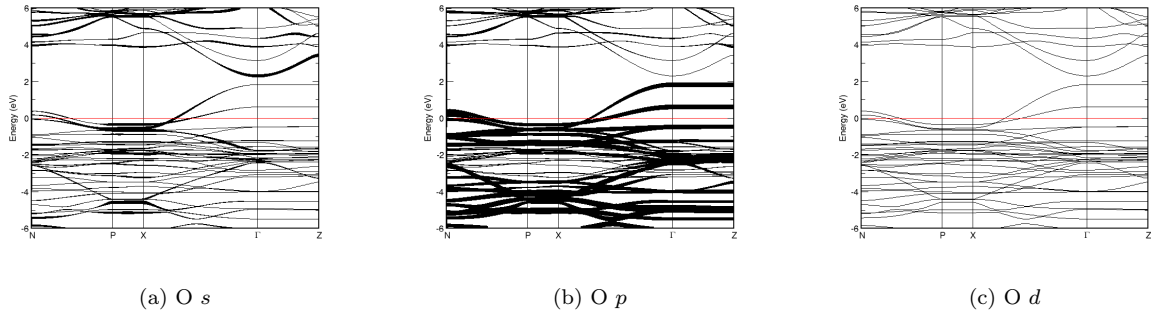
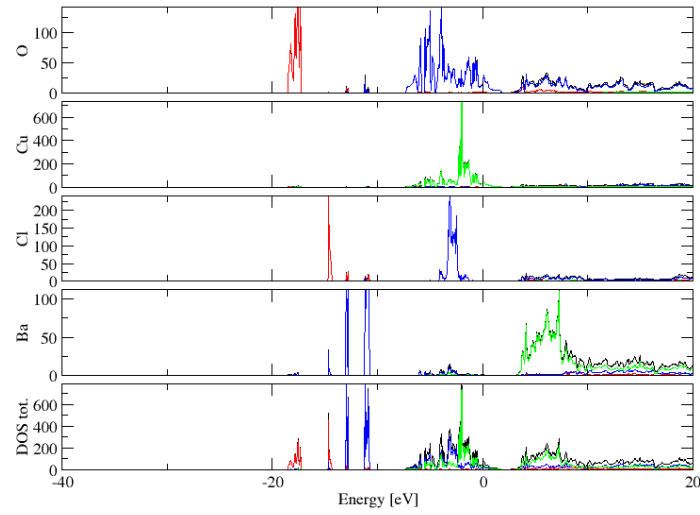
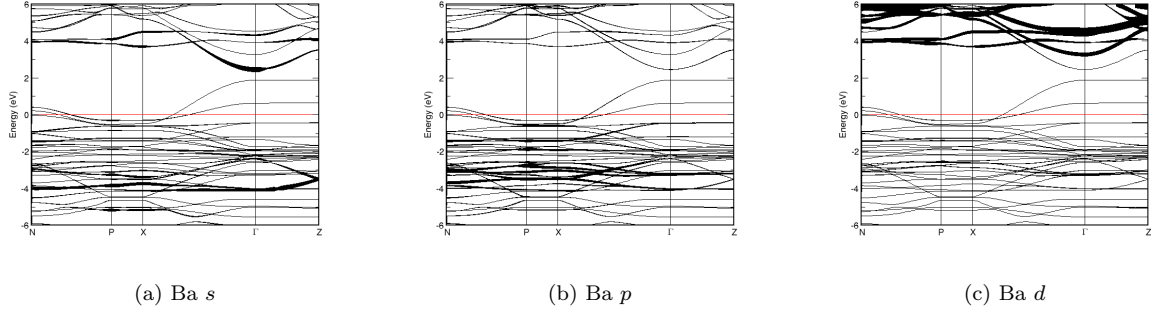
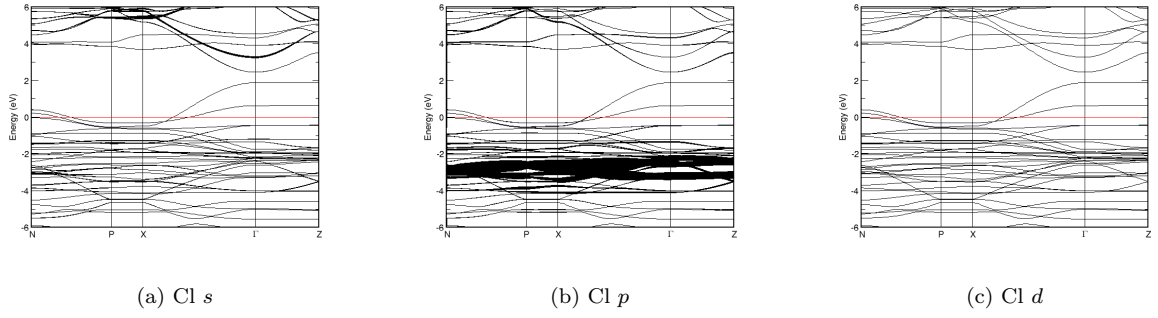
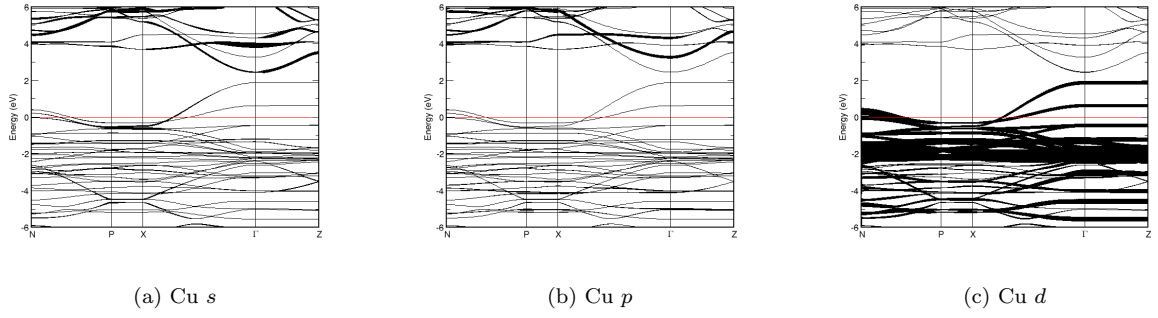
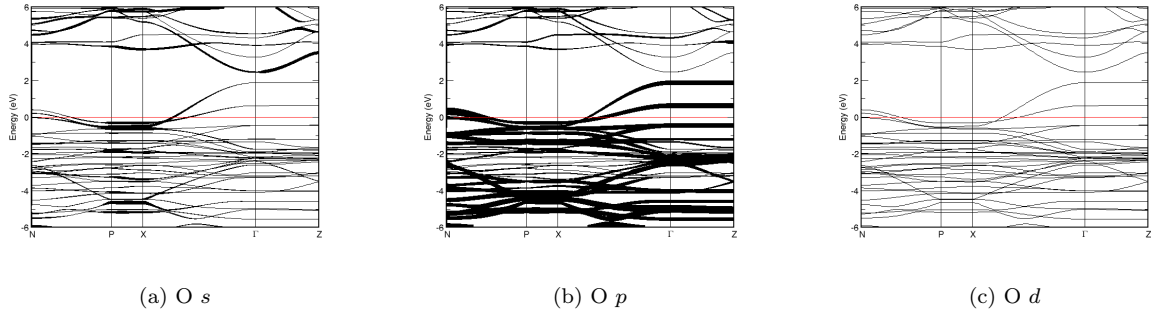
FIG. 431: Fat band representation of Cu in $\text{Ba}_2\text{Cu}_3\text{O}_4\text{Br}_2$ FIG. 432: Fat band representation of O in $\text{Ba}_2\text{Cu}_3\text{O}_4\text{Br}_2$ 

FIG. 433: (Color online) PDOS of $\text{Ba}_2\text{Cu}_3\text{O}_4\text{Cl}_2$ (ICSD #355). The *s*-, *p*- and *d*-projected states are in red, blue and green, respectively. $\text{Ba}_2\text{Cu}_3\text{O}_4\text{Cl}_2$ crystallizes in space group $I\ 4/m\ m\ m$ (#139), in a tetragonal body-centred structure.

FIG. 434: Fat band representation of Ba in $\text{Ba}_2\text{Cu}_3\text{O}_4\text{Cl}_2$ FIG. 435: Fat band representation of Cl in $\text{Ba}_2\text{Cu}_3\text{O}_4\text{Cl}_2$ FIG. 436: Fat band representation of Cu in $\text{Ba}_2\text{Cu}_3\text{O}_4\text{Cl}_2$ FIG. 437: Fat band representation of O in $\text{Ba}_2\text{Cu}_3\text{O}_4\text{Cl}_2$

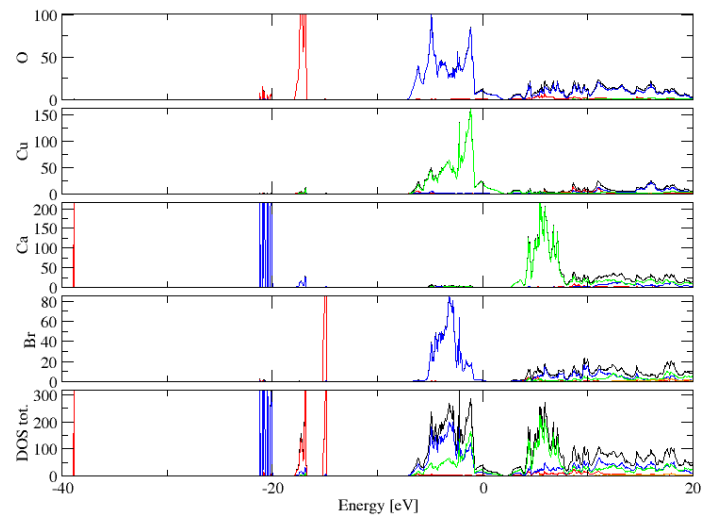


FIG. 438: (Color online) PDOS of $\text{Ca}_3\text{Cu}_2\text{O}_4\text{Br}_2$ (ICSD #69182). The s -, p - and d -projected states are in red, blue and green, respectively. $\text{Ca}_3\text{Cu}_2\text{O}_4\text{Br}_2$ crystallizes in space group I $4/m\ m\ m$ (#139), in a tetragonal body-centred structure.

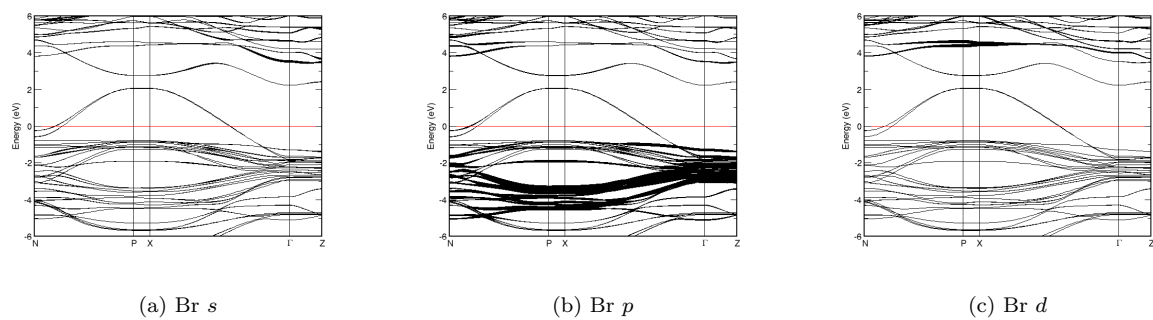


FIG. 439: Fat band representation of Br in $\text{Ca}_3\text{Cu}_2\text{O}_4\text{Br}_2$

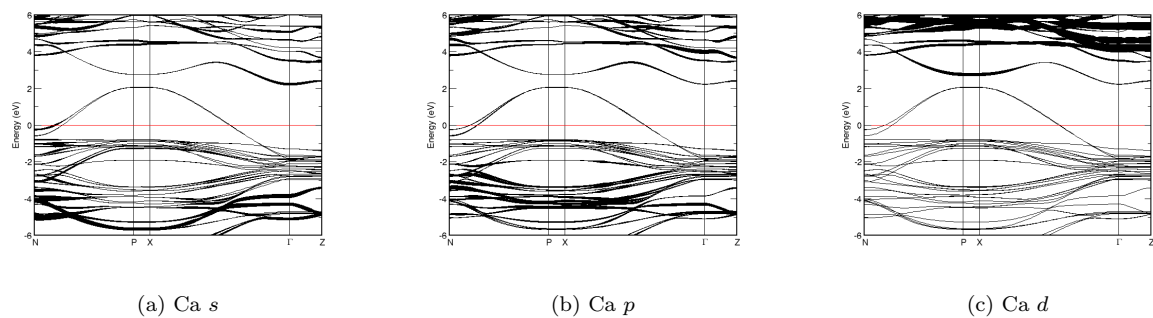


FIG. 440: Fat band representation of Ca in $\text{Ca}_3\text{Cu}_2\text{O}_4\text{Br}_2$

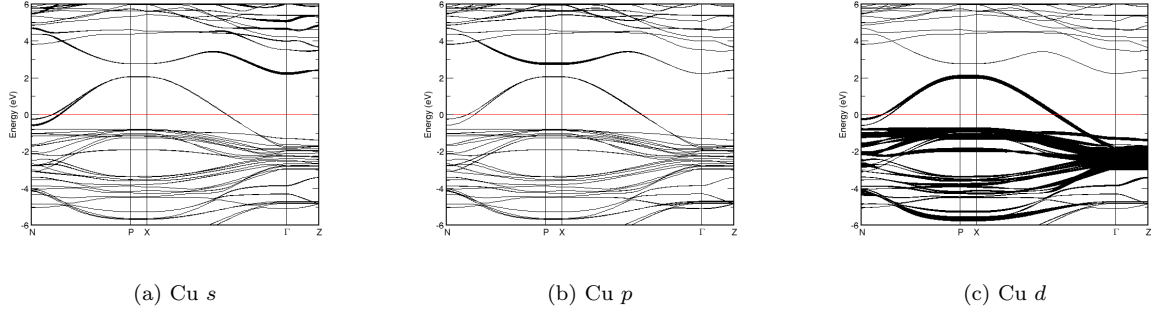
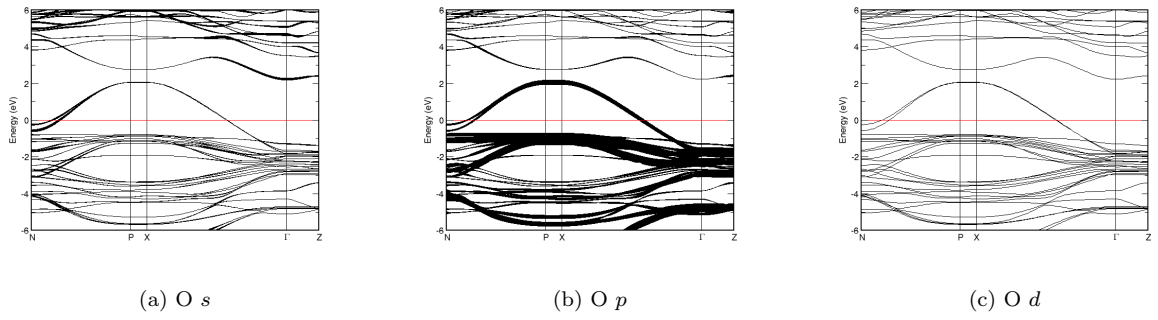
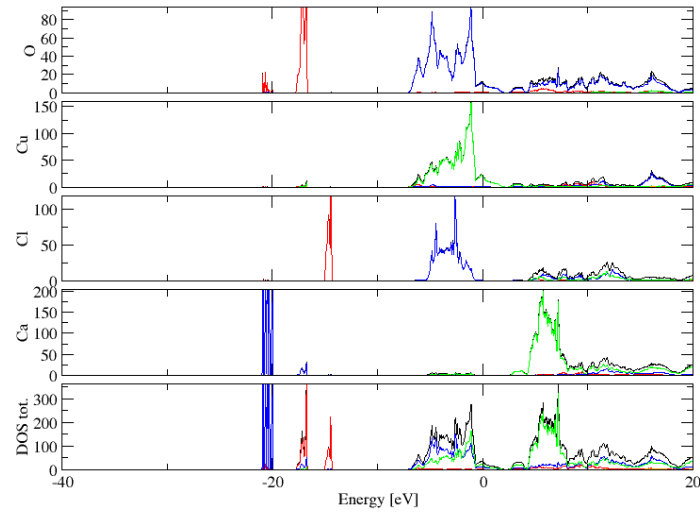
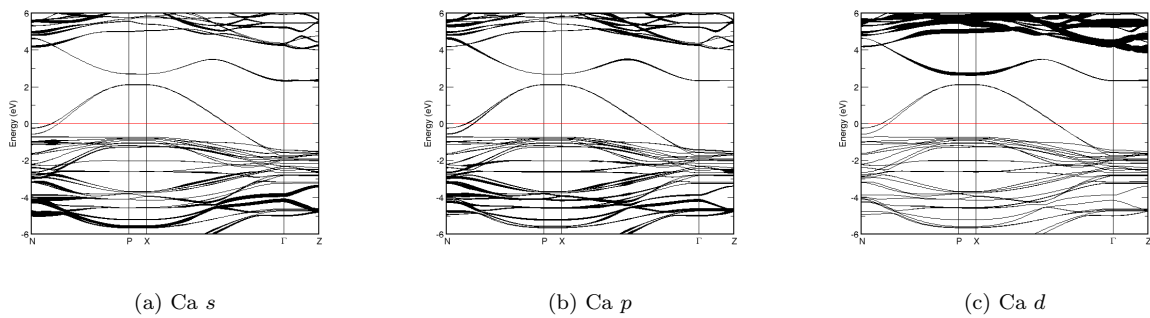
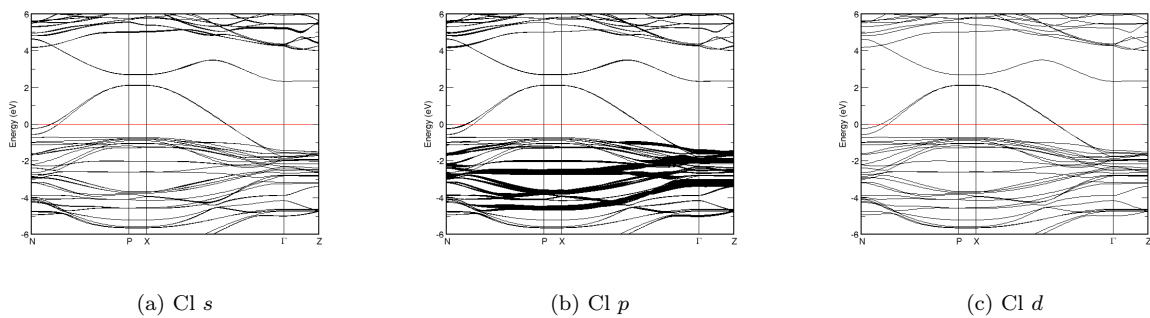
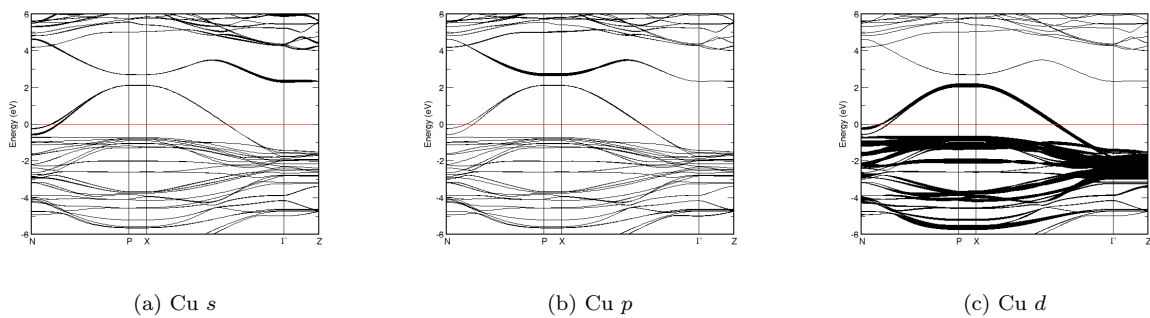
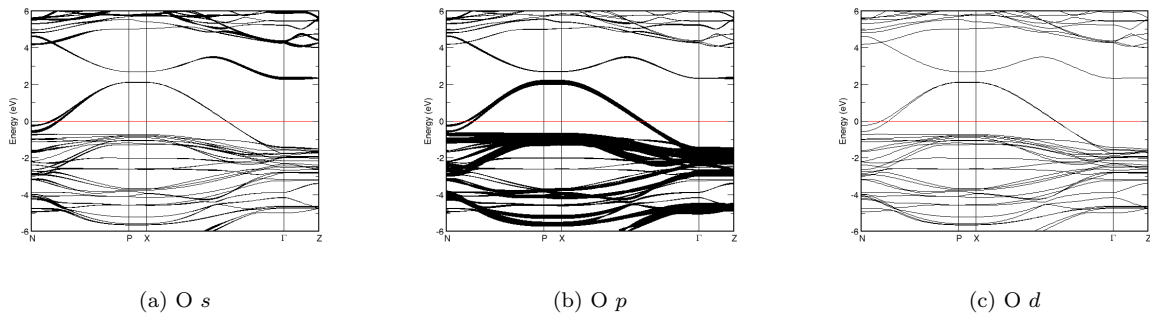
FIG. 441: Fat band representation of Cu in $\text{Ca}_3\text{Cu}_2\text{O}_4\text{Br}_2$ FIG. 442: Fat band representation of O in $\text{Ca}_3\text{Cu}_2\text{O}_4\text{Br}_2$ 

FIG. 443: (Color online) PDOS of $\text{Ca}_3\text{Cu}_2\text{O}_4\text{Cl}_2$ (ICSD #69181). The *s*-, *p*- and *d*-projected states are in red, blue and green, respectively. $\text{Ca}_3\text{Cu}_2\text{O}_4\text{Cl}_2$ crystallizes in space group $I 4/m m m$ (#139), in a tetragonal body-centred structure.

FIG. 444: Fat band representation of Ca in $\text{Ca}_3\text{Cu}_2\text{O}_4\text{Cl}_2$ FIG. 445: Fat band representation of Cl in $\text{Ca}_3\text{Cu}_2\text{O}_4\text{Cl}_2$ FIG. 446: Fat band representation of Cu in $\text{Ca}_3\text{Cu}_2\text{O}_4\text{Cl}_2$ FIG. 447: Fat band representation of O in $\text{Ca}_3\text{Cu}_2\text{O}_4\text{Cl}_2$

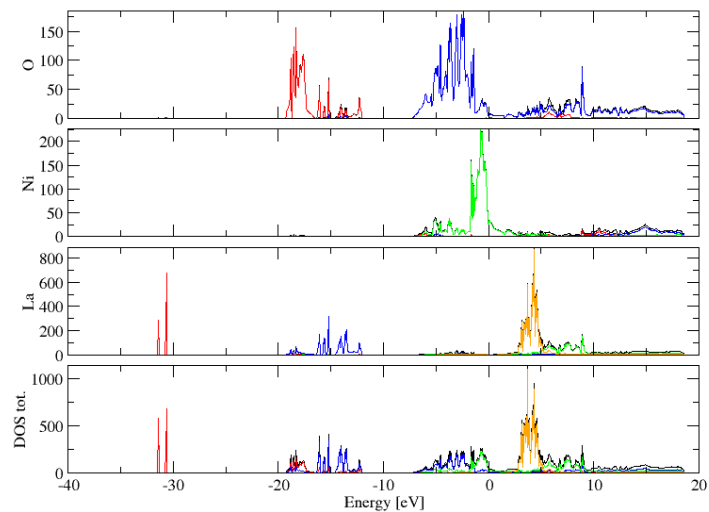


FIG. 448: (Color online) PDOS of $\text{La}_3\text{Ni}_2\text{O}_6$ (ICSD #249209). The s -, p - and d -projected states are in red, blue and green, respectively. $\text{La}_3\text{Ni}_2\text{O}_6$ crystallizes in space group I $4/m\ m\ m$ (#139), in a tetragonal body-centred structure.

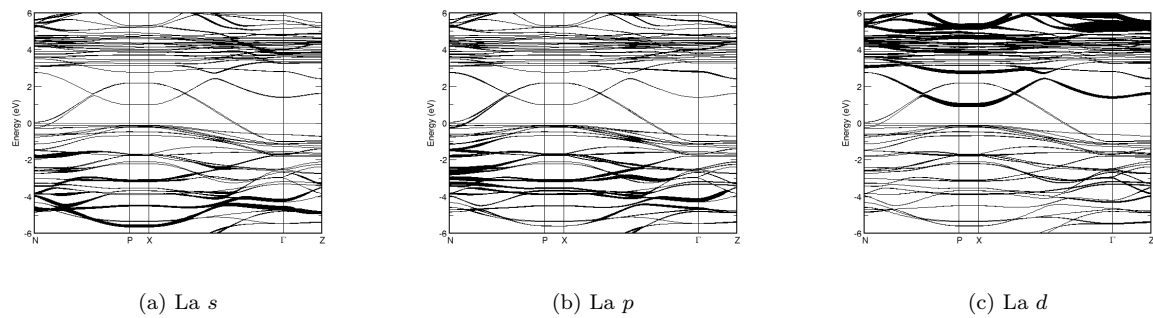


FIG. 449: Fat band representation of La in $\text{La}_3\text{Ni}_2\text{O}_6$

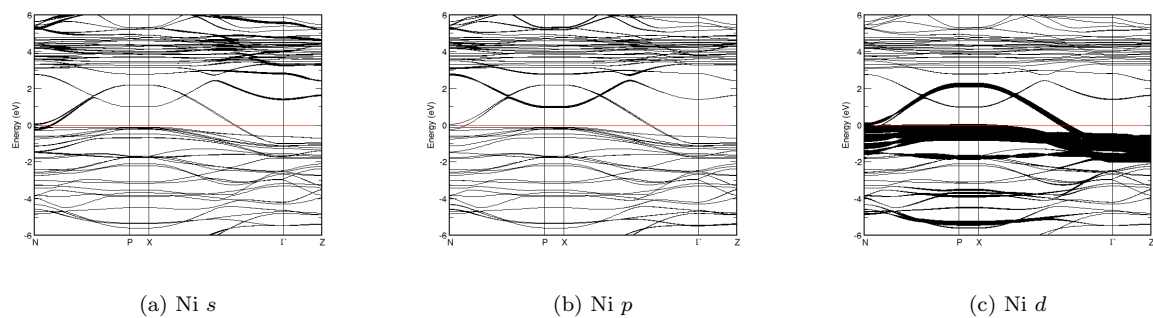
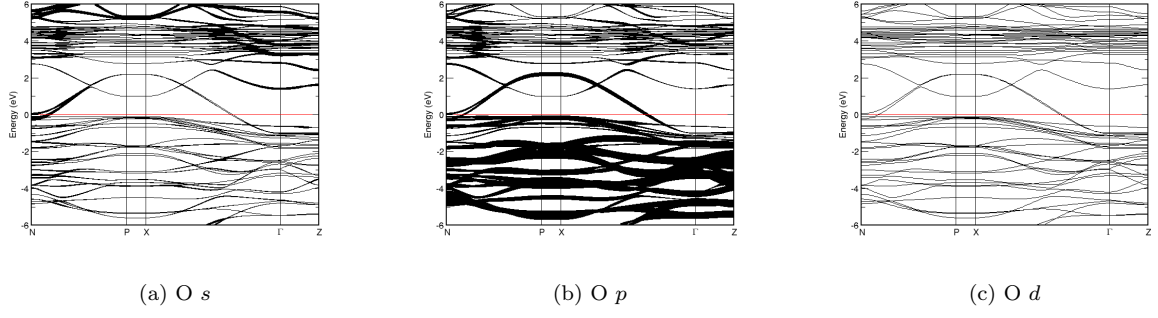
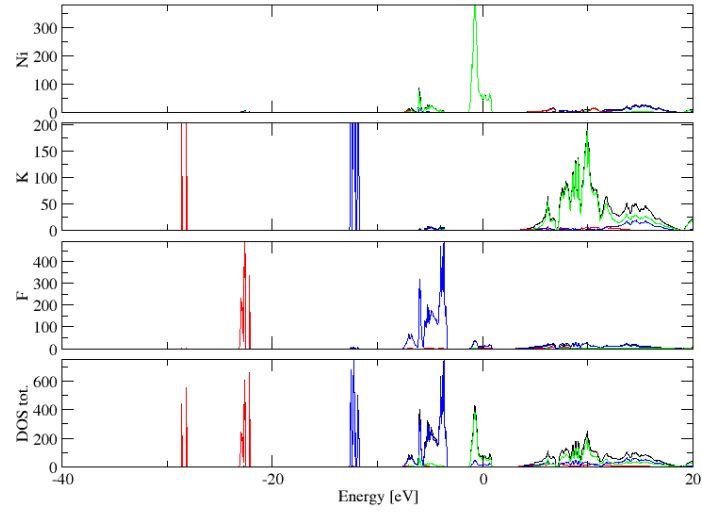
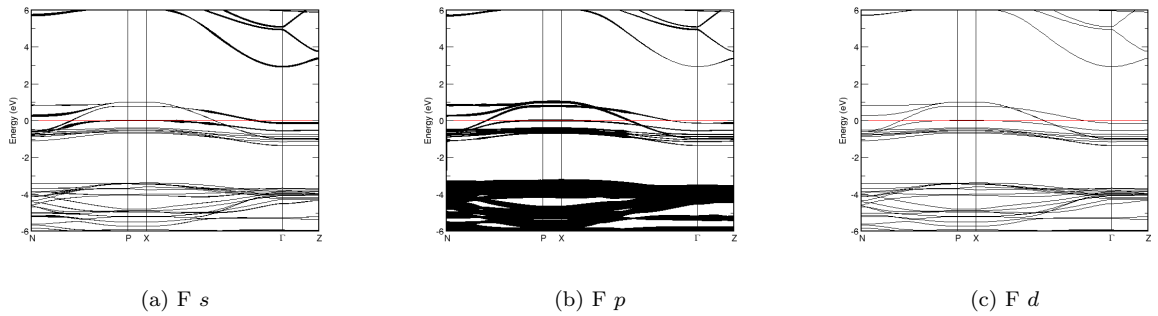
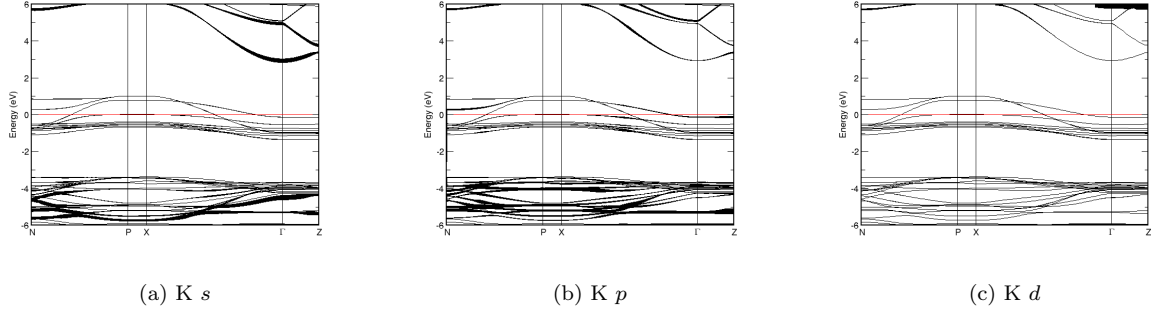
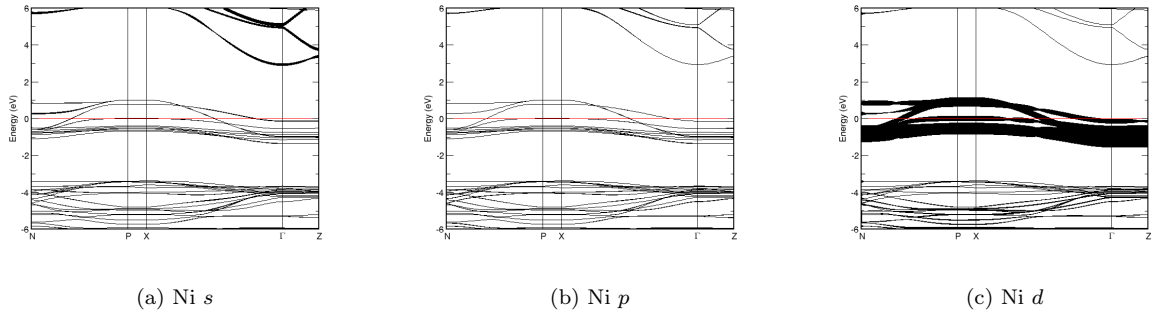
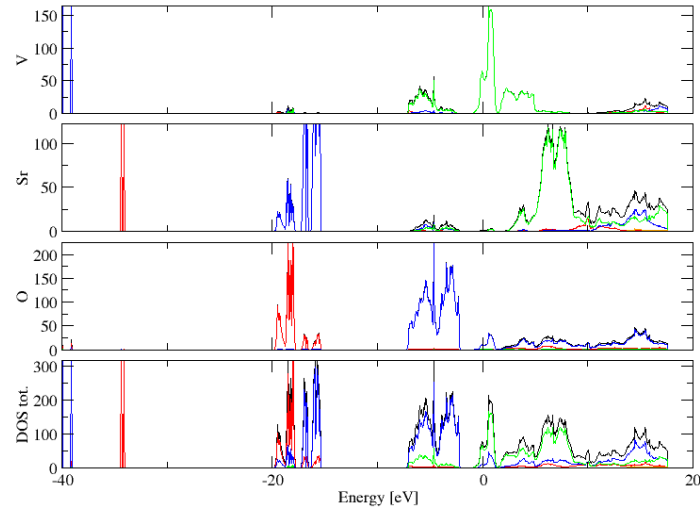
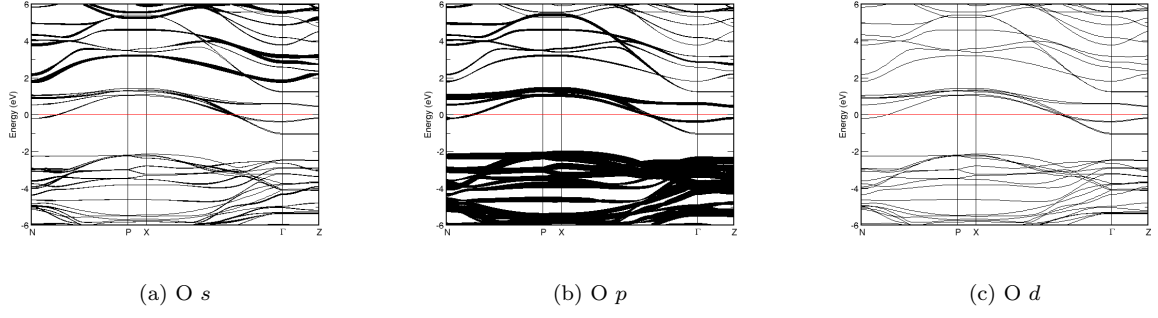
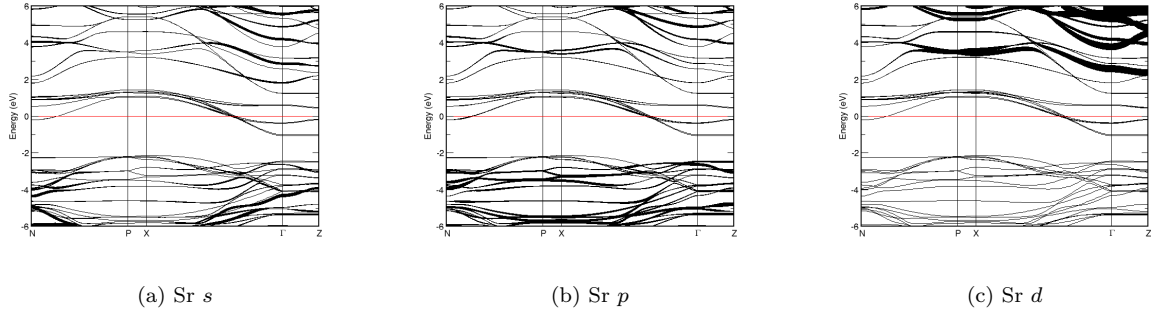
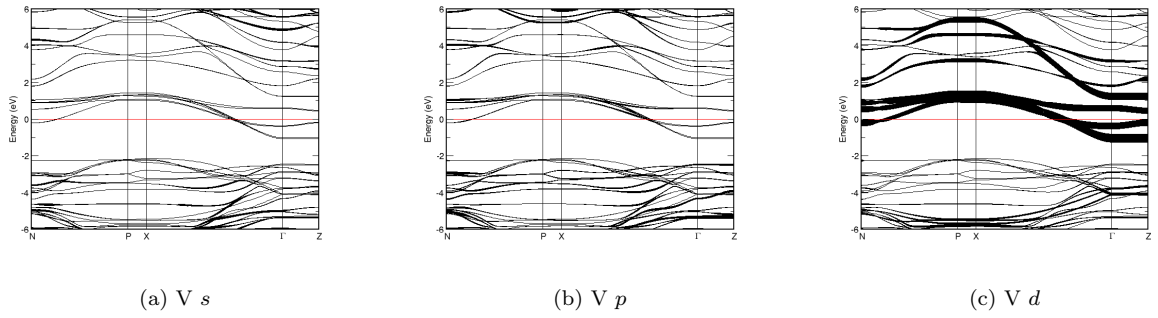


FIG. 450: Fat band representation of Ni in $\text{La}_3\text{Ni}_2\text{O}_6$

FIG. 451: Fat band representation of O in $\text{La}_3\text{Ni}_2\text{O}_6$ FIG. 452: (Color online) PDOS of $\text{K}_3\text{Ni}_2\text{F}_7$ (ICSD #33523). The *s*-, *p*- and *d*-projected states are in red, blue and green, respectively. $\text{K}_3\text{Ni}_2\text{F}_7$ crystallizes in space group $I 4/m m m$ (#139), in a tetragonal body-centred structure.FIG. 453: Fat band representation of F in $\text{K}_3\text{Ni}_2\text{F}_7$

FIG. 454: Fat band representation of K in $\text{K}_3\text{Ni}_2\text{F}_7$ FIG. 455: Fat band representation of Ni in $\text{K}_3\text{Ni}_2\text{F}_7$ FIG. 456: (Color online) PDOS of $\text{Sr}_3\text{V}_2\text{O}_7$ (ICSD #71320). The *s*-, *p*- and *d*-projected states are in red, blue and green, respectively. $\text{Sr}_3\text{V}_2\text{O}_7$ crystallizes in space group $I 4/m m m$ (#139), in a tetragonal body-centred structure.

FIG. 457: Fat band representation of O in $\text{Sr}_3\text{V}_2\text{O}_7$ FIG. 458: Fat band representation of Sr in $\text{Sr}_3\text{V}_2\text{O}_7$ FIG. 459: Fat band representation of V in $\text{Sr}_3\text{V}_2\text{O}_7$

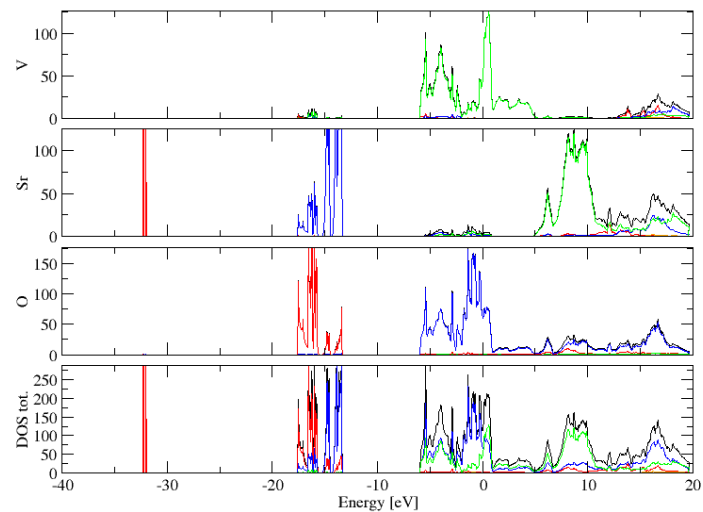


FIG. 460: (Color online) PDOS of $\text{Sr}_3(\text{V}_2\text{O}_7)$ (ICSD #71451). The s -, p - and d -projected states are in red, blue and green, respectively. $\text{Sr}_3(\text{V}_2\text{O}_7)$ crystallizes in space group $I 4/m m m$ (#139), in a tetragonal body-centred structure.

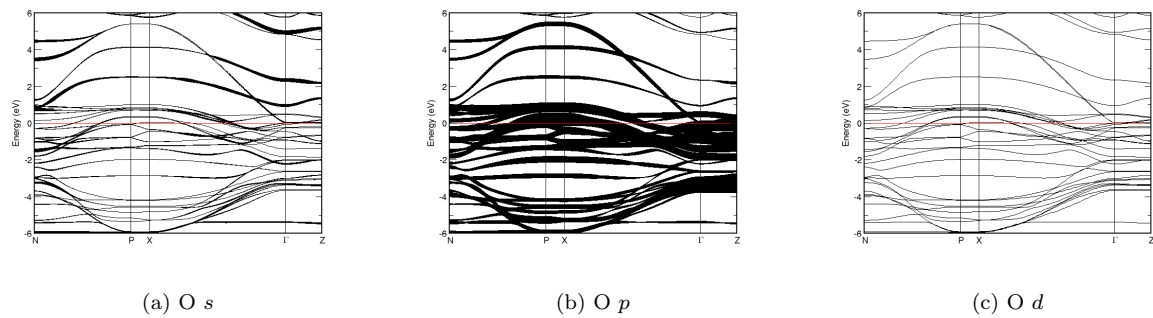


FIG. 461: Fat band representation of O in $\text{Sr}_3(\text{V}_2\text{O}_7)$

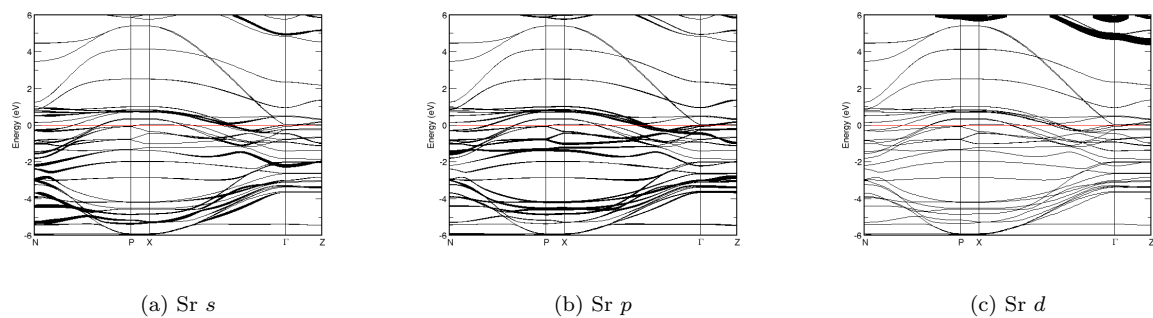
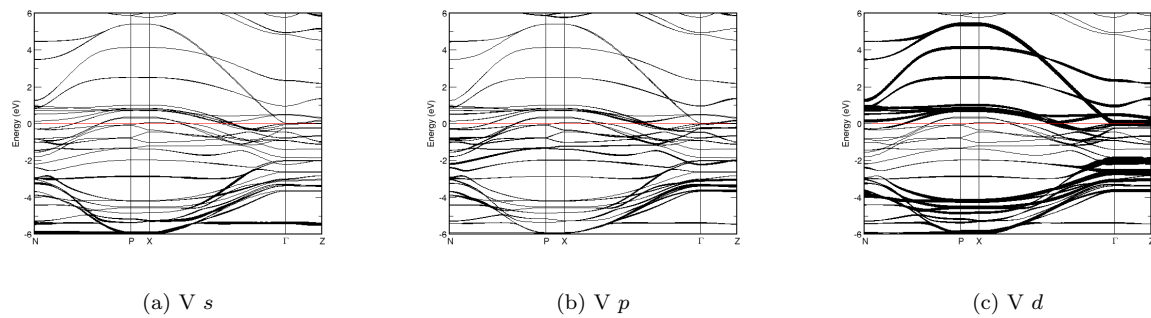
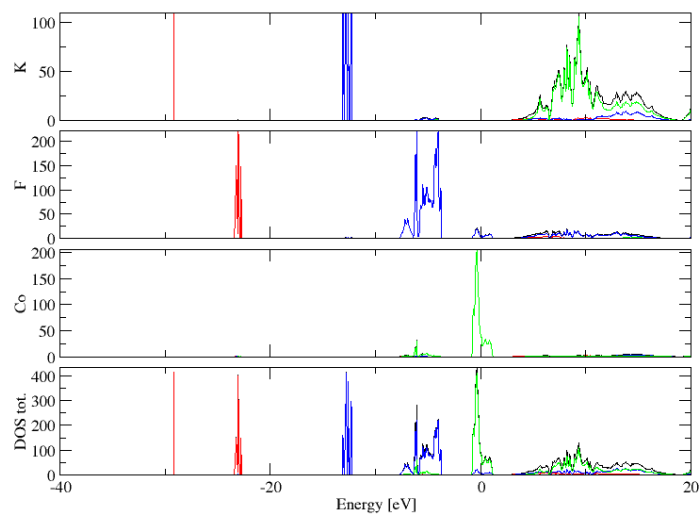
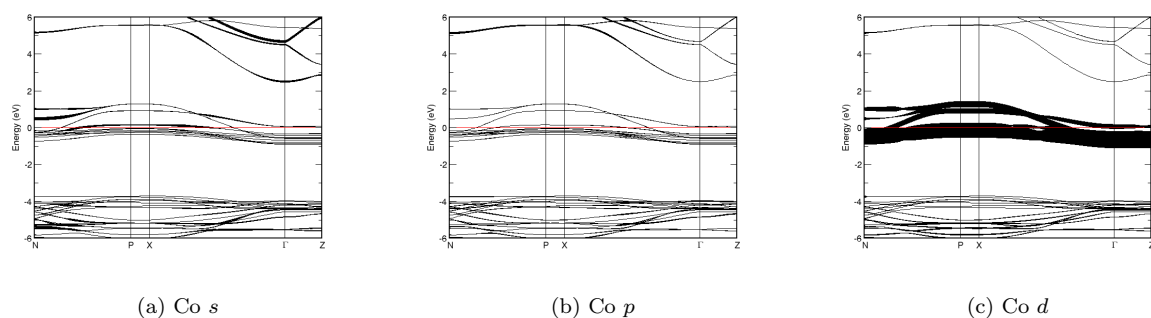
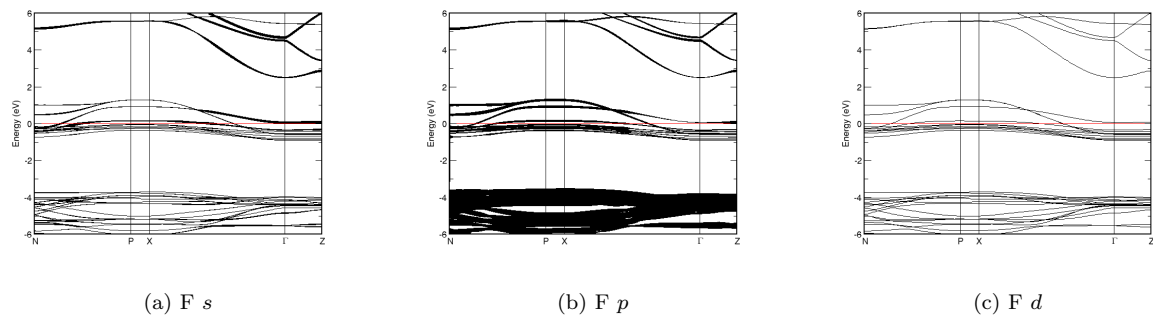
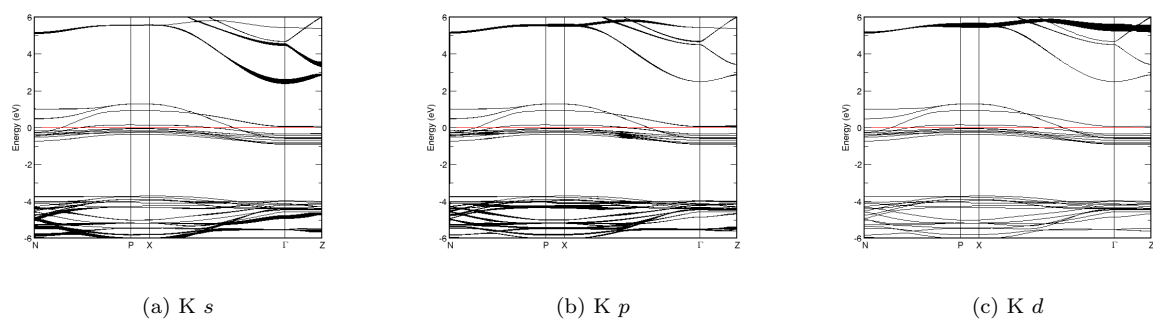
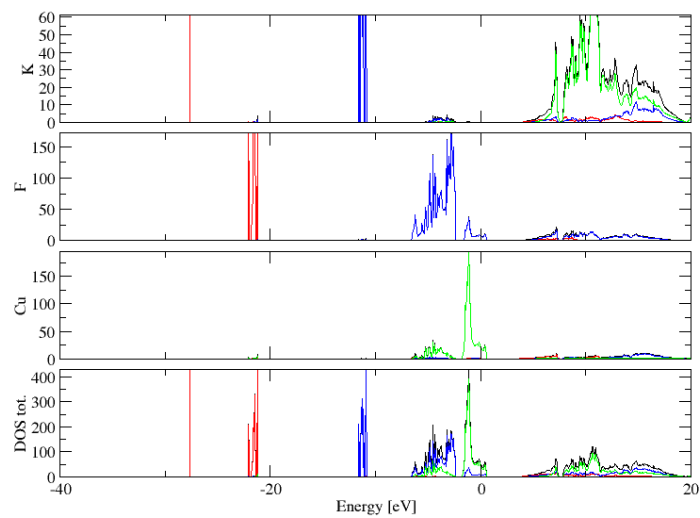
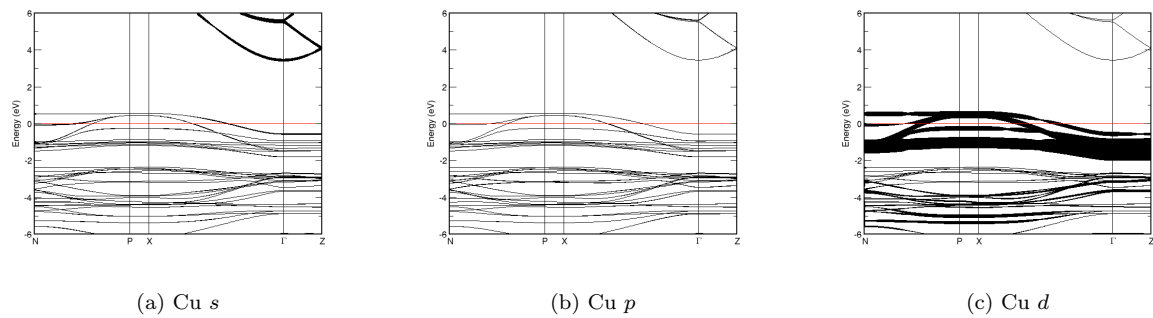
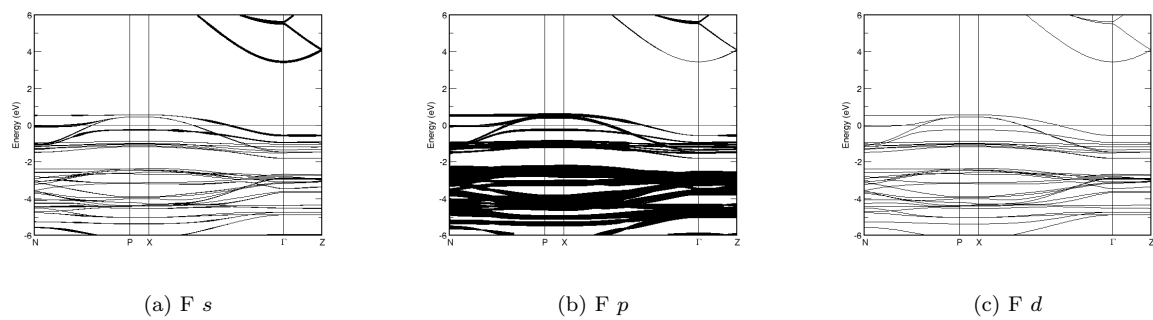
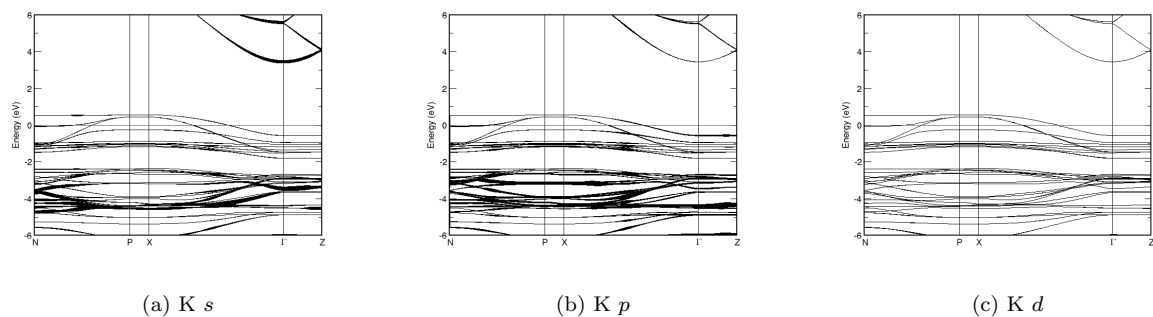


FIG. 462: Fat band representation of Sr in $\text{Sr}_3(\text{V}_2\text{O}_7)$

FIG. 463: Fat band representation of V in $\text{Sr}_3(\text{V}_2\text{O}_7)$ FIG. 464: (Color online) PDOS of $\text{K}_3\text{Co}_2\text{F}_7$ (ICSD #33524). The s -, p - and d -projected states are in red, blue and green, respectively. $\text{K}_3\text{Co}_2\text{F}_7$ crystallizes in space group $I 4/m m m$ (#139), in a tetragonal body-centred structure.FIG. 465: Fat band representation of Co in $\text{K}_3\text{Co}_2\text{F}_7$

FIG. 466: Fat band representation of F in $K_3Co_2F_7$ FIG. 467: Fat band representation of K in $K_3Co_2F_7$ FIG. 468: (Color online) PDOS of $K_3Cu_2F_7$ (ICSD #15373). The *s*-, *p*- and *d*-projected states are in red, blue and green, respectively. $K_3Cu_2F_7$ crystallizes in space group $I 4/m m m$ (#139), in a tetragonal body-centred structure.

FIG. 469: Fat band representation of Cu in $K_3Cu_2F_7$ FIG. 470: Fat band representation of F in $K_3Cu_2F_7$ FIG. 471: Fat band representation of K in $K_3Cu_2F_7$

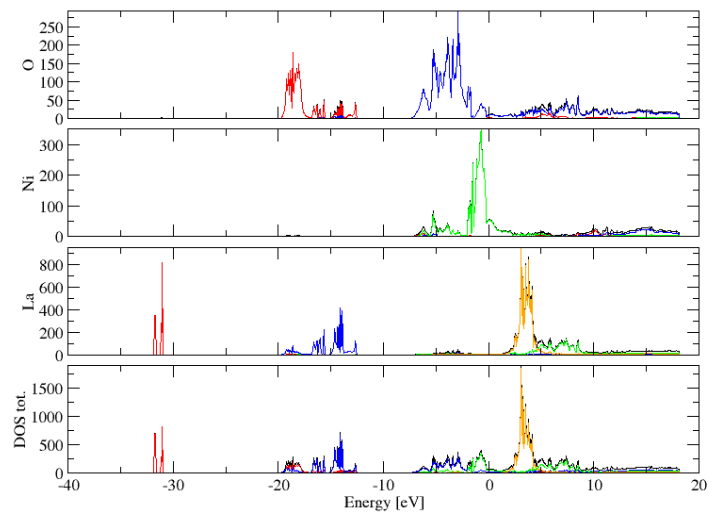


FIG. 472: (Color online) PDOS of $\text{La}_4\text{Ni}_3\text{O}_8$ (ICSD #173372). The s -, p - and d -projected states are in red, blue and green, respectively. $\text{La}_4\text{Ni}_3\text{O}_8$ crystallizes in space group I $4/m\ m\ m$ (#139), in a tetragonal body-centred structure.

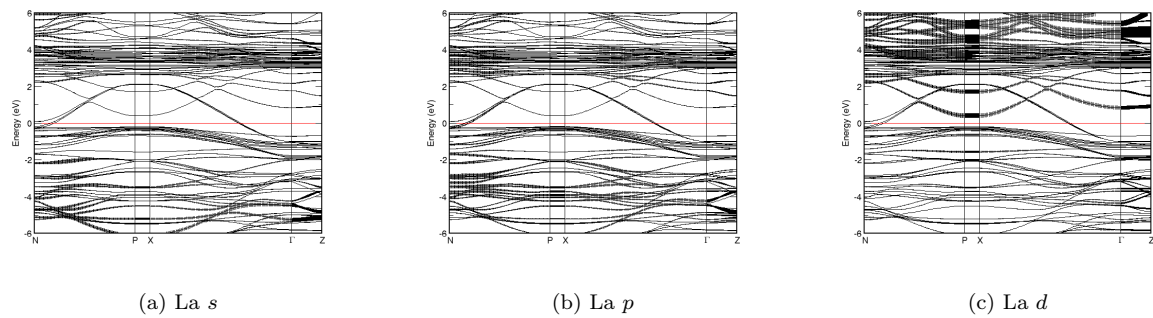


FIG. 473: Fat band representation of La in $\text{La}_4\text{Ni}_3\text{O}_8$

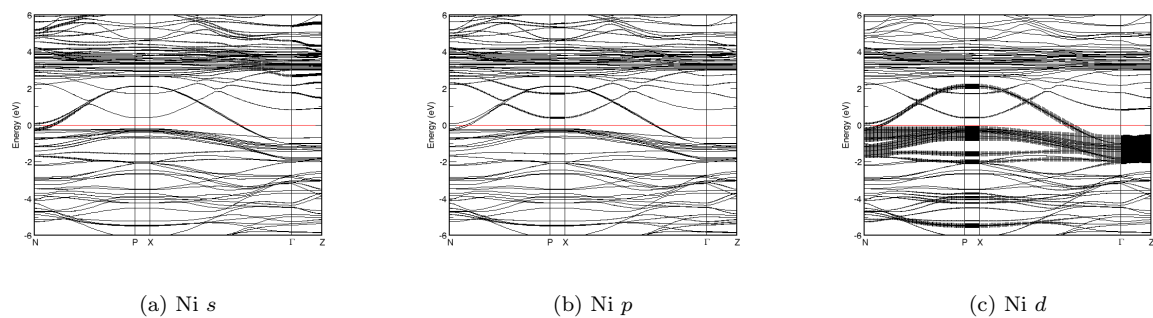
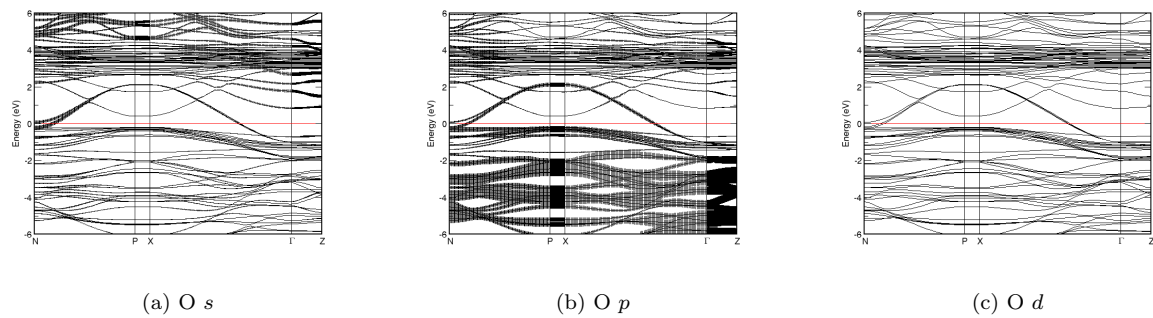
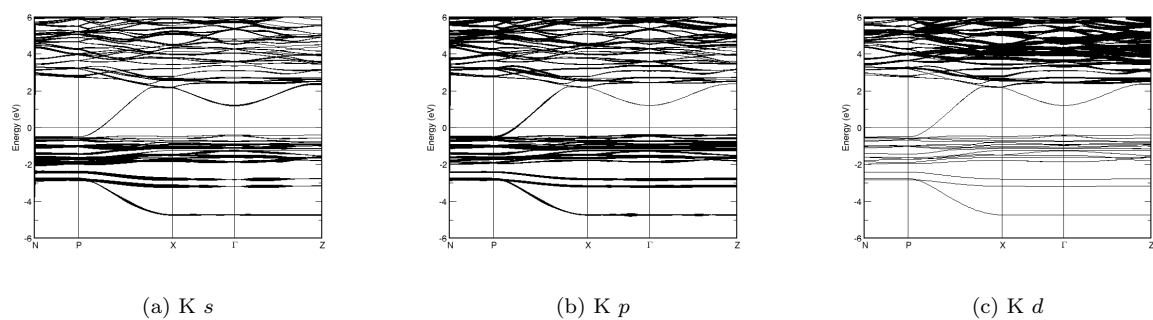
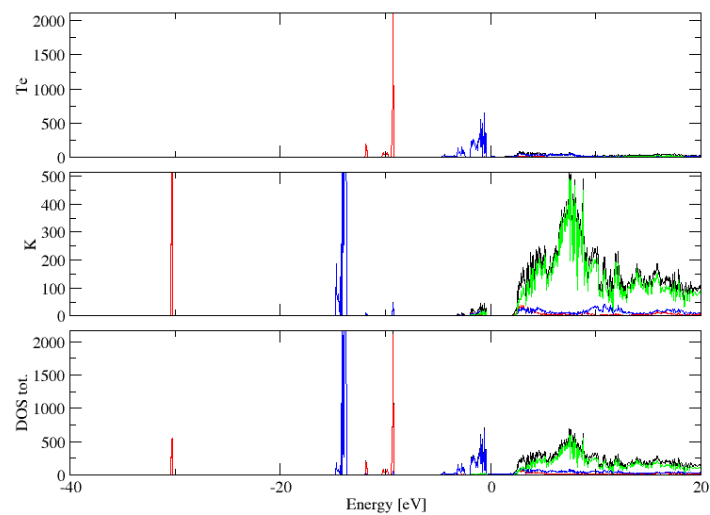
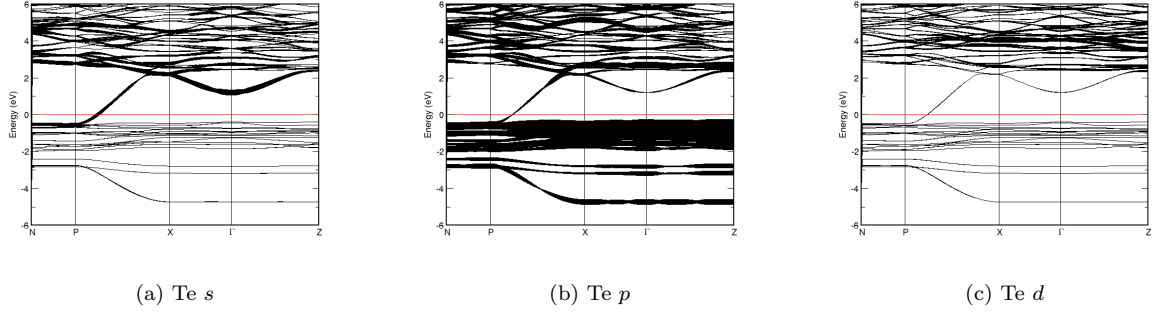
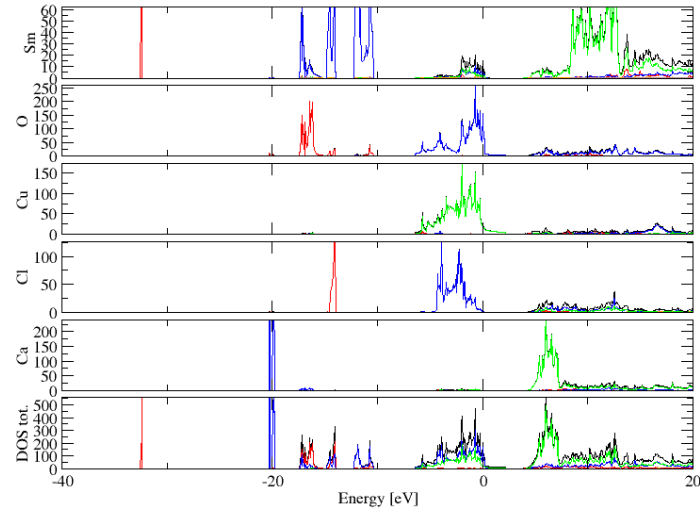
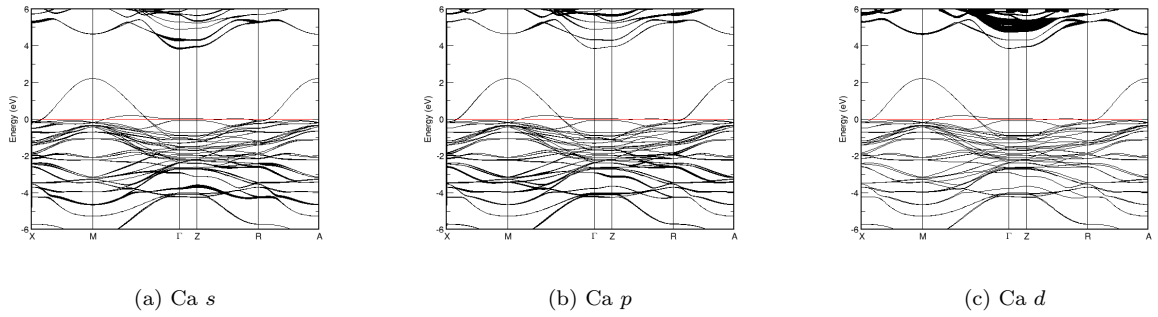
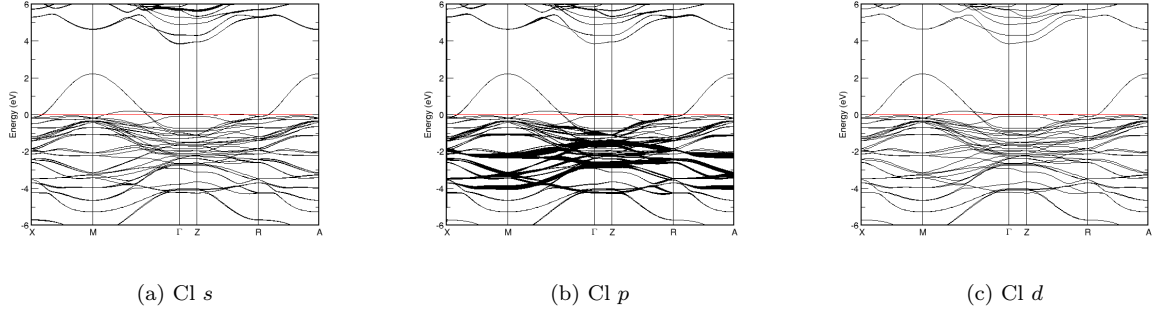
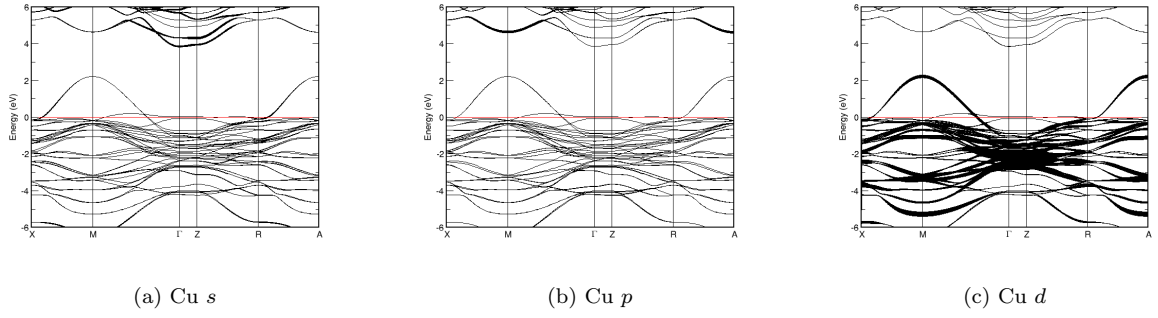
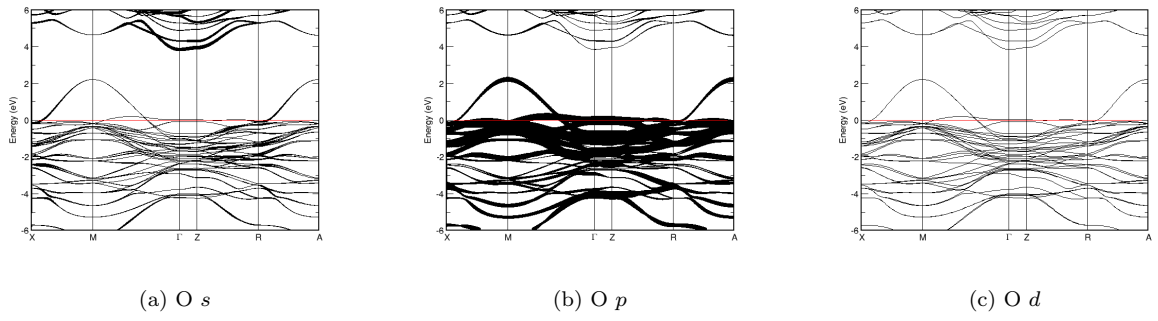
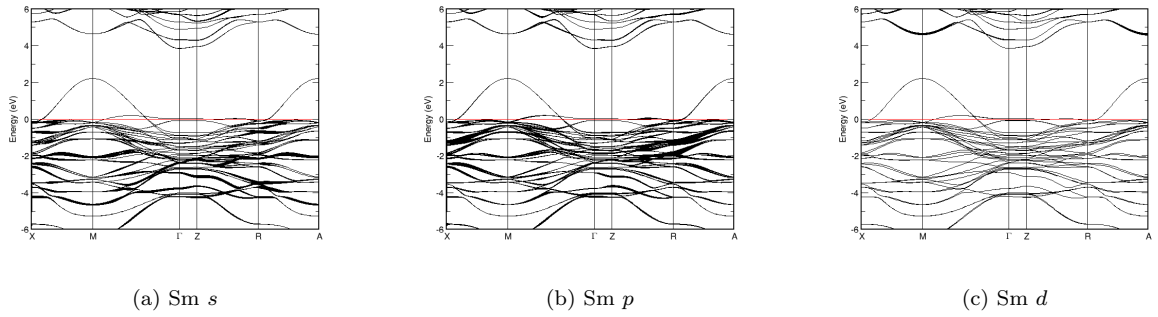


FIG. 474: Fat band representation of Ni in $\text{La}_4\text{Ni}_3\text{O}_8$

FIG. 475: Fat band representation of O in $\text{La}_4\text{Ni}_3\text{O}_8$ FIG. 477: Fat band representation of K in K_5Te_3

FIG. 478: Fat band representation of Te in K_5Te_3 FIG. 479: (Color online) PDOS of $CaSmCuO_3Cl$ (ICSD #86428). The *s*-, *p*- and *d*-projected states are in red, blue and green, respectively. $CaSmCuO_3Cl$ crystallizes in space group $P 4/n m m Z$ (#129), in a tetragonal primitive structure.FIG. 480: Fat band representation of Ca in $CaSmCuO_3Cl$

FIG. 481: Fat band representation of Cl in $\text{CaSmCuO}_3\text{Cl}$ FIG. 482: Fat band representation of Cu in $\text{CaSmCuO}_3\text{Cl}$ FIG. 483: Fat band representation of O in $\text{CaSmCuO}_3\text{Cl}$ FIG. 484: Fat band representation of Sm in $\text{CaSmCuO}_3\text{Cl}$

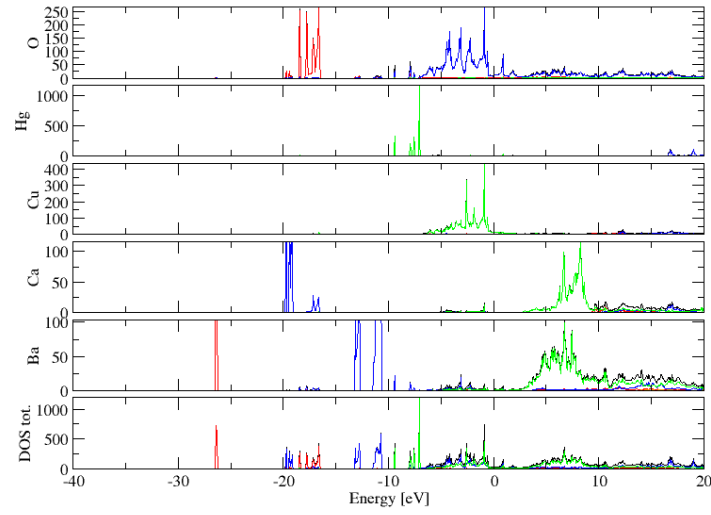


FIG. 485: (Color online) PDOS of $\text{HgBa}_2\text{CaCu}_2\text{O}_6$ (ICSD #75725). The s -, p - and d -projected states are in red, blue and green, respectively. $\text{HgBa}_2\text{CaCu}_2\text{O}_6$ crystallizes in space group $P 4/m m m$ (#123), in a tetragonal primitive structure.

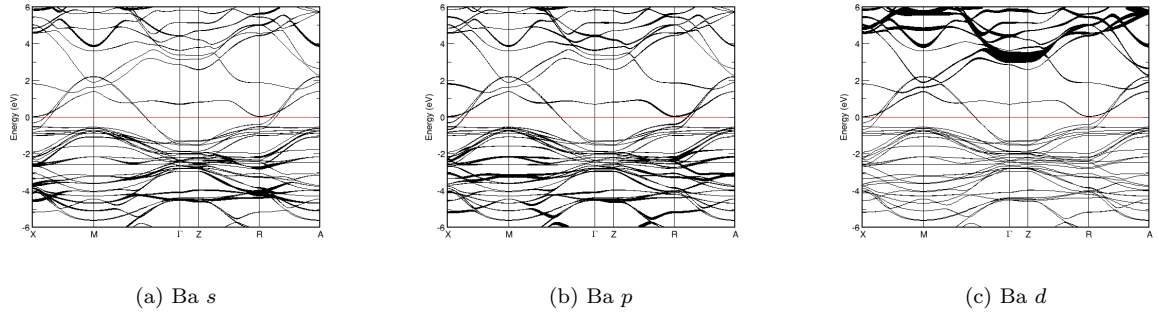


FIG. 486: Fat band representation of Ba in $\text{HgBa}_2\text{CaCu}_2\text{O}_6$

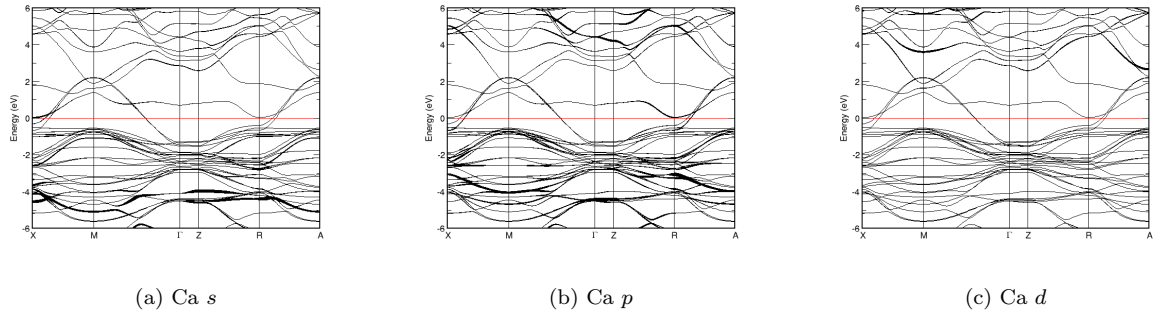
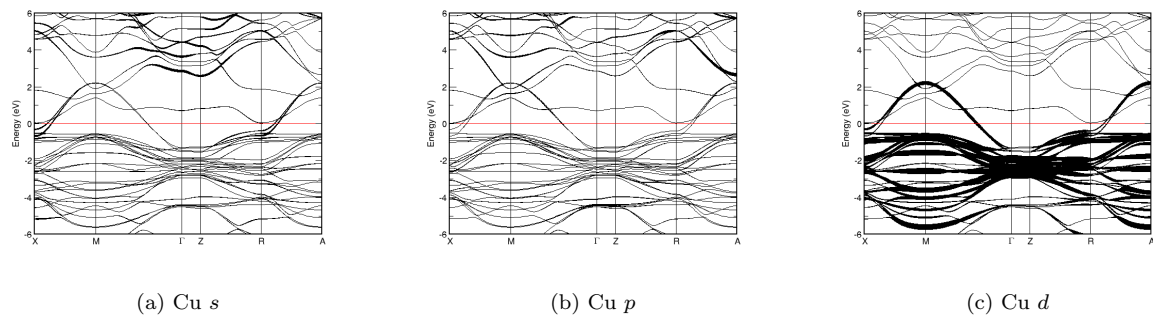
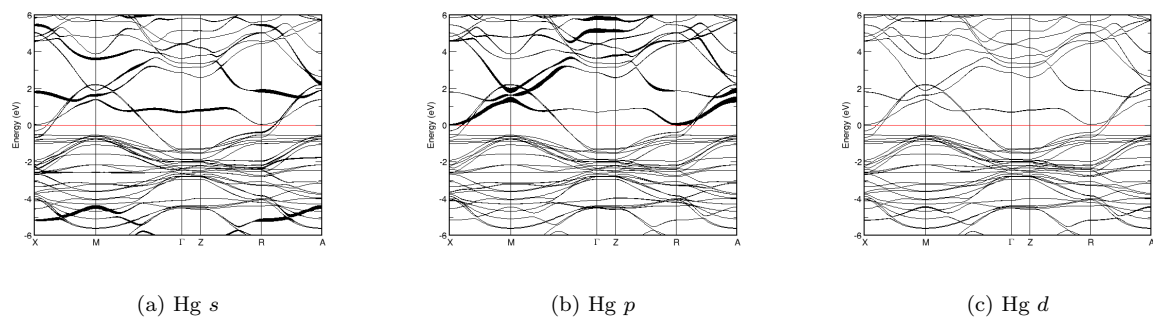
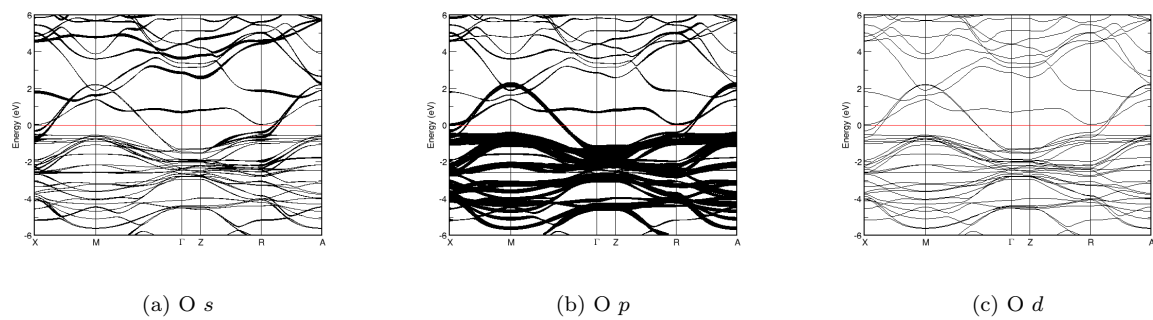


FIG. 487: Fat band representation of Ca in $\text{HgBa}_2\text{CaCu}_2\text{O}_6$

FIG. 488: Fat band representation of Cu in $\text{HgBa}_2\text{CaCu}_2\text{O}_6$ FIG. 489: Fat band representation of Hg in $\text{HgBa}_2\text{CaCu}_2\text{O}_6$ FIG. 490: Fat band representation of O in $\text{HgBa}_2\text{CaCu}_2\text{O}_6$

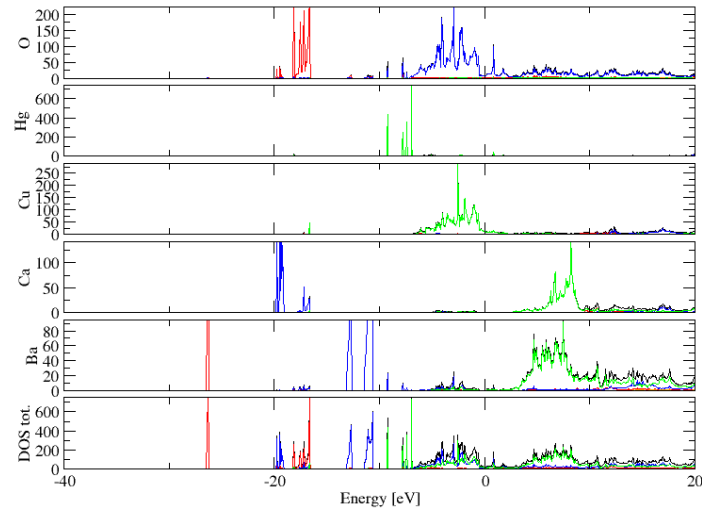


FIG. 491: (Color online) PDOS of $\text{HgBa}_2\text{CaCu}_2\text{O}_6$ (ICSD #83087). The s -, p - and d -projected states are in red, blue and green, respectively. $\text{HgBa}_2\text{CaCu}_2\text{O}_6$ crystallizes in space group $P 4/m m m$ (#123), in a tetragonal primitive structure.

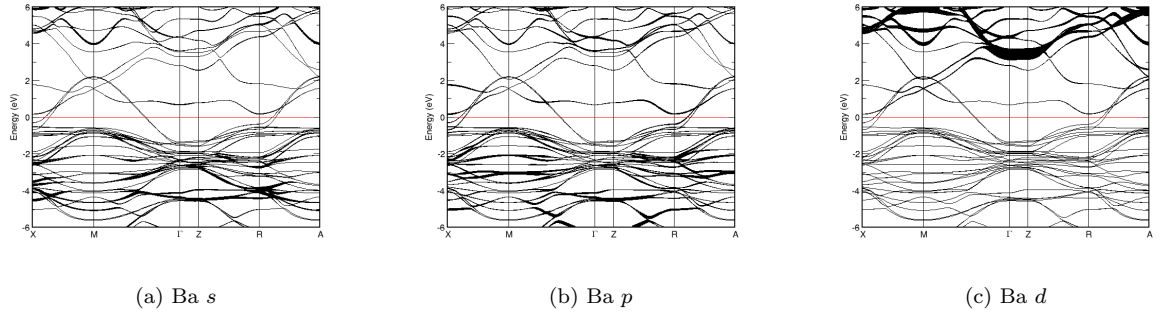


FIG. 492: Fat band representation of Ba in $\text{HgBa}_2\text{CaCu}_2\text{O}_6$

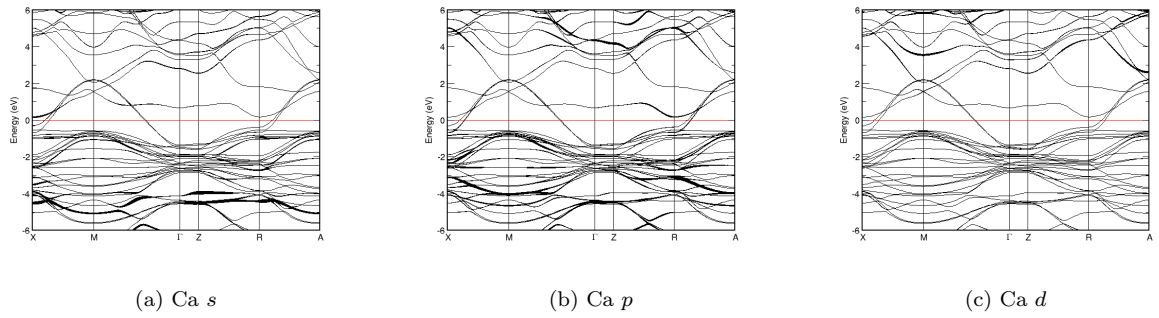
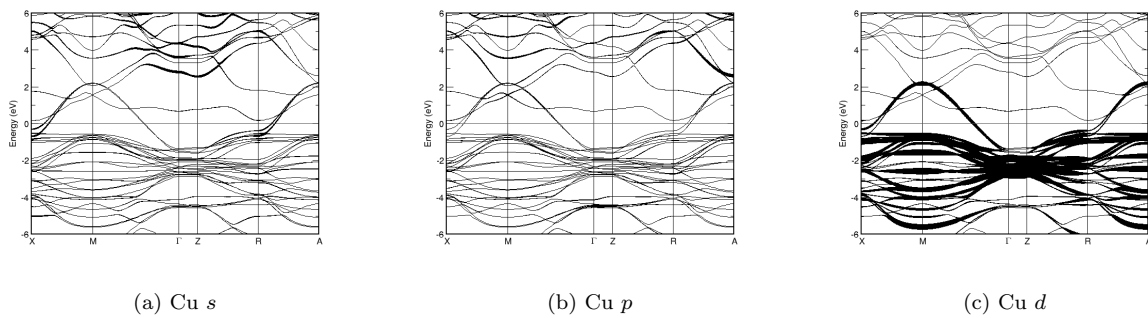
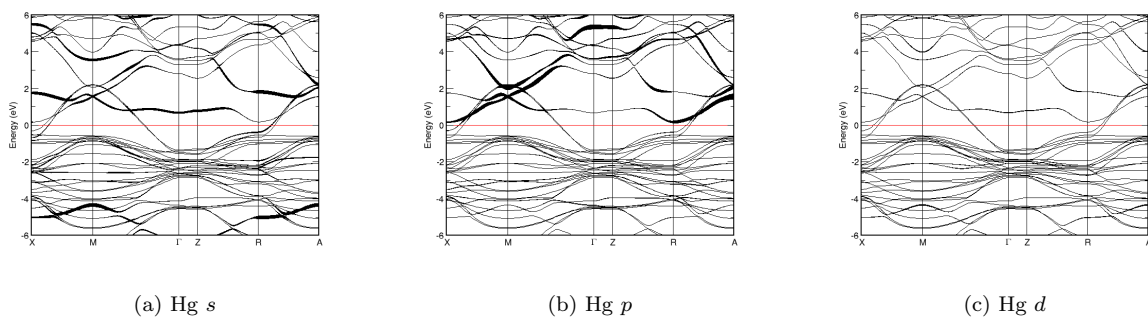
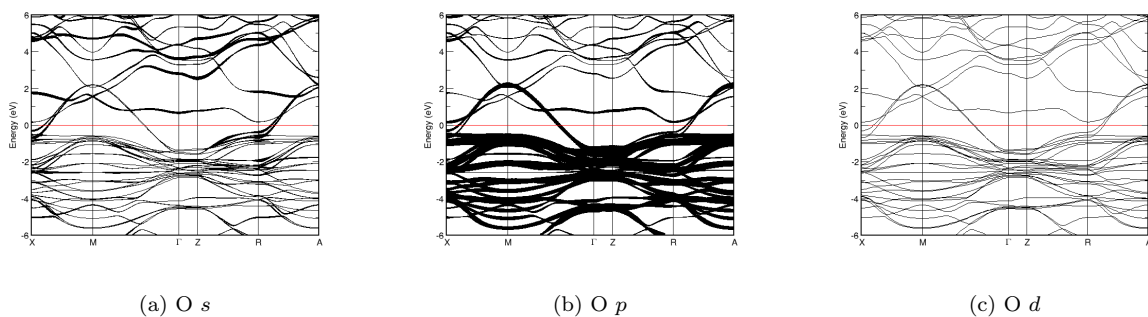


FIG. 493: Fat band representation of Ca in $\text{HgBa}_2\text{CaCu}_2\text{O}_6$

FIG. 494: Fat band representation of Cu in $\text{HgBa}_2\text{CaCu}_2\text{O}_6$ FIG. 495: Fat band representation of Hg in $\text{HgBa}_2\text{CaCu}_2\text{O}_6$ FIG. 496: Fat band representation of O in $\text{HgBa}_2\text{CaCu}_2\text{O}_6$

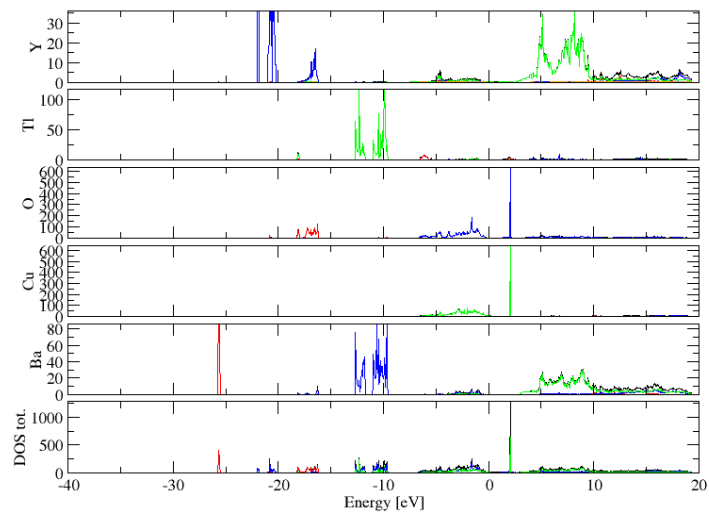
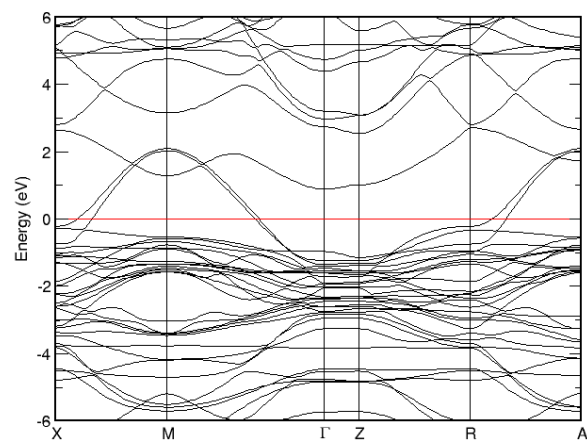


FIG. 497: (Color online) PDOS of $\text{TiYBa}_2\text{Cu}_2\text{O}_7$ (ICSD #74163). The s -, p - and d -projected states are in red, blue and green, respectively. $\text{TiYBa}_2\text{Cu}_2\text{O}_7$ crystallizes in space group $P 4/m m m$ (#123), in a tetragonal primitive structure.



(a) E vs. k

FIG. 498: Band structure of $\text{TiYBa}_2\text{Cu}_2\text{O}_7$

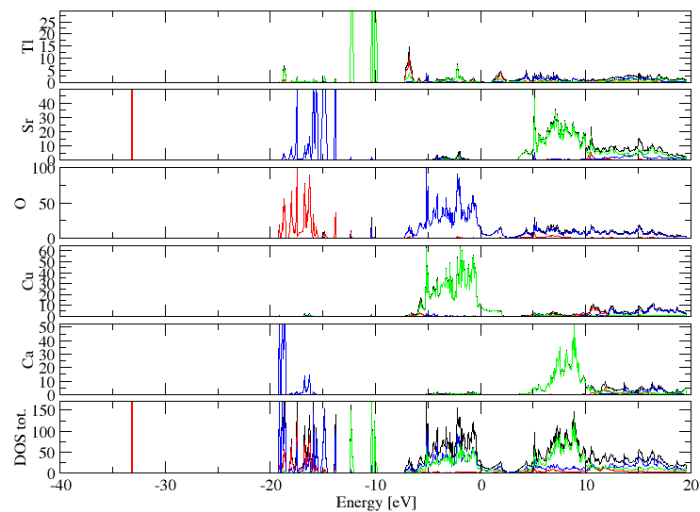


FIG. 499: (Color online) PDOS of $\text{TiCaSr}_2\text{Cu}_2\text{O}_7$ (ICSD #74165). The s -, p - and d -projected states are in red, blue and green, respectively. $\text{TiCaSr}_2\text{Cu}_2\text{O}_7$ crystallizes in space group $P 4/m m m$ (#123), in a tetragonal primitive structure.

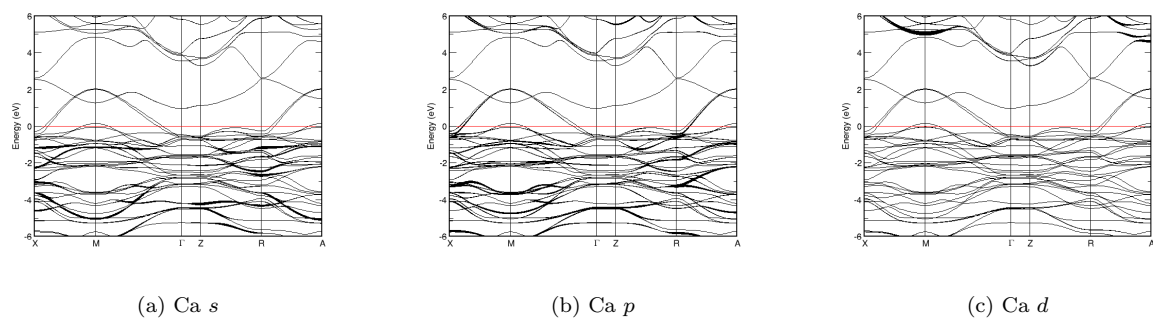


FIG. 500: Fat band representation of Ca in $\text{TiCaSr}_2\text{Cu}_2\text{O}_7$

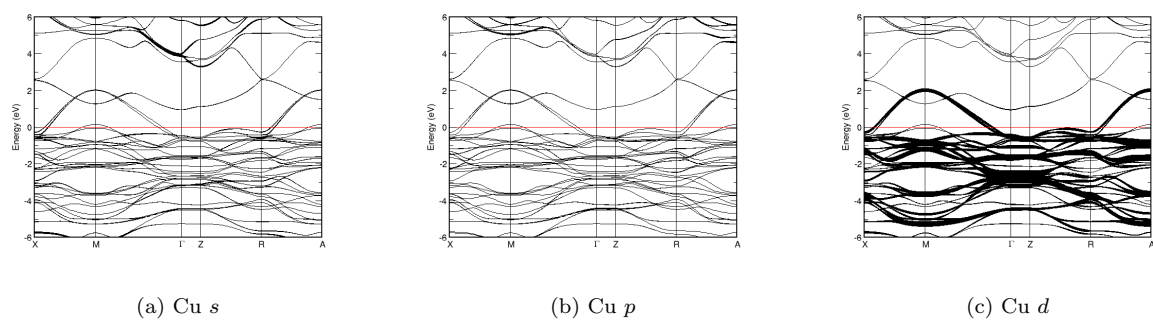
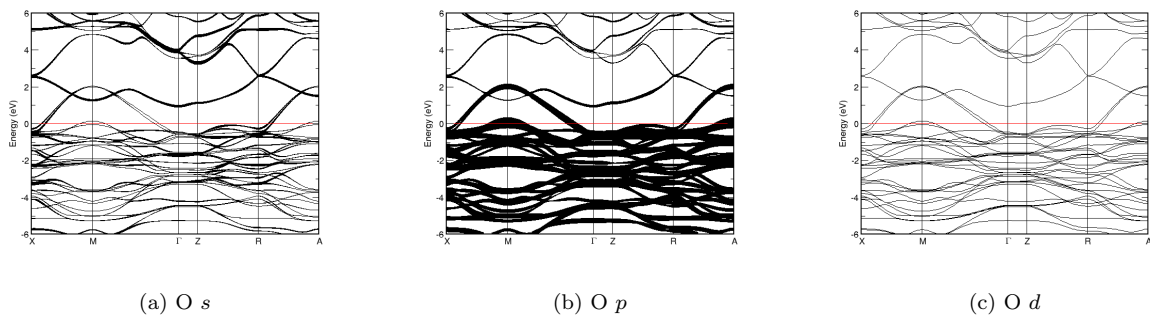
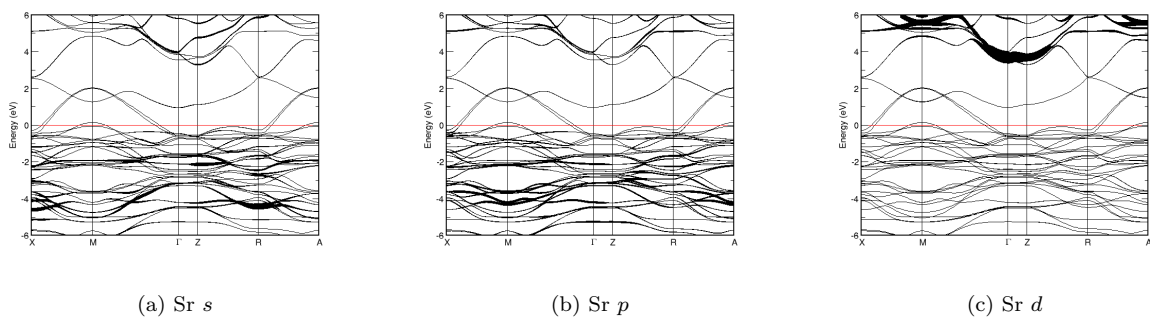
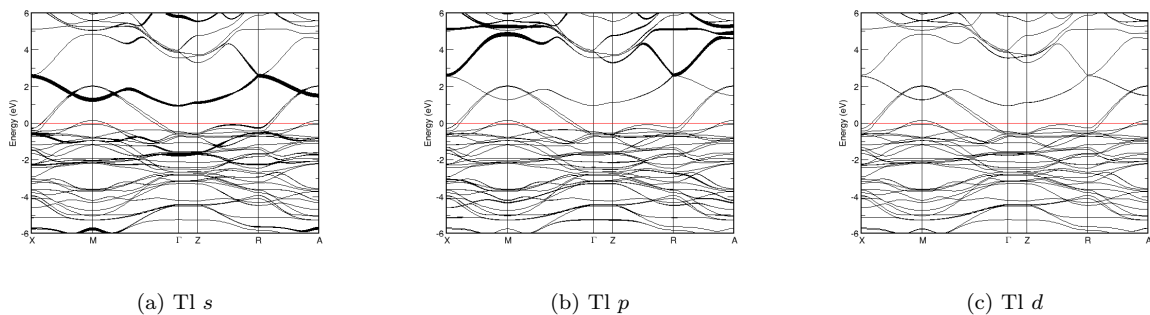


FIG. 501: Fat band representation of Cu in $\text{TiCaSr}_2\text{Cu}_2\text{O}_7$

FIG. 502: Fat band representation of O in $\text{TlCaSr}_2\text{Cu}_2\text{O}_7$ FIG. 503: Fat band representation of Sr in $\text{TlCaSr}_2\text{Cu}_2\text{O}_7$ FIG. 504: Fat band representation of Tl in $\text{TlCaSr}_2\text{Cu}_2\text{O}_7$

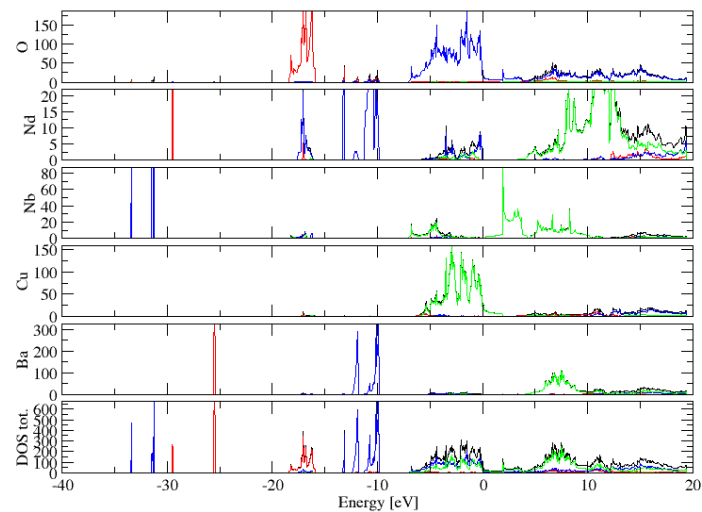


FIG. 505: (Color online) PDOS of $\text{NdBa}_2\text{Cu}_2\text{NbO}_8$ (ICSD #44255). The s -, p - and d -projected states are in red, blue and green, respectively. $\text{NdBa}_2\text{Cu}_2\text{NbO}_8$ crystallizes in space group $P 4/m m m$ (#123), in a tetragonal primitive structure.

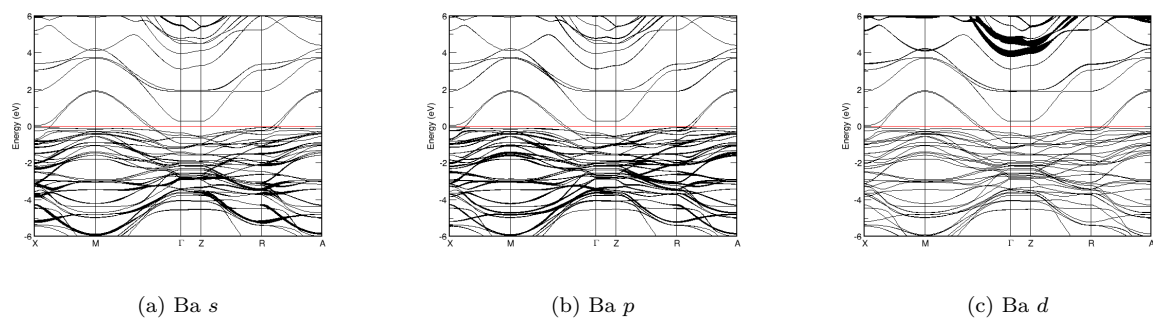


FIG. 506: Fat band representation of Ba in $\text{NdBa}_2\text{Cu}_2\text{NbO}_8$

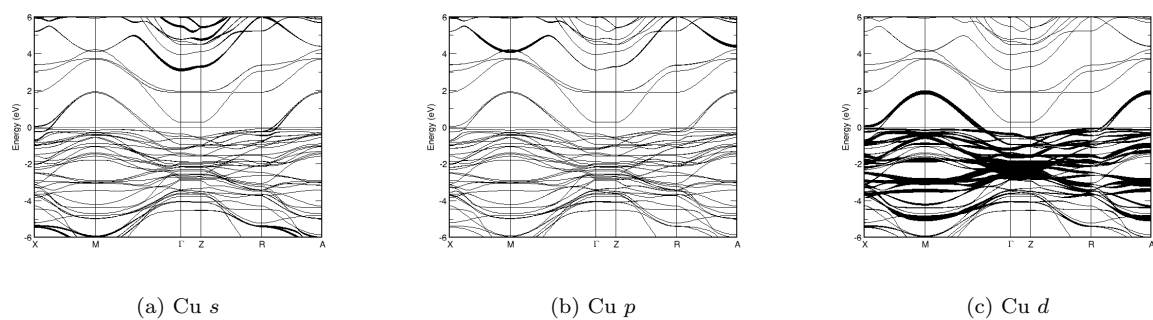
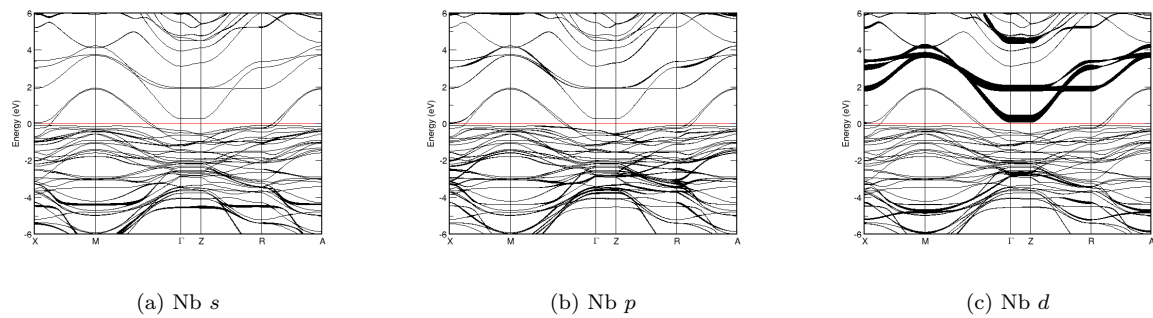
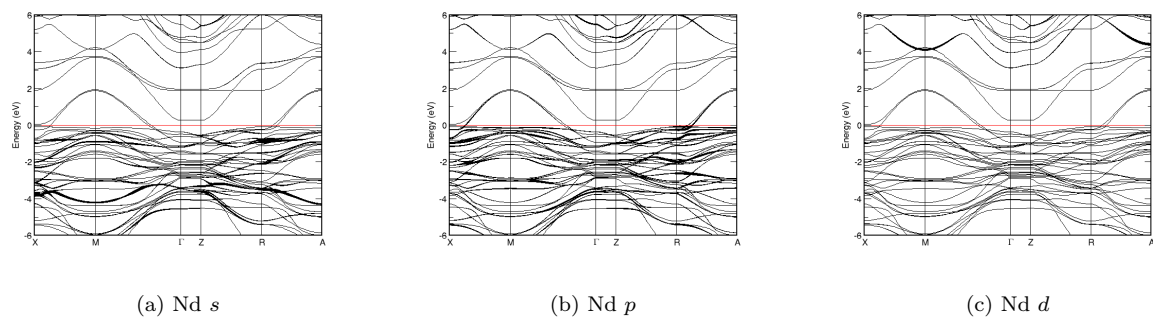
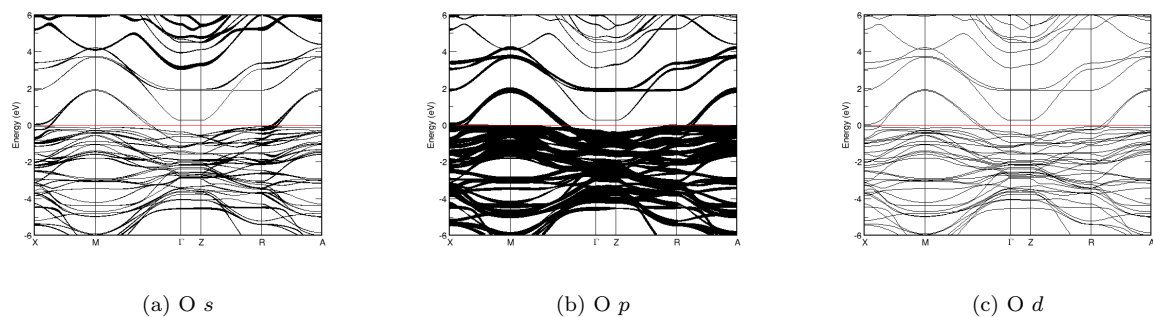


FIG. 507: Fat band representation of Cu in $\text{NdBa}_2\text{Cu}_2\text{NbO}_8$

FIG. 508: Fat band representation of Nb in $\text{NdBa}_2\text{Cu}_2\text{NbO}_8$ FIG. 509: Fat band representation of Nd in $\text{NdBa}_2\text{Cu}_2\text{NbO}_8$ FIG. 510: Fat band representation of O in $\text{NdBa}_2\text{Cu}_2\text{NbO}_8$

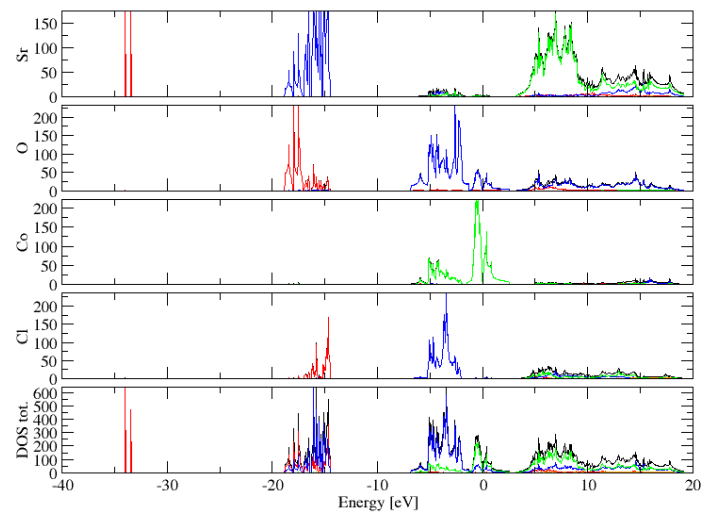


FIG. 511: (Color online) PDOS of $\text{Sr}_2\text{CoO}_3\text{Cl}$ (ICSD #91750). The s -, p - and d -projected states are in red, blue and green, respectively. $\text{Sr}_2\text{CoO}_3\text{Cl}$ crystallizes in space group $P 4/n m m Z$ (#129), in a tetragonal primitive structure.

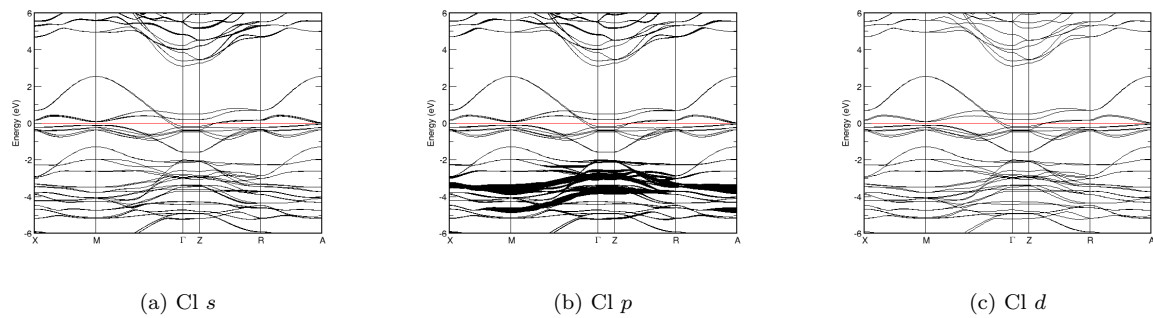


FIG. 512: Fat band representation of Cl in $\text{Sr}_2\text{CoO}_3\text{Cl}$

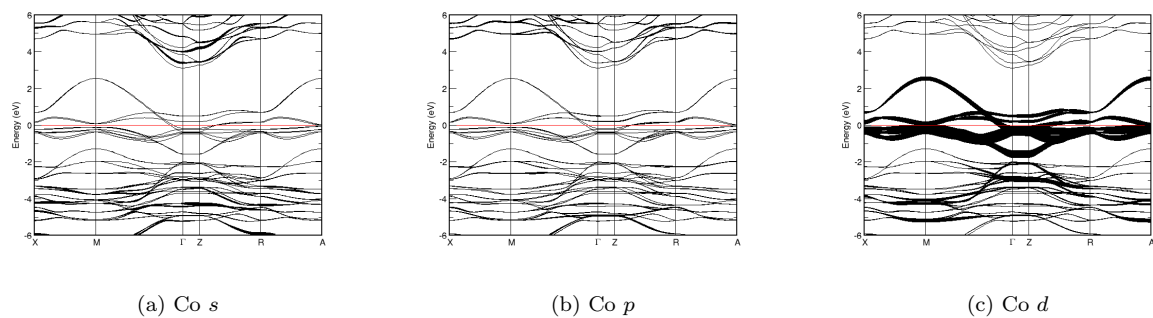


FIG. 513: Fat band representation of Co in $\text{Sr}_2\text{CoO}_3\text{Cl}$

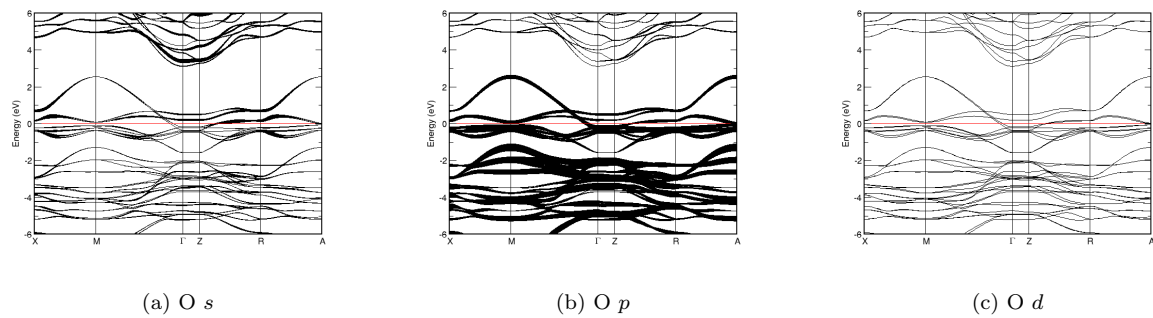
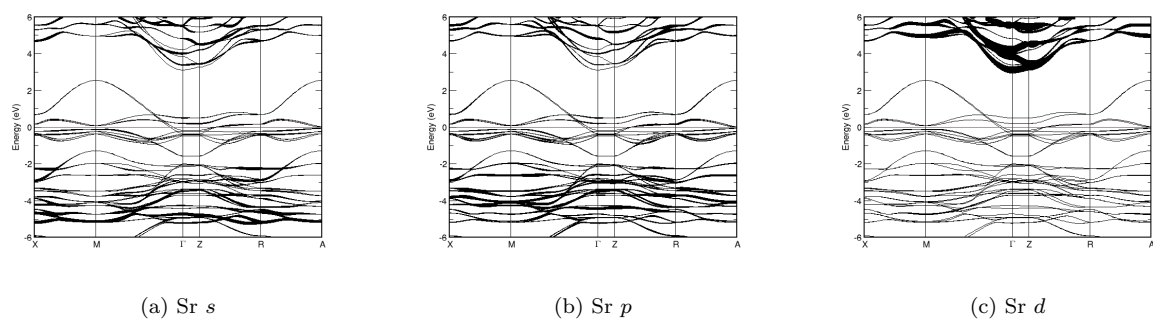
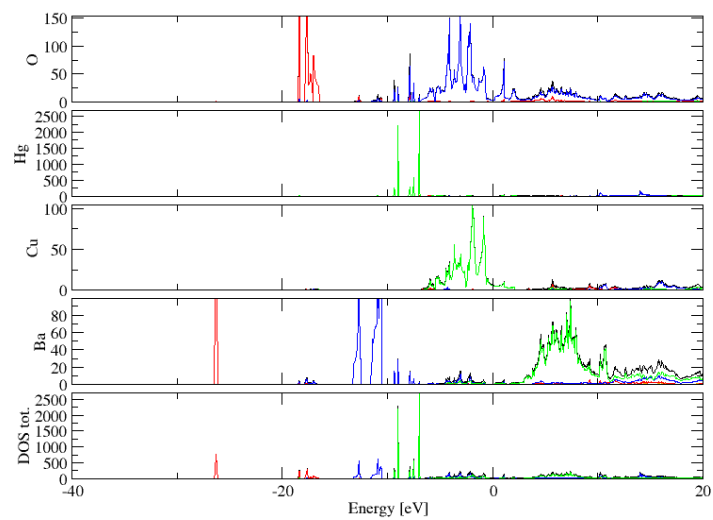
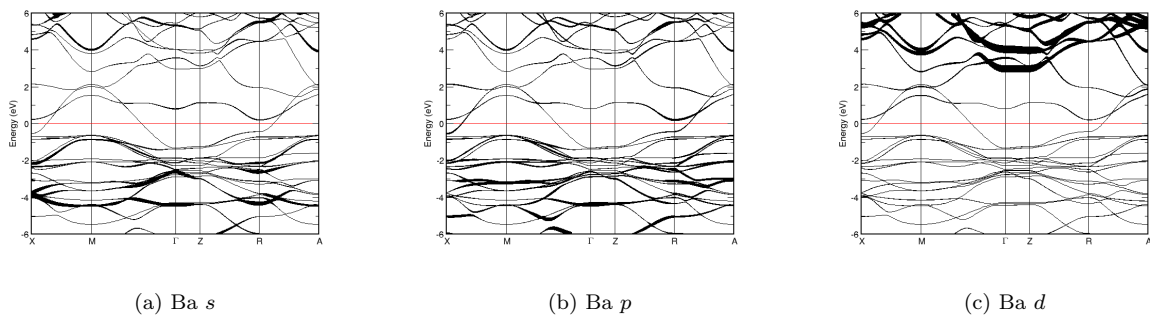
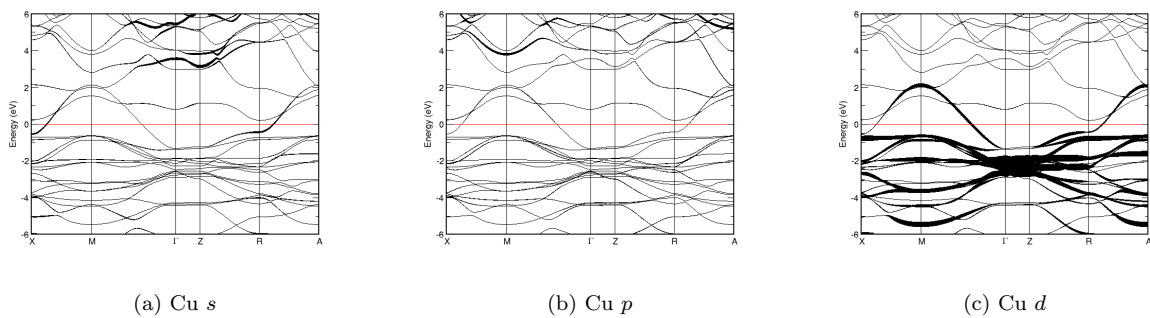
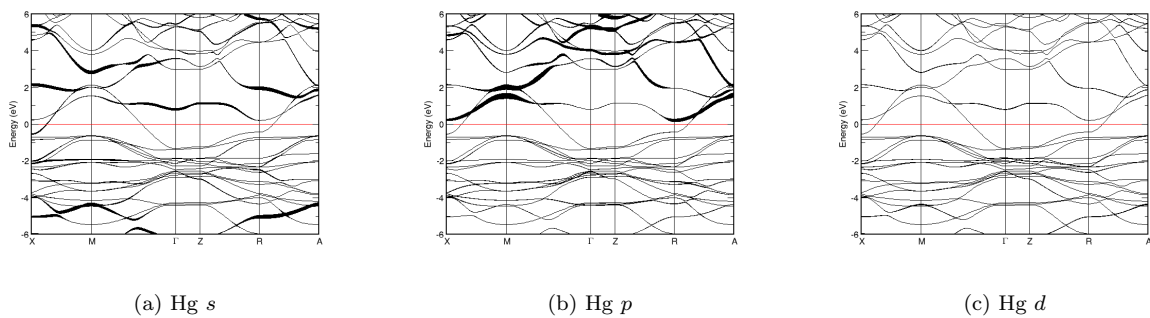
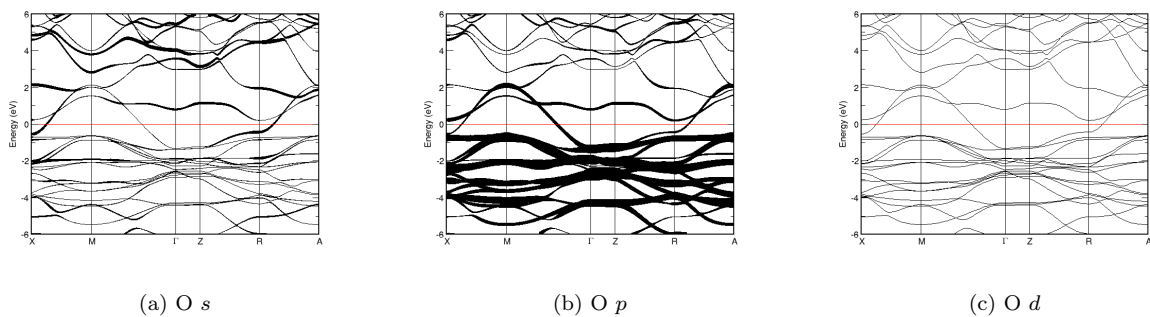
FIG. 514: Fat band representation of O in $\text{Sr}_2\text{CoO}_3\text{Cl}$ FIG. 515: Fat band representation of Sr in $\text{Sr}_2\text{CoO}_3\text{Cl}$ 

FIG. 516: (Color online) PDOS of $\text{HgBa}_2\text{CuO}_4$ (ICSD #75720). The *s*-, *p*- and *d*-projected states are in red, blue and green, respectively. $\text{HgBa}_2\text{CuO}_4$ crystallizes in space group $P 4/m m m$ (#123), in a tetragonal primitive structure.

FIG. 517: Fat band representation of Ba in $\text{HgBa}_2\text{CuO}_4$ FIG. 518: Fat band representation of Cu in $\text{HgBa}_2\text{CuO}_4$ FIG. 519: Fat band representation of Hg in $\text{HgBa}_2\text{CuO}_4$ FIG. 520: Fat band representation of O in $\text{HgBa}_2\text{CuO}_4$

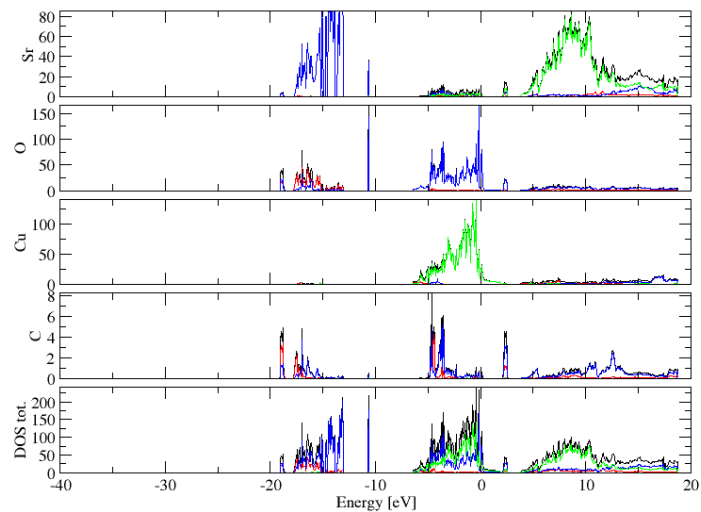
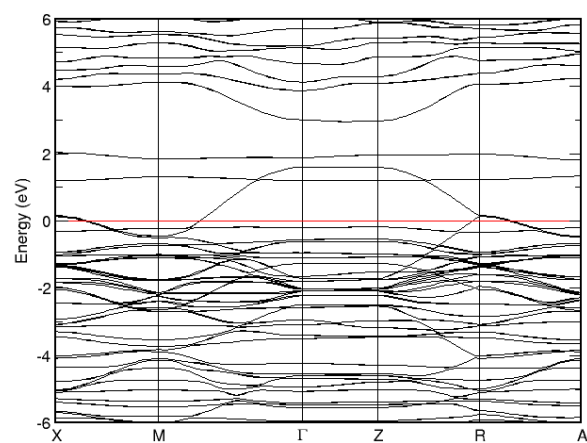


FIG. 521: (Color online) PDOS of $\text{Sr}_2\text{CuO}_2(\text{CO}_3)$ (ICSD #83096). The s -, p - and d -projected states are in red, blue and green, respectively. $\text{Sr}_2\text{CuO}_2(\text{CO}_3)$ crystallizes in space group $P 4 21 2$ (#90), in a tetragonal primitive structure.



(a) E vs. k

FIG. 522: Band structure of $\text{Sr}_2\text{CuO}_2(\text{CO}_3)$

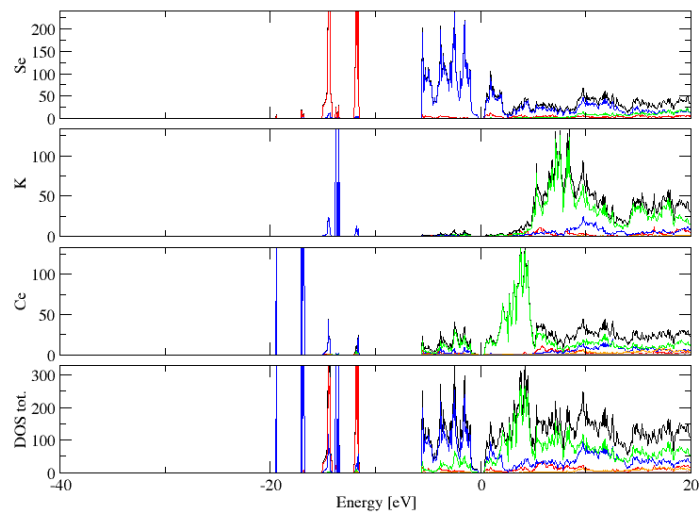


FIG. 523: (Color online) PDOS of KCeSe_4 (ICSD #67656). The s -, p - and d -projected states are in red, blue and green, respectively. KCeSe_4 crystallizes in space group $P 4/n b m Z$ (#125), in a tetragonal primitive structure.

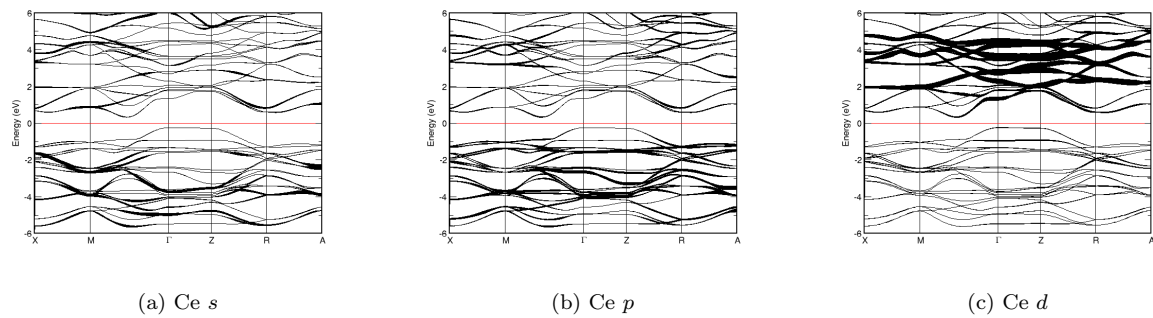


FIG. 524: Fat band representation of Ce in KCeSe_4

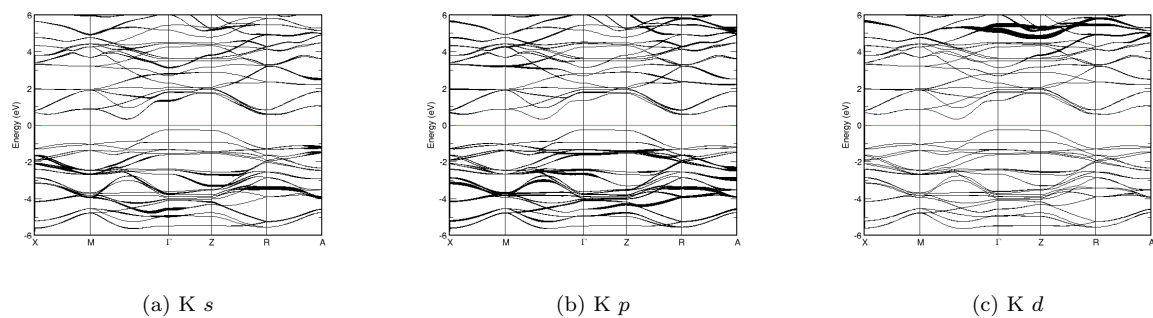
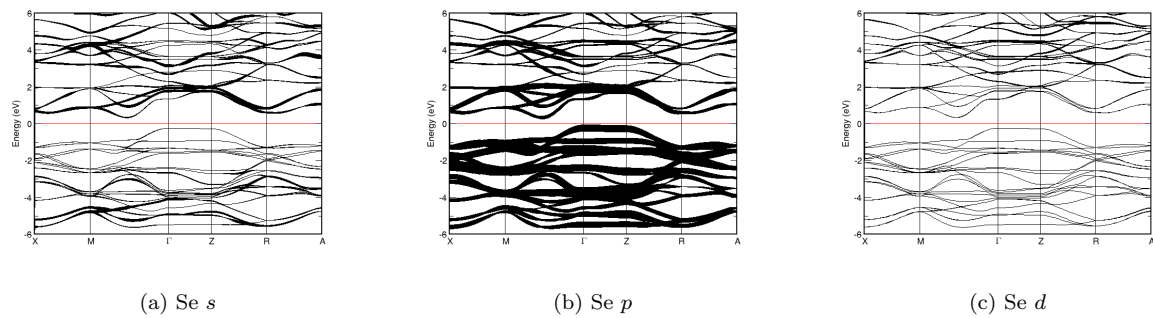
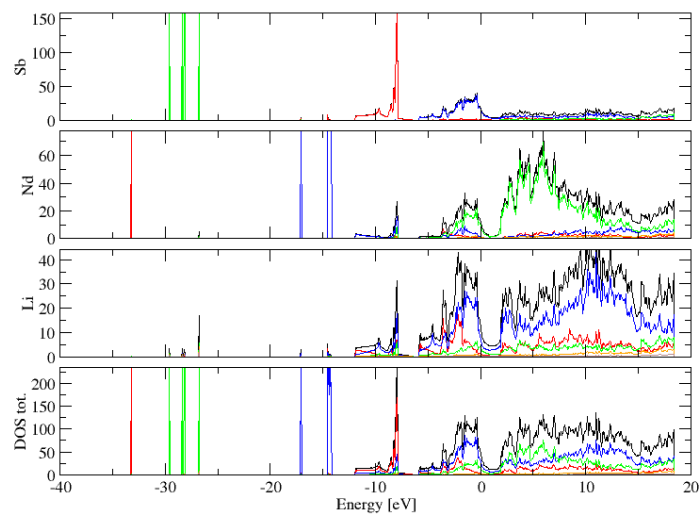
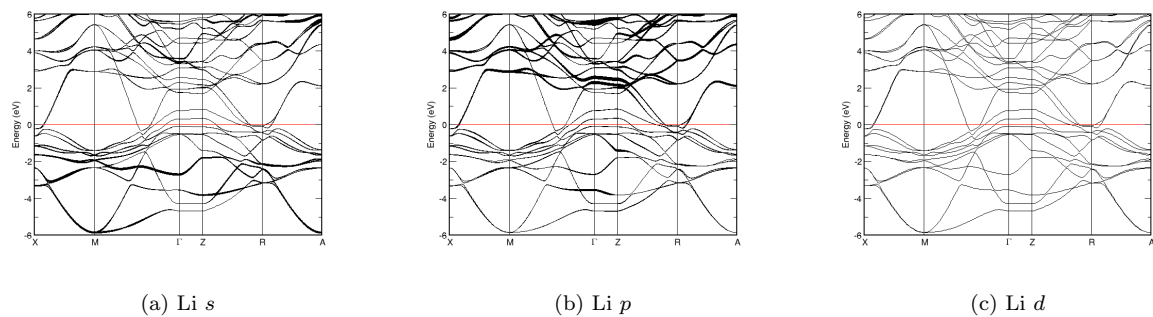


FIG. 525: Fat band representation of K in KCeSe_4

FIG. 526: Fat band representation of Se in KCeSe_4 FIG. 527: (Color online) PDOS of NdLi_2Sb_2 (ICSD #36020). The s -, p - and d -projected states are in red, blue and green, respectively. NdLi_2Sb_2 crystallizes in space group $P 4/n m m Z$ (#129), in a tetragonal primitive structure.FIG. 528: Fat band representation of Li in NdLi_2Sb_2

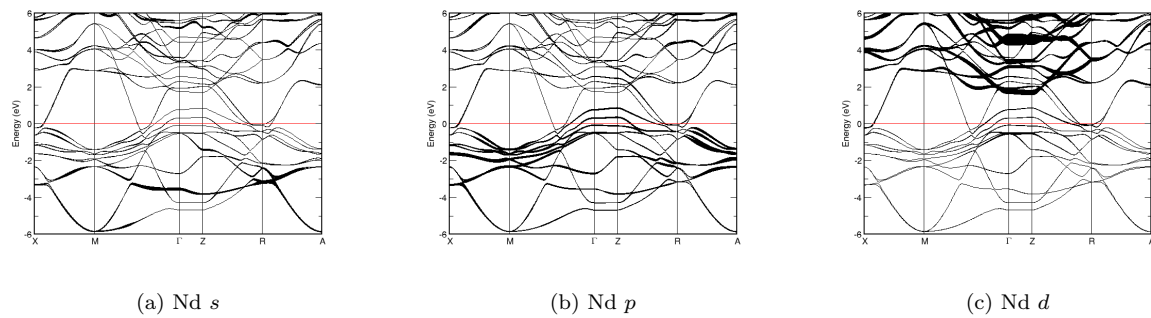
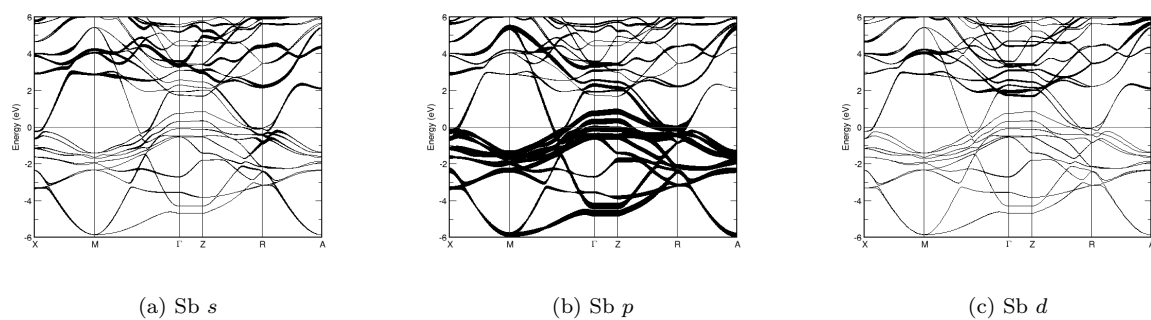
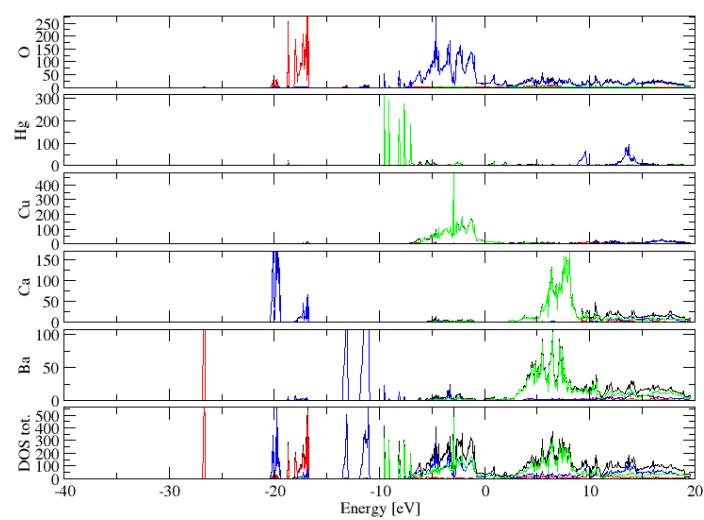
FIG. 529: Fat band representation of Nd in NdLi_2Sb_2 FIG. 530: Fat band representation of Sb in NdLi_2Sb_2 

FIG. 531: (Color online) PDOS of $\text{HgBa}_2\text{Ca}_2\text{Cu}_3\text{O}_8$ (ICSD #75730). The s -, p - and d -projected states are in red, blue and green, respectively. $\text{HgBa}_2\text{Ca}_2\text{Cu}_3\text{O}_8$ crystallizes in space group $P 4/m m m$ (#123), in a tetragonal primitive structure.

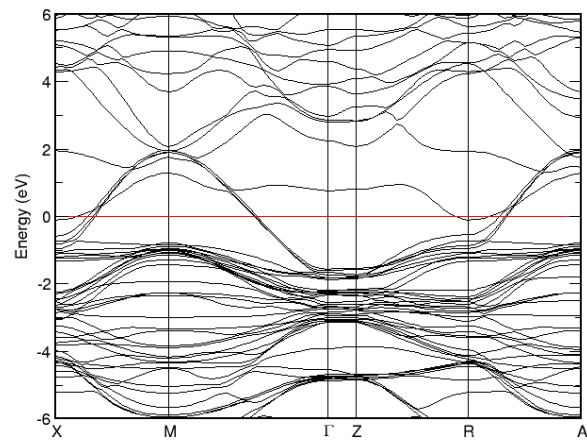
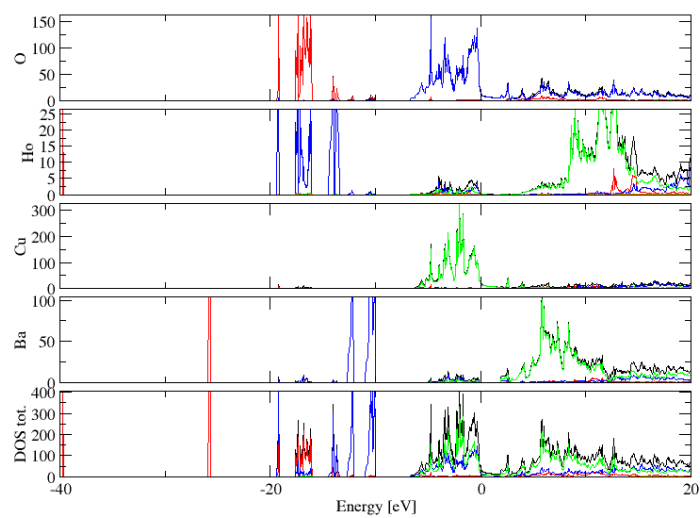
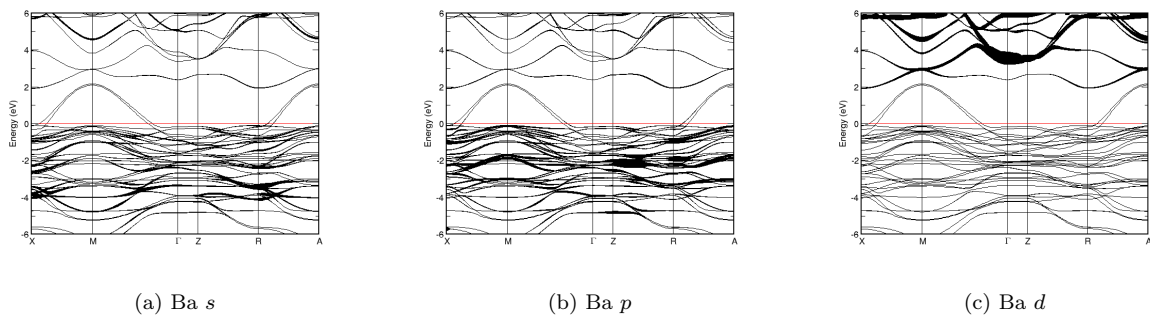
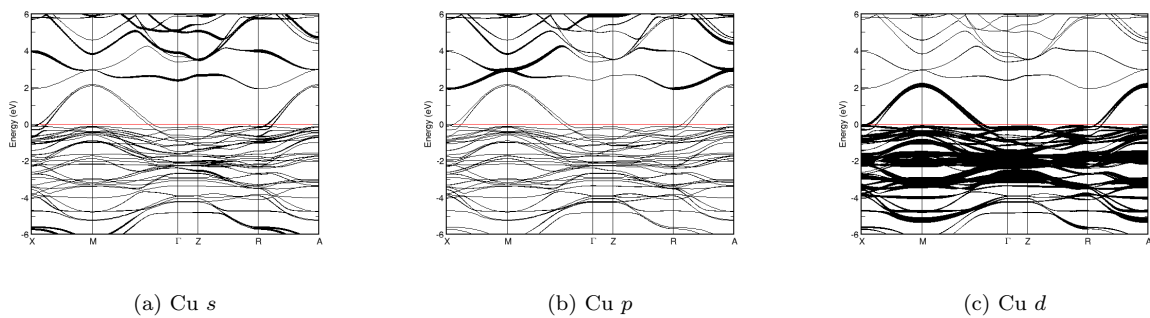
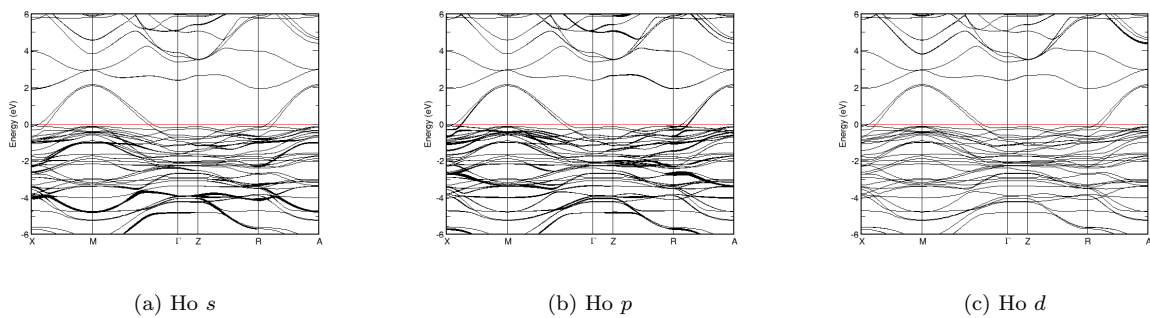
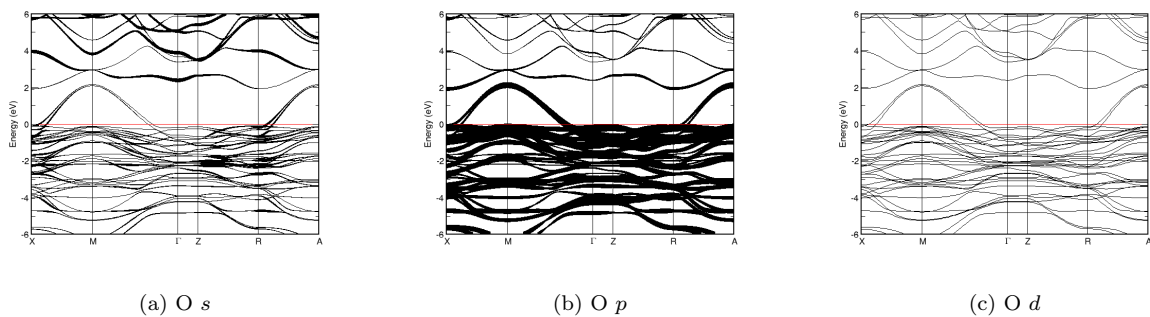
(a) E vs. k FIG. 532: Band structure of $\text{HgBa}_2\text{Ca}_2\text{Cu}_3\text{O}_8$ 

FIG. 533: (Color online) PDOS of $\text{HoBa}_2\text{Cu}_3\text{O}_6$ (ICSD #68047). The s -, p - and d -projected states are in red, blue and green, respectively. $\text{HoBa}_2\text{Cu}_3\text{O}_6$ crystallizes in space group $P 4/m m m$ (#123), in a tetragonal primitive structure.

FIG. 534: Fat band representation of Ba in $\text{HoBa}_2\text{Cu}_3\text{O}_6$ FIG. 535: Fat band representation of Cu in $\text{HoBa}_2\text{Cu}_3\text{O}_6$ FIG. 536: Fat band representation of Ho in $\text{HoBa}_2\text{Cu}_3\text{O}_6$ FIG. 537: Fat band representation of O in $\text{HoBa}_2\text{Cu}_3\text{O}_6$

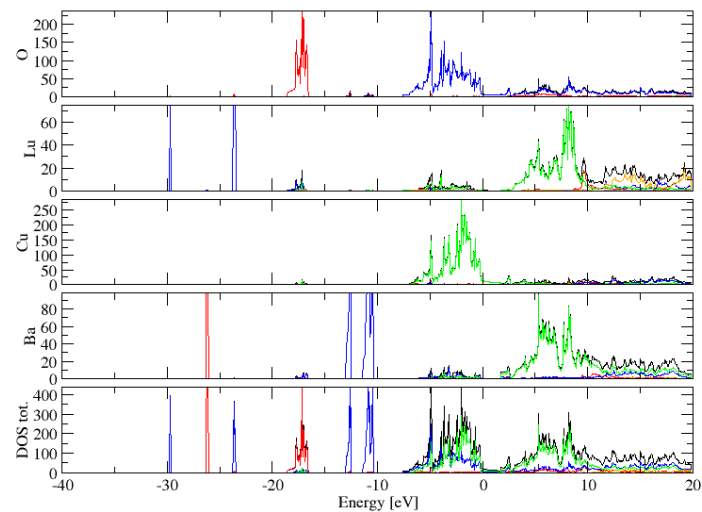


FIG. 538: (Color online) PDOS of $\text{LuBa}_2\text{Cu}_3\text{O}_6$ (ICSD #98113). The s -, p - and d -projected states are in red, blue and green, respectively. $\text{LuBa}_2\text{Cu}_3\text{O}_6$ crystallizes in space group $P 4/m m m$ (#123), in a tetragonal primitive structure.

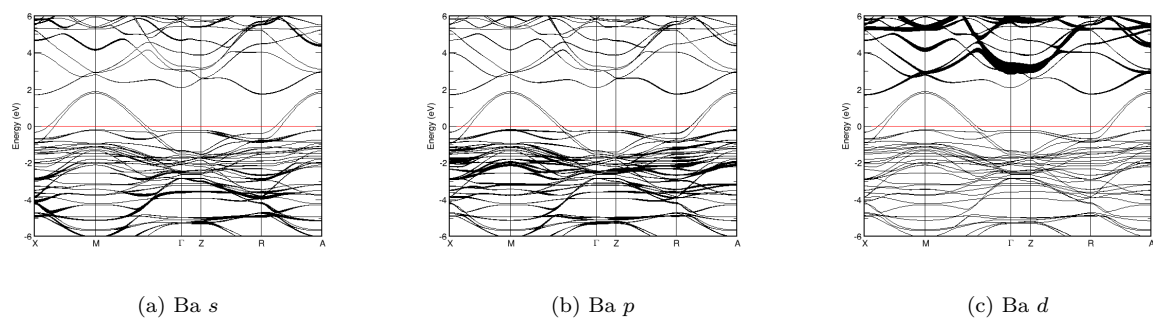


FIG. 539: Fat band representation of Ba in $\text{LuBa}_2\text{Cu}_3\text{O}_6$

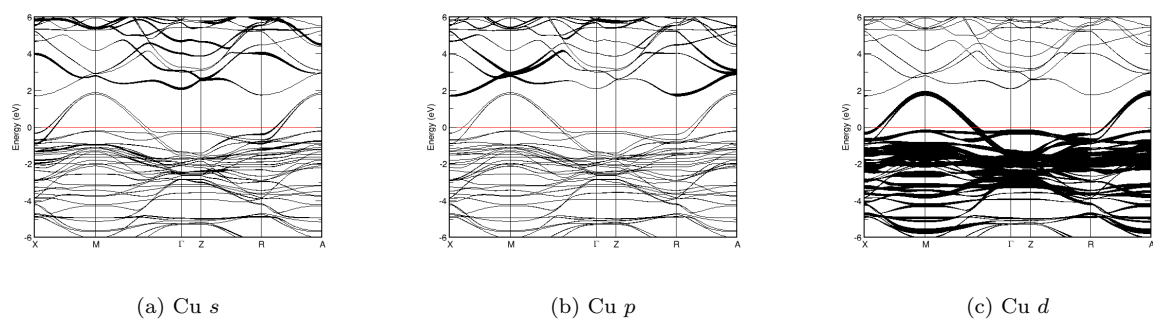


FIG. 540: Fat band representation of Cu in $\text{LuBa}_2\text{Cu}_3\text{O}_6$

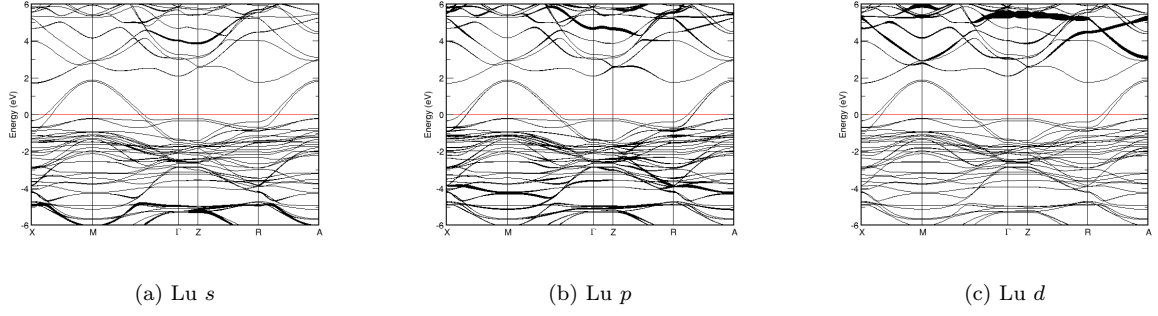
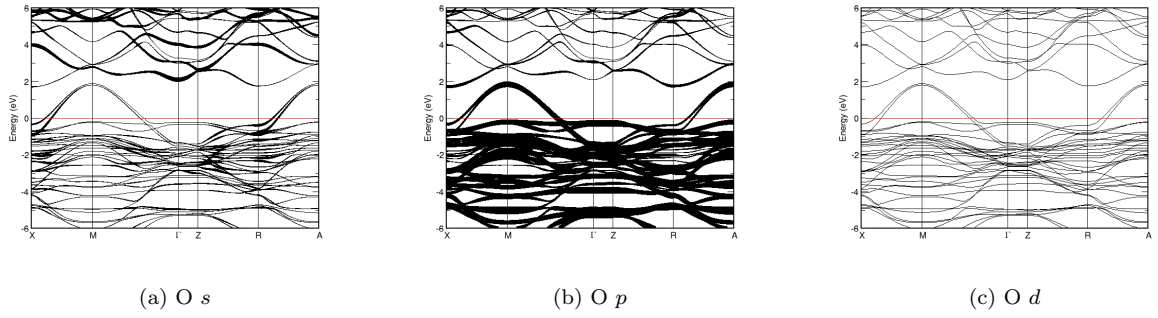
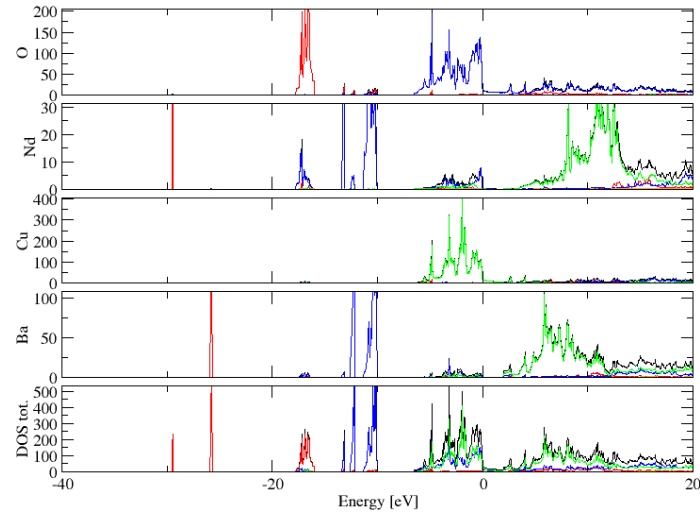
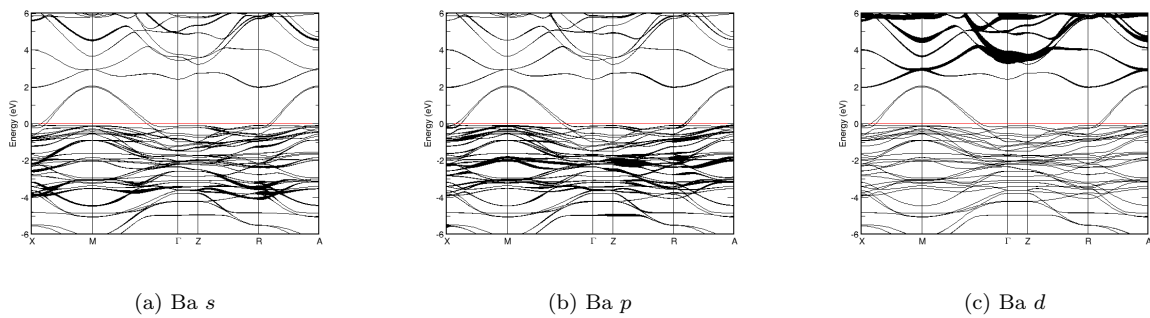
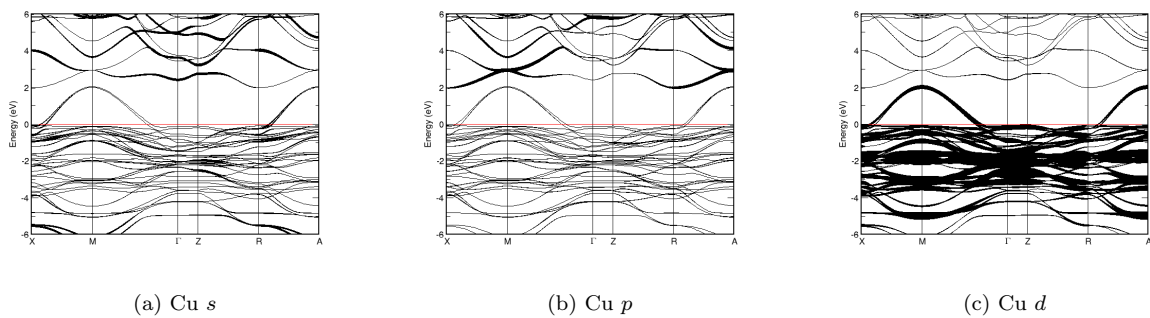
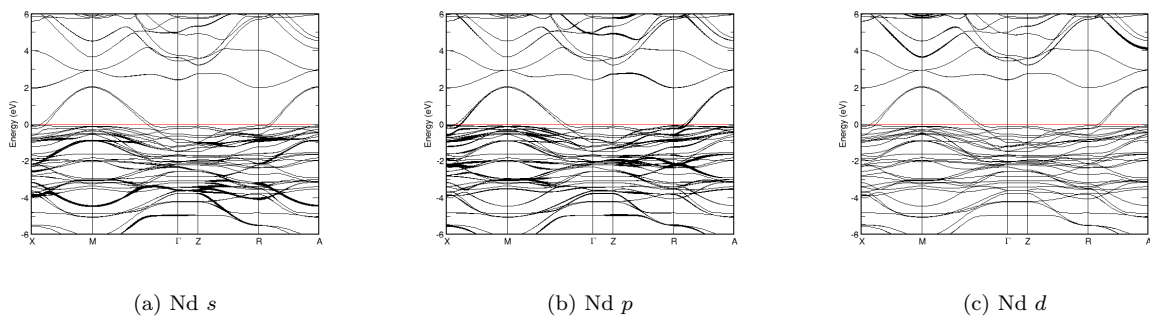
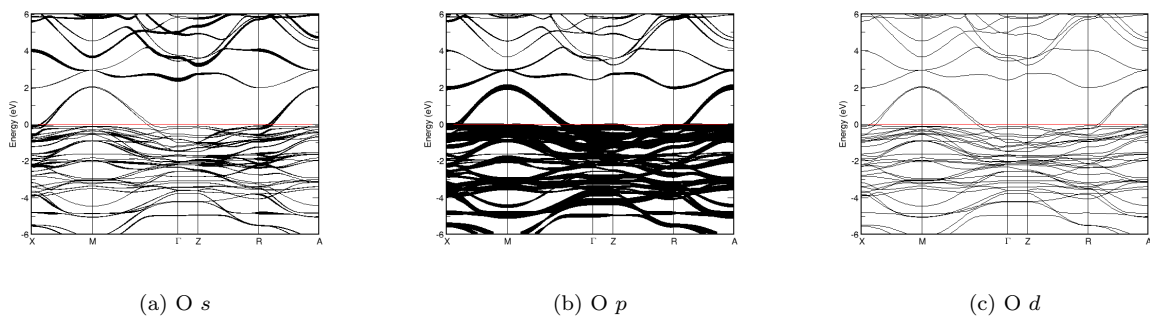
FIG. 541: Fat band representation of Lu in $\text{LuBa}_2\text{Cu}_3\text{O}_6$ FIG. 542: Fat band representation of O in $\text{LuBa}_2\text{Cu}_3\text{O}_6$ 

FIG. 543: (Color online) PDOS of $\text{NdBa}_2\text{Cu}_3\text{O}_6$ (ICSD #83074). The *s*-, *p*- and *d*-projected states are in red, blue and green, respectively. $\text{NdBa}_2\text{Cu}_3\text{O}_6$ crystallizes in space group $P 4/m m m$ (#123), in a tetragonal primitive structure.

FIG. 544: Fat band representation of Ba in $\text{NdBa}_2\text{Cu}_3\text{O}_6$ FIG. 545: Fat band representation of Cu in $\text{NdBa}_2\text{Cu}_3\text{O}_6$ FIG. 546: Fat band representation of Nd in $\text{NdBa}_2\text{Cu}_3\text{O}_6$ FIG. 547: Fat band representation of O in $\text{NdBa}_2\text{Cu}_3\text{O}_6$

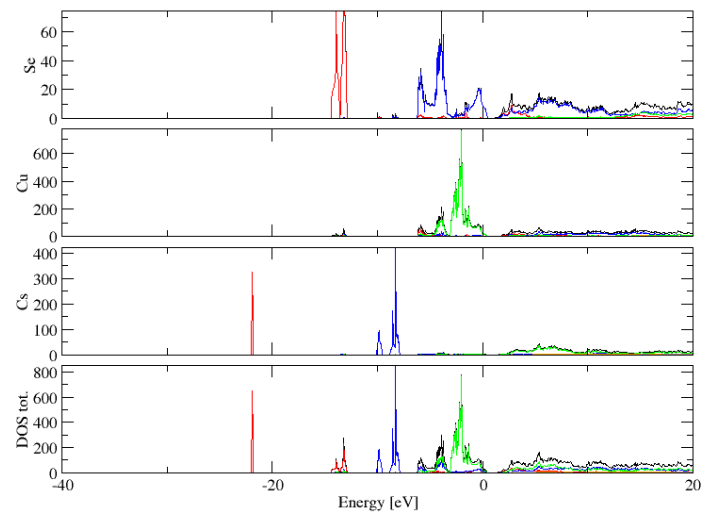


FIG. 548: (Color online) PDOS of $\text{Cs}(\text{Cu}_4\text{Se}_3)$ (ICSD #75196). The s -, p - and d -projected states are in red, blue and green, respectively. $\text{Cs}(\text{Cu}_4\text{Se}_3)$ crystallizes in space group $P 4/m m m$ (#123), in a tetragonal primitive structure.

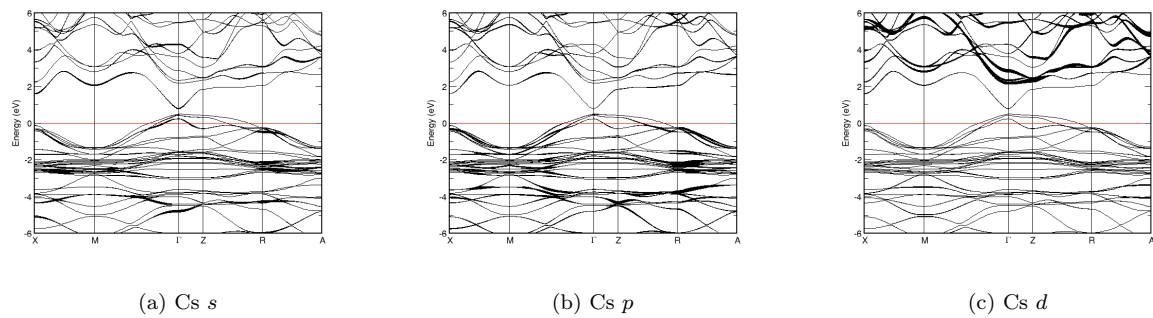


FIG. 549: Fat band representation of Cs in $\text{Cs}(\text{Cu}_4\text{Se}_3)$

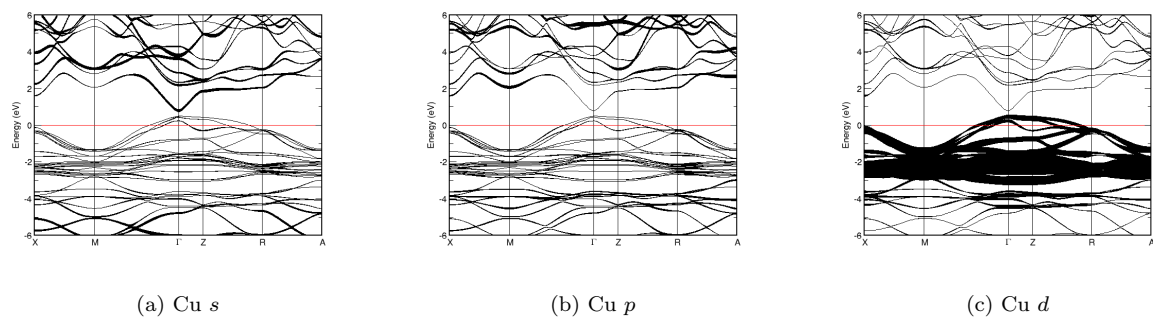
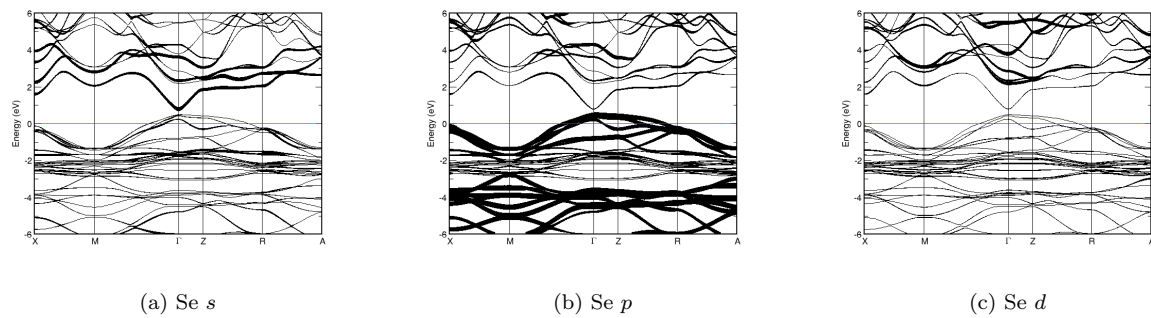
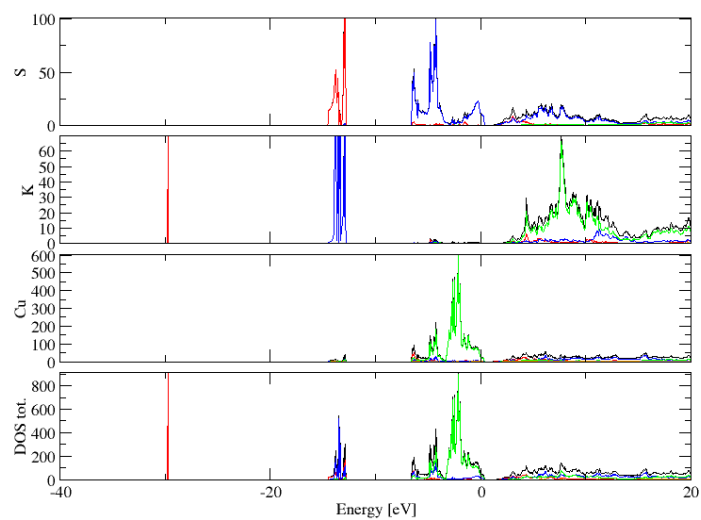
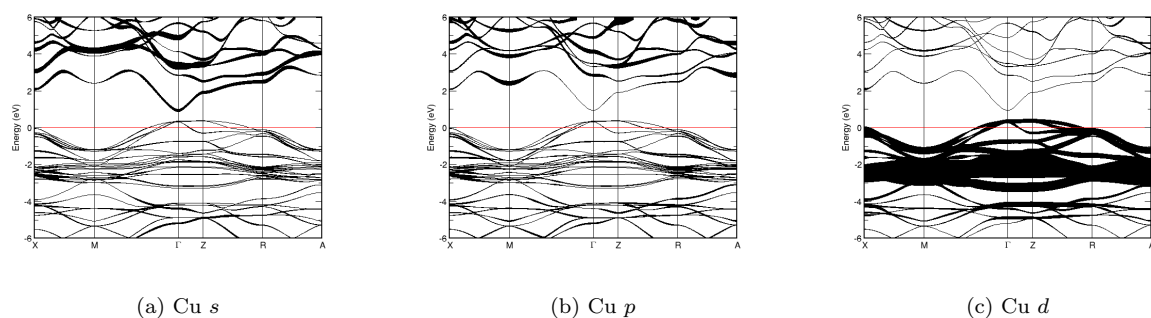
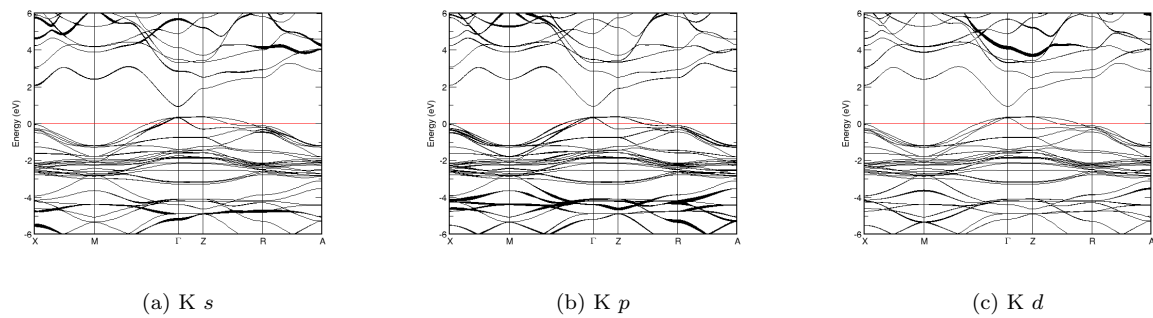
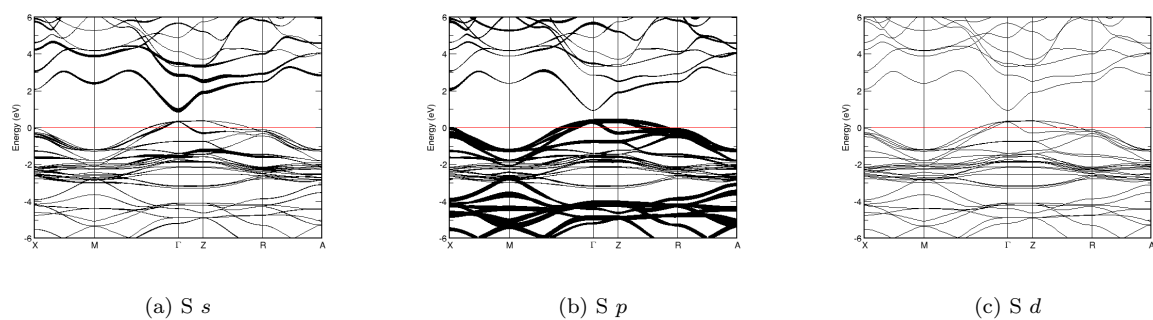
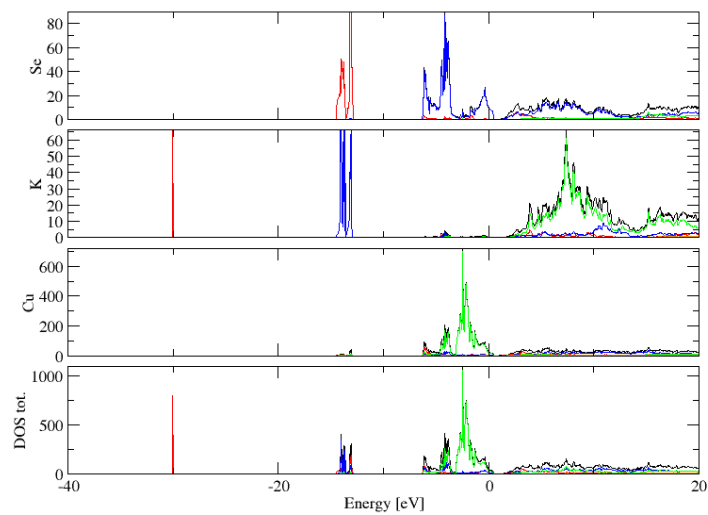
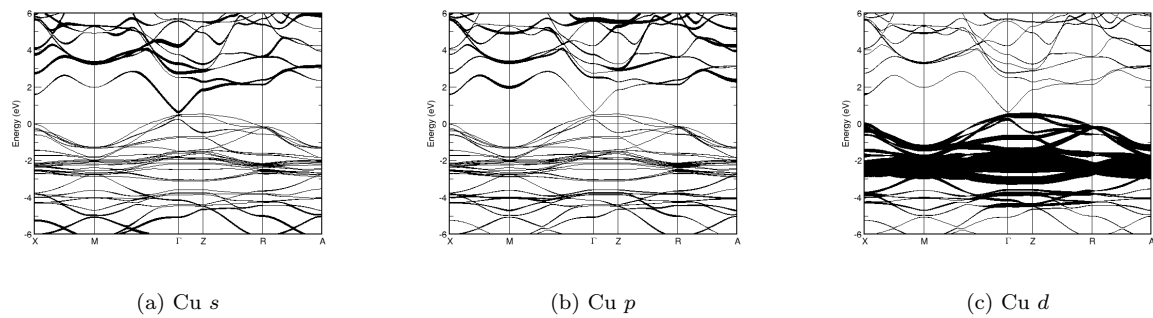
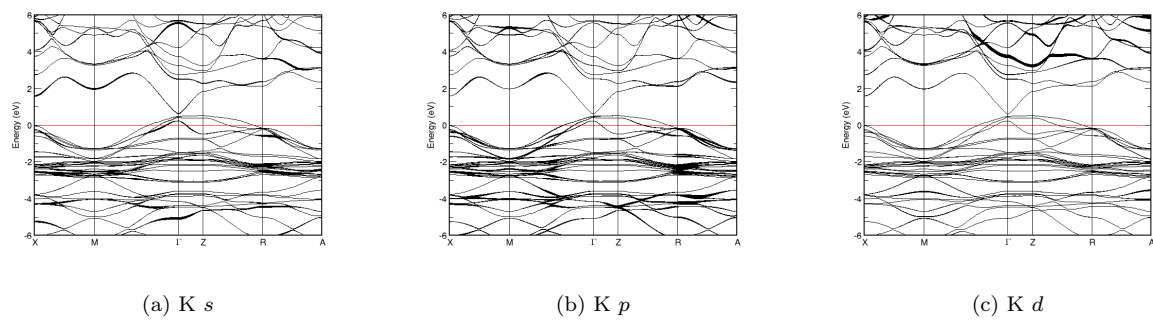
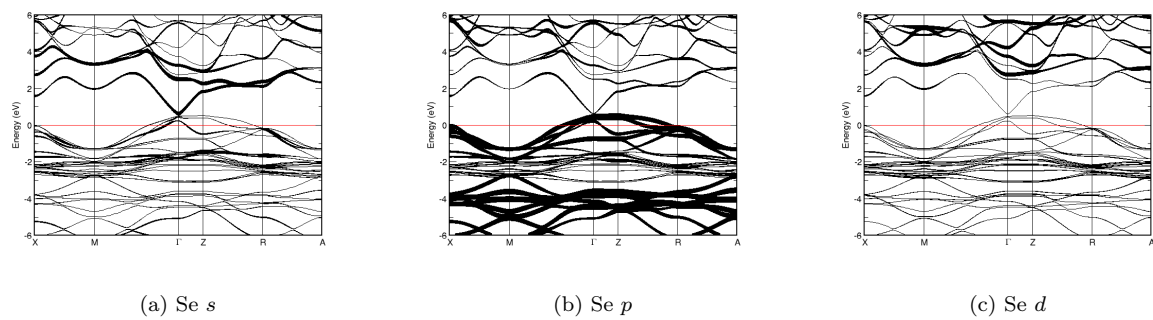


FIG. 550: Fat band representation of Cu in $\text{Cs}(\text{Cu}_4\text{Se}_3)$

FIG. 551: Fat band representation of Se in Cs(Cu₄Se₃)FIG. 552: (Color online) PDOS of KCu₄S₃ (ICSD #23336). The *s*-, *p*- and *d*-projected states are in red, blue and green, respectively. KCu₄S₃ crystallizes in space group P 4/m m m (#123), in a tetragonal primitive structure.FIG. 553: Fat band representation of Cu in KCu₄S₃

FIG. 554: Fat band representation of K in KCu_4S_3 FIG. 555: Fat band representation of S in KCu_4S_3 FIG. 556: (Color online) PDOS of KCu_4Se_3 (ICSD #280072). The *s*-, *p*- and *d*-projected states are in red, blue and green, respectively. KCu_4Se_3 crystallizes in space group $P 4/m m m$ (#123), in a tetragonal primitive structure.

FIG. 557: Fat band representation of Cu in KCu_4Se_3 FIG. 558: Fat band representation of K in KCu_4Se_3 FIG. 559: Fat band representation of Se in KCu_4Se_3